FINITE ELEMENT ANALYSIS OF STRESSES, DEFORMATIONS AND PROGRESSIVE FAILURE OF NON-HOMOGENEOUS FISSURED ROCK

OHIO STATE UNIVERSITY

PREPARED FOR
ADVANCED RESEARCH PROJECTS AGENCY

MARCH 1973

AD 768648

3200.8 (Att 1 to Encl 1)
Mar 7, 66

UNCLASSIFIED
Security Classification

DOCUMENT CONTROL DATA - R & D

(Security classification of title, body of abstract and indexing annotation must be entered when the overall report is classified)

1 ORIGINATING ACTIVITY (Corporate author)

The Ohio State University Research Foundation

2a. REPORT SECURITY CLASSIFICATION

Unclassified

2b. GROUP

3 REPORT TITLE

Finite Element Analysis of Stresses, Deformations and Progressive Failure of Non-Homogeneous Fissured Rock - Volume 1, Main Document

4 DESCRIPTIVE NOTES (Type of report and inclusive dates)

Final Report - March 31, 1973

5. AUTHOR(S) (First name, middle initial, last name)

Ranbir S. Sandhu

6 REPORT DATE	7a. TOTAL NO OF PAGES	7b. NO OF REFS
March 31, 1973	220 213	130

8a. CONTRACT OR GRANT NO	9a. ORIGINATOR'S REPORT NUMBER(S)
HO210017	
b. PROJECT NO: RF 3177 A1	OSURF 3177-73-1F
c.	9b. OTHER REPORT NO(S) (Any other numbers that may be assigned this report)
d.	

10 DISTRIBUTION STATEMENT

Distribution of this document is unlimited.

11 SUPPLEMENTARY NOTES

Computer programs available in magnetic tape, see AD-768 651.

12 SPONSORING MILITARY ACTIVITY

Advanced Research Projects Agency
Washington, D. C. 20301

13 ABSTRACT

The objective of this research program was development of finite element procedures for prediction of stresses and deformations in the vicinity of underground excavation.

Two models of rock behavior were selected. In one the rock is treated as isotropic elastic-plastic following a generalized Mohr-Coulomb law and in the other the rock is isotropic elastic-brittle subject to Griffith or modified failure theory.

For each model, mathematical relationships governing stress-strain behavior and progressive failure were developed. Finite element computer programs incorporating each of the two models were coded. Preliminary to this development, a revised version of Zienkiewicz's no-tension analysis was programmed.

The procedures developed all for initial stresses in rock, arbitrary shape and size of the opening, any given sequence of construction/excavation, material nonhomogeneity and progressive failure.

This report is in three parts: Volume 1-Main Document; Volume 2-Computer Program User's Manual; Volume 3-Computer Programs.

Volume 1, Main Document, contains the theoretical development, and discussion of application of the techniques to theoretical solutions, experimental data, published results and a parametric study of forces in structural supports for a tunnel excavation.

DD FORM 1 NOV 65 1473

Unclassified
Security Classification

14. KEY WORDS	LINK A		LINK B		LINK C	
	ROLE	WT	ROLE	WT	ROLE	WT
computation						
crack propagation						
deformation						
elasticity						
excavation						
failure						
finite element method						
foundations						
fracture						
mining						
plasticity						
progressive failure						
research						
rock mechanics						
stresses						
tunnels						
underground excavation						

AD 768648

OSURF-3177-73-1F

STRESSES, DEFORMATIONS AND PROGRESSIVE FAILURE OF NON-HOMOGENEOUS FISSURED ROCK

Final Report
Volume 1
March 1973

U.S. BUREAU OF MINES
Contract Number HO210017

Sponsored by
ADVANCED RESEARCH PROJECTS AGENCY
ARPA Order No. 1579, Amend. No. 2
Program Code 1F10

Principal Investigators

R. S. Sandhu
T.H. Wu
J.R. Hooper

THE OHIO STATE UNIVERSITY RESEARCH FOUNDATION
1314 KINNEAR ROAD COLUMBUS, OHIO 43212

FINAL REPORT

ARPA Order Number: 1579, Amend 2

Program Code Number: 1F10

Contract Number: HO210017

Principal Investigators: R. S. Sandhu
T. H. Wu
J. R. Hooper
Telephone Number: (614) 422-7531

Name of Contractor:
The Ohio State University
Research Foundation

Project Scientist or Engineer:
R. S. Sandhu
Telephone Number: (614) 422-7531

Effective Date of Contract:
February 1, 1971

Short Title of Work:
Stresses, Deformations and
Progressive Failure of
Nonhomogeneous Fissured Rock

Contract Expiration Date:
March 31, 1973

Amount of Contract:
$71,613.00

This research was supported by the Advanced Research Projects Agency of the Department of Defense and was monitored by the United States Bureau of Mines under Contract Number HO210017.

TECHNICAL REPORT SUMMARY

Program Objectives

The objective of this research program was development of finite element procedures to predict stresses, deformations and progressive failure of rock associated with underground excavations. For applicability to arbitrary sequence of excavation operations, it was necessary that the procedures developed allow for arbitrary initial stresses in rock, arbitrary size and shape of the opening and progressive failure. Plane strain conditions and two different types of material behavior were considered. Rock was treated as an isotropic elastic-plastic generalized Mohr-Coulomb material in one model and as an elastic-brittle material following Griffith theory of fracture in the other.

Background

In previous applications of the finite element method to rock mechanics, elastic-plastic behavior of rock has been modeled as nonlinear elastic for computational convenience. Further, it was assumed that the results of a one-dimensional test could be generalized to three-dimensional analysis through the use of an equivalent stress-equivalent strain curve. In some applications, two stress or strain parameters were used. These procedures are unsatisfactory. Assumption of isotropic elasticity assumes that the principal directions of stress and strain coincide. In plasticity this is not true. Also, rock behavior is characterized by a significant part of deformation being irreversible. For this reason, the mechanical behavior in unloading is different from that in loading. For rock with preexisting joints or developing tensile cracks, a 'no tension'

procedure is often adopted. In this method, a linear elastic solution is obtained and all tensile stress redistributed simultaneously. Actually, as cracking progresses, the rock on either side of the crack is relieved of stress and a stress concentration develops near the crack tip. Conventional procedures ignore these effects and the progressive nature of crack development, leading to erroneous conclusions regarding stresses around underground openings.

Accomplishments Under the Present Program

The research conducted under this contract has resulted in development of computer programs based on more realistic simulation of material behavior. The incremental theory of plasticity has been used to characterize the stress-strain behavior of elastic-plastic rock. Role of kinematic constraint of plane strain in development of residual stresses in rock has been examined on the basis of Hill's theory. New techniques have been developed for study of initiation and propagation of fracture in rock following Griffith's theory or the modified Griffith theory. Allowing for sequential fracture of various elements in a system, the effect of progressive stress redistribution in the remaining system is correctly incorporated. Arbitrary initial stress states, arbitrary sequence of excavation (or construction), arbitrary size and shape of opening, and nonhomogeneous material properties were allowed for. The actual construction operations can be simulated. The procedures developed were applied to several typical problems in rock mechanics as well as to some theoretical and laboratory studies for the purpose of verification and illustration. These were used to carry out parametric studies to examine the influence of rock properties upon the stresses in steel supports in a tunnel.

DOD Implications

The procedures developed provide useful means for study of stability of underground excavations based on stresses and deformations associated with the mining operations, structural support evaluation, safety analyses of openings, study of blasting effectiveness under certain conditions, evaluation of mining sequences, study of vulnerability and serviceability of underground structures etc.

Organization of the Report

This report is in three parts as follows:

Volume 1 - Main Document
Volume 2 - Computer Program User's Manual
Volume 3 - Computer Programs

Volume 1 contains the main body of the report including the theoretical development, program verification and case studies. Chapter I reviews previous efforts in the general research area and describes the objectives and methods of the present research in the historical context. Chapter II describes the mechanical behavior of rock and the idealizations used in the research under report. The basis and methods of the finite element theory are briefly discussed in Chapter III leading to the formulation of matix equations. Chapter IV gives details of the analysis technique for isotropic elastic-plastic generalized Mohr-Coulomb rock materials and Chapter V gives the numerical analysis procedure for jointed rock and rock subjected to progressive fracture following Griffith or modified Griffith theory. Examples of application are included in Chapters IV and V. Chapter VI presents application of the elastic-plastic analysis computer program to a parametric study to evaluate the influence of rock properties on stresses in steel supports for specified initial stresses and design of the opening.

In the original proposal, model testing to verify some aspects of rock behavior under plane strain conditions was foreseen. The effort under the present contract covered procurement of suitable plane strain test equipment and design of suitable test material. Appendix B includes a report on this effort.

Volume 2 of the report contains description of the three computer programs developed under the contract along with fortran listings and instructions for input preparation. The input definition and the listings are for the IBM 370/165 version.

The programs are the primary content of volume 3. These are available on magnetic tape from DDC-TC, U.S. Department of Commerce, Springfield, Virginia 22151, telephone (703) 321-8517.

ACKNOWLEDGEMENTS

The research was supported by the U.S. Government through the Advanced Research Projects Agency, ARPA, and its agent the U.S. Bureau of Mines, Department of the Interior. James J. Olson, Twin Cities Mining Research Center, was the ARPA program coordinator and Dr. William J. Karwoski, Spokane Mining Research Center, was the Project Officer. In early stages of work. Dr. Syd Peng, Twin Cities Mining Research Center acted as the Project Officer. Constant cooperation and several constructive suggestions from these individuals are gratefully appreciated.

A number of graduate students worked on the project. The contributions of Messrs. Ram Dhan Singh, S. W. Huang and Kamar Jit Singh were specially noteworthy. The Instruction and Research Computer Center of the Ohio State University provided the computational facilities.

R. S. Sandhu
Project Supervisor

TABLE OF CONTENTS

TABLE OF CONTENTS (Continued)

TABLE OF CONTENTS (Continued)

LIST OF FIGURES

LIST OF FIGURES (Continued)

LIST OF FIGURES (Continued)

LIST OF FIGURES (Continued) Page

LIST OF FIGURES (Continued)

CHAPTER I. INTRODUCTION

The terrestrial crust is in a complex state of stress. Excavations in this stressed medium profoundly influence the distribution of stress which in turn determines the stability of the pit, slope or underground opening as the case may be. Feasibility of a project is related to economics of safe and stable construction. As an aid to decision making, it is necessary to develop quantitative information regarding the 'state' of insitu rock and predict the stability characteristics of rock under a change in mechanical environment associated with the proposed construction or excavation operations. Accordingly, engineering investigations in rock mechanics are motivated by the following two objectives:

i. Evaluation of the 'state' of insitu rock. This includes, among others, investigation of pre-existing stresses in the rock and mapping of discontinuities, material symmetries and other physical data relevant to engineering decision process.

ii. Evaluation of changes from the initial state, associated with excavation or construction operations, including among other factors, changes in the stress field, along with consequent yield of material, extension of existing faults and discontinuities and development of new ones.

The research effort covered by this report was directed towards the second objective. In order to realistically predict the stresses, deformations and distress of rock, it is necessary that the method of analysis used take account of the following:

i. The initial state including pre-existing stresses,

discontinuities, nonhomogeneity, and material symmetries, if any.

ii. The sequence of excavation or construction operations.

iii. The mechanical behavior of rock i.e., deformation, yield, failure or fracture of rock under changes in stress environment.

iv. Interaction with structural supports, if any, used to improve safety and stability.

Traditionally, limit equilibrium methods have been used to predict stress states and factors of safety. The theory of elasticity has been extensively used to evaluate stresses in rock in the vicinity of underground openings. However, these methods are applicable only for linear elasticity, homogeneous materials, simple geometry (e.g. circular or elliptical openings), and isotropic materials. None of these assumptions are valid for rock. Furthermore, the excavation was assumed to be carried out in a single step. Influence of sequential nature of any construction could not be taken into account by these methods.

With the advent of high speed digital computers, numerical methods of analysis have proved to be increasingly useful. Of available techniques, the most powerful is the finite element method. The method was introduced by Clough (1960) and was essentially an offshoot of the general matrix structural analysis techniques developed in the aerospace industry (Argyris (1960), Turner et al. (1956)). Development of the method has been rapid and a considerable volume of literature has accumulated over a relatively short period. Among the more important references are

the text books by Zienkiewicz (1972), Oden (1972), Desai (1972) and proceedings of conferences and symposia (WPAFB (1965, 1968, 1971), Vanderbilt (1969), U.S.-Japan Seminar (1969), IUTAM Symposium (1970)). Mathematical foundations of the method (Zlamal (1968), Oliviera (1968), Oden (1969), Aubin (1972)), its relationship to variational methods (Melosh (1963), Pian and Tong (1968)), convergence of sequences of approximate solutions (Walz et al. (1968), Yamamoto and Tokuda (1971), Key (1966), Oliviera (1968)) have received attention.

The finite element method has been applied to rock mechanics problems and its special suitability stems from the fact that any geometrical configuration can be considered and nonhomogeneity of material does not present any difficulty in the solution process. Also arbitrary loads, including body forces and surface loads, and displacements can be prescribed for the problem.

King (1965) developed finite element techniques for incremental construction which were used by Clough and Woodward (1965) and Sandhu et al. (1967). King also incorporated a technique for relieving stresses in individual elements in analysis of time-dependent problems. This procedure has been since used to simulate excavations by Nair et al. (1968), Dunlap and Duncan (1969), Duncan and Chang (1970), among others. It also forms the basic procedure in analysis of rock as 'no tension' material by Zienkiewicz et al. (1968) and also in Zienkiewicz et al.'s (1968) analysis of elastic-plastic materials. Kulhawy (1972) improved the procedure somewhat by using stresses at the excavated surface rather than stresses at centers of surface

elements to simulate stress relief due to excavation.

Nonlinear material behavior was treated by Gallagher et al. (1962) using the 'initial strain' approach. Finite element analysis procedures were developed for nonlinear elasticity by several investigators. The approach was to approximate a one-dimensional stress-strain curve by a mathematical relationship. Wilson (1965) used the bilinear law. Multi-linear laws have been proposed by Dunlap et al. (1968). Salmon, Berke and Sandhu (1969) incorporated Richard-Goldberg (1965) and Ramberg-Osgood law (1943) and Wilson's bilinear representation in a single program. Kulhawy and Duncan (1969) and Kulhawy (1972) adopted Kondner's (1963) hyperbolic representation of the stress-strain curve. These mathematical equations use one or more parameters to get best fits and are unsatisfactory insomuch as the slope of the curve is not closely approximated. Desai (1971) used spline functions to obtain the best fit. This way he was able to obtain the best fit,not only to the stress-strain plot,but also to the slope of the curve which is the information actually used in the computer program. Desai (1972) extended his work to allow for the effect of confining pressure. This was achieved by using bi-cubic splines. Singh and Chang (1972) further developed upon Desai's work to use spline fit by approximating curves independent of stress path and calculated secant modulus and poisson's ratio. The procedure has been extended to laminates.

To extend the procedure to three-dimensional analysis, the general approach has been to interpret the one-dimensional test data as equivalent stress-equivalent strain plot. Second invariant of the stress derivative and the octahedral shearing

strain are the quantities most often used. Defining a shear modulus in this manner, the Poisson's ratio is assumed constant. Kulhawy (1972) defined both elastic modulus and Poisson's ratio as stress-dependent quantities. This approach assumes isotropic behavior throughout. Another approach using the laws of plasticity was used by Salmon, Berke and Sandhu (1969) and Sutherland (1970). All these approaches are essentially empirical. If the material is indeed nonlinear elastic, one can either treat it as Green-elastic and set up on energy functional for isothermal or adiabatic conditions as the case might be, or directly treat the stress tensor as a nonlinear function of the strain tensor and for isotropic materials using the Cayley-Hamilton theorem to obtain a representation. Evans and Pister (1966) showed that for energy functional cubic in strain, five constants are required to define the stress-strain law, and these cannot be obtained from any single test. Similarly the constants in any Cayley-Hamilton representation cannot be obtained from a single test. It is well-known that equivalent stress-equivalent strain plots obtained from different tests on rocks and soils are path dependent and therefore different.

For finite element analysis, elastic-plastic materials (rate independent materials exhibiting path dependent behavior above certain stress level) were treated as nonlinear elastic by several workers. In rock mechanics the deformation theory of plasticity has been used (Jaeger and Cook (1969), Brady (1970), Malina (1970)). This theory assumes the principal strain directions to coincide with the principal stress directions, assumes no volume change during plasticity, and is inapplicable

to nonmonotonic loading. Hill (1950) has discussed the shortcomings of this theory in detail. It suffices to note here that this theory is unsound and for this reason it was not considered in the present research program as a possible model for mechanical behavior of rock.

Incremental theory of plasticity was used by Zienkiewicz et al. (1968), Swedlow et al. (1965), Marcal (1969), Marcal and King (1967). Drucker's method for evaluation of λ in the 'normality rule' was used leading to the tangent modulus approach for von Mises materials. Felippa (1966) developed stress-strain relations in terms of total incremental strain (elastic and plastic) and incremental stress. This relation is identical to the one proposed by Naghdi (1960) and Prager (1949) for work-hardening materials but has the additional advantage that it is valid for perfectly plastic solids for which Naghdi-Prager relationships are undefined. Reyes (1965) and Reyes and Deere (1966) used a rate of work equation to develop stress-strain relations for Mohr-Coulomb materials. This approach has the limitation that it cannot be generalized to other failure laws. Yamada (1968) used an energy rate approach for von Mises materials. These energy rate approaches are limited in application and can be derived from Felippa's more general formulation. Zienkiewicz et.al. (1968) used this approach in conjunction with an 'initial stress' technique to solve for stresses without interest in displacements. Baker, Sandhu and Shieh (1969) used Reyes and Deere's formulation for finite element analysis of stresses and deformations in rock. It was noticed that under plane strain

conditions, a radial path eannot be followed in the Westergaard-Haigh stress spaee.

Diseontinuities in rock appear as joints, fissures and faults. Modeling of diseontinuities has reeeived eonsiderable attention. However, exclusively, the geometry of the eraeks and joints was assumed to be known. With this as the starting point, researeh effort has principally been eoncentrated on eharaeterization of stress-strain behavior of jointed roek and on ineorporating limiting shear strength of joints in finite element analyses. Anderson and Dodd (1966) considered open joints or faults as surfaees with no resistanee to shear, ineapable of withstanding tensile stresses normal to their planes. This capability is now routinely ineorporated in most finite element programs. A two-dimensional 'soft' material element has long been used to represent weak joint planes in roek. Duncan and Goodman (1968) objeet to this on the basis of the large number of elements needed to ensure a reasonable 'aspect ratio' in the shape of elements. This becomes a problem for elements representing very thin joints. For rock systems having thin, elosely spaeed parallel joint planes, an equivalent orthotropic elastie eontinuum representation regarding the orientation of the joints as the plane for refleetive symmetry in the material was proposed by Dunean and Goodman (1968). A one-dimensional element with shear and normal stiffness eharaeteristies was developed by Goodman et al. (1968). Reeently, Heuze et al. (1971) have introduced nonlinear meehanieal properties in this element. Christian is eredited with development of an element capable of simulating eonstant shear and residual shear

characteristics. All these investigations were concerned with setting up stress-strain relationships for rock with pre-existing joints. Propagation of fracture has been considered by several investigators. Chan et al. (1970), Gross et al. (1968) sought to calculate stress intensity factors at crack tips to determine whether a given crack would propagate. To improve accuracy, Wilson (1971), Byskov (1970) and Levy (1971) introduced stress singularity elements at crack tips. Pian (1971) used hybrid finite elements to obtain improved stress intensity factors without recourse to singularity elements. Throughout, it was assumed the geometry of the crack was known beforehand. These procedures cannot be used to study discontinuities arising as a result of fracture under changes in stress environment. Also these cannot consider propagation of fracture. To use the same procedure for pre-existing as well as post-failure cracks, it is necessary to allow cracks and joints within elements. Then, the mesh layout is more flexible and arbitrary failure laws can be used. Malina (1970) used this approach to study failure along joint planes and then went on to compute the amount of slip and the accompanying stress redistributuion on the basis of deformation or slip theory of plasticity. Recently, Bock (1971) has used Malina's technique to study propagation of faulting in rock.

Simulation of rock behavior after cracking develops can be achieved using a bimodular elastic representation (Sandhu, 1969). However, recognizing the crack to be a plane of material symmetry, the material is bimodular orthotropic with no resistance

to tension in the direction normal to crack. For cracks in two independent directions, an element under uniform stress can be regarded as bimodular isotropic. The 'no tension' method used by Zienkiewicz et al. (1968) is an iterative procedure of obtaining tension free stress states. The philosophy reflects an iterative solution of a bimodular orthotropic problem. However, the mechanics of solution eliminates only the tensile principal stresses. This amounts to using a non-symmetric stress-strain relationship and is open to objection. This situation was corrected by Sandhu (1971).

New procedures for finite element analysis of elastic-plastic Mohr-Coulomb materials and elastic-brittle materials following Griffith's theory under plane strain conditions were developed in the course of the present research. Arbitrary geometric configurations, complex boundary conditions, nonhomogeneity of rock are allowed for as is usual in finite element techniques. Variational formulations of the field equations shows that arbitrary initial stresses and pore-water pressures, if any, can be directly included in the problem. Stress-strain relations in plasticity follow Reyes and Deere (1966) and Felippa's (1966) formulation. At early stages of work (Sandhu, 1971), it was assumed that in plane strain plasticity, the elastic and plastic components of strain on planes normal to the axis separately vanish. Thus a sudden jump in axial stress was introduced to ensure continuity of deformation. Later, Hill's (1950) analysis of plane strain was adopted using the vanishing of total strains. In an arbitrary construction sequence, a given element may be subjected to excursions to, from and within the yield surface in the stress space. Capability

to allow for loading followed by unloading has been incorporated in the analysis. For jointed rock subject to progressive fracture, Griffith and Modified Griffith theories were used to predict fracture initiation. Bimodular elastic orthotropy describes the post-fracture behavior of rock and an iterative-incremental process is used to define the sequential fracture of elements in a system giving the extent of various fractures. The new procedure differs significantly from the 'no tension' concepts. The latter define a region where the elastic solution indicates tensile stresses and the solution process neutralizes all tensions simultaneously. This is incorrect and does not allow for the stress redistribution, in its neighborhood, caused by the formation of a crack. Sequential cracking constitutes a nonlinearity in material behavior and linear superposition implied in simultaneous release of all tensions in the 'no tension' procedure is not valid.

The procedures developed allow for arbitrary construction or excavation sequence, and can allow for pre-existing joints, open or closed. Linear elastic elements can be included in the analysis. The procedures can include tunnel supports as part of the sequential construction scheme. These were used to obtain numerical solutions to several problems. Results are included in the report.

Chapter II of the report discusses mathematical modeling of mechanical behavior of rock. In Chapter III basis of the finite element method is outlined. Chapters IV and V present details of application of the finite element method respectively to plane strain analysis of elastic-plastic Mohr-Coulomb rock and plane strain analysis of progressive cracking of rock following Griffith's theory.

Chapter VI reports the application of the elastic-plastic incremental structure analysis to a parametric study. The objective of this study was to determine the influence of rock property data on stresses in steel supports of a tunnel. Chapter VII contains a discussion of results of this research effort. Appendices A and B present, respectively, Griffith's theory of fracture propagation and the experimental research effort under the contract.

CHAPTER II. MATHEMATICAL MODELING OF MECHANICAL BEHAVIOR OF ROCK

2.1. Mechanical Behavior of Rock

Figs. II-1 and II-2 show, respcetively, typical stress-strain plots for a granite and a marble. Upon loading the stress-strain eurve is almost linear and reversible over a short portion. Unloading from higher loads does not coincide with initial loading. This eharacteristie along with rate independenee distinguishes elastic-plastie behavior. Reloading closely follows unloading until the previous maximum is reached; whereupon, the original curve is followed. This leads to some simplifying assumptions.

i. A yield point exists below which the material is linear elastic.

ii. The yield point corresponds to the maximum stress level previously attained.

iii. Unloading and reloading paths are linear, coincident and parallel to the initial elastie loading eurve.

Fig. II-3 shows this simplifieation. Clearly the yield point ean be deseribed by the permanent or irreeoverable strain or the area bounded by the loading curve, the unloading curve and the horizontal axis. Whereas in generalization to the three-dimensional ease, the stresses and strains beeome seeond rank tensors and are therefore unordered; the area is still a scalar product and retains its ordering eharacteristies. To this extent, it is often preferred as a measure of the elastie limit. Other approaehes treat the elastic limit as a sealar function of the strain tensor.

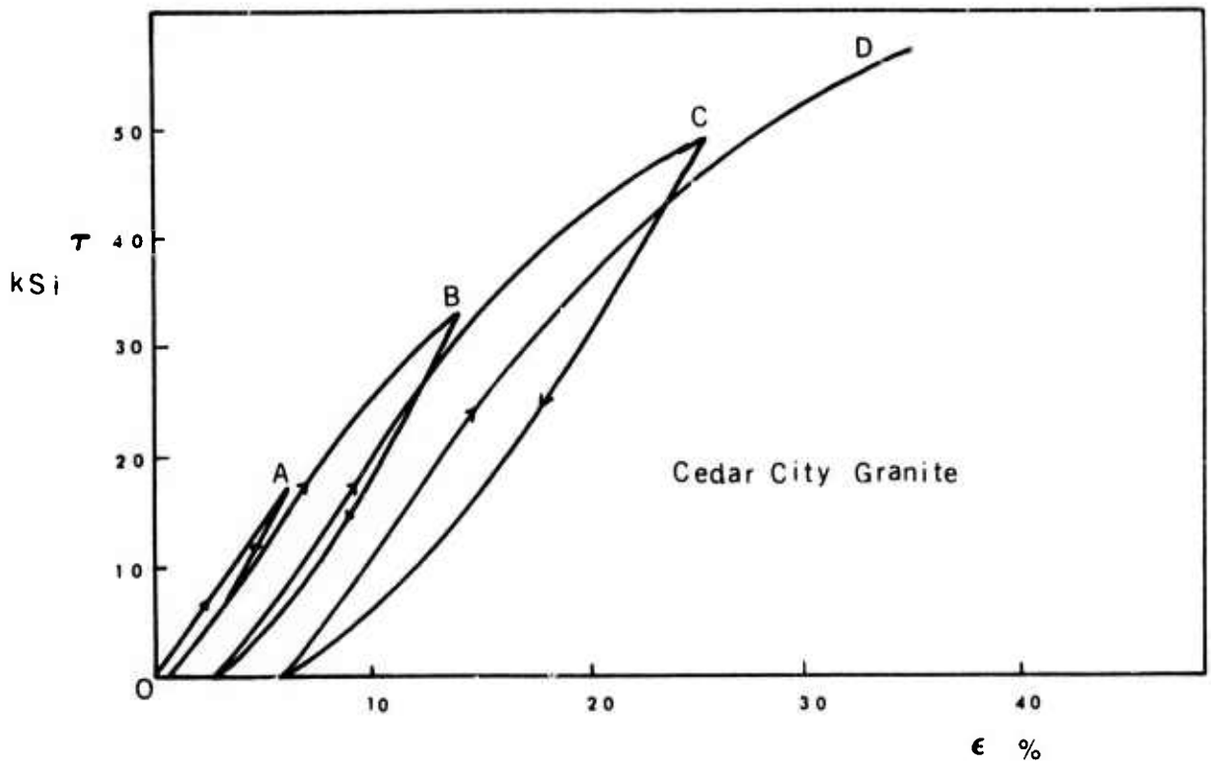

FIG. II-1. Stress-Strain Curves for Cedar City Granite
(Swanson, 1970)

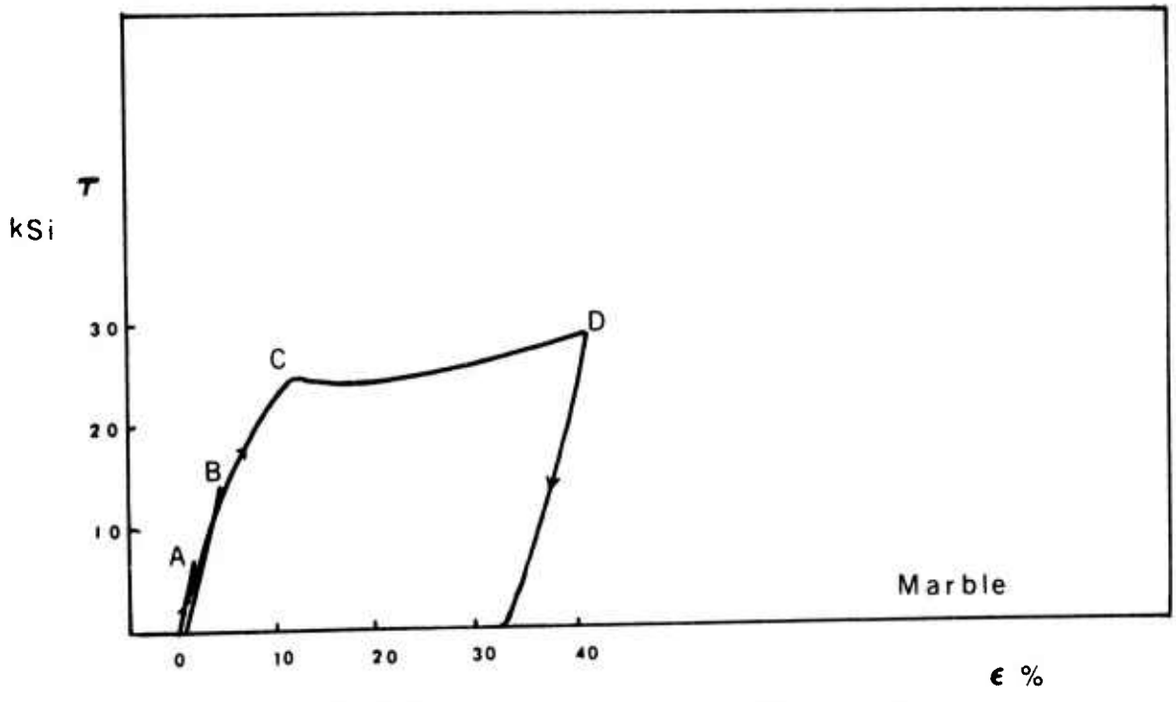

FIG. II-2. Stress-Strain Curves for Marble
(Swanson, 1970)

Mechanical behavior of rock under polyaxial state of stress has been examined in the light of brittle failure theories. Four regions of behavior are identified in Fig. II-4. The first region corresponds to closure of preexisting open cracks and is peculiar to compressional loading. In region II material behavior is linear elastic. Fracture initiation occurs near the end of this region in accordance with Griffith or Modified Griffith theory. This stage also corresponds to onset of nonlinearity in the relationship of stress to volumetric strain (Brace, 1966). Stable fracture propagation characterizes region III. In region IV, unstable fracture propagation results in strength failure and rupture. Differences in loading and unloading behavior are observed (Walsh, 1965).

We have, thus, two general approaches to the characterization of stress-strain behavior of rock. One follows the theory of elastic-plastic solids without consideration of micro-mechanics of the system. The other uses Griffith theory or Modified Griffith theory to relate deformation and failure to initiation and propagation of fracture. It has been observed (Swanson, 1970) that Mohr-Coulomb failure law applies for moderate values of confining pressure and that at low confining pressures, failure is by rupture. Contrary to plastic behavior, strength of material drops to almost zero in the direction normal to the crack if rupture theory is followed. Figs. II-5 and II-6 depict typical relationships of failure strength and post-failure behavior in relation to confining pressures. It is reasonable to assume that the material is linear-elastic upto yield or rupture, as the case may be, and that the post-failure behavior only is

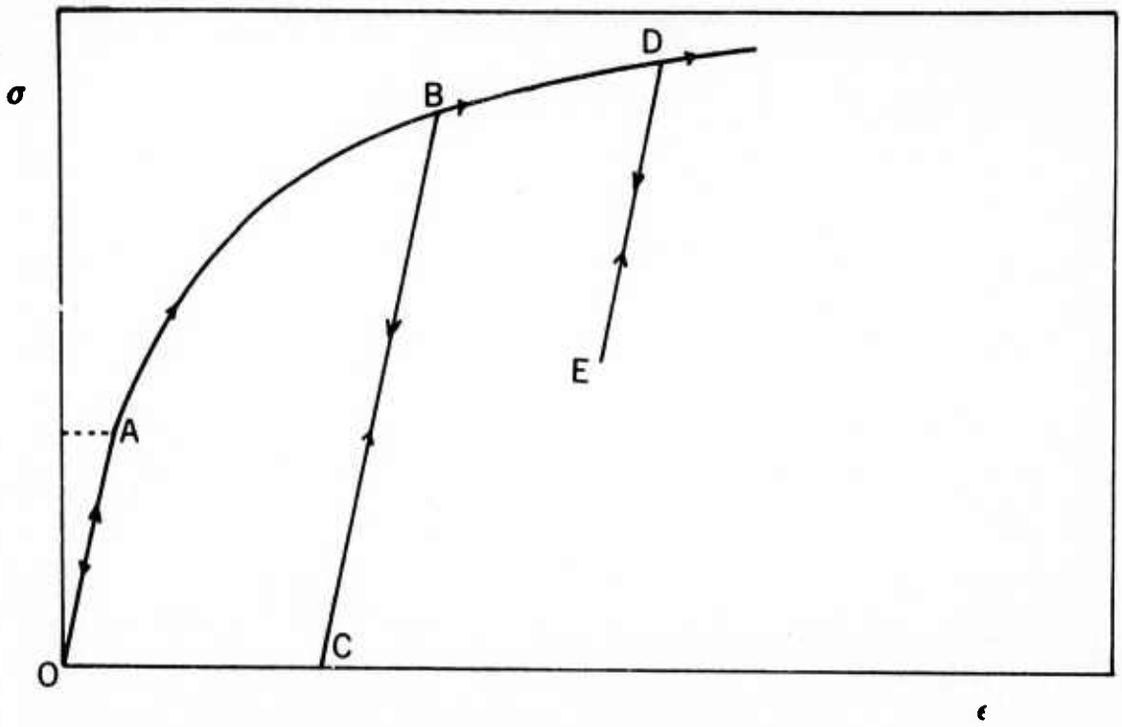

FIG. II-3. Idealization of Elastic-Plastic Stress-Strain Behavior for Rocks

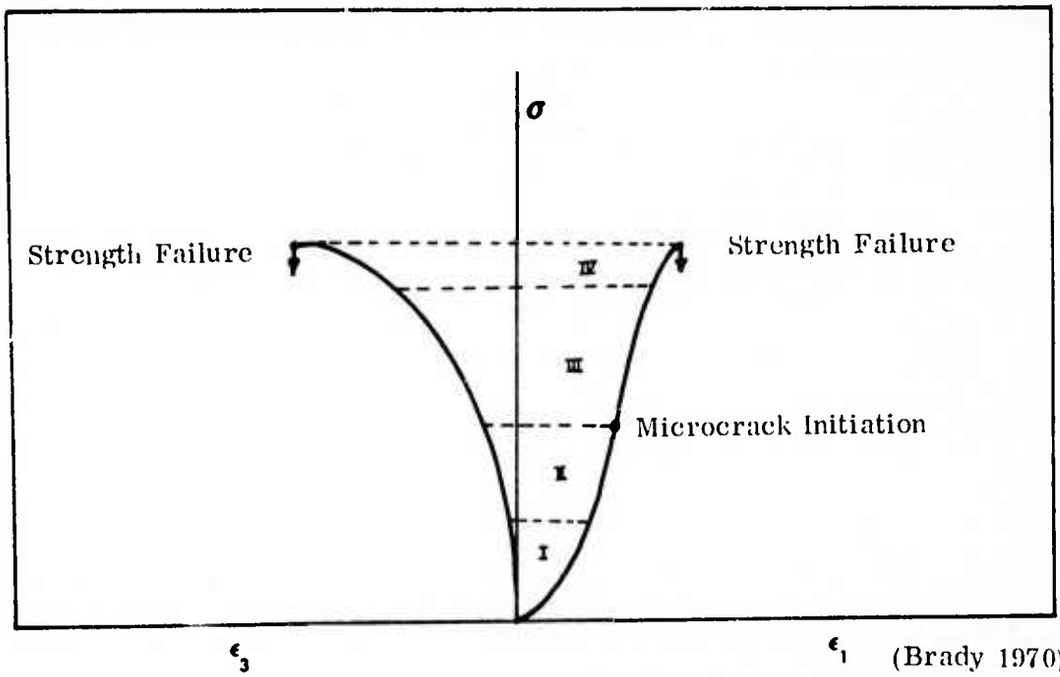

(Brady 1970)

FIG. II-4. Typical Axial and Lateral Stress-Strain Behavior of Brittle Rock

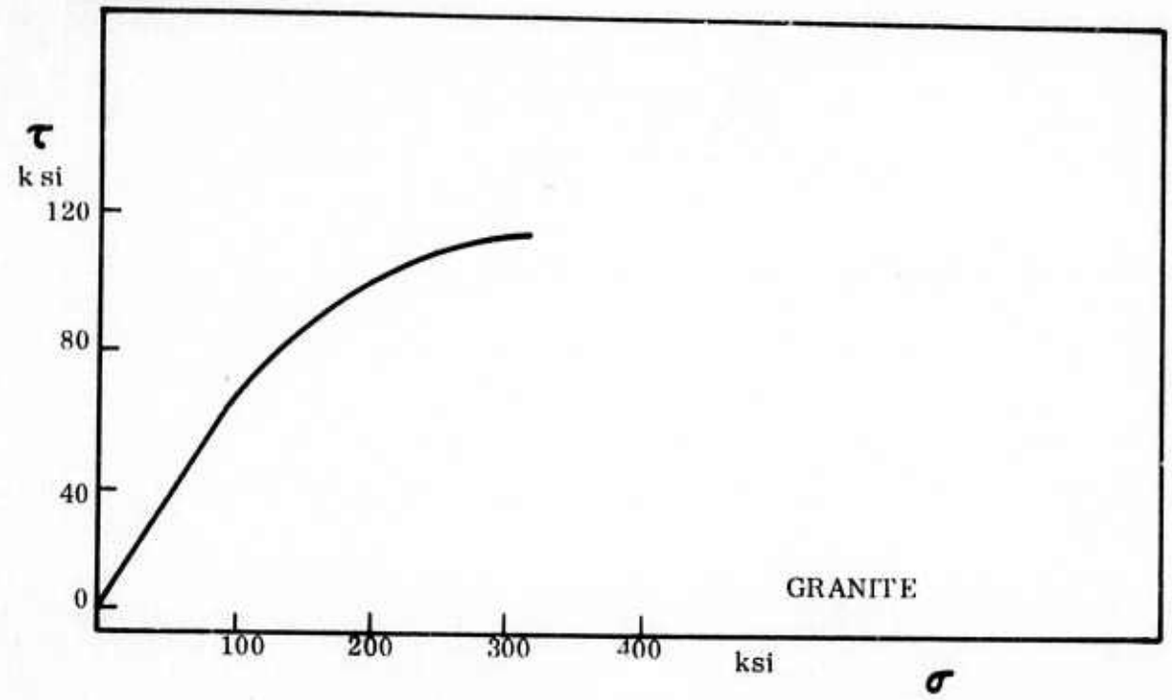

FIG. II-5. Proportional Limit in Shear for Westerly Granite (Swanson, 1970)

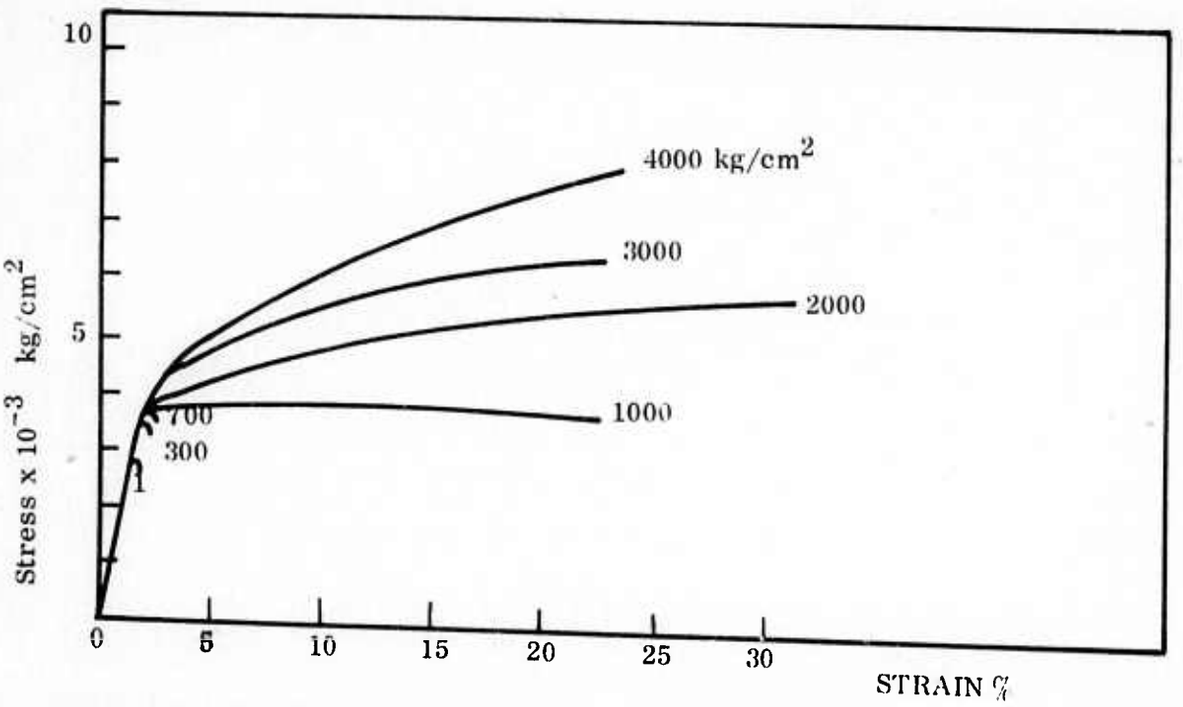

FIG. II-6. Effect of Confining Pressure on Stress-Strain Behavior of Limestone

governed by the theory used to define failure. In the present research program, both the elastic-plastic Mohr-Coulomb failure theory and the Griffith theory have been used for analysis of stresses, deformation, and failure of rock.

2.2. Characterization of Elastic-Plastic Behavior

Several approaches have been used for formulation of elastic-plastic behavior of rock. One approach is to treat rock as nonlinear elastic material. It is argued that this assumption is a reasonable one in case unloading does not occur and loading is 'proportional' (or radial in the stress space). Under such circumstances, the state of stress is described completely by a single parameter. If stress-strain data for the actual stress path are available, these can be directly used to predict deformation response to applied loads. This approach is attractive because of its apparent simplicity. However, stress path dependence of material behavior results in difficulties in correct representation of behavior under arbitrary stress changes. Attempts have been made to represent strain invariants as functions of stress invariants and vice versa, thereby permitting generalizations to arbitrary stress paths. It is customary to use a stress or strain dependent Young's modulus and Poisson's ratio. Wilson's bilinear law (1965), Goldberg-Richard equation (1965), Ramberg-Osgood equation (1943), Prager's formulation (1938), the work of Kondner (1963), Duncan and Chang (1970), Kulhawy (1971), Vallabhan and Reese (1968), Desai (1971) and recent work by Singh (1972), are all based on this philosophy.

In general, there are two distinct approaches to characterization of nonlinear elastic materials. One is to assume the existence of energy functional such that its

derivative with respect to any strain component is the corresponding component of the stress tensor. The other directly writes stress as a tensor function of strain. Assuming the existence of strain energy functional, Rivlin (1960) proposed

$$U = \sum_{\alpha,\beta,\gamma} I_1^{\alpha} \; I_2^{\beta} \; I_3^{\gamma} \qquad \text{(II-1)}$$

where $I_1 = \epsilon_{ii}$, $I_2 = 2\,\epsilon_{ii} + \epsilon_{ii}\,\epsilon_{jj} - \epsilon_{ij}\,\epsilon_{ij}$ and I_3 = determinant $(\delta_{ij} + 2\,\epsilon_{ij}) - 1$. Toupin and Bernstein (1961) proposed

$$U = \frac{1}{2} E_{ijkl}\,\epsilon_{ij}\,\epsilon_{kl} + \frac{1}{6} E_{ijklmn}\,\epsilon_{ij}\,\epsilon_{kl}\,\epsilon_{mn} + \ldots . \qquad \text{(II-2)}$$

Neuber (1969) used

$$U = U(\phi_1, \phi_2, \phi_3) \qquad \text{(II-3)}$$

where

$$\begin{aligned} \phi_1 &= A_{ij}\,\epsilon_{ij} \\ \phi_2 &= A_{ijkl}\,\epsilon_{ij}\,\epsilon_{kl} \\ \phi_3 &= A_{ijklmn}\,\epsilon_{ij}\,\epsilon_{kl}\,\epsilon_{mn} \end{aligned} \qquad \text{(II-4)}$$

Neuber's formulation includes Toupin and Bernstein's as a specialization. For isotropy A_{ij}, A_{ijkl}, A_{ijklmn} are taken as identity tensors. Evans and Pister (1966) proposed, for isotropic elasticity

$$U = U(\phi_1, \phi_2, \phi_3) \qquad \text{(II-5)}$$

as a cubic or biquadratic expression in ϵ_{ij}. For biquadratic expansion

$$\begin{aligned} U = {} & \frac{A_{11}}{2}\,\phi_1^2 + \frac{A_{21}}{3}\,\phi_1^3 + \frac{A_{31}}{4}\,\phi_1^4 + A_{34}\,\phi_1\,\phi_3 \\ & + A_{33}\,\phi_1^2\,\phi_2 + 2A_{22}\,\phi_1\,\phi_2 + A_{32}\,\phi_2^2 + A_{12}\,\phi_2 + A_{23}\,\phi_3 \end{aligned} \qquad \text{(II-6)}$$

requiring nine constants to describe the energy functional. Here $\phi_1 = \epsilon_{ii}$, $\phi_2 = \frac{1}{2}\epsilon_{ij}\epsilon_{ij}$, $\phi_3 = \frac{1}{3}\epsilon_{ij}\epsilon_{jk}\epsilon_{ki}$. It is important to note that $\epsilon_{ij} \longrightarrow 0$ does not imply linearity in the limit. Using a cubic expansion, there are five constants.

Alternatively, writing stress directly as a polynomial function of strain, Cayley-Hamilton theorem leads to the following relationship for isotropic materials

$$\sigma_{ij} = a\ \delta_{ij} + b\ \epsilon_{ij} + c\ \epsilon_{ik}\ \epsilon_{kj} \qquad \text{(II-7)}$$

where a,b,c are functions of strain invariants.

It is clear that the characterization of material behavior based on a single type of test cannot be expected to completely represent nonlinear elasticity. Even if it were possible, the analysis could not simulate elastic-plastic behavior in which the plastic strain increments are normal to the stress increments in loading. It is necessary therefore that elastic-plastic behavior of rock be modeled using the theory of elastic-plastic continua.

A general theory of elastic-plastic continua was presented by Green and Naghdi (1965). Stress-strain relationships in plasticity and thermo-plasticity have been reviewed, among others by Drucker (1950), Naghdi (1960), Koiter (1953) and Hill (1950). In general, theoretical concepts have been based on generalization of material behavior in a one-dimensional test.

The deformation theory of plasticity relates increments in components of the strain tensor to corresponding components of the stress deviation tensor. This theory

is unsound theoretically and fails to properly explain physical behavior of materials. It has been used to represent material behavior under proportional or almost proportional loading (Budiansky (1959), Havner (1969), Ilyushin (1945)). Hill (1950) has examined the shortcomings of the theory in his text. These will not be discussed here, and we shall confine our attention to the incremental or rate type theory of plasticity.

Using Prandtl's idealization, shown in Figure II-3, it is assumed that in one-dimensional loading:

1. There is a yield point σ_{yield} such that any loading beyond this level is accompanied by permanent deformation and any stress changes below σ_{yield} have linear reversible response independent of prior deformation history.

2. The yield point is a function of history of prior permanent deformation.

3. The stress-strain behavior is independent of sign of the stress.

In generalization to arbitrary stress states, it is customary to introduce a yield surface in the six-dimensional (three-dimensional for isotropic materials and nine-dimensional for non-symmetric stress tensor) stress space. Allowing for history of deformation and material properties, the yield condition is:

$$f(\sigma_{ij}, \epsilon''_{ij}, k_i) = 0 \qquad \text{(II-8)}$$

where ϵ''_{ij} are components of the plastic strain tensor (irreversible) and k_i are material parameters depending upon history. The mapping f in Eq. II-8 defines a functional on the linear vector space V spanned by σ_{ij}, ϵ''_{ij}, k_i, and orders the space

V such that 'loading' and 'unloading' can be defined analogous to the one-dimensional test where the set of stress states is an interval on the real line and is naturally ordered. Thus $f < 0$ will imply elastic states and plastic deformation is possible only for $f = 0$. We shall denote the interior of the surface defined by $f = 0$ as D. Thus $f(u) < 0$ for $u \in D$. Assuming only one material constant k, the time rate of f is

$$\dot{f} = \frac{\partial f}{\partial \sigma_{ij}} \dot{\sigma}_{ij} + \frac{\partial f}{\partial \epsilon''_{ij}} \dot{\epsilon}''_{ij} + \frac{\partial f}{\partial k} \dot{k} \qquad \text{(II-9)}$$

For $\dot{f} < 0$, $f + \dot{f}\,dt < f$. Hence the stress change associated with $\dot{f} < 0$ must lead to an elastic state in D. This constitutes unloading. Prandtl's assumption for unloading $\Rightarrow \dot{\epsilon}''_{ij} = 0$ and consequently $\dot{k} = 0$. Hence during unloading,

$$\dot{f} = \frac{\partial f}{\partial \sigma_{ij}} \dot{\sigma}_{ij} < 0 \qquad \text{(II-10)}$$

If the change in state is from one point on $f = 0$ to another on the surface, $\dot{f} = 0$. If $\dot{\epsilon}''_{ij} = \dot{k} = 0$, i.e. the change is not accompanied by any plastic strain, then

$$\dot{f} = \frac{\partial f}{\partial \sigma_{ij}} \dot{\sigma}_{ij} = 0 \qquad \text{(II-11)}$$

i.e. the stress path is tangential to the surface $f = 0$. This is termed neutral loading. When the stress change is accompanied by changes in ϵ''_{ij}, k,

$$\dot{f} = 0 \quad \text{and} \quad \frac{\partial f}{\partial \sigma_{ij}} \dot{\sigma}_{ij} > 0 \qquad \text{(II-12)}$$

This constitutes loading.

In order to obtain stress-strain relations in plasticity, Drucker (1950) used a thermodynamic postulate to obtain the normality rule

$$\dot{\epsilon}''_{ij} = \lambda \frac{\partial f}{\partial \sigma_{ij}} \tag{II-13}$$

where λ is a positive scalar which, for rate independence, must be homogeneous of order one in $\dot{\sigma}_{kl}$. For von Mises materials, Equation (II-13) reduces to the well-known Prandtl-Reuss relationships. To evaluate λ, Drucker defined equivalent stress σ_e and equivalent plastic strain rate $\dot{\epsilon}''_e$ as second invariants of the stress deviation tensor and of the plastic strain rate tensor respectively. These invariants are proportional to the L_2 norm on the linear vector spaces spanned respectively by the components s_{ij} of the stress deviation tensor and the components $\dot{\epsilon}''_{ij}$ of the plastic strain rate tensor. Thus

$$\sigma_e = (\tfrac{1}{2} s_{ij} s_{ij})^{\frac{1}{2}} \tag{II-14}$$

$$\dot{\epsilon}''_e = (\tfrac{1}{2} \dot{\epsilon}''_{ij} \dot{\epsilon}''_{ij})^{\frac{1}{2}} \tag{II-15}$$

where the components of the stress deviation tensor are related to the stress tensor by the relationship

$$s_{ij} = \sigma_{ij} - \delta_{ij} \frac{\sigma_{kk}}{3} \tag{II-16}$$

Then

$$\lambda^2 = \frac{\frac{1}{2} \dot{\epsilon}''_{ij} \dot{\epsilon}''_{ij}}{\frac{1}{2} \frac{\partial f}{\partial \sigma_{kl}} \frac{\partial f}{\partial \sigma_{kl}}} \tag{II-17}$$

or

$$\lambda = \frac{\dot{\epsilon}''_e}{\left(\frac{1}{2} \frac{\partial f}{\partial \sigma_{kl}} \frac{\partial f}{\partial \sigma_{kl}} \right)^{\frac{1}{2}}} \tag{II-18}$$

Writing $\frac{\dot{\sigma}_e}{\dot{\epsilon}''_e}$, the slope of the σ_e, ϵ''_e curve as H, we obtain upon substitution of Equation (II-18) in Equation (II-13),

$$\dot{\epsilon}''_{ij} = \frac{\frac{\partial f}{\partial \sigma_{ij}} \frac{\dot{\sigma}_e}{H}}{\left(\frac{1}{2} \frac{\partial f}{\partial \sigma_{kl}} \frac{\partial f}{\partial \sigma_{kl}}\right)^{\frac{1}{2}}} \qquad \text{(II-19)}$$

$$= \frac{1}{2H\sigma_e} \frac{\frac{\partial f}{\partial \sigma_{ij}} s_{mn} \dot{s}_{mn}}{\left(\frac{1}{2} \frac{\partial f}{\partial \sigma_{kl}} \frac{\partial f}{\partial \sigma_{kl}}\right)^{\frac{1}{2}}} \qquad \text{(II-20)}$$

This formulation was used in the so called tangent-modulus methods e.g. Swedlow and Yang (1965). Clearly this analysis satisfies the condition $f = 0$ and the normality rule but fails to satisfy $\dot{f} = 0$ in plastic deformation.

Hill (1950) used the normality rule assuming λ to be a fourth rank tensor linear in $\dot{\sigma}_{kl}$ and introduced a plastic potential. Using normality as well as the condition $\dot{f} = 0$, Prager (1949) obtained for $f = f(\sigma_{ij}, \epsilon''_{ij})$

$$\lambda = \frac{-\frac{\partial f}{\partial \sigma_{ij}} \dot{\sigma}_{ij}}{\frac{\partial f}{\partial \epsilon''_{mn}} \frac{\partial f}{\partial \sigma_{mn}}} \qquad \text{(II-21)}$$

Naghdi (1960) also obtained the above equation. This formulation breaks down for elastic perfectly plastic solids where f is independent of ϵ''_{mn}. Felippa (1966) obtained λ in terms of $\dot{\epsilon}_{ij}$, the total strain increment as follows.

The incremental stress is related to the incremental elastic strain by the equation

$$\dot{\sigma}_{ij} = E_{ijkl} \dot{\epsilon}'_{kl} \qquad \text{(II-22)}$$

where $\dot{\epsilon}'_{kl}$ are components of the elastic strain rate tensor and E_{ijkl} is the fourth rank isothermal elasticity tensor satisfying the symmetry properties

$$E_{ijkl} = E_{jikl} = E_{ijlk} = E_{klij} \qquad \text{(II-23)}$$

Writing $\dot{\epsilon}'_{kl} = \dot{\epsilon}_{kl} - \dot{\epsilon}''_{kl}$ and using normality rule, (II-24)

$$\dot{\sigma}_{ij} = E_{ijkl}\ \dot{\epsilon}_{kl} - E_{ijkl}\ \lambda\ \frac{\partial f}{\partial \sigma_{kl}} \tag{II-25}$$

Also $\dot{f}(\sigma_{ij}, \epsilon''_{ij}) = 0$ implies

$$\frac{\partial f}{\partial \sigma_{ij}}\ \dot{\sigma}_{ij} + \frac{\partial f}{\partial \epsilon''_{ij}}\ \dot{\epsilon}''_{ij} = 0 \tag{II-26}$$

Using normality rule, Equation (II-26) gives

$$\frac{\partial f}{\partial \sigma_{ij}}\ \dot{\sigma}_{ij} + \frac{\partial f}{\partial \epsilon''_{ij}}\ \lambda\ \frac{\partial f}{\partial \sigma_{ij}} = 0 \tag{II-27}$$

Substituting Equation (II-25) in Equation (II-27),

$$\frac{\partial f}{\partial \sigma_{ij}}\ E_{ijkl}\ \dot{\epsilon}_{kl} = \left[-\frac{\partial f}{\partial \epsilon''_{ij}}\ \frac{\partial f}{\partial \sigma_{ij}} + \frac{\partial f}{\partial \sigma_{ij}}\ E_{ijkl}\ \frac{\partial f}{\partial \sigma_{kl}} \right] \lambda \tag{II-28}$$

Hence

$$\lambda = \frac{\dfrac{\partial f}{\partial \sigma_{ij}}\ E_{ijkl}\ \dot{\epsilon}_{kl}}{B} \tag{II-29}$$

where

$$B = -\frac{\partial f}{\partial \epsilon''_{ij}}\ \frac{\partial f}{\partial \sigma_{ij}} + \frac{\partial f}{\partial \sigma_{ij}}\ E_{ijkl}\ \frac{\partial f}{\partial \sigma_{kl}} \tag{II-30}$$

Substituting Equation (II-29) in Equation (II-25)

$$\dot{\sigma}_{ij} = E_{ijkl} \left[\dot{\epsilon}_{kl} - \lambda\ \frac{\partial f}{\partial \sigma_{kl}} \right]$$

$$= E_{ijkl} \left[\delta_{km}\ \delta_{ln} - L_{klmn} \right]\ \dot{\epsilon}_{mn} \tag{II-31}$$

where

$$L_{klmn} = \left[-\frac{\partial f}{\partial \epsilon''_{ij}} \frac{\partial f}{\partial \sigma_{ij}} + \frac{\partial f}{\partial \sigma_{ij}} E_{ijpq} \frac{\partial f}{\partial \sigma_{pq}} \right]^{-1} \frac{\partial f}{\partial \sigma_{rs}} E_{rskl} \frac{\partial f}{\partial \sigma_{mn}}$$

(II-32)

This formulation relates the total stress increment to the total strain increment and is valid for all cases including perfect plasticity. For work-hardening plasticity, it can be shown to be identical to the Prager-Naghdi formulation of Equation (II-21).

Using rate of work equations, it is possible to evaluate λ in terms of stress rates for von Mises or generalized Mohr-Coulomb materials. Yamada (1968) used shear deformation energy rate to set up incremental stress-strain relationships for von Mises materials. Assuming ϵ''_{ij} to occur in f as the second invariant only, a tangent modulus approach was introduced. Reyes (1965) developed the incremental stress-strain relations for generalized Mohr-Coulomb materials using the total energy rate. The general forms of these equations can be shown to be specializations of the more general formulation developed by Felippa.

The stress-strain relations expressed by Equations (II-22) and (II-31) for the elastic and elastic-plastic deformation respectively have to be specialized for any kinematic constraints that may exist in the case of plane strain, for example

$$\dot{\epsilon}_{i3} = 0; \quad i = 1,2,3 \tag{II-33}$$

Thus in the elastic domain, if E_{ijkl} is invertible such that

$$C_{ijkl} = (E_{ijkl})^{-1} \tag{II-34}$$

the kinematic constraint is expressed by a linear relationship between components

of incremental stress tensor,

$$\dot{\epsilon}_{i3} = C_{i3kl}\,\dot{\sigma}_{kl} = 0 \tag{II-35}$$

For the elastic-plastic deformation, writing

$$\overline{C}_{ijkl} = \left[E_{ijkl}\,(\delta_{km}\,\delta_{ln} - L_{klmn})\right]^{-1} \tag{II-36}$$

the kinematic constraint is

$$\dot{\epsilon}_{i3} = \overline{C}_{i3kl}\,\dot{\sigma}_{kl} = 0 \tag{II-37}$$

It is important to note that $\overline{C}_{ijkl}$ depends upon σ_{ij} and ϵ''_{ij}. Consequently the relationship expressed by Equation (II-37) is nonlinear and involves σ_{ij}, ϵ''_{ij} as well as $\dot{\sigma}_{kl}$. For a perfectly plastic solid, $\overline{C}_{i3kl}$ is a function of stress and elastic properties. For a von Mises solid the problem was studied by Hill (1950). Figure II-7 shows a plane strain loading and unloading cycle for $\sigma_{11} = \sigma_{22}$, $\tau_{12} = 0$. Path OA represents elastic loading to yield at A. Continued loading requires the stress path to follow AD, the trace of the loading surface on the σ_{11}, σ_{33} plane. Loading from A to D is accompanied by development of plastic strains ϵ''_{11}, ϵ''_{22} and a residual stress σ_{33}. Upon elastic unloading from D to E, the path is parallel to OA. The intercept OE represents the residual stress σ_{33}. This stress remains in the material upon removal of the two-dimensional load. Accompanying this residual stress are elastic as well as plastic strains satisfying the kinematic constraints. The above theory was used to develop mathematical model representative of plane strain elastic-plastic behavior of Mohr-Coulomb rock. The details are contained in Chapter IV of this report.

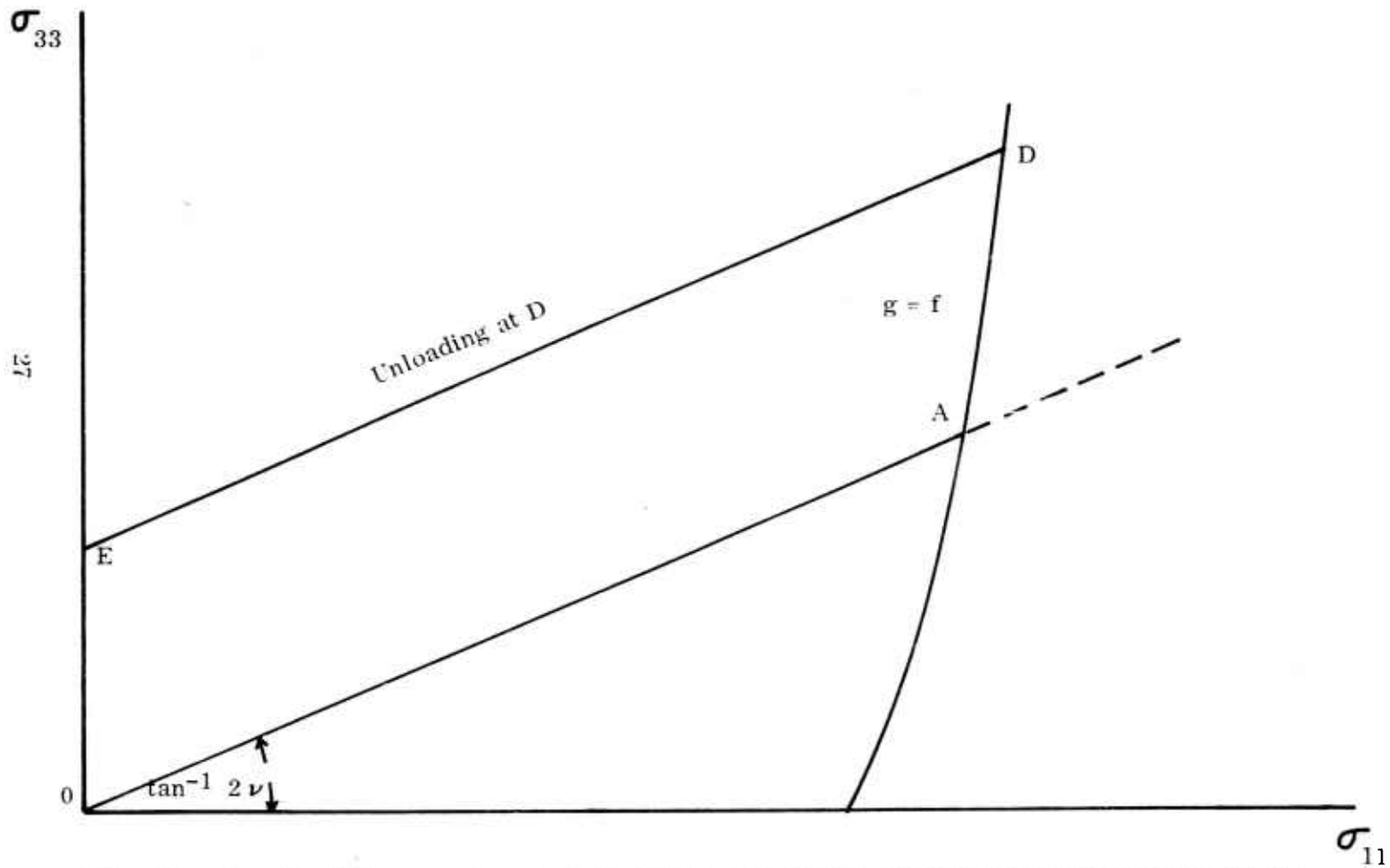

FIG. II-7. Residual Stresses Associated with Elastic-Plastic Deformation Under Plane Strain

2.3. Mechanical Behavior of Brittle Rock

Stress-strain behavior of rock under polyaxial compression has received considerable attention (Brace (1964), Cook (1965), Bieniawski (1967), Brady (1970)). In a one-dimensional test the stress-strain curve can be divided into four regions. Figure II-4 taken from Brady (1970) shows the different regions. These are characterized by the following:

i. Closure of initial flaws under compression

ii. Microcrack initiation

iii. Stable fracture propagation

iv. Unstable crack propagation leading to rupture

In compression, closure of precxisting microcracks is essentially completed over a small increment of stress. A nonlinear stress-strain relation has been observed for this zone, showing the high deformability due to open cracks decreasing as the cracks close. Friction is developed when surfaces of the initial flaws contact each other, resulting in an increase in the observed modulus of elasticity.

When the applied stress is increased further, the mechanical behavior as seen from the stress-strain curve is essentially linear elastic, and the modulus of elasticity is constant. However, some sliding across the faces of closed cracks may occur. Walsh (1965) demonstrated that the loading-unloading process at this stage shows hysteresis in the stress-strain curve (Figure II-8). Some of the frictional strength contributed by the roughness on the crack surfaces is overcome by sliding, and upon

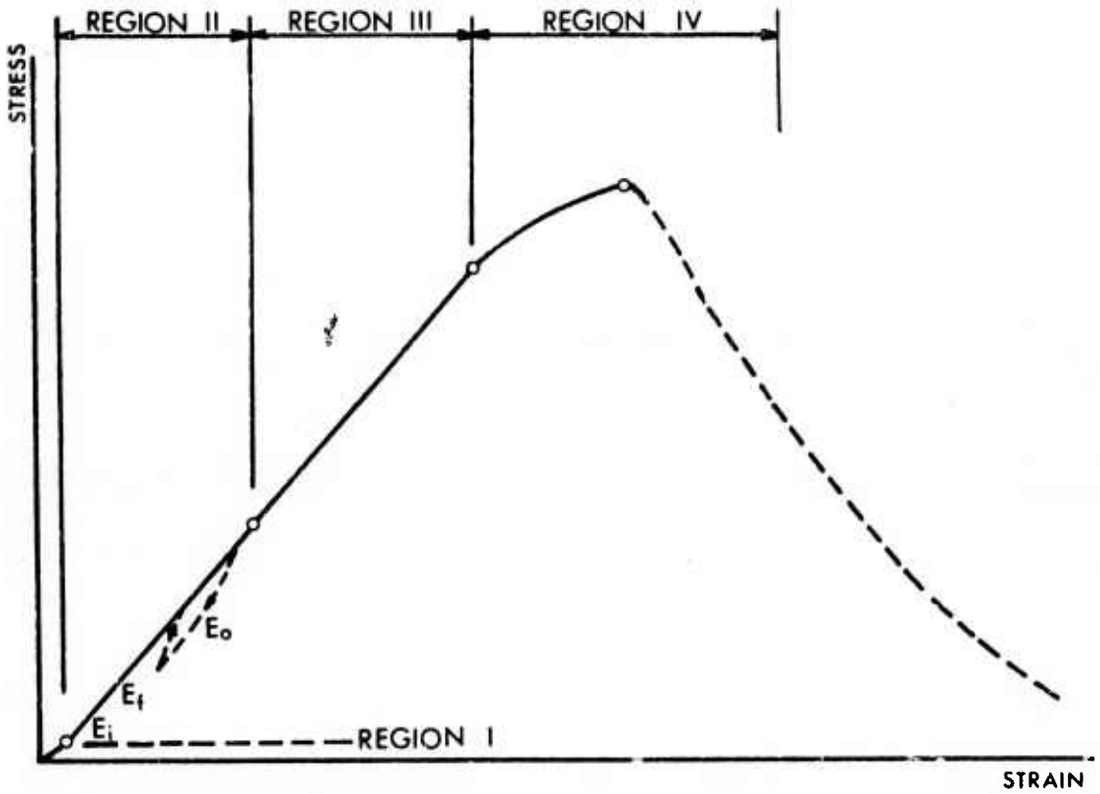

FIG. II-8. Typical Stress-Strain Curve for a Rock Specimen Under Multiple-Axial Loading (Walsh, 1965a)

unloading, the crack does not move back to the original position immediately. Thus, even in the linear elastic region II, rocks may exhibit irreversibility as well as hysteresis (Figure II-1).

Sliding along each initial crack produces new cracks at the ends of the initial crack. Tests on quartzite led Bieniawski (1967) to conclude that the relative displacement of crack surfaces is the primary factor which influences fracture initiation. In region III, the microcracks propagate with increasing stress level. Stable fracture propagation is a function of stress only and the process is quasi-static. Initiation and propagation of cracks is reflected in the departure from linearity of the stress-strain curve (Brace, (1966)). Crack growth starts right after the initiation of new surfaces. Tests in glass and rock (Hoek and Bieniawski, (1965)) have shown that stable fracture propagation follows a curved path leading to a direction parallel to the major compressive stress, and the length of propagation is related to the ratio of major principal stress to minor principal stress and related to the initial crack as well (Paul, et. al. (1967)). Pattern of crack array can also influence the fracture propagation.

Before the applied stress reaches its peak, some abrupt changes on propagation behavior would happen. Although the stress is still increasing, the slope of the stress-strain curve is decreasing. As soon as slope reaches its stationary position, it drops down rapidly and rupture begins. In terms of Irwin's concept (1958), the rate of strain energy released at this stage is equal to a critical value, G_c, which marks a state of instability.

Compression tests have revealed (Bieniawski (1967)) that the major type of unstable fracture propagation is still following the direction of major principal stress. It has been commonly observed by researchers (Bieniawski, et.al. (1969), Brady (1970)) that the unstable fracturing process is greatly affected by the type of loading, rate of loading and type of machine used in the testing.

Mechanical properties of rock containing flaws or cracks are somewhat different from those of intact rock. From a statistical point of view, flaws or cracks in the rock can be assumed to be randomly distributed and oriented. Therefore, no definite expression of the material properties can be obtained unless the distribution function of flaws is known. In a series of papers Walsh (1965-a, b, c) derived mathematical formulas for effective compressibility, modulus of elasticity and Poisson's ratio as functions of mean crack length and mean unit volume which contains the mean crack length. Those mathematical expressions were shown to be qualitatively justified by a limited number of experiments. In general, it was found that compressibility decreased as the cracks closed under pressure and remained almost constant with further change in pressure. Brace (1965) reported that linear compressibility is a function of applied pressure and is related quantitatively to porosity, grain size and dimensional orientation. If the elastic modulus is defined as the tangent to the stress-strain curve, the initial tangent in region I (Figure II-4) represents Young's modulus of a rock with initial open cracks (E_i); the constant slope in regions II and III represents the modulus for rock with closed crack (E_f); and the initial tangent to the un-

loading curve in regions II and III represents the intrinsic modulus of an intact rock (E_o) (Walsh (1965-b)). The magnitudes of these quantities can be ordered as

$$E_i < E_f < E_o$$

Walsh (1965) observed that the Poisson's ratio of a rock having open cracks is slightly lower than that of a solid rock. The value of Poisson's ratio ranges from zero to 0.5 as E_i changes from zero to the value of E_o, and ν_f is greater than ν_o but within the limit of 0.5.

For study of crack initiation and propagation in tensile stress fields, Griffith (1920, 1924) proposed a theory postulating the propagation of elliptical cracks as an instability phenomenon. A crack was expected to extend if the energy released in propagation exceeded the surface energy of the additional surface created by the extended crack. Initial flaws exist randomly in a solid body and have random orientation. Fracture propagation can occur at the extremities of these flaws. The theory is briefly outlined in Appendix A to this report. For nonuniform multi-axial stress fields, a crack may propagate until it stabilizes on reaching a region of low stress. Also for finite systems, this effect of stress redistribution associated with crack propagation may be significant in relation to the extension of other microcracks in the system.

Crack propagation can also occur at the ends of closed cracks in compressive stress fields. McClintock and Walsh (1962) developed the modified Griffith theory applicable to these situations. This theory is also discussed in Appendix A.

Extensive surveys (Hoek and Bieniawski (1965)) of published experimental data have shown the Griffith and modified Griffith theories to be satisfactory criteria for fracture initiation. Tests by Brace (1963) and Lajtai (1971) confirmed that in compressive stress fields, cracks started at the ends of closed joints, in the direction normal to the maximum tensile stress and then became parallel to the direction of the major compressive stress applied to the specimen. At this stage, the crack stabilized and additional compression was needed for further growth. Brace (1963) observed cracks propagating at stress levels much lower than required to extend a single crack. Experimental evidence (Hahn (1972)) exists to show that the energy absorption associated with fracture may be one or two orders of magnitude higher than the energy of surfaces created. Moreover, the experimental results show considerable scatter. Thus energy balance does not appear to be a useful means to examine crack propagation in rock.

Irwin (1956) proposed the use of stress intensity factor to predict crack propagation. Stresses or displacements could be used to obtain the value of the stress intensity factor and propagation would occur if the value equaled or exceeded a critical value characteristic of the material. Compliance or energy balance methods have also been used. The finite element method has been used to evaluate the stress intensity factor for complex geometries and loadings. However, this approach is unsatisfactory inasmuch as the extent of propagation and stress redistribution associated with such propagation cannot be directly evaluated. Also, the crack geometry

has to be known before hand. It is not possible to study initiation of fractures at microcracks or Griffith flaws arbitrarily oriented and located in the material.

In the current research program, the Griffith and modified Griffith theory were used to predict microcrack initiation and propagation. Post-fracture behavior across a crack was simulated on the assumption that an open crack cannot transmit tensile and shear stresses. In the finite element idealization, an element was presumed to have flaws in all directions such that fracture was entirely dependent upon the stress field. Also, for small elements it is reasonable to assume that if an element cracks, the fracture extends throughout the element at a constant orientation. With this modeling, the exact location of the crack within an element is unimportant.

CHAPTER III. THE FINITE ELEMENT METHOD

3.1. Basic Concepts in Direct Method of Solution

A boundary value problem can be stated in the form

$$Au = f \text{ on } F \tag{III-1}$$

where u is the unknown function to be determined, A is an operator, and f is the "forcing" function. F is the domain of interest and may be an open, connected, bounded spatial region embedded in R^3 or in a cartesian product $R^3 \times [0, \infty)$ where $[0, \infty)$ is the non-negative time interval. In addition to the field equation (III-1), there will be some conditions to be satisfied on boundary $\mathcal{S}$ of F. For A linear positive, it can be shown that Equation (III-1) has a unique solution. Necessarily, any approximate solution will in general not coincide with the unique solution of Equation (III-1) and consequently no approximate solution is expected to satisfy the field equation as well as the boundary conditions completely.

Solutions to engineering problems as well as the forcing functions are, in general, bounded and therefore belong to L_2, the space of square integrable functions. L_2 is a Hilbert space. However, u may be contained in a subset D of L_2 such that A is defined on D. We assume that D is dense in L_2. If the set of functions $\{\phi_k, k=1,2,\ldots,\infty\}$ is a basis in D, then any function $u \in L_2$ can be expressed as an infinite sum:

$$u = \sum_{k=1}^{\infty} a_k \phi_k \tag{III-2}$$

A scheme to generate approximate solutions is to use a finite set of terms in the

infinite sum above. Thus, we use

$$\bar{u} = \sum_{k=1}^{N} a_k \phi_k \qquad \text{(III-3)}$$

as an approximation. The approximation process then consists of appropriate choice of N, ϕ_k and the coefficients a_k. Several alternative procedures are available. The finite element method is a special process of selection of finite subset of the basis $\{\phi_k\}$. The coefficients a_k are evaluated by requiring the approximate solution to satisfy the field equations. Often a more systematic approach is to use a variational formulation and obtain a_k by requiring the approximate solution (Eq. III-3) to satisfy the variational principle. Ritz' method, Galerkin's method, least squares method, all belong to this category.

The finite element method is well documented in literature (Zienkiewicz (1972), Bell and Holand (1969), WPAFB Conferences (1965,1968,1971), Felippa (1966), Clough (1960,1965)). Its theoretical basis (Oden (1969), de Arantes e Oliveira (1968), Zlamal (1968), Melkes (1970), Aubin (1972)) and relationship to variational principles (Melosh (1963), Pian and Tong (1969)) have been examined. Essentially a finite element idealization partitions the spatial region F into a finite number of nontrivial discrete elements or subregions. The geometry of the elements is defined by a set of points in space called the nodal points of the system.

Over an element e, let an approximation to u be

$$u^e = \sum_{k=1}^{N^e} a_k^e \bar{\phi}_k^e \qquad \text{(III-4)}$$

or in matrix form

$$u^e = \{\bar{\phi}^e\}^T \{a^e\} \tag{III-5}$$

where $\{\bar{\phi}^e\}^T$ is a row vector consisting of $\bar{\phi}^e_k$ as its elements and $\{a^e\}$ is a column vector of coefficients a^e_k. Evaluating the function at nodal points

$$\{u^e_i\} = [\bar{\phi}^e_i]^T \{a^e\} \tag{III-6}$$

where $\{u^e_i\}$ is the vector of nodal point values of the function and $[\bar{\phi}^e_i]^T$ is the matrix of basc functions evaluated at eaeh nodal point. Rows and columns of $[\bar{\phi}^e_i]^T$ are linearly independent. If square, the matrix is invertible. If the number of nodal points is not equal to the number of independent base funetions, a least squares procedure ean be used for inversion. Hence, we can write

$$\{a^e\} = [[\bar{\phi}^e]^T]^{-1} \{u^c_i\} \tag{III-7}$$
$$= [A]^{-1} \{u^e_i\}$$

where $A = [\bar{\phi}^c_i]^T$

Substituting Equation (III-7) in Equation (III-5)

$$u^e = \{\bar{\phi}^c\}^T [A]^{-1} \{u^e_i\} \tag{III-8}$$
$$= \{\phi^e\}^T \{u^e_i\}$$

where $\{\phi^e\}$ ean now be regarded as a set of interpolating funetions relating nodal point values of a function to the value at an arbitrary point within the element e.

3.2. Variational Methods in Continuum Mechanics

3.2.1. Underlying Philosophy

Let A be an operator such that

$$A : V \longrightarrow V^* \tag{III-9}$$

where V, V* are linear vector spaces over a field F or a finite connected subset thereof. For $u \in V$, we introduce the operator equation

$$Au = f \; . \; \ni \; . \; f \in V^* \tag{III-10}$$

Let B be a bilinear map on V*

$$B : V^* \times V^* \longrightarrow S \tag{III-11}$$

where S is a linear vector space. To each ordered pair of vectors $u, v \in V^*$, B assigns a point $B(u, v) \in S$, such that

$$\begin{aligned} B(\alpha u_1 + u_2, v) &= \alpha B(u_1, v) + B(u_2, v) \\ B(u, \alpha v_1 + v_2) &= \alpha B(u, v_1) + B(u, v_2) \end{aligned} \tag{III-12}$$

For simplicity, in the sequel we shall use the notation $< u, v >$ as equivalent to $B(u, v)$.

In order to set up variational principles corresponding to the field problem expressed by Eq. (III-10), we introduce a pair $\{\Omega, \Delta\}$. The first element, Ω, defined through a bilinear map B on V*, is a function of the quantities appearing in Eq. (III-10), and for given A and f can be regarded as a function of u. The other element of the pair, Δ, is a variation operator defined on the range of Ω in S. By appropriate selection of B, Ω, Δ, different variational formulations of a problem are realized. In the context of obtaining an approximate solution to Eq. (III-10), if B is continuous and V, S are

metric spaces, the distance of an approximation u_o from the correct solution u is intuitively related to the distance between their respective images under Ω, thus providing a basis for study of convergence of sequences of approximate solutions.

Many variational formulations use R, the space of real numbers, as the range of B. For this case, two alternative approaches are used. One defines Δ so that

$$\Delta\Omega > 0 \tag{III-13}$$

whenever (III-10) is satisfied. This yields a class of 'minimum' principles. Another, somewhat more versatile approach applicable to bilinear maps in general is to define Δ so that

$$\Delta\Omega = 0 \tag{III-14}$$

is equivalent to Eq. (III-10). An interesting feature of this second alternative is that if Ω, Δ are defined such that

$$\Delta\Omega(u) = Au - f \tag{III-15}$$

Eq. (III-14) is directly equivalent to Eq. (III-10). Thus Δ can be viewed as a gradient operator or derivative. In literature, this has been identified with the Gateaux derivative, the Frechet derivative or the variation operator used by Gurtin. The Gateaux derivative of Ω, denoted by $G_{\bar{u}}\ \Omega(u)$, is defined such that

$$< G_{\bar{u}}\ \Omega(u), \bar{u} > = \lim_{a \to o} \frac{\Omega(u + a\bar{u}) - \Omega(u)}{a} \tag{III-16}$$

Here $< , >$ indicates the bilinear map appropriate to the problem and $\bar{u} \in V^*$ is the 'path' or the 'direction' of the derivative such that $u + a\bar{u} \in V$; a is a scalar. We note

here that for the notion of a limit, we require a suitable topology is S and continuity of Ω. These analytical aspects are not discussed in this report. It is assumed that such conditions where necessary are satisfied. The right hand side of Eq. (III-16), denoted $V\,\Omega(u, \bar{u})$, is the Gateaux differential of Ω at u in the direction $\bar{u}$; assumed to be linear in $\bar{u}$ to establish $G_{\bar{u}}\,\Omega(u)$. Following Vainberg (1964), we write a linear Gateaux differential as $D\,\Omega(u,\bar{u})$. To ensure a norm, S has traditionally been identified with R, the set of real numbers, although clearly, this is not necessary.

If V* and S are normed, the Frechet derivative, denoted by $F_{\bar{u}}\,\Omega(u)$ is defined such that

$$|< F_{\bar{u}}\,\Omega(u), \bar{u} >| \leq \lim_{|\bar{u}| \to 0} |\Omega(u+\bar{u}) - \Omega(u)| \qquad \text{(III-17)}$$

where $|\ \ |$ denotes a norm. Gurtin (1963, 1964) regards $\Omega(u+\alpha\bar{u})$ as a function of α, a scalar. Then,

$$\Delta_{\bar{u}}\,\Omega(u) = \frac{d}{d\alpha}\,\Omega(u+\alpha\bar{u})\Big|_{\alpha\ 0} \qquad \text{(III-18)}$$

provided the derivative exists. $\Delta_{\bar{u}}\,\Omega(u)$ is expected to be of the form

$$\Delta_{\bar{u}}\,\Omega(u) \quad < Au - f, \bar{u} > \qquad \text{(III-19)}$$

such that vanishing of the variation for arbitrary $\bar{u} \in V^*$ is equivalent to Eq. (III-10). Indeed $\Delta_{\bar{u}}\,\Omega(u)$ can be shown to be identical to the linear Gateaux differential. For Eq. (III-10) to be equivalent to Eq. (III-19), in conjunction with Eq. (III-14), the bilinear map must have the property[1]

[1] We do not use special notations to distinguish between zero elements of V, V*, S. The nature of the zero is apparent from the context in which it is used.

$$< u, o > \quad 0 = < o, v > \; ; \forall\, u, v \in V^* \tag{III-20}$$

$$< u, v > \quad 0 \Rightarrow u = 0 \text{ or } v = 0 \tag{III-21}$$

A class of variational principles dircetly uses Eq. (III-20) along with its converse, i.e., if $< u, v > = 0 \; \forall \; v \in V^*, u = 0$. Thus if we define Ω as a bilinear map on V* x V* sueh that

$$\Omega(u,v) = < Au - f, v > \tag{III-22}$$

$\Omega(u, v) = 0 \; \forall \; v \in V^*$ direetly implies Eq. (III-10). This approach, for operators with suitable symmetry properties, leads to prineipal of 'virtual work' type. In this formulation, based on the orthogonality of zero with the linear veetor spaee V*, the variation operator plays no part and may be taken to be the identity operator. For obtaining approximate solutions to Eq. (III-10), Eq. (III-20) ean be used as a starting point for several well-known procedures. For example, if $v = Au - f$, defining $\Omega(v) = |< v, v >|$ leads to a generalization of the least squares method.

3.2.2. A Formulation for Linear Operators

Consider, eorresponding to the field problem expressed by Eq. (III-10),

$$\Omega(u) = < u, Au > - 2 < u, f > \tag{III-23}$$

where $< , >$ denotes a bilinear map satisfying Eqs. (III-12, III-20, III-21). Using the variation operator of Eq. (III-18), we obtain for linear A,

$$\Delta_{\bar{u}} \Omega(u) = < u, A\bar{u} > + < \bar{u}, Au > - 2 < \bar{u}, f > \tag{III-24}$$

If A is symmetric, i.e.,

$$< u, Av > = < v, Au > \; ; u, v \in V \tag{III-25}$$

then

$$\Delta_{\bar{u}} \Omega(u) = < Au, \bar{u} > + < \bar{u}, Au > - 2 < \bar{u}, f > \tag{III-26}$$

If, further, the bilinear map is symmetric,[#] i.e.,

$$< u,v > = < v,u > \; ; \; u, v \in V^* \tag{III-27}$$

it follows that

$$\Delta_{\bar{u}} \, \Omega(u) = 2 < \bar{u}, \, Au - f > \tag{III-28}$$

Eq. (III-28) seen with Eqs. (III-20) and (III-21) implies

$$\Delta_{\bar{u}} \, \Omega(u) = 0 \text{ for arbitrary } \bar{u} \in V^* \tag{III-29}$$

if and only if Eq. (III-10) is satisfied.

We recognize $\Delta_{\bar{u}} \, \Omega(u)$ as the generalized Gateaux differential such that Eq. (III-28) implies

$$G_{\bar{u}} \, \Omega(u) = 2(Au - f) \tag{III-30}$$

Clearly $G_{\bar{u}} \, \Omega(u)$ vanishes if and only if Eq. (III-10) is satisfied.

The foregoing discussion shows that for linear bounded symmetric operator A, solution of equation $Au = f$ is equivalent to vanishing of variation of $\Omega(u)$ where in the pair $\{\Omega, \Delta\}$, $\Omega = < u, Au > - 2 < u, f >$, and Δ is the variation operator defined by Eq. (III-18) or, alternatively, is the Gateaux derivative. The bilinear map $< \, , \, >$ satisfied Eqs. (III-12), (III-20), (III-21) and (III-27).

If the symmetric bilinear map has its range in R, and in addition to Eqs. (III-12), (III-20), and (III-27) satisfies

$$< u, u > \; \geq 0, \; \forall \; u \neq 0 \tag{III-31}$$

the bilinear map defines an inner product. In this case, for A positive, i.e.

$$< u, Au > \; \geq 0, \qquad u \neq 0 \tag{III-32}$$

[#]Magri (1972) has shown that for every linear operator, A, there exists a bilinear form B such that A is symmetric in the sense of B.

using the pair $\{\Omega, \Delta\}$ where $\Omega(u)$ is defined by Eq. (III-23) and Δ is defined as

$$\Delta_{\bar{u}} \Omega(u) = \Omega(u + \bar{u}) - \Omega(u) \tag{III-33}$$

minimum principles can be developed for positive or positive definite operators. A comprehensive exposition has been presented by Mikhlin (1965) for this case.

Traditionally, variational principles have been based on an inner product, which is a bilinear functional satisfying Eq. (III-31) but not Eq. (III-21). The motivation has been to use positive property (Eq. (III-32)) of the operator to establish uniqueness of the solution. Also the functionals have their range in R, the set of reals, a Hilbert space. However, other bilinear maps are available.

The above discussion for a single field variable u is easily extended to the case of several dependent field variables. If there are n variables, V is defined as the direct sum space $V_1 \oplus V_2 \oplus \ldots \oplus V_n$ and an element $u \in V$ is an n-tuple $(u_1, u_2, \ldots, u_n)$ with $u_i \in V_i$ for $i = 1, 2, \ldots, n$. A bilinear map on V is now defined as

$$< u, v > = < u_1, v_1 >_1 + < u_2, v_2 >_2 + \ldots + < u_n, v_n >_n \tag{III-34}$$

(no sum on n)

where $< , >_r$ is a bilinear map from $V_r^* \times V_r^* \longrightarrow S$. Symmetry of each of $< , >_r$ implies symmetry of $< u, v >$. The operator A is defined as a two-dimensional array of linear operators with n x n elements such that an element A_{ij} maps a set $M_{ij} \subseteq V_j$ into V_i. Corresponding to Eq. (III-25), we define symmetry of A as

$$< u_i , A_{ij} u_j >_i = < u_j, A_{ji} u_i >_j \quad \text{(no sums)} \tag{III-35}$$

For diagonal elements of the array, Eq. (III-35) is identical to Eq. (III-25). The operator equation (III-10) is now a set of linear equations for the problem

$$A_{ij}\, u_j = f_i \quad , \qquad i,j = 1,2,\ldots,n \tag{III-36}$$

Equation (III-23) will then define $\Omega(u)$ and we shall require each of the variations

$$\Delta_{\bar{u}_i}\, \Omega(u) = 2 < \bar{u}_i,\ A_{ij}\, u_j - f_i > \tag{III-37}$$

for $\bar{u}_i \in V_i$; $i = 1,2,\ldots,n$ to vanish. Examples of this type of formulation have been presented by Sandhu and Pister (1970, 1971). Often problems which are not in linear symmetric form can be manipulated to write them in the form of Eq. (III-36) with A_{ij} satisfying Eq. (III-35). Symmetry of the operator matrix leads to extended variational principles such that the unique intersection of the sets of solutions associated with these alternative formulations is the problem solution. Generalizations to include nonlinear operators on the diagonal of the operator matrix arise as natural extensions. These aspects of the problem have been discussed in detail by Sandhu and Pister (1971) who also presented a general discussion of variational principles in continuum mechanics (1972).

3.2.3. The Elastostatics Problem

The variational formulation of problems in elasticity has been discussed by Washizu (1968) and by Sandhu and Pister (1971). Herein we only present generalized potential energy formulation in which the variation of the functional

$$\Omega = \int_F (2U - u_i\, \sigma_{ij,j} - 2\, \epsilon_{ij}\, \sigma_{ij} + u_{i,j}\, \sigma_{ij} - 2\, u_i\, f_i)\ dF$$
$$+ \int_{S_1} u_i\, (\sigma_{ij}\, n_j - 2\, \hat{t}_i)\ ds - \int_{S_2} (u_i - 2\, \hat{u}_i)\, \sigma_{ij}\, n_j\ ds \tag{III-38}$$

vanishes at the correct solution to the field equations

$$\sigma_{ij,j} + f_i = 0 \tag{III-39}$$

$$\sigma_{ij} = \frac{\partial U}{\partial \epsilon_{ij}} \tag{III-40}$$

and

$$\epsilon_{ij} = u_{(i,j)} \tag{III-41}$$

subject to the boundary conditions

$$\sigma_{ij}\, n_j = \hat{t}_i \quad \text{on } \mathcal{S}_1 \tag{III-42}$$

$$u_i = \hat{u}_i \quad \text{on } \mathcal{S}_2 \tag{III-43}$$

Here $\mathcal{S}_1, \mathcal{S}_2$ are complcmentary subsets of $\mathcal{S}$, the boundary of F. U is the strain energy function. σ_{ij}, ϵ_{ij} are respectively the components of the symmetric Cauchy stress tensor and the infinitesimal strain tensor. u_i, f_i arc the components of the displacement vector and the body force vector. n_j are direction cosines of the outward normal to $\mathcal{S}$.

Using the symmetry property of the field equations, and requiring u_i to identically satisfy the strain displacement equation as well as the boundary conditions on $\mathcal{S}_2$, Eq. (III-38) reduces to the potential energy functional

$$\Omega_1 = \int_F (U - u_i f_i)\, dF - \int_{\mathcal{S}_1} u_i \hat{t}_i\, ds \tag{III-44}$$

To allow for initial stresses, the Eq. (III-40) is written as

$$\sigma_{ij} = \frac{\partial U}{\partial \epsilon_{ij}} + \bar{\sigma}_{ij} \tag{III-45}$$

where $\bar{\sigma}_{ij}$ is the initial stress. Then the potential energy functional has the form

$$\Omega_2 = \int_F (U - u_i f_i + u_{i,j} \bar{\sigma}_{ij}) \, dF - \int_{S_1} u_i \hat{t}_i \, ds \qquad \text{(III-46)}$$

Equation (III-46) is the functional used in development of stiffness type finite element formulations.

In the analysis for progressive failure according to Griffith's theory, the above formulation was used assuming the system to be piecewise linear elastic -- changes in structural properties being introduced in a stepwise fashion as elements in the system develop cracks in a sequential manner.

3.2.4. Variational Formulation for Elastic-Plastic Solids

The field equations of incremental plasticity in symmetric form are

$$\begin{bmatrix} 0 & 0 & -\frac{1}{2}\left(\delta_{ik}\frac{\partial}{\partial j} + \delta_{jk}\frac{\partial}{\partial i}\right) \\ 0 & E_{ijkl} & -1 \\ \frac{1}{2}\left(\delta_{ki}\frac{\partial}{\partial l} + \delta_{li}\frac{\partial}{\partial k}\right) & -1 & 0 \end{bmatrix} \begin{Bmatrix} \dot{u}_i \\ \dot{\epsilon}_{kl} \\ \sigma_{ij} \end{Bmatrix} = \begin{Bmatrix} F_k \\ -\bar{\sigma}_{ij} \\ 0 \end{Bmatrix} \qquad \text{(III-47)}$$

Here E_{ijkl} are components of the symmetric tensor relating the components of the incremental stress tensor σ_{ij} to the components of the incremental strain tensor $\dot{\epsilon}_{ij}$. $\dot{u}_i$, F_k, $\bar{\sigma}_{ij}$ are respectively the components of the incremental displacement vector, the body force vector (including seepage forces if any), and the initial stress tensor

for the specific increment under consideration. Following Sandhu and Pister (1970, 1971) the governing functional is

$$J = \int_F \Big[\dot{\epsilon}_{ij} E_{ijkl} \dot{\epsilon}_{kl} - \dot{u}_i \sigma_{ij,j} - 2 \dot{u}_i F_i - \dot{\epsilon}_{ij} \sigma_{ij} + 2 \dot{\epsilon}_{ij} \bar{\sigma}_{ij} + \sigma_{ij} \dot{u}_{i,j} - \sigma_{ij} \dot{\epsilon}_{ij} \Big] dF + \int_{S_1} \dot{u}_i (\sigma_{ij} n_j - 2 \hat{t}_i) ds - \int_{S_2} (u_i - 2 u_i) \sigma_{ij} n_j ds \quad \text{(III-48)}$$

where we have included the boundary conditions (Eqs. III-42, III-43) in the formulation. Noting that

$$\int_F \dot{u}_i \sigma_{ij,j} dF = - \int_F \dot{u}_{i,j} \sigma_{ij} dF + \int_S \dot{u}_i \sigma_{ij} n_j ds \quad \text{(III-49)}$$

and defining $\dot{U}$ as $\frac{1}{2} \dot{\epsilon}_{ij} E_{ijkl} \dot{\epsilon}_{kl} = \dot{U} (\epsilon_{ij})$ (III-50)

J can be written as follows:

$$J_1 = \int_F \Big[2 \dot{U} - 2 \dot{u}_i F_i - \dot{\epsilon}_{ij} \sigma_{ij} + \dot{u}_{i,j} \sigma_{ij} + 2 \dot{\epsilon}_{ij} \bar{\sigma}_{ij} + \sigma_{ij} \dot{u}_{i,j} - \sigma_{ij} \dot{\epsilon}_{ij} \Big] dF - 2 \int_{S_1} \dot{u}_i (\hat{t}_i) ds - 2 \int_{S_2} (\dot{u}_i - \hat{\dot{u}}_i) \sigma_{ij} n_j ds \quad \text{(III-51)}$$

Requiring that the strain displacement relationship and the displacement boundary conditions be identically satisfied,

$$J_2 = \int_F (\dot{U} - \dot{u}_i F_i + \dot{u}_{i,j} \bar{\sigma}_{ij}) \, dF - \int_{S_1} \dot{u}_i \hat{t}_i \, ds \qquad \text{(III-52)}$$

which is of the same form as Ω_2 in Eq. (III-46) except for the displacement components u_i being replaced by the incremental displacement $\dot{u}_i$ and $\dot{U}$ replacing U. Explicitly, introducing the seepage force into the formulation,

$$F_i = \rho f_i + \pi_{,i} \qquad \text{(III-53)}$$

where π is the hydrostatic pore water pressure. Eq. (III-52) then becomes

$$J_3 = \int_F (\dot{U} - \dot{u}_i \rho f_i - \dot{u}_i \pi_{,i} + \dot{u}_{i,j} \bar{\sigma}_{ij}) \, dF - \int_{S_1} \dot{u}_i \hat{t}_i \, ds \qquad \text{(III-54)}$$

The above formulation would reduce to that given by Washizu (1968) if the equilibrium equation were to be written in the form

$$(\bar{\sigma}_{ij,j} + \dot{\sigma}_{ij,j}) + (\bar{F}_i + \dot{F}_i) = 0 \qquad \text{(III-55)}$$

with the boundary condition $t_i = \bar{t}_i + \dot{t}_i$ (III-56)

Then upon using symmetry and the specialization of displacements satisfying the boundary conditions and the strain displacement equation, the governing functional would have the form

$$J_4 = \int_F (\dot{U} - \dot{u}_i \dot{F}_i) \, dF - \int_{S_1} \dot{u}_i \hat{\dot{t}}_i \, ds \qquad \text{(III-57)}$$

The finite element procedure for elastic-plastic Mohr-Coulomb rock described in Chapter IV was based on the variational principle using the functional J_2.

3.3. Matrix Formulation of Field Equations

Following the proeedure indieated in seetion 3.1, a finite dimensional approximation to the problem solution is written using the values of the funetion at the nodal points of the system as the generalized coordinates. The spatial domain F is partitioned into a finite number of nontrivial disjoint elements sueh that their union approximates F. Eaeh point in F belongs to one distinet element. The ambiguity regarding points on interelement boundaries is resolved by ensuring that the funetion value will be the same regardless of whieh element the point is assigned to. This is the requirement of 'eompatibility' on finite element modelling. For a point within an element, the funetion value is expressed in terms of nodal point values (the generalized eoordinates) through a set of interpolating funetions. The approximate funetion is inserted in the governing funetional so that the funetional ean now be regarded as a funetion of the generalized eoordinates. Vanishing of variation of the funetional yields the matrix equations for evaluation of the generalized eoordinates and henee the approximate solution. We give below the formulation for ineremental analysis of elastie-plastie solids. The treatment for the elastie ease is similar.

The funetional J_3 in Equation (III-54) has ineraments of the displaeement veetor as the field variable. In an approximate solution, the ineremental displaeement field within the mth element is defined in terms of the nodal point values as

$$\overset{\cdot m}{u_i}(\underset{\sim}{x}) = \{\phi^m\}^T \{\dot{u}_i\} \qquad \text{(III-58)}$$

Here $\overset{\cdot m}{u_i}(\underset{\sim}{x})$ is the ith eomponent of the incremental displaeement vector at spatial

location defined by the vector $\underset{\sim}{x}$ in a global reference frame, $\{\phi^m\}$ is the set of displacement interpolation functions and $\{u_i\}$ is the set of the ith components of nodal point incremental displacements for the entire system.

The strain displacement relationship can be written as

$$\{\dot{e}^m(\underset{\sim}{x})\} = \left[\phi_e^m\right]^T \{\dot{u}\} \tag{III-59}$$

Here $\{e^m(\underset{\sim}{x})\}$ is the reduced strain tensor. For the two-dimensional case,

$$\{\dot{e}^m(\underset{\sim}{x})\} = \begin{Bmatrix} e_x \\ e_y \\ \gamma_{xy} \end{Bmatrix} \tag{III-60}$$

$\left[\phi_e^m\right]^T$ is the transformation matrix derived from the displacement interpolation functions $\{\phi^m\}$ by suitable differentiation and rearrangement of terms and $\{\dot{u}\}$ is the vector of nodal point incremental displacements for the system.

Writing the stress-strain relationship as matrix $[H^m]$ for the mth element and replacing integration over the spatial domain by sum of integrals over individual elements, the governing functional Eq. (III-54) becomes

$$J_3 = \{\dot{u}\}^T [K] \{\dot{u}\} + 2\{\dot{u}\}^T \{M_1\} - 2\{\dot{u}\}^T \{M_2\} - 2\{\dot{u}\}^T \{P\} \tag{III-61}$$

where

$$[K] = \sum_{m=1}^{M} \int_{v_m} \left[\phi_e^m\right][H^m]\left[\phi_e^m\right]^T dv_m \tag{III-62}$$

$$\{M_1\} = \sum_{m=1}^{M} \int_{v_m} \left[\phi_e^m\right] \{\bar{\sigma}^m\} dv_m \tag{III-63}$$

$$\{M_2\} = \sum_{m=1}^{M} \int_{v_m} [\phi^m] \{\rho f^m\} \, dv_m \qquad \text{(III-64)}$$

$$\{P\} = \sum_{m=1}^{M} \int_{S_1} [\phi^m] [\phi^m]^T \{\hat{t}^m\} \, ds_m \qquad \text{(III-65)}$$

Application of the variational principle to Equation (III-61) yields the matrix equation

$$[K] \{\dot{u}\} = \{\dot{R}\} \qquad \text{(III-66)}$$

where

$$\{\dot{R}\} = \{M_1\} - \{M_2\} + \{P\} \qquad \text{(III-67)}$$

$\{M_1\}$, $\{M_2\}$, $\{P\}$ respectively represent the contribution of the residual stresses, the body forces and the boundary loads. For incremental formulation, the residual stresses are the stresses at the beginning of the increment. Pore water pressures are included in the form of seepage force in the body force contribution.

For the elastic case, the function to be approximated is the displacement vector. Equations (III-66), (III-67) will apply with the difference that $\{\dot{u}\}$, $\{\dot{R}\}$ will be replaced by $\{u\}$, $\{R\}$ and $\{\bar{\sigma}_i\}$ will represent the initial stresses in the system.

The computer programs developed both for elastic-plastic rock and progressive failures following Griffith theory used a quadrilateral element made from four constant strain triangles. This element as well as other quadrilateral elements have been discussed by Wilson (1965) and Dougherty et. al. (1968).

3.4. Initial Stresses in Rock

The initial stresses present in rock in the 'insitu' state are the stresses corresponding to reference displacement field generally taken as zero. These are easily included in the stress-strain relationships by assuming that the total stress is the sum of the initial stresses and the stresses associated with the displacements. Thus

$$\dot{\sigma}_{ij} = E_{ijkl}\ \epsilon_{kl} + \bar{\sigma}_{ij} \qquad \text{(III-68)}$$

where $\dot{\sigma}_{ij}$, ϵ_{kl} are components of stress and strain increments and $\bar{\sigma}_{ij}$ are components of the initial stress. With this formulation, the initial stresses appear in the variational formulation and vector $\{M_1\}$ in Equation (III-61) represents a pseudo-load corresponding to the initial stresses. This technique is the basis of stress-relief methods used by various investigators. The analyses described in Chapters IV and V use this approach.

3.5. Incremental Procedures

In finite element analysis, allowance for incremental loading or incremental construction is quite straightforward. For any step of loading or construction (excavation), the initial state is used as a reference state and increments of stresses and displacements worked out for the particular step. Thus

$$[K]_n \{\Delta u\}_n = \{\Delta R\}_n \qquad \text{(III-69)}$$

where $[K]_n$, $\{\Delta u\}_n$, $\{\Delta R\}_n$, are respectively the system stiffness matrix, the incremental displacement vector and the incremental loading vector for the nth step of construction/excavation/loading. In cases where $[K]_n$ is dependent upon displacements or stresses, iterative procedures or Runge-Kutta methods can be used to im-

prove accuracy. In the research described in this report, essentially the method was 'initial stiffness' for each increment in the case of elastic-plastic analysis. For the case of progressive cracking, the influence of stress redistribution and stiffness change due to cracking was allowed for in an iterative process.

CHAPTER IV. FINITE ELEMENT PLANE STRAIN ANALYSIS OF ELASTIC-PLASTIC MOHR-COULOMB ROCK

4.1. Review of Previous Work

Attempts to use the finite element method for stress and deformation analysis of elastic-plastic materials may be classified on the basis of the modeling of mechanical behavior or the computational technique. Early attempts noticed the nonlinearity of deformation response to applied loads. The material was regarded as nonlinear elastic having stress or strain dependent elastic 'moduli'. In order to extend the results of the one-dimensional test to the six-dimensional stress-state, an equivalent stress to equivalent strain curve was adopted. Bilinear (Wilson 1963) or multilinear (Zienkiewicz 1967) approximations, Richard-Goldberg law (1965), Ramberg-Osgood law (1943), Kondner's hyperbolic equation (1963), cubic spline functions (Desai 1971) have been used to approximate test data by smooth or piecewise smooth curves for ease of data handling within the computer.

Swedlow and Yang (1965) used the normality rule and Drucker's (1952) method for evaluating the constant of proportionality in the Prandtl-Reuss equation. This was a tangent modulus approach. It did not satisfy the 'loading' condition $\dot{f} = 0$. Marcal (1968) and Marcal and King (1967) used similar formulation. Reyes (1966) and Reyes and Deere (1966) used a rate of work equation to develop stress-strain relations for Mohr-Coulomb materials under plane strain conditions. This was consistent with the incremental theory of plasticity. Felippa (1966) developed

equations for incremental theory of plasticity which include Reyes work as a specialization. Marcal and King (1967) and Zienkiewicz et al. (1969) use a formulation identical to Felippa's. Baker et al. (1969) used Reyes formulation in their work. Yamada (1968) used a rate of work in distortion to set up equations for von Mises materials. Isakson et al. (1967) developed the incremental stress-strain relationship for kinematic hardening using Ziegler's (1959) modification of Prager's rule (1955).

Numerical procedures for elastic-plastic analysis have been either the ineremental type using Euler or Runge-Kutta methods, or the initial tangent type using the initial stress or initial strain approach. In the first type the system stiffness matrix has to be developed at each increment whereas in the initial tangent method, the same stiffness is used throughout with the effect of nonlinearity being introduced as a corrective pseudo-load in conjunction with an iterative solution scheme. The initial strain approach was used by Argyris (1965), Gallagher (1962), Lansing et al. (1965) among others. Zienkiewicz (1969) used the initial stress approach. Baker et al. (1969) found the iterative procedure to be unsatisfactory as convergence was often very slow.

All the research workers mentioned above used triangular elements in their analysis. It is well-known that the triangular elements do not give correct stress field. In this report quadrilateral elements were used to get a good stress distribution. In the present research program the incremental approach reflected in the variational formulation of the problem was used. The formulation follows Felippa (1966) and Reyes (1966).

4.2. Stress-Strain Relations for Mohr-Coulomb Materials

The Mohr-Coulomb failure criterion for isotropic materials is

$$\tau_f = c + \sigma_n \tan\phi \qquad \text{(IV-1)}$$

where τ_f, σ_n are the failure shearing stress and the normal stress on the failure plane and c, ϕ are, respectively, the cohesion and the angle of internal friction for the material. Drucker and Prager (1952) proposed a generalization of the Mohr-Coulomb law to a cone, in the three-dimensional principal stress-space, symmetrical about the principal diagonal. The loading surface is defined as

$$f = \alpha J_1 + J_2^{\frac{1}{2}} - k = 0 \qquad \text{(IV-2)}$$

where J_1, J_2 are the first and the second invariants of the stress tensor, and α, k are material constants.

Using Drucker and Prager's generalization of the Mohr-Coulomb law, Reyes (1966) developed the stress-strain relationship for elastic perfectly-plastic solids under plane strain conditions. A rate of work equality was used. The same relationship can be obtained by directly using Equation (IV-2) in Felippa's general approach already discussed in Chapter II.

4.2.1. Stress-Strain Formulation for Elastic-Plastic Mohr-Coulomb Solids

Define a tensor with components q_{ij} such that

$$q_{ij} = \frac{\partial f}{\partial \sigma_{ij}} \qquad \text{(IV-3)}$$

For Drucker and Prager's generalization of Mohr-Coulomb yield surface

$f = \alpha J_1 + J_2^{\frac{1}{2}} = k$. This gives

$$q_{ij} = \alpha \delta_{ij} + \frac{s_{ij}}{J_2^{\frac{1}{2}}}$$

$$= \alpha \delta_{ij} + \frac{1}{J_2^{\frac{1}{2}}} \left(\sigma_{ij} - \frac{1}{3} J_1 \delta_{ij}\right) \qquad \text{(IV-4)}$$

where s_{ij} are components of the stress deviation tensor and δ_{ij} is Kronecker's delta.

Define a tensor with components p_{ij} such that

$$p_{ij} = \frac{\partial f}{\partial \epsilon''_{ij}} \qquad \text{(IV-5)}$$

For perfect plasticity, the yield surface is independent of the plastic strain and $p_{ij} = 0$.

Let q be a reduced representation for q_{ij} such that

$$q = < q_{11} \; q_{22} \; q_{33} \; 2q_{12} \; 2q_{23} \; 2q_{31} > \qquad \text{(IV-6)}$$

where

$$q_{11} = \alpha + \frac{1}{J_2^{\frac{1}{2}}} \left(\sigma_{11} - \frac{1}{3} J_1\right)$$

$$q_{22} = \alpha + \frac{1}{J_2^{\frac{1}{2}}} \left(\sigma_{22} - \frac{1}{3} J_1\right)$$

$$q_{33} = \alpha + \frac{1}{J_2^{\frac{1}{2}}} \left(\sigma_{33} - \frac{1}{3} J_1\right)$$

$$2q_{12} = \frac{2}{J_2^{\frac{1}{2}}} \sigma_{12} \qquad \text{(IV-7)}$$

$$2q_{23} = \frac{2}{J_2^{\frac{1}{2}}} \sigma_{23}$$

$$2q_{31} = \frac{2}{J_2^{\frac{1}{2}}} \sigma_{31}$$

Following the notation used in Chapter II, Equation (II-30),

$$B = \left\{ - \frac{\partial f}{\partial \epsilon''_{ij}} \frac{\partial f}{\partial \sigma_{ij}} + \frac{\partial f}{\partial \sigma_{ij}} E_{ijkl} \frac{\partial f}{\partial \sigma_{kl}} \right\}$$

$$= q^T E q \qquad \text{(IV-8)}$$

where E is the reduced elasticity tensor. Equation (II-32) gives the tensor L as

$$L = \frac{1}{B} q q^T E \qquad \text{(IV-9)}$$

Hence,

$$\left\{ \dot{\sigma} \right\} = \left[E - \frac{1}{B} E q q^T E \right] \left\{ \dot{\epsilon} \right\} \qquad \text{(IV-10)}$$

Equation (IV-10) gives the relation between the stress rate tensor $\dot{\sigma}$ and total strain rate tensor $\dot{\epsilon}$, for an elastic-perfectly plastic material. Explicitly, these relations for the generalized Mohr-Coulomb material, assuming isotropic elastic behavior, are:

$$\dot{\sigma}_{ij} = 2G (\dot{\epsilon}_{ij} - a\delta_{ij} - b\sigma_{ij})$$

where $a = h_2 \dot{\epsilon}_{kk} + h_1 \sigma_{ij} \dot{\epsilon}_{ij}$

$$b = h_1 \dot{\epsilon}_{kk} + h_3 \sigma_{ij} \dot{\epsilon}_{ij}$$

and $$h_1 = \frac{h_o}{J_2^{\frac{1}{2}} H}$$

$$h_2 = \frac{1}{H} \left[2 h_o \frac{\sigma_{ij}}{J_2^{\frac{1}{2}}} - \frac{\nu K}{[1 - 2\nu] J_2^{\frac{1}{2}}} \right]$$

$$h_3 = \frac{1}{2 J_2 H}$$

$$h_o = \frac{3}{2} \alpha \frac{K}{G} - \frac{\sigma_{ij}}{6 J_2^{\frac{1}{2}}}$$

$$H = 1 + 9\alpha^2 \frac{K}{G}$$

ν, K, G are respectively, the Poisson's ratio, the bulk modulus and the shear modulus in elasticity.

For plane strain

$$a = h_2 \dot{\epsilon}_{\alpha\alpha} + h_1 \sigma_{\alpha\beta} \dot{\epsilon}_{\alpha\beta}$$

$$b = h_1 \dot{\epsilon}_{\alpha\alpha} + h_3 \sigma_{\alpha\beta} \dot{\epsilon}_{\alpha\beta}$$

where summation on repeated indices is over the range 1,2.

4.3. Analysis of Progressive Failure

4.3.1. Basic Methodology

In applying the finite element method to elastic-plastic continuum, it was assumed that the stress field is constant within each element. Under applied loads, an element was assumed to be either totally yielded or elastic. For sufficiently small elements, this appears to be a reasonable assumption. The stiffness of the system represents the collective stiffness of its elements. For each element after yield, the stress-strain behavior was defined by the relationships developed in section 4.2. Thus as each element yields, the system stiffness is altered resulting in a non-linear structural response. In the study of progressive failure, it is important to allow for the effect of this nonlinearity. In the current research program, the system was assumed to be stepwise linear within yield of successive elements. In the incre-

mental procedure, the load was divided into increments with each increment large enough to introduce yield in another element. This was subject to checks on the validity of assumption of linear stress-strain relationship. As several elements may yield at almost the same load, a lower limit on load increment size was used to avoid excessive computational effort. Also, elements yielding within a prescribed load range of the computed increment for any step were treated as if these had yielded simultaneously with the elements controlling the increment size. The total load vector $\{R\}$ was treated as a sum of load increments $\{\Delta R_i\}$, i = 1, 2, ..., n where n is the total number of increments, not necessarily equal.

$$\{R\} = \sum_{i=1}^{n} \{\Delta R_i\} \qquad \text{(IV-11)}$$

The first increment of load, $\{\Delta R_1\}$ applied to an elastic system was sufficiently large to allow at least one element to reach the yield surface. To evaluate the load increment for any step as a proportion of the load yet to be applied to the system, a stress ratio was introduced. Figure IV-1 shows the calculation of the stress ratio S_r for a typical element. The point A represents the initial stress state and C the stress state that would result if all the load was applied. The curve f - k = 0 represents the yield surface. If A and C both were in the interior of the yield surface, all the load could be applied and S_r was defined as unity. However, if A was in the interior and C in the exterior of the yield surface, clearly it would not be possible to

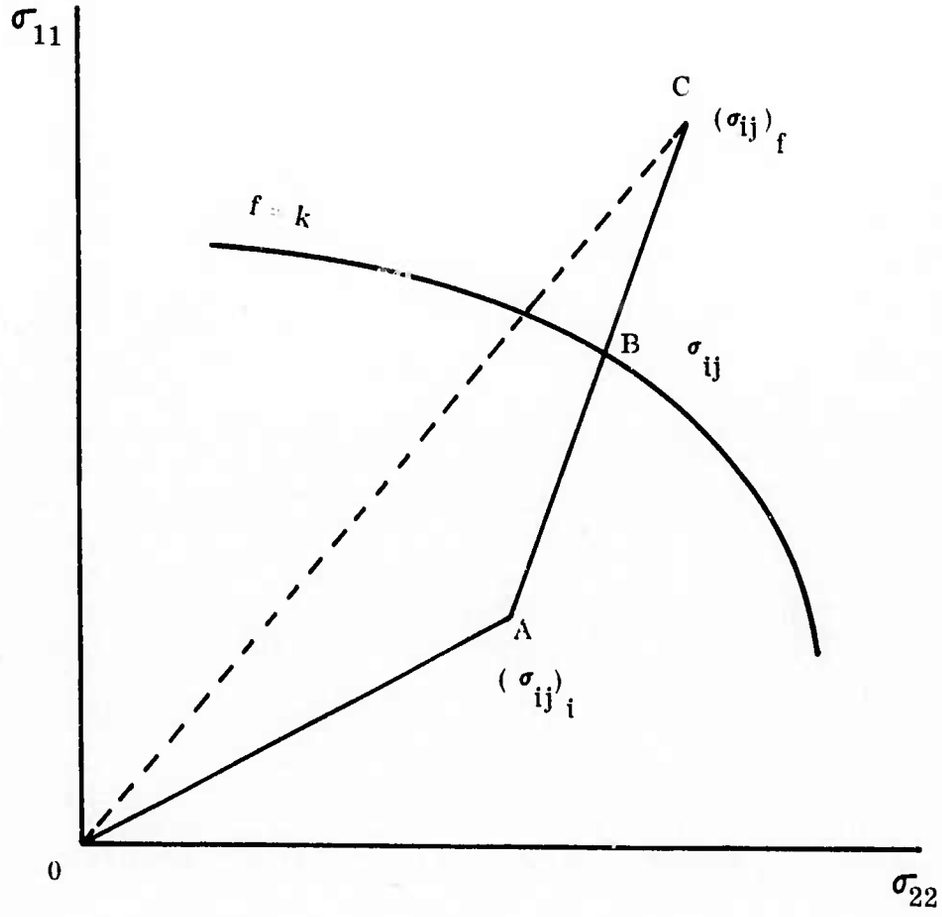

FIG. IV-1. Calculation of Stress Ratio

load the element to C and that it could only be loaded to B before onset of yield. Here B is the intersection of line AC with the yield surface. Then

$$S_r = \frac{|AB|}{|AC|} \qquad \text{(IV-12)}$$

Calculation of S_r is simple. Let $(\sigma_{ij})_i$, $(\sigma_{ij})_f$ represent the stress states associated with A and C respectively. Then the stress state for B is σ_{ij} such that

$$\sigma_{ij} = (\sigma_{ij})_i \ (1 - S_r) + S_r \ (\sigma_{ij})_f \qquad \text{(IV-13)}$$

S_r is calculated from the relationship

$$f(\sigma_{ij}) - k = 0 \qquad \text{(IV-14)}$$

The stress ratio S_r for an element represented the fraction by which the load would have to be scaled to ensure that after application of the load increment, the element was within or on the yield surface. The value of S_r was calculated for all the elements. The element with the lowest stress ratio was the next to yield and governed the system load ratio. S_r thus defined the load increments in progressive failure assuming stepwise linear behavior. As each load increment was applied, cumulative stresses and displacements were calculated. The stresses at the end of the ith step were the initial stresses for the (i + 1)th step.

4.3.2. Nonmonotonic Loading

To allow for non-monotonic loading, at any structural increment or excavation, a pilot analysis is carried out assuming all elements to be linearly elastic. In case of unloading, any element already on yield surface can unload either plastically or elastic-

ally as shown in Figure IV-2 . The two modes are distinguished by the fact that in elastic loading, the strain decreases whereas if the element stays on the yield surface in the unstable region the strain will increase. If the element is assigned the stress-strain behavior corresponding to the yield state, it is forced to stay in the yield surface because the stress-strain laws satisfy $\dot{f} = 0$. In the pilot analysis, assuming elastic behavior,the element will either follow the path AB or AC. Path AC corresponds to elastic unloading. Path AB would indicate increasing strain under applied load and therefore the element is likely to stay in the yield surface. This preliminary information is used to assign appropriate material behavior to each element previously in state of plastic yield.

4.3.3. Allowance for Nonlinear Stress-Strain Behavior

The stress-strain relationship for plasticity is stress-dependent. As the stresses change during application of a load increment, it is desirable to reflect this change in the stress computation. Assuming $c_{ij}^{(o)}$, $c_{ij}^{(f)}$ to be the compliances at the initial and final stress states, respectively, we may write

$$u_i^{(f)} = u_i^{(o)} + \frac{c_{ij}^{(o)} + c_{ij}^{(f)}}{2} \triangle P_j$$

where $u_i^{(f)}$, $u_i^{(o)}$, $\triangle P_j$ are the final displacement, the initial displacement and the increment load vectors, respectively. Further

$$c_{ij}^{(f)} = c_{ij}(\sigma_{kl}^{(f)})$$

and

$$\sigma_{kl}^{(f)} = \sigma_{kl}(u_i^{(f)})$$

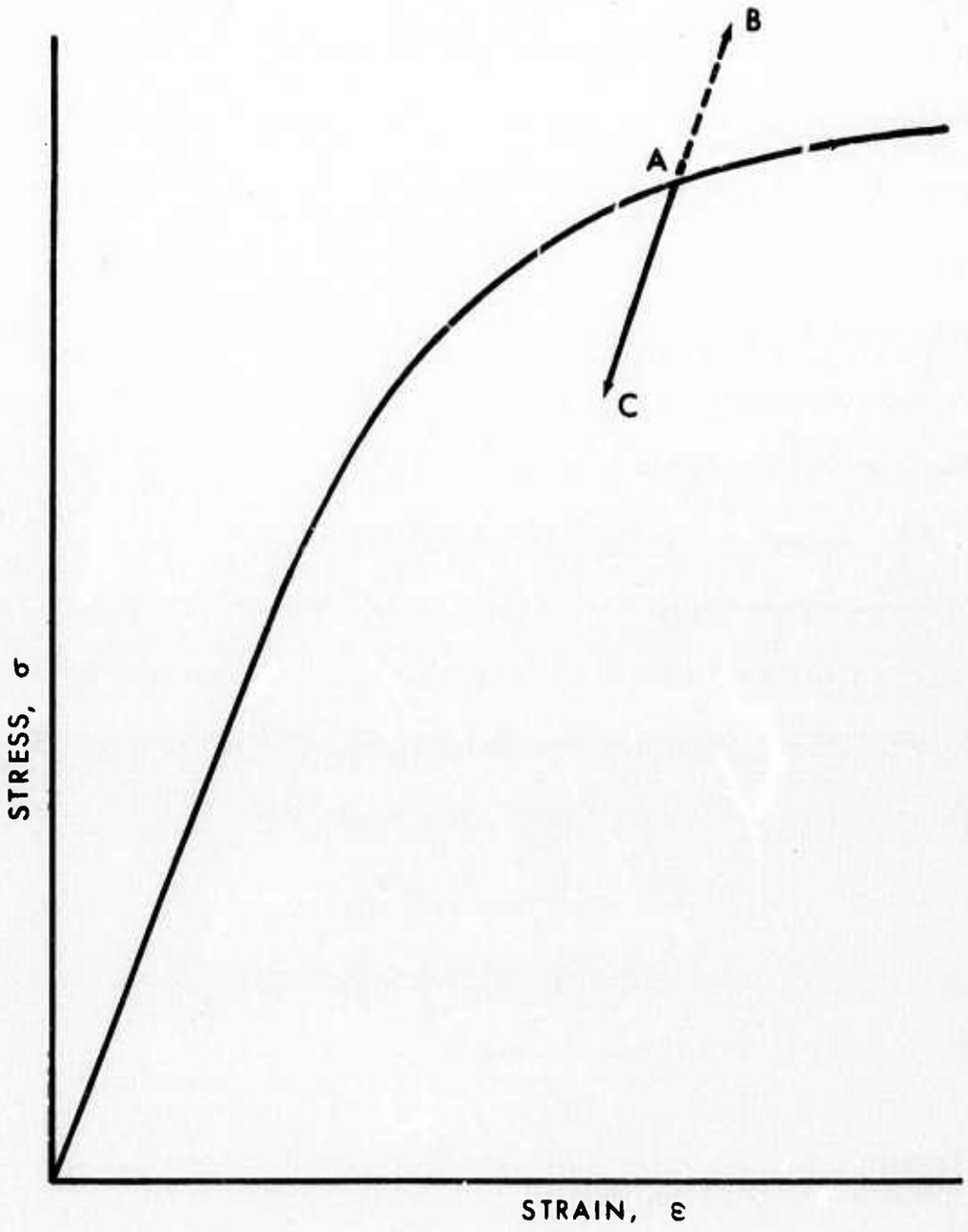

FIG. IV-2. Loading or Unloading for an Initial State of Plastic Yield

An iterative scheme would consist of the following steps

$$u_i^{(f)(n+1)} = u_i^{(o)} + \frac{c_{ij}^{(o)} + c_{ij}^{(f)(n)}}{2} \triangle P_j$$

$$c_{ij}^{(f)(n)} = c_{ij}\left(\sigma_{kl}^{(f)(n)}\right)$$

$$\sigma_{kl}^{(f)(n)} = \sigma_{kl}\left(u_i^{(f)(n)}\right)$$

$$n = 0, 1, \ldots\ldots$$

Such an iterative procedure has been used by Sandhu (1973) along with a criterion for convergence which defines the maximum increment of $\triangle P_j$ consistent with the non-linear characteristics of $c_{ij}^{(f)}$. However, repeated solution for displacements may be very expensive in terms of computation. Also, because, in general, the plasticity will be confined to local regions, the displacement solution is not likely to change significantly. Therefore, it is considered sufficient to assume constant displacements and to iterate only on stress using mean stiffness k_{ijkl} as under:

$$\sigma_{ij}^{(f)(n+1)} = \sigma_{ij}^{(0)} + \frac{k_{ijkl}^{(0)} + k_{ijkl}^{(f)(n)}}{2} \triangle \epsilon_{kl}$$

$$k_{ijkl}^{(f)(n)} = k_{ijkl}\left(\sigma_{mn}^{(f)(n)}\right)$$

where $\triangle \epsilon_{kl}$ is the strain increment. The procedure converges very rapidly. The procedure is shown schematically in Figure IV-3a.

An alternative procedure is to use

$$\sigma_{ij}^{(f)(n+1)} = \sigma_{ij}^{(0)} + k_{ijkl}^{(m)(n)} \Delta\epsilon_{kl}$$

where the mean stiffness corresponding to the load increment is defined as the stiffness at the mean stress for the increment, i.e.

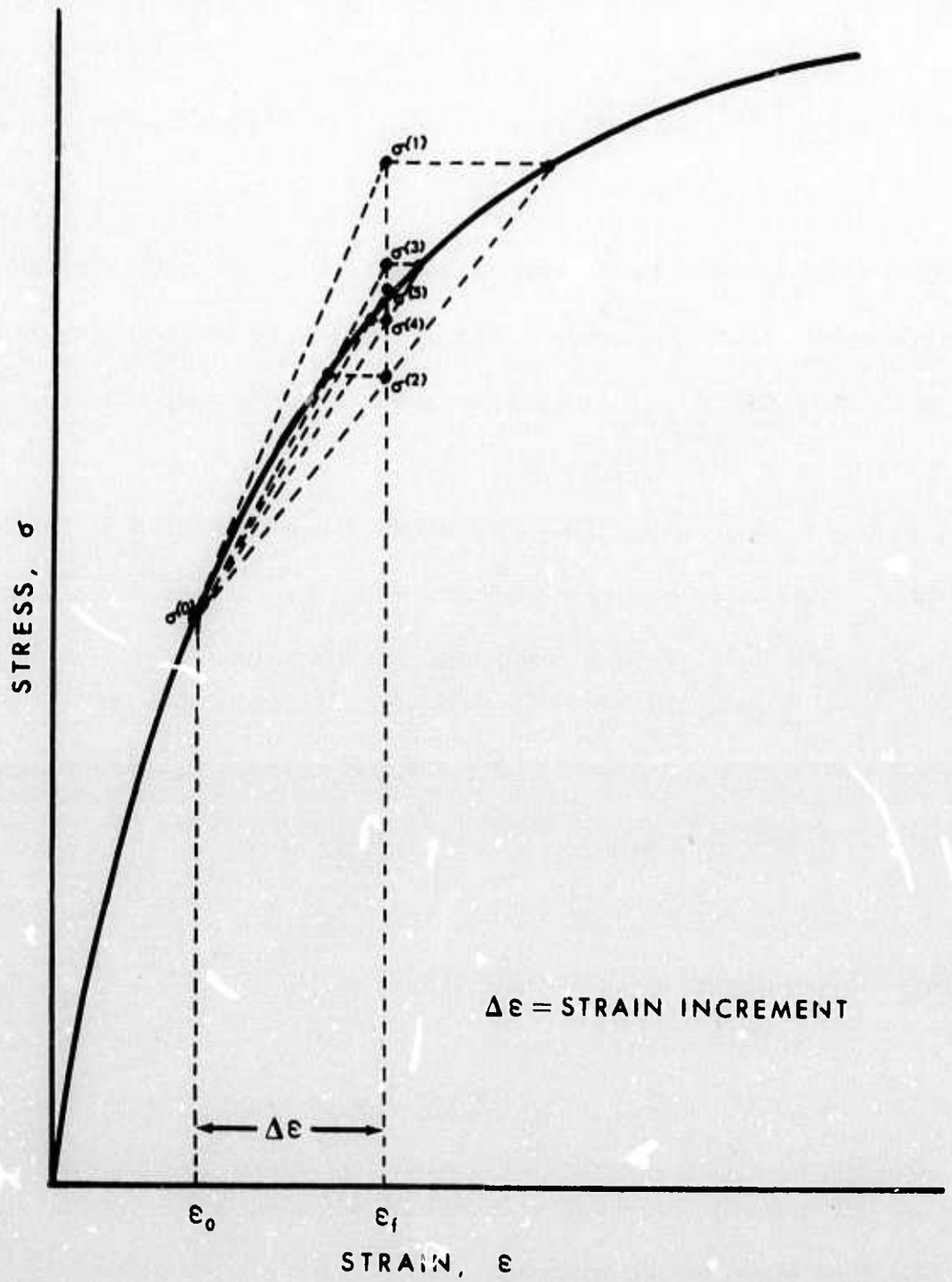

FIG. IV-3a. Calculation of Stress for a Strain Increment - Method 1

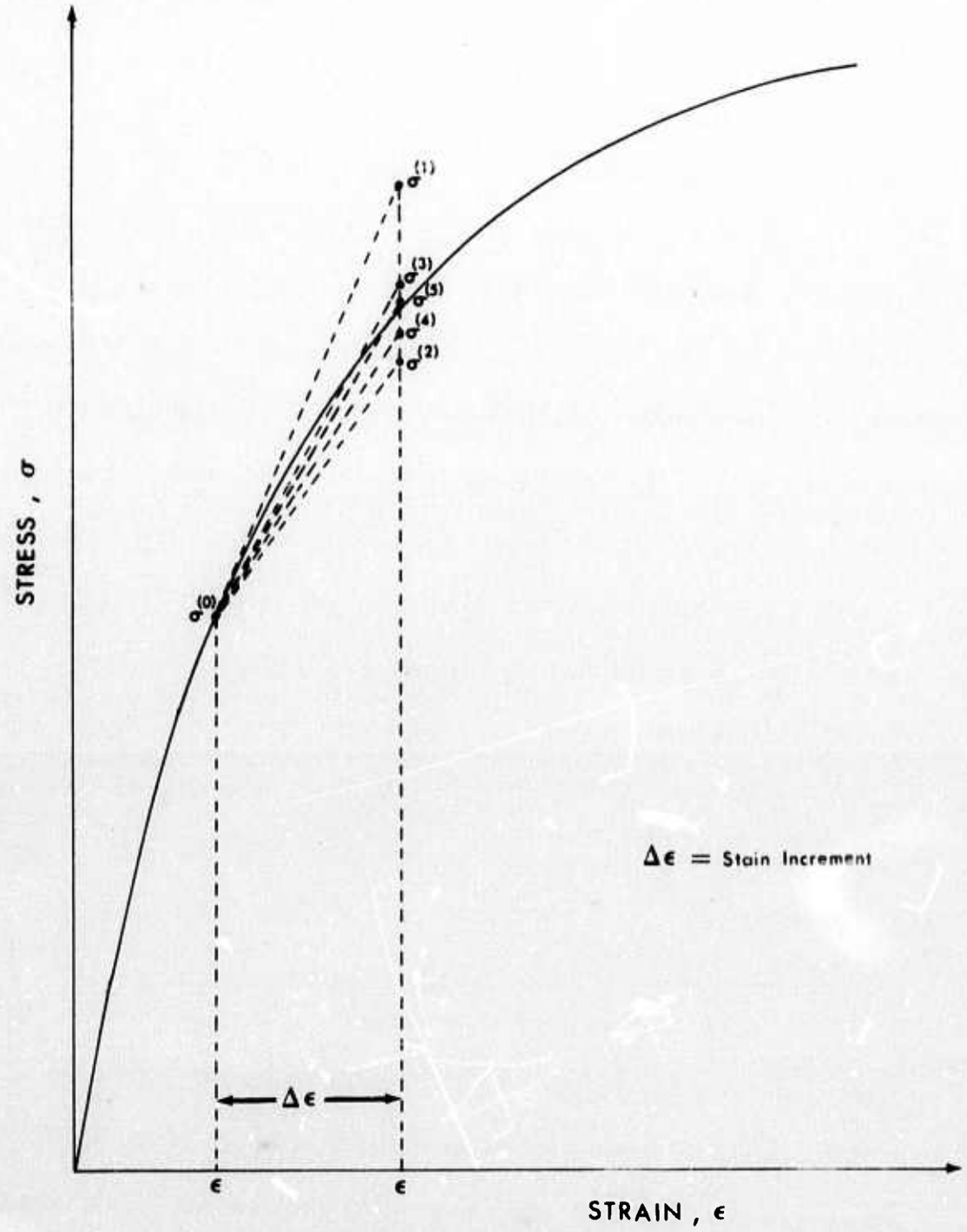

FIG. IV-3b. Calculation of Stress for a Strain Increment - Method 2

$$k_{ijkl}^{(m)(n)} = k_{ijkl}\left(\frac{\sigma_{mn}^{(0)} + \sigma_{mn}^{(f)(n)}}{2}\right)$$

This approach is illustrated in Figure IV-3b. Both the alternatives were found to be satisfactory.

4.4. Examples of Application

A computer program for plane strain analysis of elastic-plastic Mohr-Coulomb rocks was developed using the mathematical model and the discretization procedures described in the foregoing sections. The technique was used to solve several problems. There are very few problems in the theory of plasticity for which closed form solutions are available. However Naghdi (1957) solved the problem of an elastic perfectly plastic wedge under uniform loading on one face (Fig. IV-4). The Naghdi solution is for a wedge infinite in extent, made of von Mises material and loaded in plane strain. This type of material is a special case of Mohr-Coulomb material obtained by setting the angle of internal friction $\phi = 0$. This example was used earlier by Baker et al. (1969) to verify their computer code. Another example involves analysis of stresses and deformation of a notched bar of perfectly plastic von Mises material. The last example is of frequently used laboratory test. Excellent agreement with theoretical results for the wedge were obtained.

4.4.1. Elastic-Plastic Wedge

Figure (IV-4) shows a finite element idealization for the Naghdi wedge. Figures (IV-5) and (IV-6) show the theoretical and computed results for the distribution of radial and circumferential stresses at various stages of loadings. The angle Ψ denotes the angle upto which the yielding has progressed from the boundaries. Figure (IV-7) shows the radial strain distribution at various ranges.

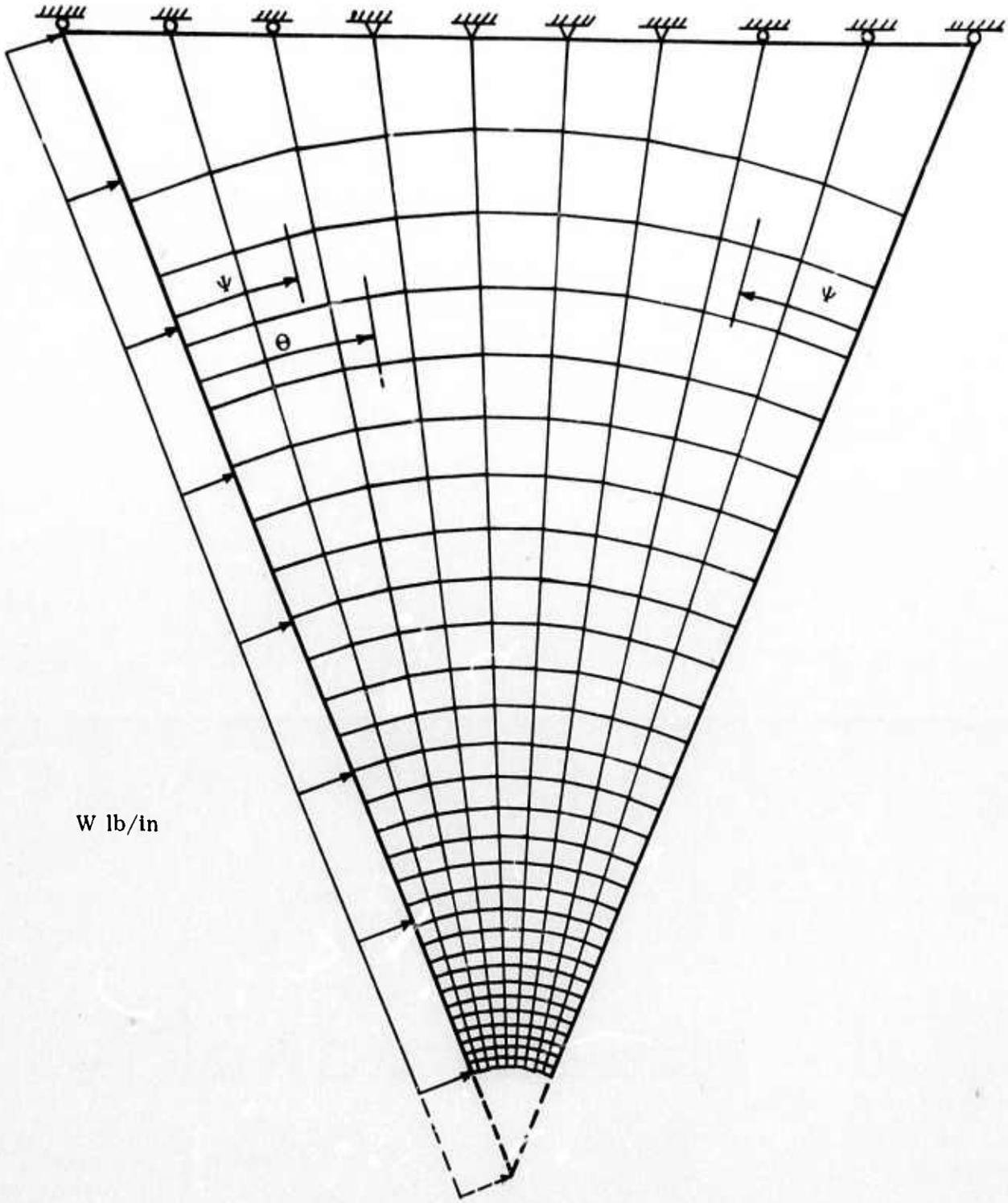

FIG. IV-4. Finite Element Idealization for Elastic-Plastic Wedge
(Baker et. al., 1969)

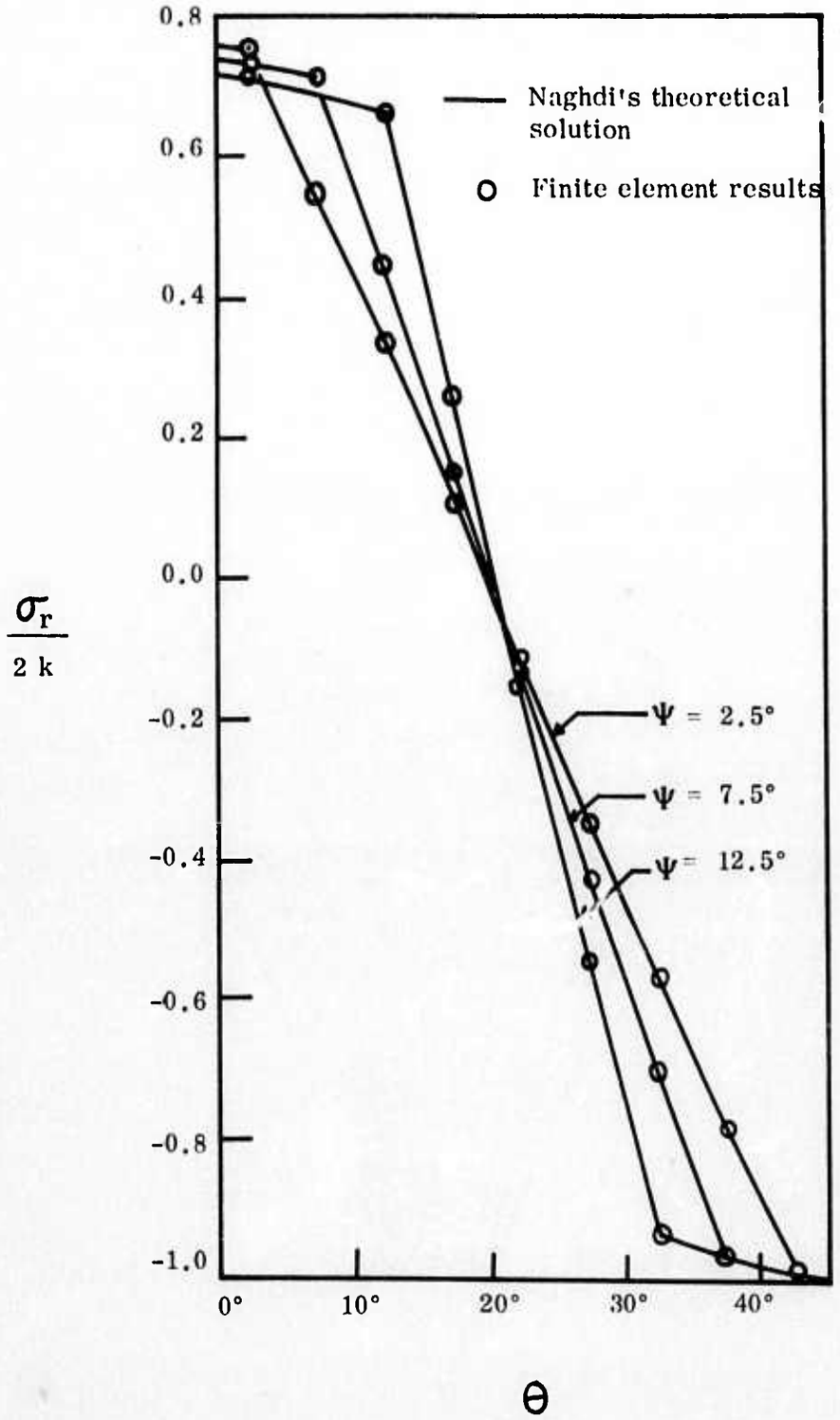

FIG. IV-5. Distribution of Radial Stress for Wedge at Various Loads

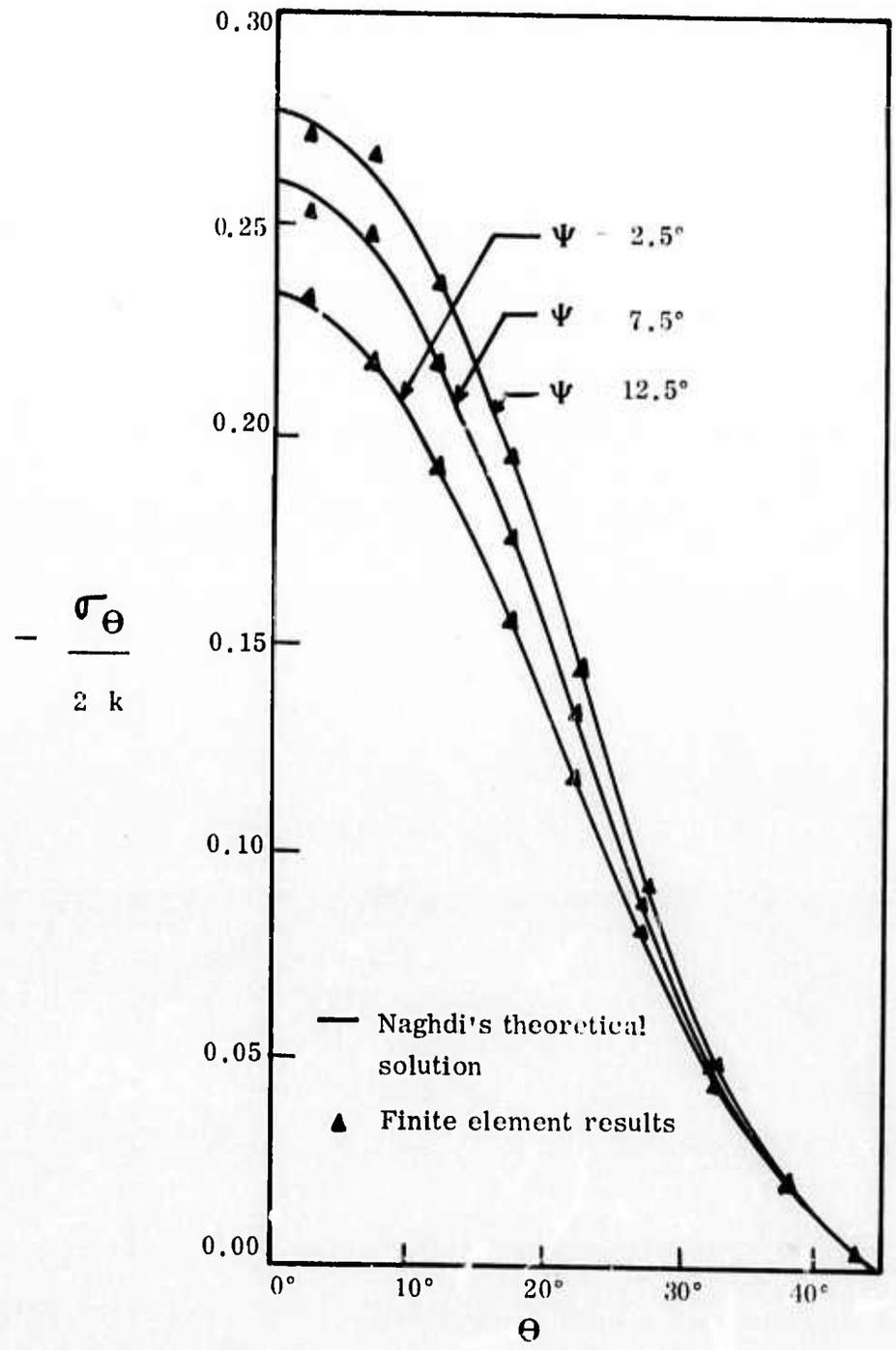

FIG. IV-6. Distribution of Circumferential Stress for Wedge at Various Loads

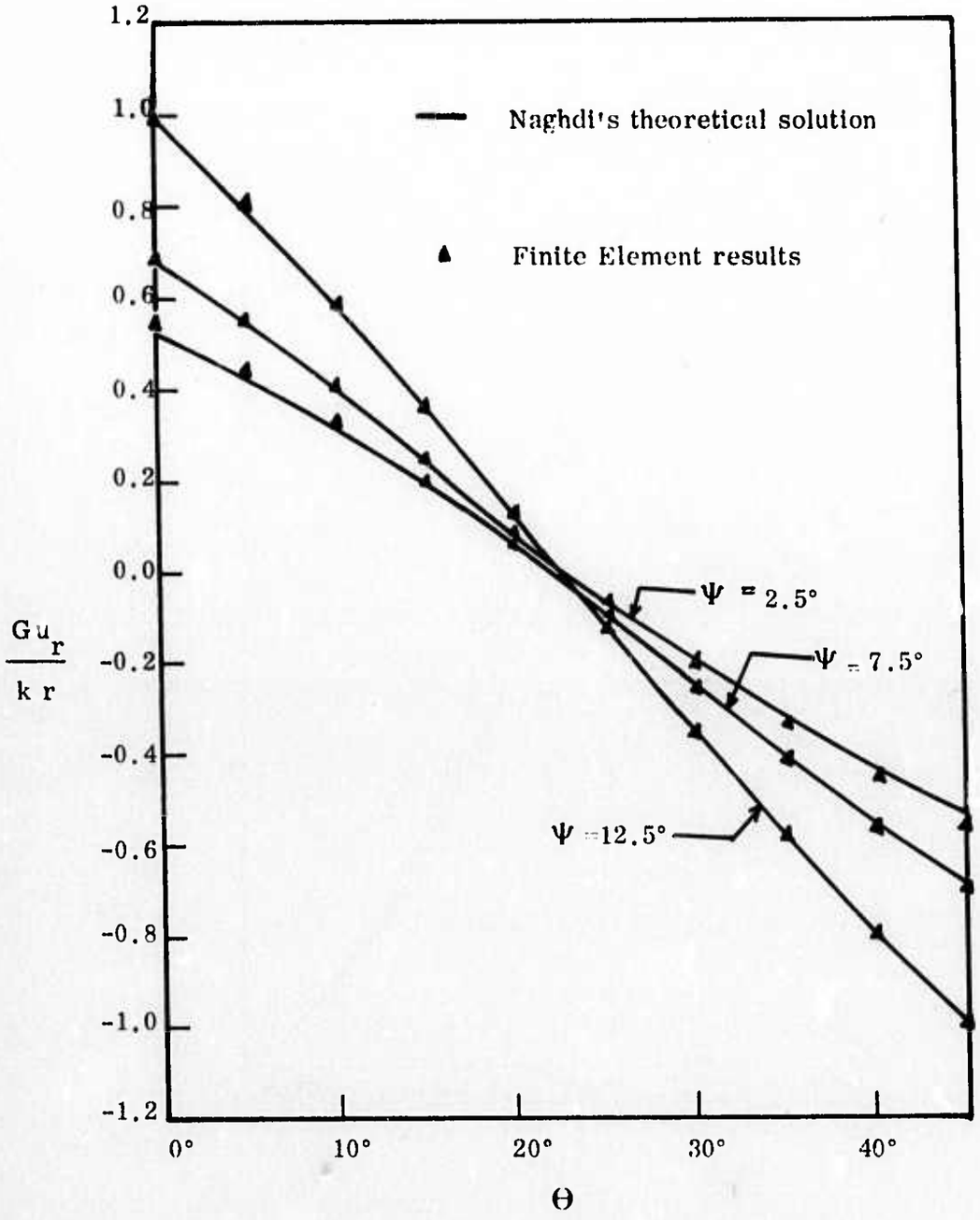

FIG. IV-7. Distribution of Radial Displacements

Generally the agreement between results computed by the method outlined and the exact analysis was found to be good.

4.4.2. Notched Specimen

A notched specimen of perfectly plastic von Mises material with a 90° notch and subjected to a uniformly distributed load was analyzed. The finite element idealization for one quarter of the specimen is shown in Figure IV-8. The value of c was taken as 12.15 kilogram per square millimeter (corresponding to a yield stress of 24.3 kg./mm. in uniaxial tension test) and ϕ was set equal to zero. Figure IV-9 shows the principal stresses at a load intensity of 19.2 kilogram per square millimeter. Figure IV-10 shows contours of failure ratio for this load as well as the boundary of the plastic zone at different values of the load. This problem was solved by Marcal and King (1968) and Zienkiewicz et al. (1969). The results are slightly different from those presented in this report for reasons discussed earlier.

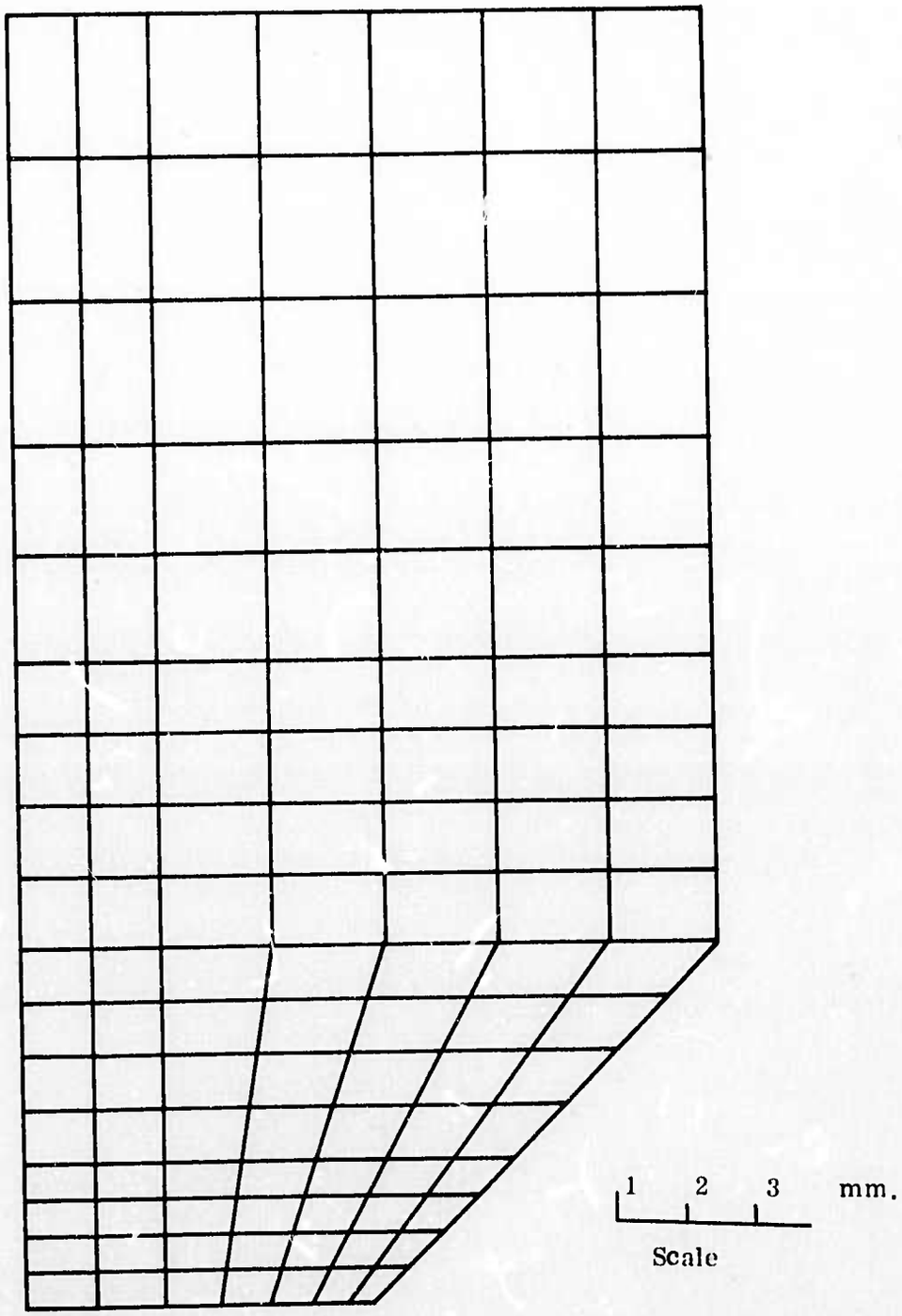

FIG. IV-8. NOTCHED SPECIMEN-- FINITE ELEMENT IDEALIZATION

$c = 14.05\ kg/mm^2$ $p = 20\ kg/mm^2$

$\phi = 0$

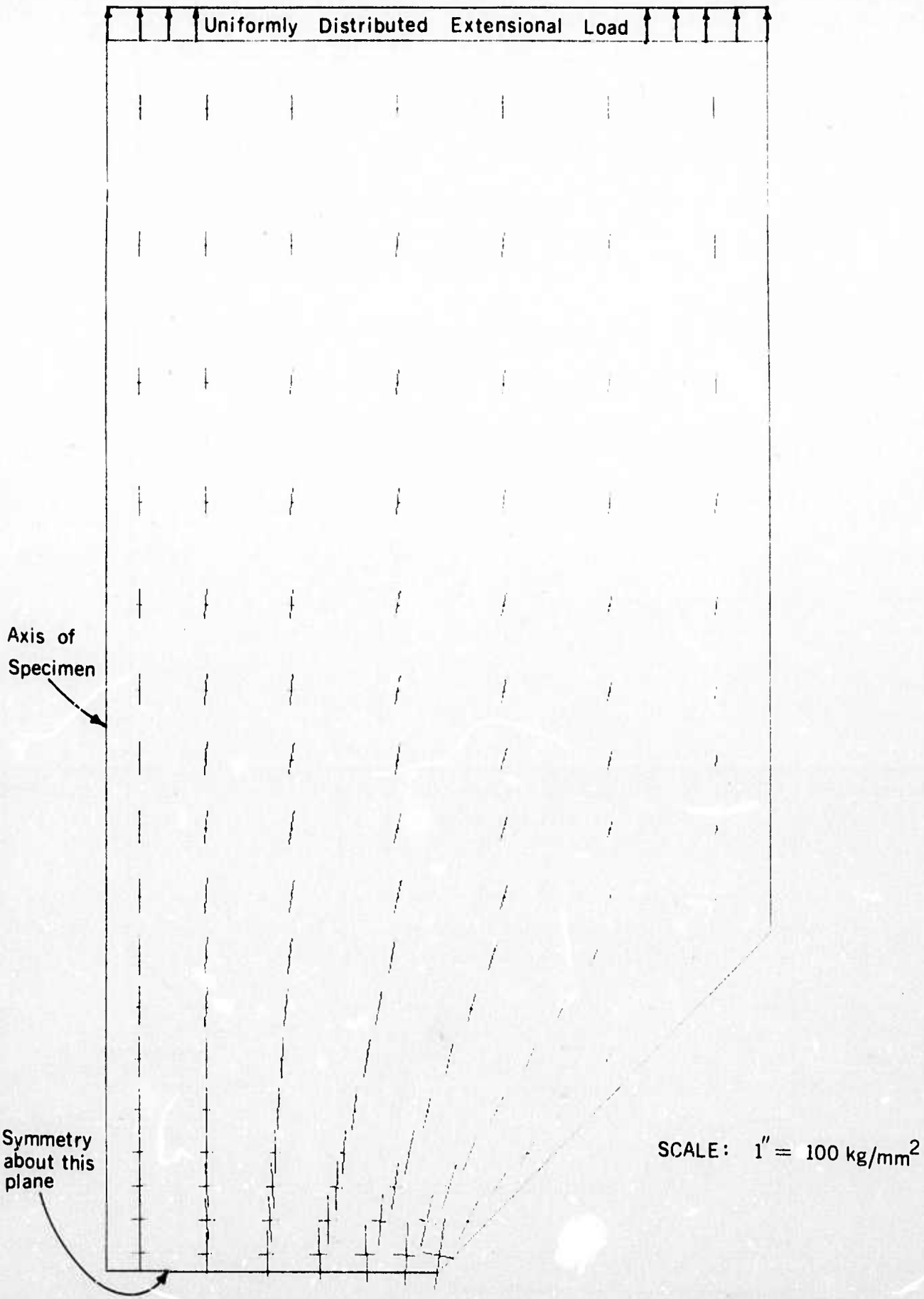

FIG. IV-9. Notched Specimen (One Quarter) - Elastic-Plastic Stress Distribution Under Uniform Load of 19.2 kg./mm.^{2} Applied at Ends

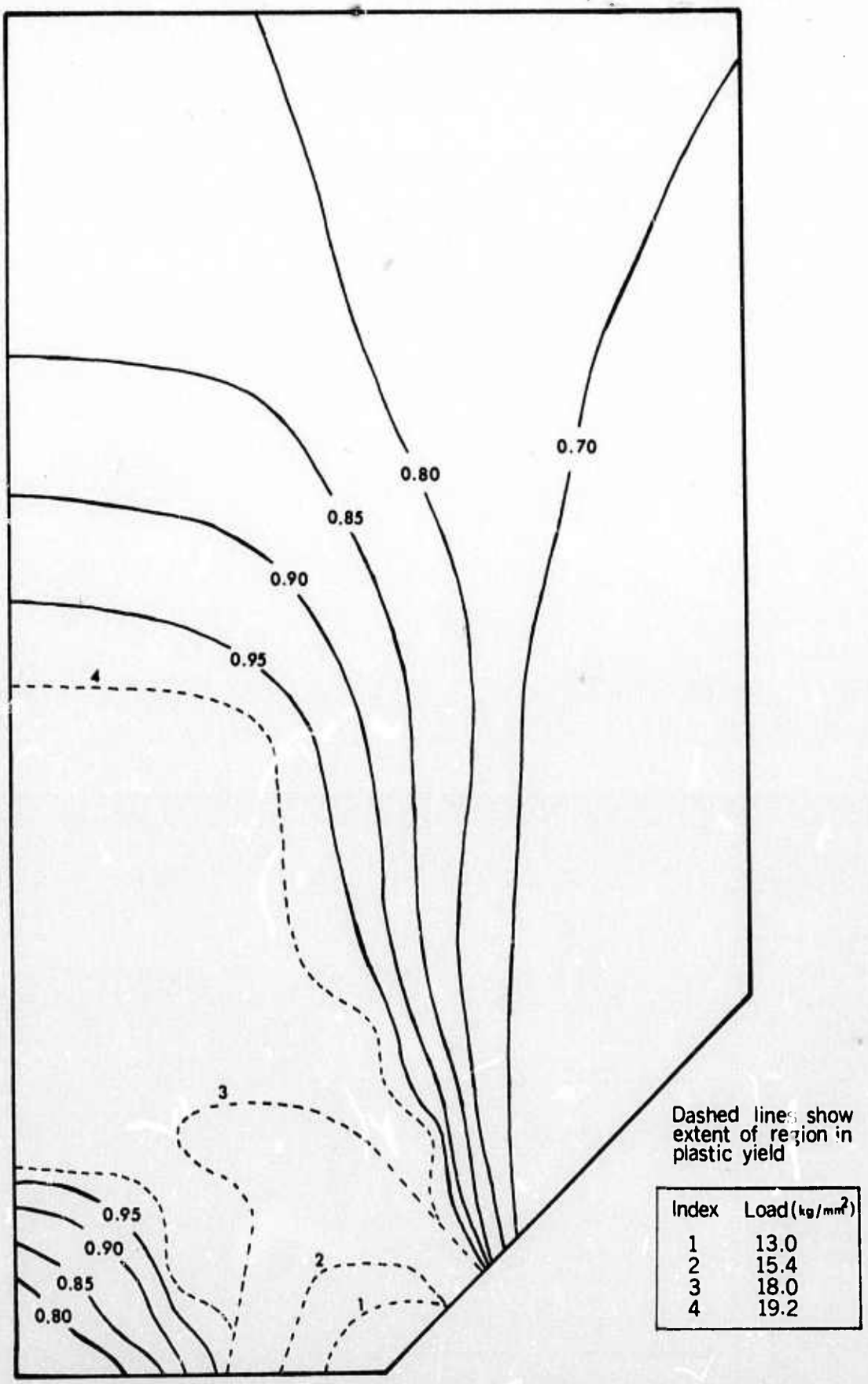

FIG. IV-10. Notched Specimen - Contours of Failure Ratio at Uniform Extensional Load of 19.2 kg./mm.^{2} Applied at Ends

CHAPTER V. FINITE ELEMENT PLANE STRAIN ANALYSES OF PROGRESSIVE CRACKING OF ROCK FOLLOWING GRIFFITH'S THEORY

5.1. Review of Previous Work

Stability of excavations in rock is deeply influenced by the presence of cracks and fissures. These discontinuities may be preexisting or might arise as a consequence of the stress-redistribution associated with excavation. Classical methods of analysis are inadequate for study of initiation and propagation of fracture.

Several attempts have been made to apply the finite element method to jointed rock systems. Zienkiewicz et al. (1968) proposed the 'no tension' analysis procedure. This consisted of the following steps:

1. Analysis of the system treating intact rock as linear elastic, isotropic.
2. Check to identify tensile principal stresses, if any, in various elements.
3. Reanalysis assigning zero resistance to deformation in the direction of the principal tensile stresses.
4. Repeat 2 and 3 to convergence, i.e. until the solution shows no appreciable tension anywhere.

In order to economize on computational effort, a stress relief procedure was introduced. The tensile principal stresses were relieved by introducing equivalent nodal point loads using the linear elastic stiffness for an iterative correction scheme. The procedure has poor convergence characteristics and even after several cycles of iterations, tension zones do not completely disappear. Moreover, for the case of one

principal stress being tensile and the other compressive, relieving tensile stress by applying equivalent nodal point loads amounts to using a non-symmetrical constitutive relationship. In the present research effort, a correction was introduced in the no-tension approach to correctly simulate the orthotropic material behavior of cracked elements. For intact linear isotropic elastic elements,

$$\begin{Bmatrix} \sigma_1 \\ \sigma_2 \end{Bmatrix} = \begin{bmatrix} C_{11} & C_{12} \\ C_{21} & C_{22} \end{bmatrix} \begin{Bmatrix} \epsilon_1 \\ \epsilon_2 \end{Bmatrix} \tag{V-1}$$

where σ_1, σ_2 are the principal stresses; ϵ_1, ϵ_2 are the principal strains and C_{11}, C_{12}, C_{21}, C_{22} are elements in a symmetric matrix. In the no-tension method $\sigma_1 > 0$, $\sigma_2 < 0$, σ_1 would be relieved by applying nodal loads $\left[b^T\right]\begin{Bmatrix}\sigma_1 \\ 0\end{Bmatrix}$ where $\left[b^T\right]$ represents the equilibrium transformation. The stress σ_2 is retained i.e. for the cracked element,

$$\begin{Bmatrix} \sigma_1 \\ \sigma_2 \end{Bmatrix} = \begin{bmatrix} 0_+ & 0_+ \\ C_{21} & C_{22} \end{bmatrix} \begin{Bmatrix} \epsilon_1 \\ \epsilon_2 \end{Bmatrix} \tag{V-2}$$

is the stress-strain relationship. Clearly, for symmetry in material behavior, the part of σ_2 corresponding to C_{21} ϵ_1 must also be relieved so that for cracked element

$$\begin{Bmatrix} \sigma_1 \\ \sigma_2 \end{Bmatrix} = \begin{bmatrix} 0_+ & 0_+ \\ 0_+ & C_{22} \end{bmatrix} \begin{Bmatrix} \epsilon_1 \\ \epsilon_2 \end{Bmatrix} \tag{V-3}$$

Even the corrected approach was not considered worthwhile. Aside from the poor convergence of the numerical solution procedures, there is a basic objection to eliminating tension from several elements simultaneously. Cracking must necessarily be progres-

sive and as each crack forms, the rock in the immediate vicinity experiences a significant stress-redistribution. The no-tension approach does not allow for the sequential cracking of elements and is therefore not realistic.

Duncan and Goodman (1968) examined the effect of preexisting joints at arbitrary orientations. A linear elastic analysis was used to establish the stress field. Normal and shear stresses on arbitrarily oriented planes (ubiquitous joint) were computed and the shearing strength based on Mohr-Coulomb law compared with the shearing stress. This analysis is useful in predicting local failure. However, the analysis did not take into account the stress-redistribution and progressive failure associated with local failure.

In a comprehensive report, Duncan and Goodman (1968) also used an orthotropic continuum to simulate rock with orthogonal sets of parallel and evenly spaced joints. Again the progressive failure and deformation could not be allowed for.

For preexisting joints, it is possible to simulate their mechanical behavior through the use of two-dimensional elements or one-dimensional elements. The two-dimensional elements have the drawback of poor 'aspect ratios' (Duncan and Goodman (1968)) in the case of very thin joints leading to inaccuracy in the results. One-dimensional elements to simulate joints were developed by Goodman et al. (1968) and have proved quite useful. These elements can transmit shear as well as compressive stresses. Figure (V-1) shows the representation discussed by Duncan and Goodman.

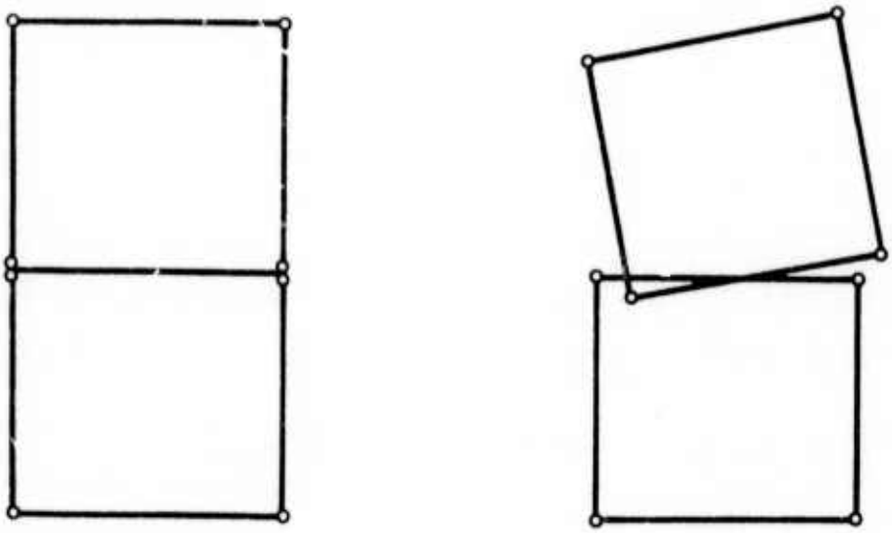

a. Before Loading

b. After Loading

Fig. V-1. One-Dimensional Element
(Goodman, 1968)

Propagation of preexisting cracks has also been studied in conjunction with the concept of stress-intensity factors. Assuming the crack geometry to be known, finite element procedures were developed by Chan et al. (1970) and Gross et al. (1968) to determine the stress intensity factors at crack tip. Displacements, stresses and compliance were all used as the basis for calculation of the factors. To improve accuracy, Wilson (1971), Byskov (1970), Levy (1971) introduced stress-singularity elements at crack tips (Figs. V-2 & V-3). Pian (1971) suggested use of hybrid elements. The stress-singularity elements improve the accuracy. However, they are severely restrictive in the study of crack propagation as the analysis applies only for crack tip at the center of the elemen . Use of quadrilateral elements with stress criterion is sufficient, in most cases, to establish the stress-intensity factors.

A common drawback of all the previous work is that the geometry of the cracks and their location must be known beforehand. For new cracks originating at Griffith flaws, the crack geometry is not known beforehand. The present research program treated the problem of fracture initiation at arbitrarily oriented Griffith flaws using the stress formulation. Assigning orthotropic no-tension material behavior to cracked elements, it was possible to trace the progressive failure of rock following Griffith's theory. The procedural details are given in the following sections.

5.2. Analysis for Crack Initiation

In the case of preexisting cracks, it is sometimes possible to plan a finite element mesh including the crack surface as a free boundary. However, where intact

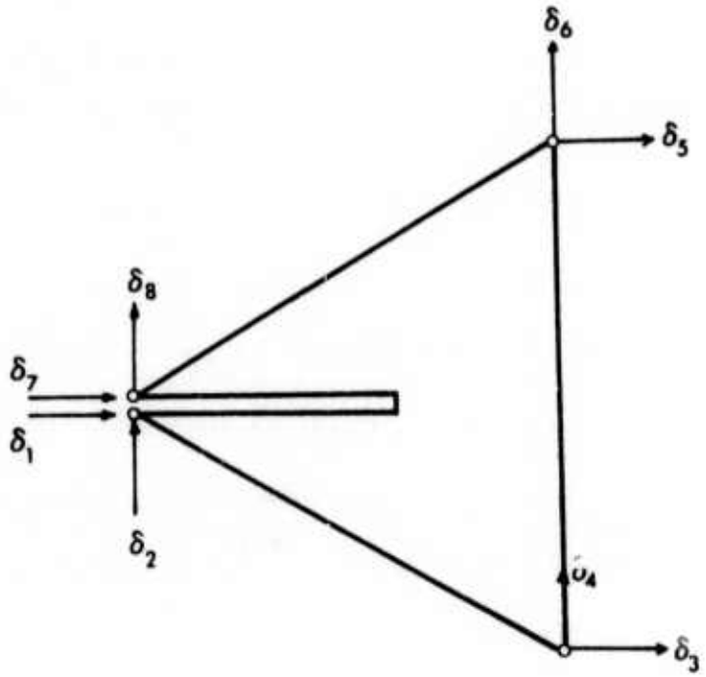

FIG. V-2. Cracked Element (Byskov, 1970)

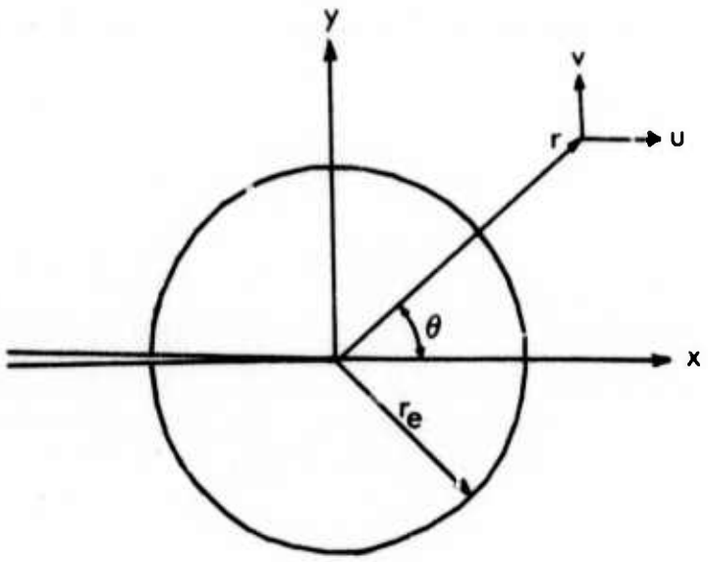

Fig. V-3. Cracked Element (Wilson, 1971)

rock cracks under changes in stress environment, it is necessary to check for crack initiation in accordance with Griffith or modified Griffith theory. As element properties change only at cracking, for a given initial mechanical state, a linear elastic analysis is valid upto cracking of an additional element in the system.

Assuming Griffith flaws are oriented in every direction in each element, an analysis based on stresses in the element is carried out to verify crack initiation. The theoretical basis for this is outlined in Appendix A. Upon application of full load, several elements may satisfy the criterion for crack initiation. In this case, a stress ratio is established for each element. The stress ratio is the factor by which the stress increment must be multiplied such that the total stress corresponds to the critical stress environment for the element. The stress ratio is a function of the initial stress and the stress path. The minimum stress ratio indicates the next element to crack in a progressive failure sequence.

5.3. Analysis of Progressive Cracking of Rock

As each element cracks, its stiffness changes reflecting a change in the system stiffness. Thus the total load deformation behavior of rock is piecewise linear in a finite element representation, changes in slope being associated with sequential cracking of various elements. In actual situations, the nonlinearity may be continuous.

In the process of analysis, the system is assumed to be piecewise linear elastic. At each stage the live load is applied and the stress response calculated. As fracture of one element, next in the sequence, marks a change in stiffness, stress-ratio is

calculated for each element as shown in Figure (V-4). Point A represents the initial state of stress. Point C along stress path AC represents the stress state if the system were linear elastic for the load increment applied. If point C satisfied the fracture criterion, it was necessary to find the stress ratio $S_r = \frac{/AB/}{/AC/}$ such that the point B defined a critical stress state. As fracture angle depends upon the stress environment, calculation of the stress ratio involved an iterative procedure. For fracture angle β corresponding to C, a stress ratio was calculated. Then for this stress ratio, the corresponding stress state was evaluated and the critical angle for this stress state represented a better approximation to the correct fracture angle. Convergence was rapid. The stress ratios for all elements were compared. The minimum value represented the end of the particular step in the multilinear stress path dependent system, and the element yielding the minimum ratio was the next to crack. Repetitive application of this procedure defined the progressive failure of rock.

In order to ensure stability in computation, the total load was applied in several increments. This served to keep the stress change in individual elements for a given load increment within reasonable limits. Figure (V-5) illustrates incremental loading analysis. For a typical load increment ΔP, the initial stiffness yields point C and allowance for sequential fracture of several elements within this load increment shifts the (P, u) point to B. The different arrows indicate sequential corrections to displacement allowing for progressive fracture.

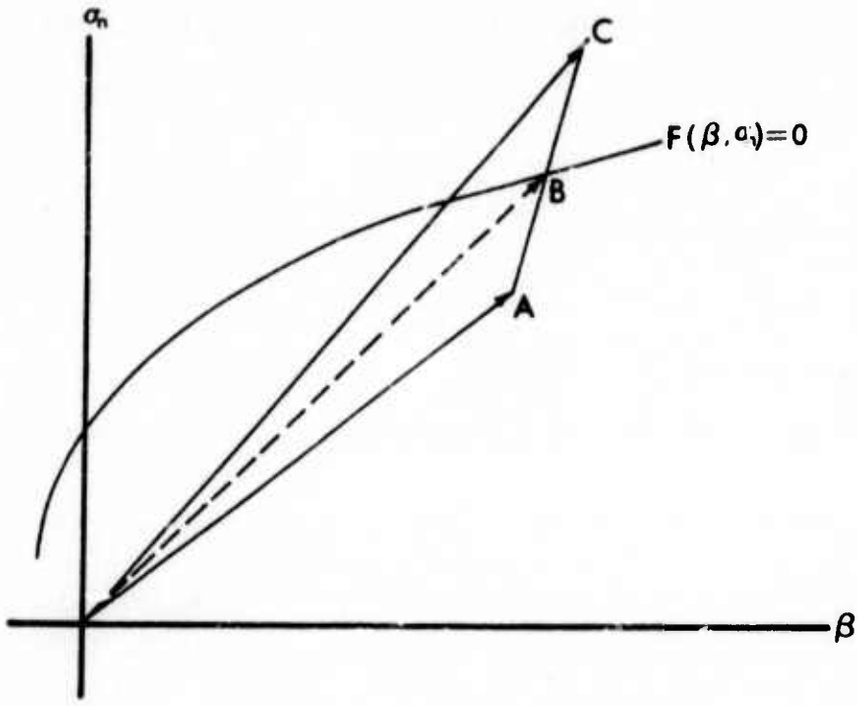

A = Initial Stress for the Load Increment
C = Stress for Full Load Increment
B = Scaled Increase of Stress to Crack Initiation

Note: β calculated for state B will in general not be the same as β for state C.

FIG. V-4. Calculation of Stress Ratio, S_r

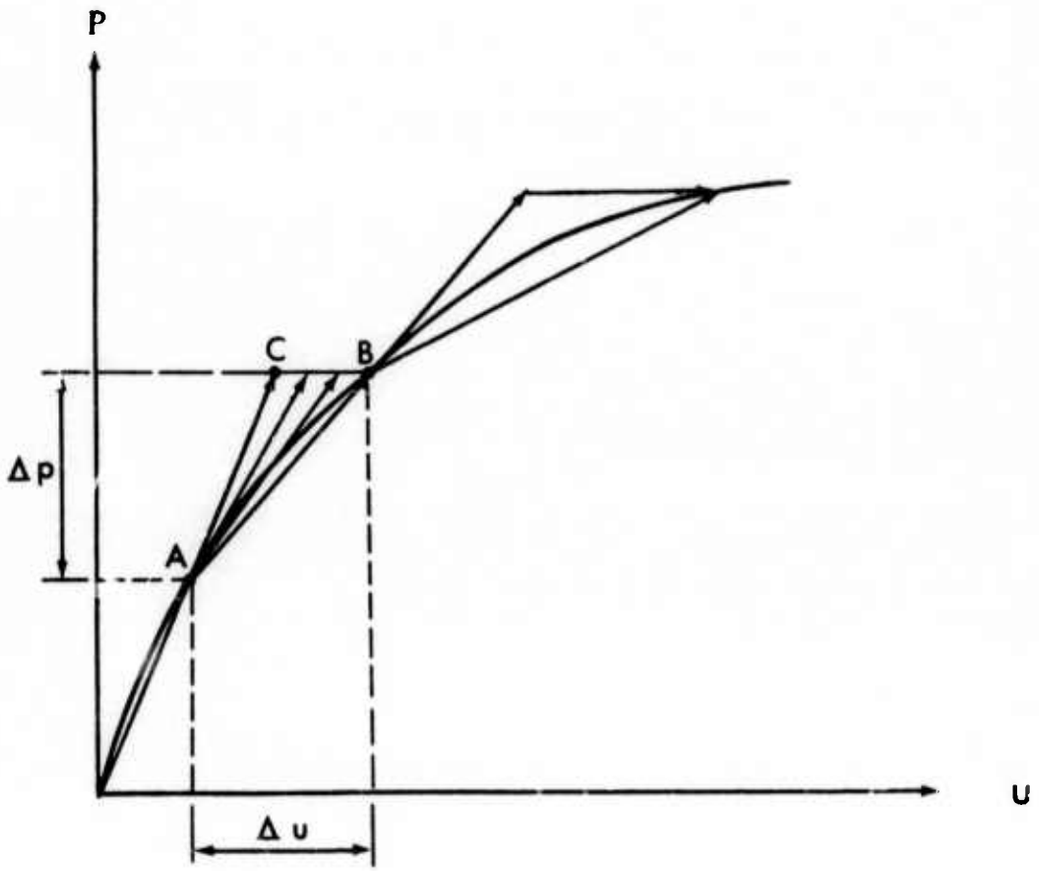

Fig. V-5. Incremental Loading Analysis

5.4. Modelling of Cracked Rock

Referred to axes of material symmetry, the constitutive relationship for linear orthotropic isothermal elasticity can be written as

$$\begin{Bmatrix} \epsilon_{11} \\ \epsilon_{22} \\ \epsilon_{33} \\ \gamma_{23} \\ \gamma_{31} \\ \gamma_{12} \end{Bmatrix} = \begin{bmatrix} \frac{1}{E_1} & \frac{-\nu_2}{E_2} & \frac{-\nu_3}{E_3} & 0 & 0 & 0 \\ \frac{-\nu_1}{E_1} & \frac{1}{E_2} & \frac{-\nu_3}{E_3} & 0 & 0 & 0 \\ \frac{-\nu_1}{E_1} & \frac{-\nu_2}{E_2} & \frac{1}{E_3} & 0 & 0 & 0 \\ 0 & 0 & 0 & G_{23} & 0 & 0 \\ 0 & 0 & 0 & 0 & G_{31} & 0 \\ 0 & 0 & 0 & 0 & 0 & G_{12} \end{bmatrix} \begin{Bmatrix} \sigma_{11} \\ \sigma_{22} \\ \sigma_{33} \\ \sigma_{23} \\ \sigma_{31} \\ \sigma_{12} \end{Bmatrix} \qquad \text{(V-1)}$$

Symmetry of the compliance matrix requires

$$\frac{\nu_1}{E_1} = \frac{\nu_2}{E_2} = \frac{\nu_3}{E_3} \qquad \text{(V-2)}$$

For plane strain $\epsilon_{33} = 0$, $\gamma_{23} = \gamma_{31} = 0$

$$\epsilon_{33} = \left\langle -\frac{\nu_1}{E_1} - \frac{\nu_2}{E_2} \right\rangle \begin{Bmatrix} \sigma_{11} \\ \sigma_{22} \end{Bmatrix} + \frac{1}{E_3} \sigma_{33} = 0 \qquad \text{(V-3)}$$

Using Eq. (V-2),

$$\sigma_{33} = \nu_3 \langle 1 \quad 1 \rangle \begin{Bmatrix} \sigma_{11} \\ \sigma_{22} \end{Bmatrix} \qquad \text{(V-4)}$$

Substituting Equation (V-4) in Equation (V-1),

$$\begin{Bmatrix} \epsilon_{11} \\ \epsilon_{22} \end{Bmatrix} \quad \begin{bmatrix} \frac{1}{E_1}(1-\nu_1\nu_3) & \frac{-\nu_2}{E_2}(1+\nu_3) \\ \frac{-\nu_2}{E_2}(1+\nu_3) & \frac{1}{E_2}(1-\nu_2\nu_3) \end{bmatrix} \begin{Bmatrix} \sigma_{11} \\ \sigma_{22} \end{Bmatrix} \qquad \text{(V-5)}$$

Inverting

$$\begin{Bmatrix} \sigma_{11} \\ \sigma_{22} \end{Bmatrix} = \frac{1}{(1-\nu_1\nu_3)(1-\nu_2\nu_3) - k\nu_2^2(1+\nu_3)^2} \begin{bmatrix} E_1(1-\nu_2\nu_3) & E_1\nu_2(1+\nu_3) \\ E_1\nu_2(1+\nu_3) & E_2(1-\nu_1\nu_3) \end{bmatrix} \begin{Bmatrix} \epsilon_{11} \\ \epsilon_{22} \end{Bmatrix} \qquad \text{(V-6)}$$

where $k = \frac{E_1}{E_2}$

Upon development of fracture surface in an element, the plane of the crack can be regarded as a plane of mechanical symmetry. Also the crack plane is a principal plane for the element. This involves an assumption that the crack is planar and extends throughout the element. It appears to be reasonable for sufficiently small element size.

Assuming that σ_{11} corresponds to the stress normal to the fracture plane, the elastic modulus E_1 is reduced to a very small value. The element is still capable of withstanding stresses σ_{22} parallel to the crack plane. However, when σ_{22} also attains values such that another fracture plane develops within an element, the material cannot sustain any load. This is modelled by letting E_2 also become very small.

As crack orientation may not be along the reference directions, it is necessary to transform the stress-strain relationship from the principal axes to the reference

axes. Let the angle of rotation be β. Then from Figure (A-4)

$$\beta = \gamma - \alpha \tag{V-7}$$

where γ = the angle between σ_x and σ_1

α = the angle between σ_2 and the fracture plane

For Griffith failure criterion, it can be shown that

$$\alpha = \tan^{-1} \left\{ \left[(k-1) \sin^2\theta + 1 - \sqrt{(k^2 - 1) \sin^2\theta + 1} \right] \Big/ \tfrac{1}{2} (1 - k) \sin 2\theta \right\} - \theta \tag{V-8}$$

where $k = \sigma_2 / \sigma_1$, and θ is identical to β defined by A-4 in Appendix A.

For the modified Griffith criterion,

$$\alpha = \frac{\pi}{4} - \theta \tag{V-9}$$

where θ is the same angle as β defined by Eq. (A-15) in Appendix A.

Let the relation between principal strains and strains in global coordinates be represented by

$$\left\{ \epsilon_p \right\} = \left[J \right] \left\{ \epsilon \right\} \tag{V-10}$$

Here $\left\{ \epsilon_p \right\}$, $\left\{ \epsilon \right\}$ are the strains referred to the principal axes and the reference axes respectively and

$$\left[J \right] = \begin{bmatrix} \cos^2 \beta & \sin^2 \beta & \cos \beta \sin \beta \\ \sin^2 \beta & \cos^2 \beta & - \cos \beta \sin \beta \end{bmatrix} \tag{V-11}$$

The relation between principal stress and stresses in the reference frame is

$$\left\{ \sigma \right\} = \left[J^T \right] \left\{ \sigma_p \right\} \tag{V-12}$$

It can be shown that if

$$\left\{ \sigma \right\} = \left[D \right] \left\{ \epsilon \right\} \tag{V-13}$$

and

$$\left\{ \sigma_p \right\} = \left[D_p \right] \left\{ \epsilon_p \right\} \tag{V-14}$$

then

$$\left[D \right] = \left[J \right]^T \left[D_p \right] \left[J \right] \tag{V-15}$$

5.5. Pre-existing Discontinuities

Pre-existing discontinuities in rock may be initial weak planes or initial open joints. In either case, strength of material would be reduced. For an initial open joint, the orthotropic stress-strain relation described in Section 5.4. can be used, and the initial fracture angle would be defined by the initial crack plane or by the inclination of joint. In the case of initial weak plane, we propose an orthotropic stress-strain relation with certain amount of shear resistance along the weak plane.

A relation similar to those in Section 5.4 can be written as

$$\left[D'_p\right] = \frac{1}{\zeta_1}\begin{bmatrix} E_1 & \nu_2 E_1 & 0 \\ \nu_2 E_1 & E_2 & 0 \\ 0 & 0 & G\,\zeta_1 \end{bmatrix} \quad \text{for plane stress} \qquad \text{(V-16)}$$

where $\zeta_1 = 1 - k\nu_2^2$

$$G = \frac{E_1}{2\,(1 + k^2\,\nu_1)}$$

and for plane strain,

$$\left[D'_p\right] = \frac{1}{2}\begin{bmatrix} E_1\,(1 - \nu_2\nu_3) & E_1\,\nu_2\,(1 + \nu_3) & 0 \\ E_1\,\nu_2\,(1 + \nu_3) & E_2\,(1 - \nu_1\,\nu_3) & 0 \\ 0 & 0 & G\,\zeta_2 \end{bmatrix} \qquad \text{(V-17)}$$

where $\zeta_2 = (1 - \nu_1\,\nu_3)\,(1 - \nu_2\,\nu_3) - k\,\nu_2^2\,(1 + \nu_3)^2$.

Following a procedure similar to that in Section 5.4, we obtain

$$\left[D'\right] = \left[J'\right]^T \left[D'_p\right] \left[J'\right]$$

where $\left[J'\right] = \left[\frac{J}{K}\right]$

$$\left[K\right] = \langle -\sin 2\beta \quad \sin 2\beta \quad \cos 2\beta \rangle$$

In general, the fracture plane does not coincide with the weak plane. The elasticity matrix in such a case can be obtained by deleting the third column and the third row of $\left[D'\right]$, and in the transformation, β is replaced by the angle between the fracture plane and the weak plane.

To deal with closure of open joints, it was assumed that the crack opening is planar

and that it can be measured normal to the crack plane. This measured quantity can be either the initial opening of a preexisting joint or the equivalent opening tolerance for an element fractured under a load increment to close again. The initial opening is equivalent to a set of nodal displacements corresponding to the initial opening. The equivalent nodal displacements thus obtained were further transformed into element strains, and the possibility of closing was checked on the basis of computed strains.

5.6. Incremental Excavation

Execution of an excavation project is a sequential process. In discretized analysis procedure, the results at the end of one stage constitute the initial state for the next step. History of the system in terms of stresses and deformations is determined corresponding to the discrete steps in excavation or construction.

For each stage, an incremental loading analysis was used. The equilibrium equation corresponding to each load increment can be written as

$$\left[K_i \right] \left\{ \Delta r_i \right\} = \left\{ \Delta P_i \right\} \qquad \text{(V-18)}$$

where i denotes the ith increment. To take account of the effect of crack propagation, $\left[K_i \right]$ was modified for elements cracked and $\left\{ \Delta P_i \right\}$ corrected to include the load resulting from the releasing of the initial stresses from the cracks. The total displacement and loading for N increments at jth stage are given by

$$\{r_j\} \quad \sum_{i=1}^{N} \{\Delta r_i\} \tag{V-19}$$

and

$$P_j = \sum_{i=1}^{N} \{\Delta P_i\} \tag{V-20}$$

The final displacement and loading for a complete construction of M stages are

$$\{r\} = \sum_{j=1}^{M} \sum_{i=1}^{N} \{\Delta r_i\} \tag{V-21}$$

$$\{P\} = \sum_{j=1}^{M} \sum_{i=1}^{N} \{\Delta P_i\} \tag{V-22}$$

5.7. Examples of Application

The procedure developed, for analysis of progressive failure of rock following Griffith's or modified Griffith theory, in accordance with the mathematical model described in the preceding paragraphs were used to solve several problems. On cracking of concrete beams, considerable volume of data is available. The procedures were also applied to analysis of crack propagation in tunnels of circular and elliptical shape. Effect of incremental construction/excavation was allowed for. A simple model was used to simulate loading in underground blasting.

5.7.1. Crack Propagation in Concrete Beams

Application of the finite element method in the study of cracking in reinforced concrete members was first proposed by Ngo and Scordelis in 1967. In their analysis,

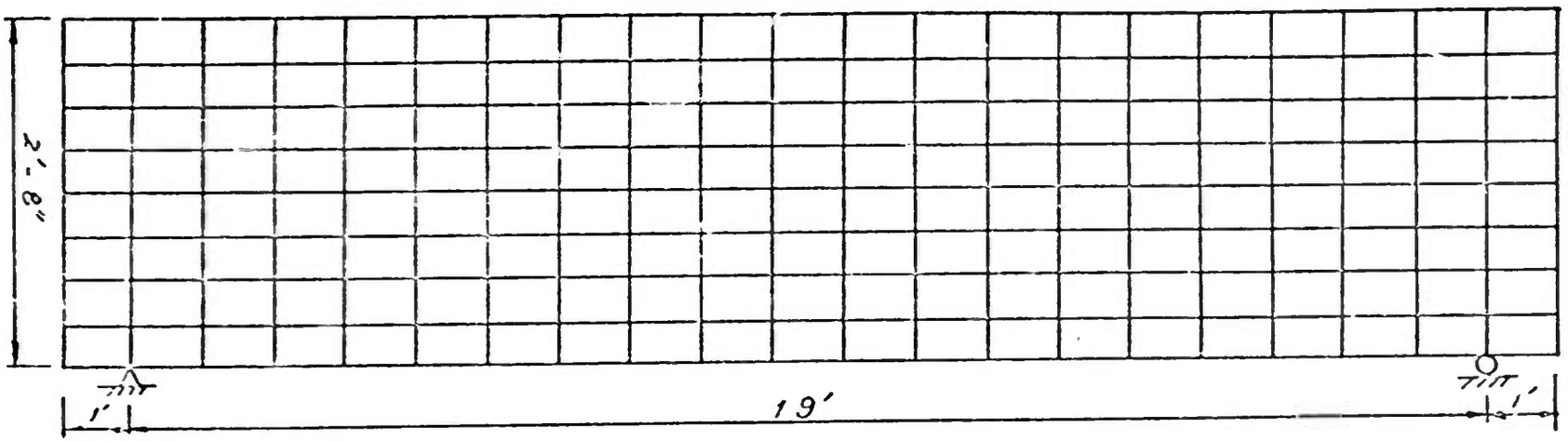

a. System Analyzed

Number of Nodes = 198
Number of Elements = 168

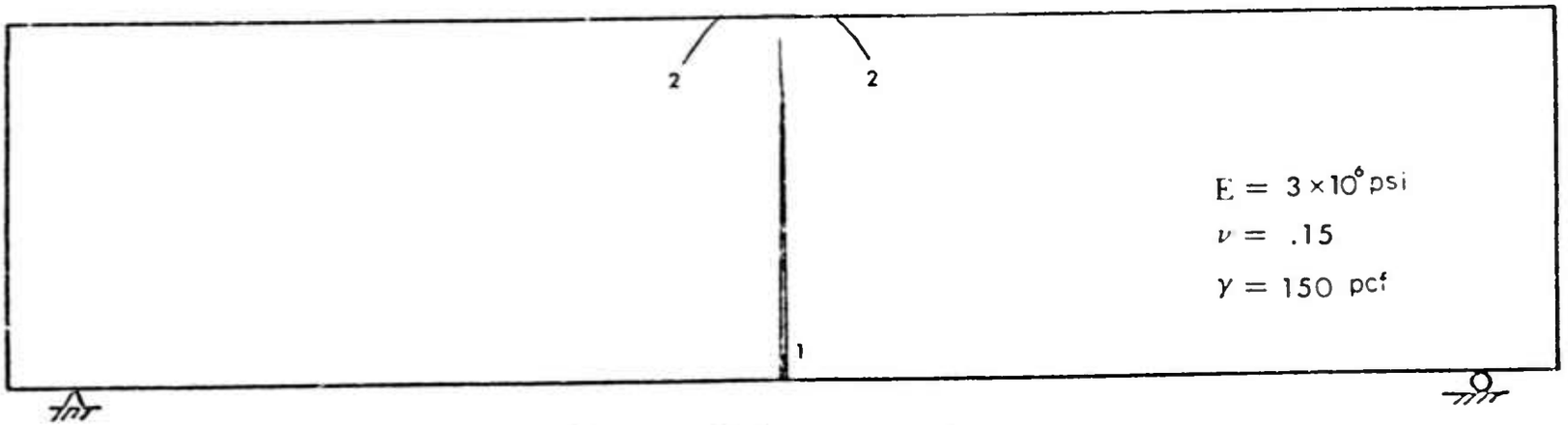

b. Crack Pattern Under Dead Load

FIG. V-6. Crack Propagation in Plain Concrete Beam

two-dimensional triangular elements were used for idealization of concrete and steel reinforcement. The bond action between concrete and steel bars was modeled by special links. Geometry of crack was defined by disconnecting nodes as preexisting openings and progressive cracking in concrete was not allowed. Nilson (1968) incorporated an incremental loading process along with a simple cracking criterion allowing for progressive cracking. Again, the cracks were defined by disconnecting nodes when the average stress at that nodal point satisfied the cracking criterion.

Using the method of analysis described in preceding sections, sequential cracking in simply supported beams was investigated. Results of these investigations are summarized in the following paragraphs.

A. A Plain Concrete Beam

Fig. (V-6) gives the configuration of a simply supported beam without any reinforcement. Crack commenced at midspan and propagated throughout the cross-section. A collapse mechanism developed when the crack extended to the top element. Severe compression caused by the hinge action produces two secondary cracks which follow the modified Griffith criterion.

B. A Concrete Beam with Tension Reinforcement

A finite element representation of a reinforced concrete beam with 19 feet effective span and a depth of 32 inches is shown in Fig. (V-7a). Two concentrated loads of 300 lbs. each were applied at two one-third points along the total span. The sequence of cracking is indicated by numbers as shown in Fig. (V-7b) and (V-7c). The cracking may be roughly grouped into three stages. Upon application of the load,

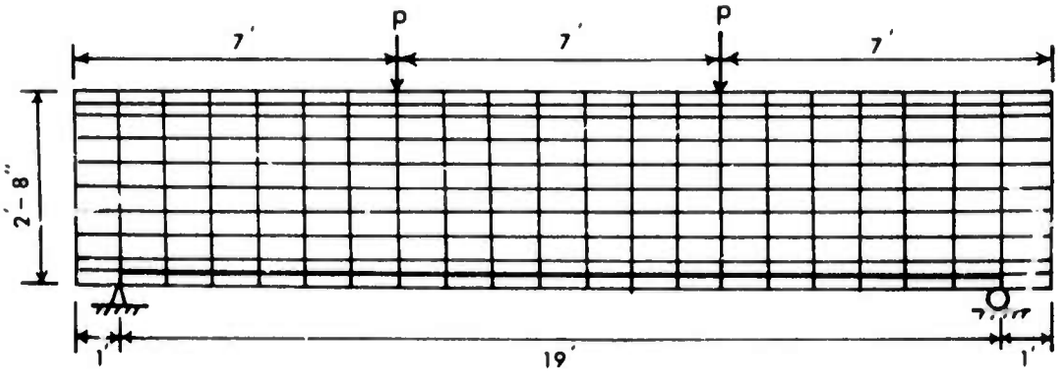

a. System Analyzed Number of Nodes = 242

Number of Elements 229

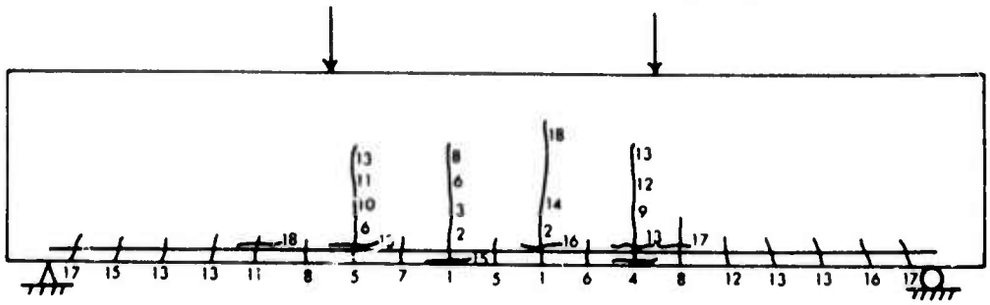

b. Sequence of Cracking

CONCRETE:
$E = 3 \times 10^6$ psi
$\upsilon = 0.15$
$\gamma = 150$ pcf
$\sigma_t = 75$ psi

REINFORCEMENT:
$E = 3 \times 10^7$ psi
$A_s = 0.32$ in^2/in

LOAD: P = 300 lbs

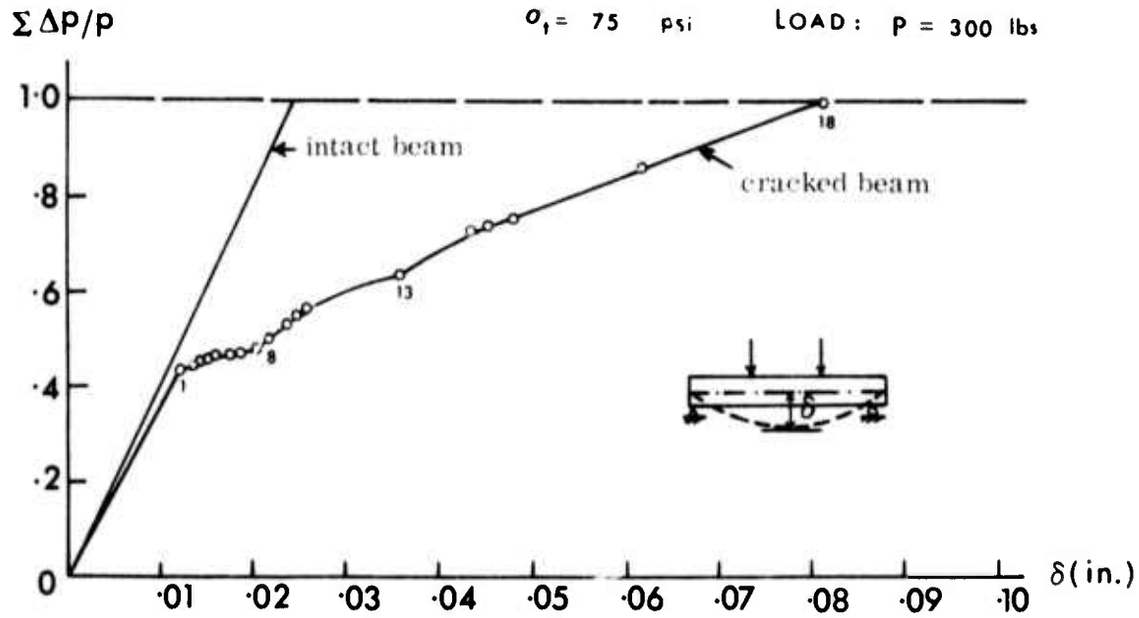

c. Load-Displacement Curve

FIg V-7. Progressive Cracking of Simple Reinforced Concrete Beam

primary eracks start and propagate in the middle third of the span and stop after travelling eertain distanees. Seeondary eraeks then follow and spread over the outer one-third of the span. Some bond slippage assoeiated with extension of the primary eraeks oeeurs at the last stage. The load-defleetion eurve in Fig. (V-7e) refleets the eontinuous proeess of eraeking.

C. A Conerete Beam with Tension Reinforeement (Bresler and Scordelis, 1963)

A series of tests on reinforeed eonerete beams was eondueted by Bresler and Seordelis (1963). The present method of analysis was applied to two of these beams to prediet the cracking behavior.

Fig. (V-8) shows the configuration of beam OA-2 and A-2 in the aforementioned tests. All the dimensions and material properties used are taken from the paper by Bresler and Seordelis (1963) (See Table V-1, V-2).

The eraeking sequenee for load up to 45 kips is shown in Fig. (V-9), and the load-midspan defleetion eurve is given in Fig. (V-10). Agreement with the experimental data both in the eraek patterns and the load-defleetion eurves is exeellent. Referring to Fig. (V-10), inereasing deviation of the eurve obtained from the finite element analysis from the eurve given by tests would be expeeted with further inerease in load.

D. A Concrete Beam with Tension, Compression and Web Reinforeement

In addition to the tension reinforcement in beam OA-2, compression as well as web reinforeement was used in beam A-2. Again the eraeking sequenee and eraek pattern were in agreement with experimental data. The midspan defleetion eurve obtained at a total load of 62 kips was slightly lower than the eurve given by the test, but in general, agreement was exeellent (see Figs. V-11, V-12).

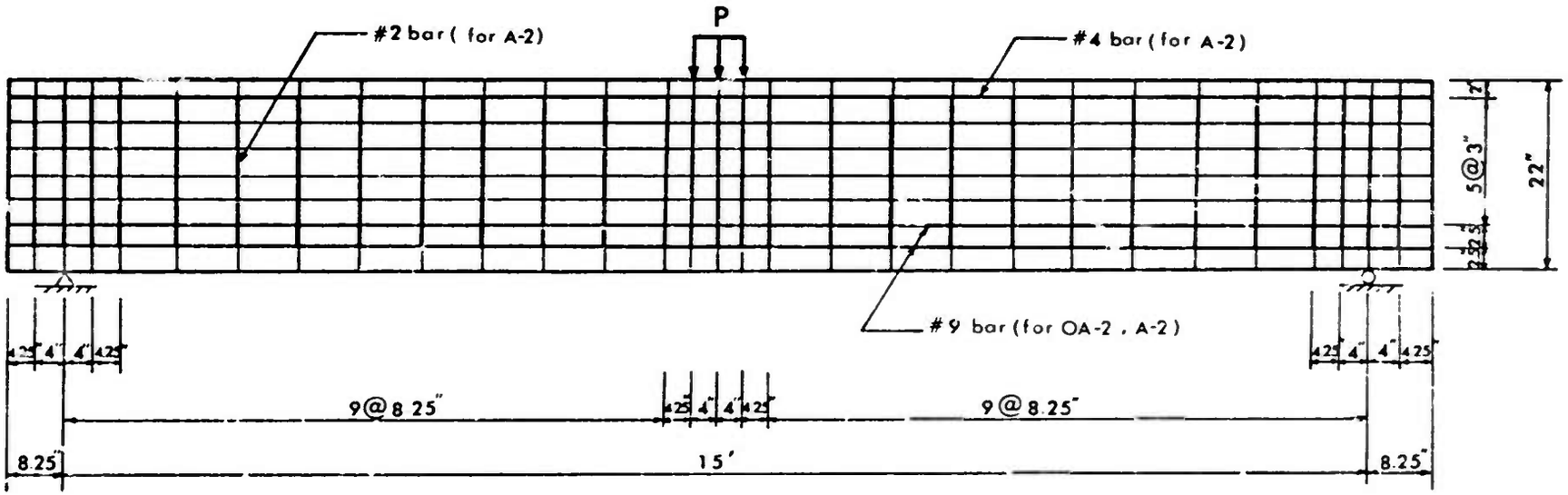

FIG. V-8. Finite Element Idealization of Reinforced Concrete Beams OA-2 and A-2

TABLE V-1. DIMENSIONS & PROPERTIES OF R.C. BEAMS

	CONCRETE		BEAM DIMENSIONS				RATIO	REINFORCEMENT					
SPECIMEN NO.	f_c' ksi	f_r' ksi	b in.	h in.	d in.	L ft.	a/d	#9 bars	P_t percent	#4 bars	p' percent	spacing #2 stirrups in.	$r f_y$ psi
OA-2	3.44	.629	12.	22.	18.35	15.	5.	5	2.27	0	0	—	0
A-2	3.52	.540	12.	22.	18.27	15.	5.	5	2.27	2	.182	@ 1/4	47.2

Note: $E_c = 3 \times 10^6$ psi.
$\nu = 0.15$

TABLE V-2. PROPERTIES OF STEEL REINFORCING BARS

BAR SIZE, #	9	4	2
GRADE	high strength	intermediate	intermediate
YIELD STRENGTH fy, ksi.	80.5	50.1	47.2
ULTIMATE STRENGTH fu, ksi.	138.9	78.6	62.3
MODULUS OF ELASTICITY Es, ksi.	31.6×10^3	29.2×10^3	27.5×10^3
WEIGHT PER LINEAL FT. lb.	3.47	.665	.17
NOMINAL AREA sq. in.	1.02	.195	.05

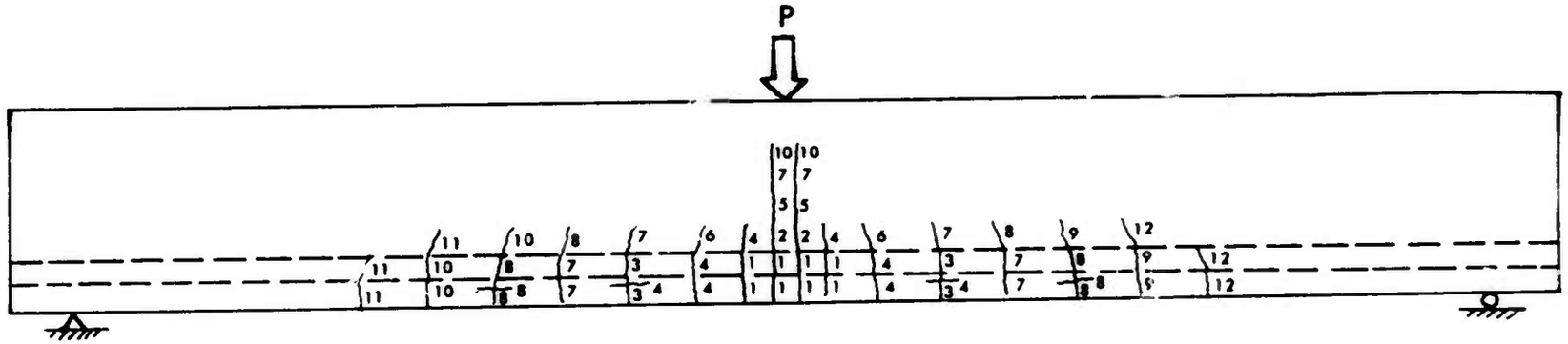

FIG. V-9. Cracking Sequence of Beam OA-2

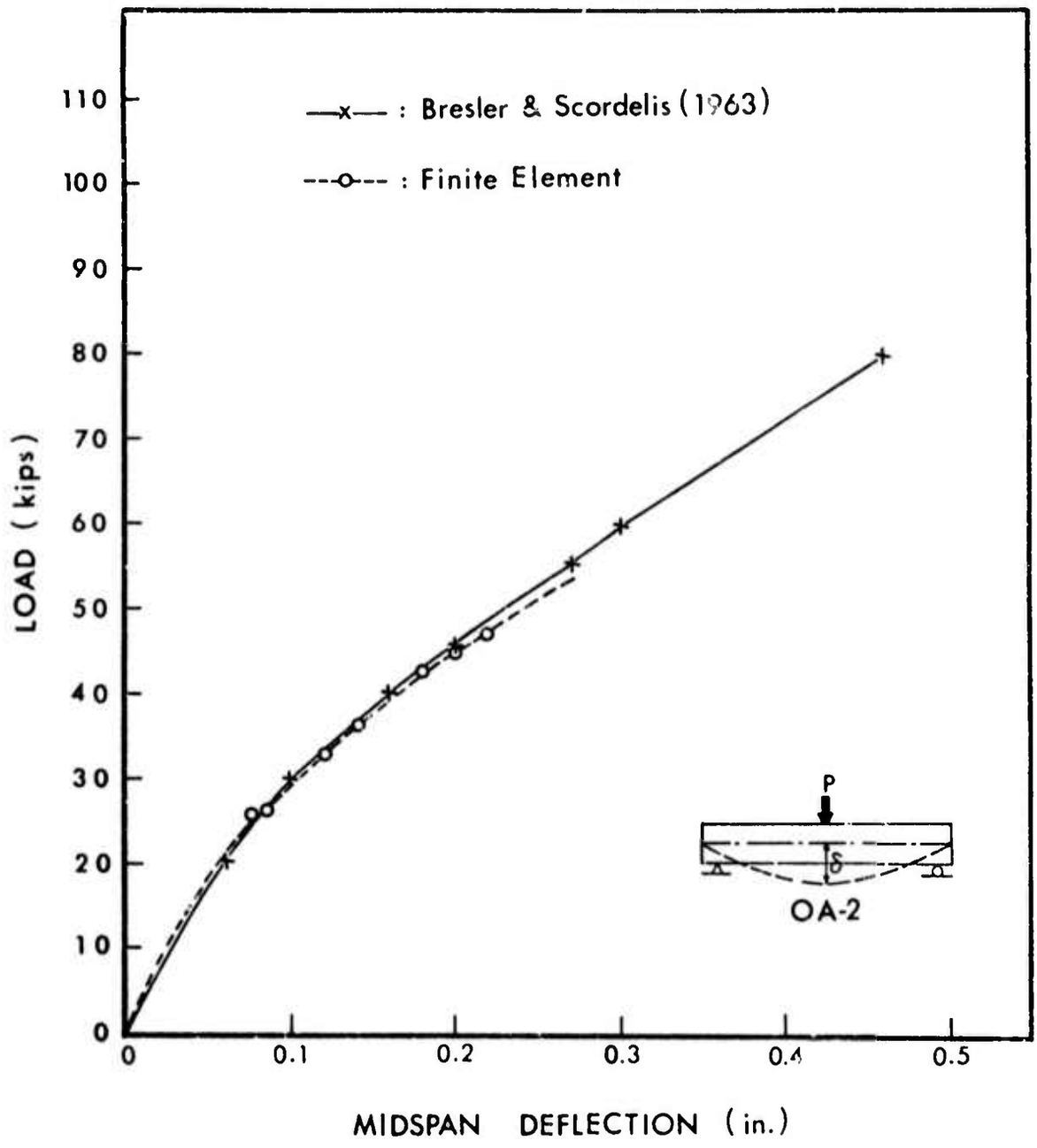

FIG. V-10. Load-Deflection Curve for Beam OA-2

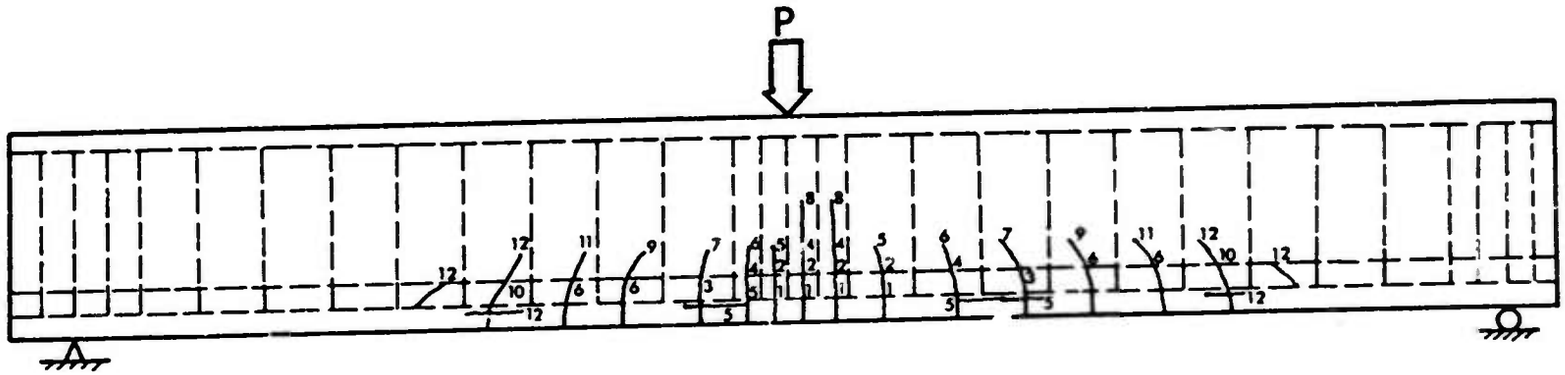

FIG. V-11. Cracking Sequence of Beam A-2

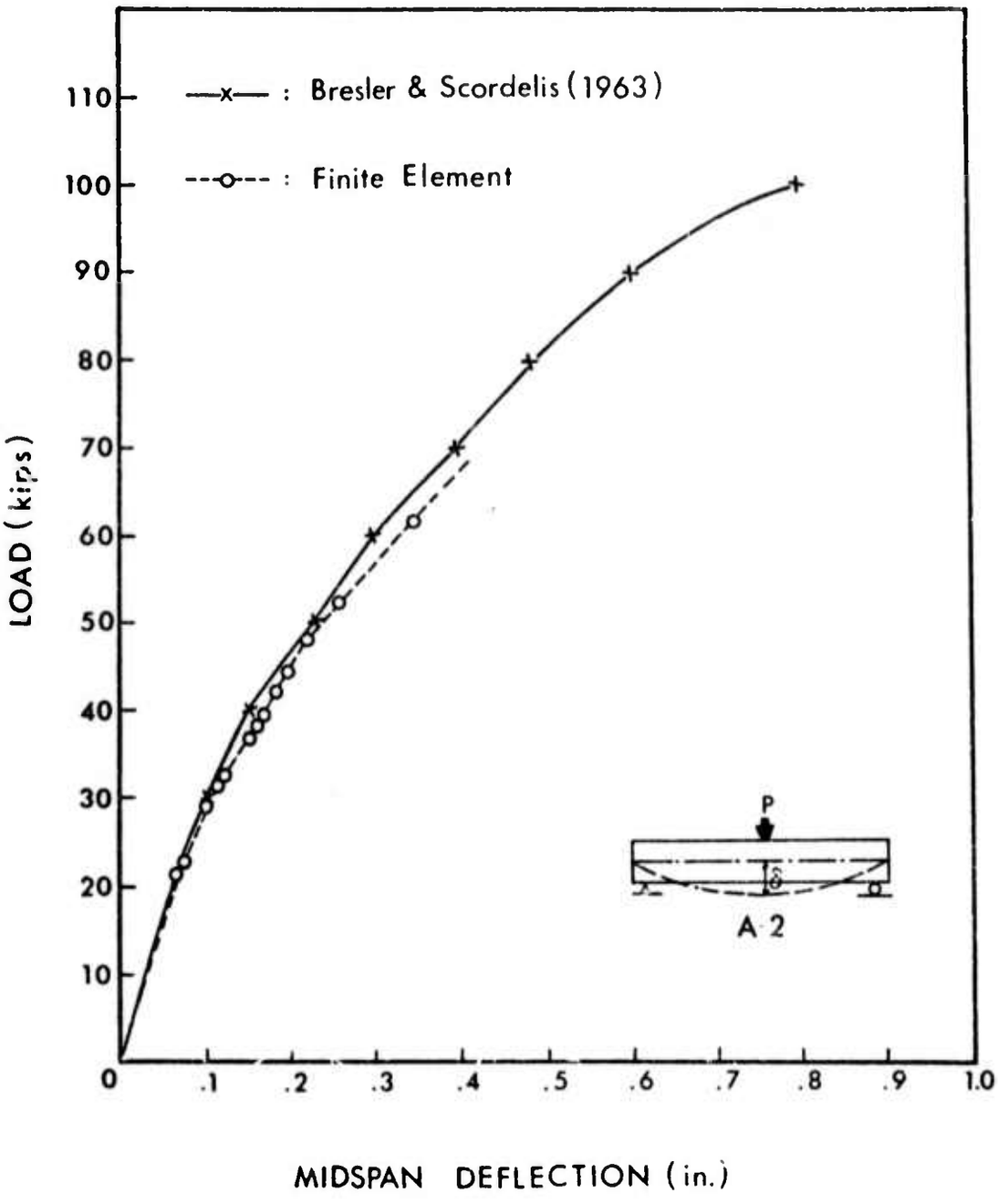

FIG. V-12. Load-Deflection Curve for Beam A-2

5.7.2. Progressive Cracking Around a Semi-Circular Tunnel

The configuration of a lined semi-circular tunnel analyzed by Zienkiewicz et al. (1968) using the no-tension approach is shown in Fig. (V-13). Limitation of this approach has been discussed in Section 5.1. Fig. (V-15) shows the initial tension zones in the linear elastic solution. This is similar to the solution obtained by Zienkiewicz (Fig. (V-14a)). Upon application of fracture criteria, the crack was found to initiate and propagate sequentially (Fig. V-16). Figs. (V-16, V-17, V-18) show that stress redistribution around the tunnel resulted in reduction of the tensile zones. The cracks occur mainly along the contact between the lining and the rock. Cracking of this kind may be interpreted as failure of bond between the concrete lining and the rock.

5.7.3. Progressive Cracking Around an Elliptic Tunnel

One major concern during an incremental excavation in rock mass is fragmentation of the material caused by progressive fracture occurring in the vicinity of excavated area. To prevent such situation from occurring, supports or lining can be applied immediately following the excavation. A system consisting of an elliptic tunnel was used to study the progressive cracking in an incremental excavation process.

A. An Unlined Tunnel

Fig. (V-19a) shows a system assuming excavation to be completed in a single step. Fracture first commences in the surface of the tunnel, then proceeds upward layer by layer. The cracking sequence is shown in Fig. (V-19b).

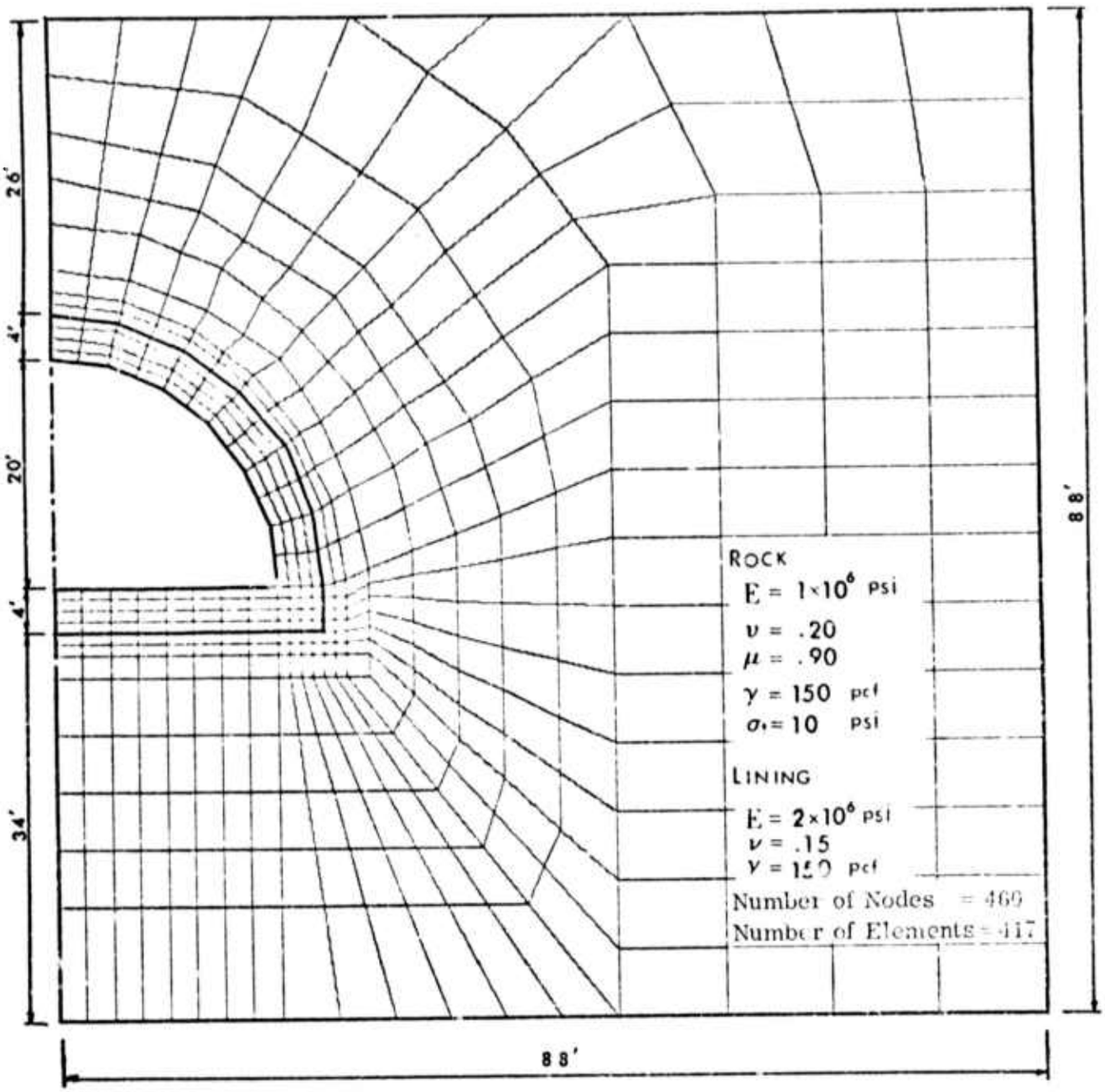

FIG. V-13 Configuration of a Semi-Circular Tunnel

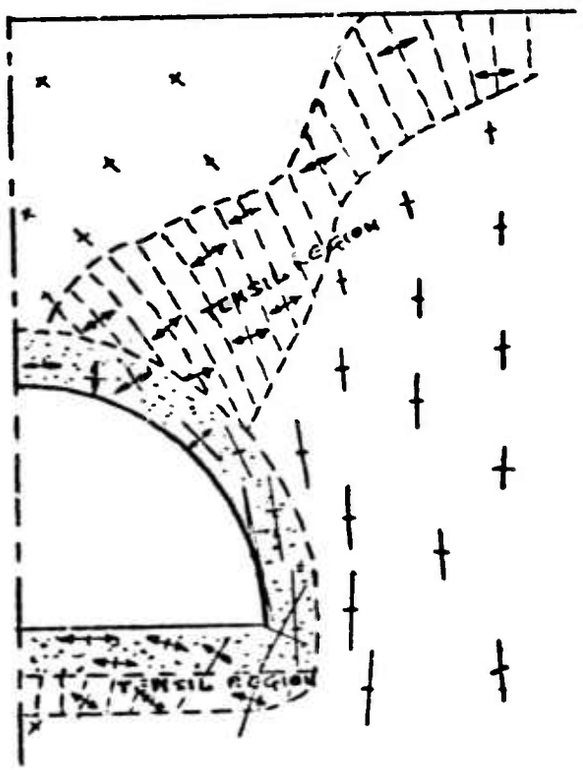

a. Initial Tensile Zones in Rock

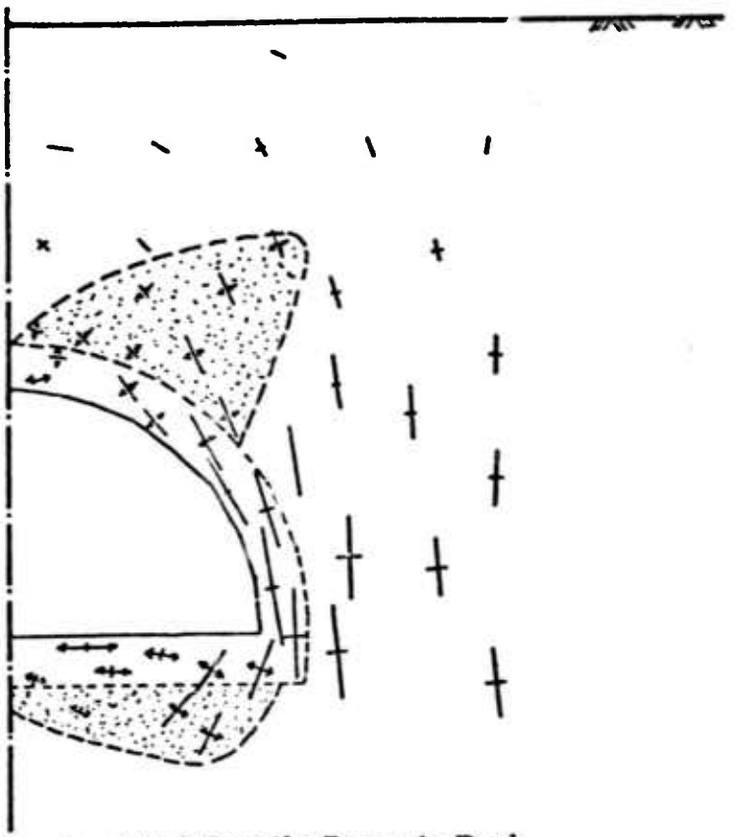

b. Final Tensile Zones in Rock

FIG. V-14 Zienkiewicz's Solution of Tunnel Problem

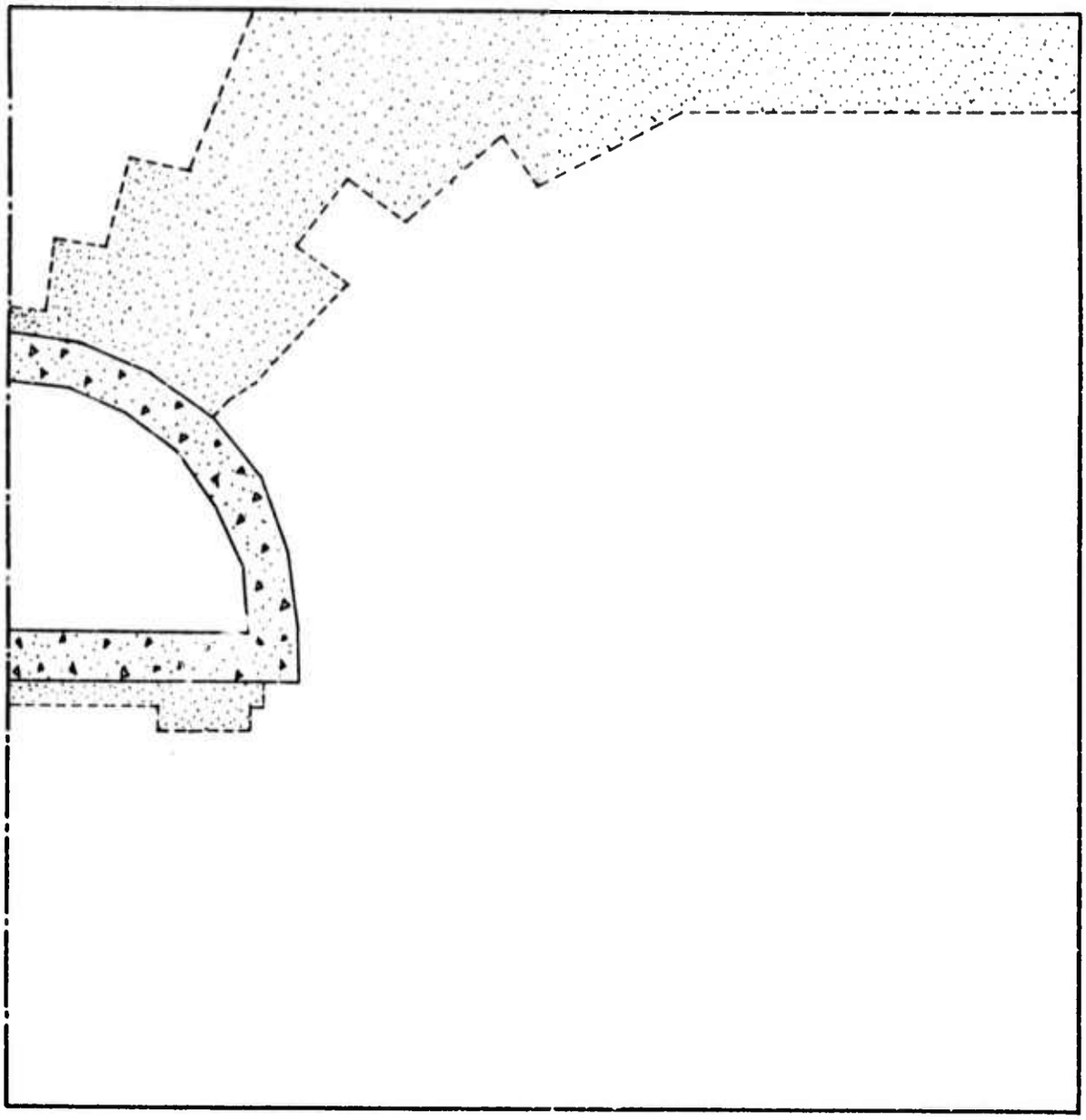

FIG. V-15 Initial Tensile Zones in Rock

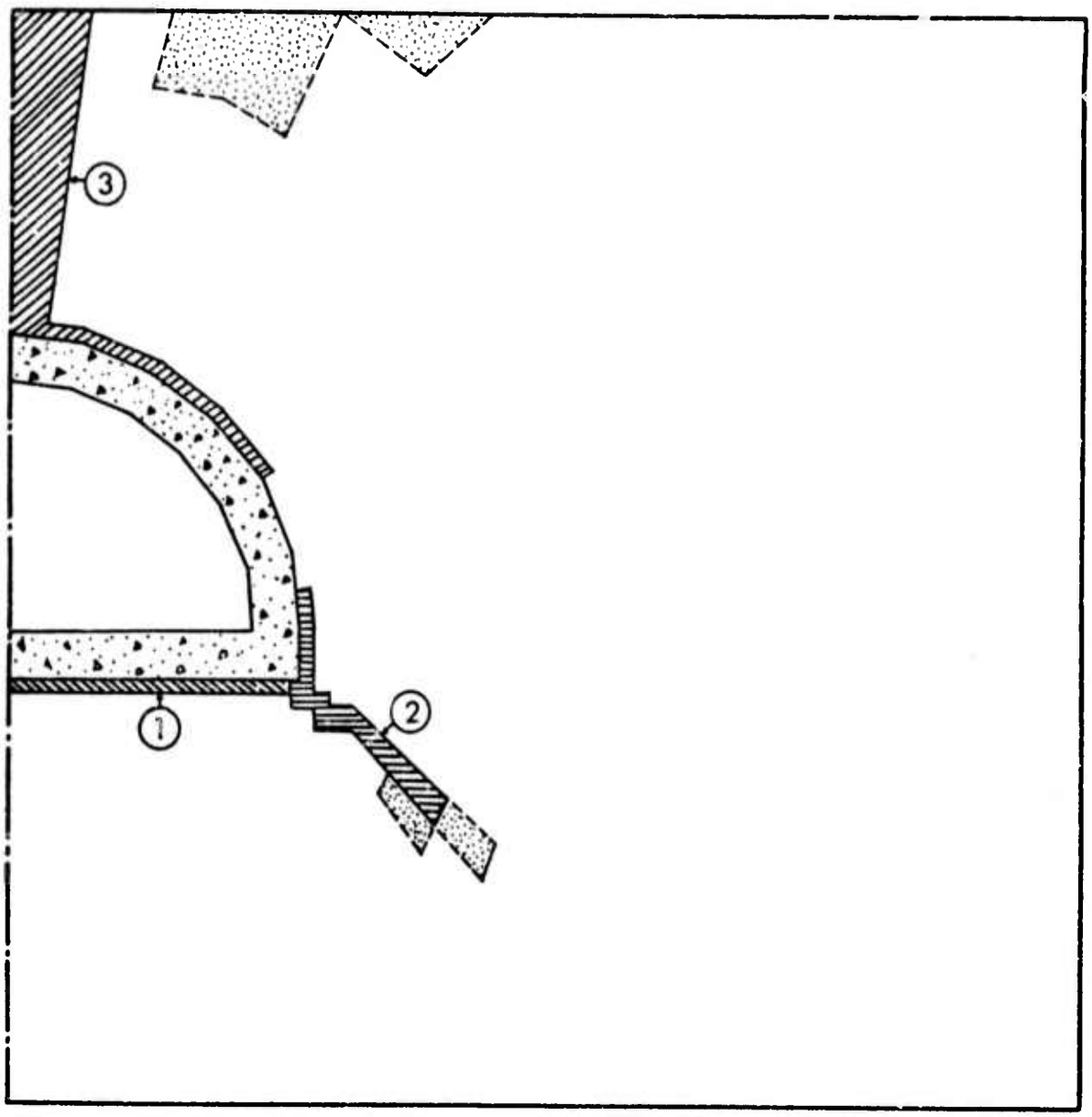

FIG. V-16 Sequence of Cracking and Final Tensile Zones in Rock

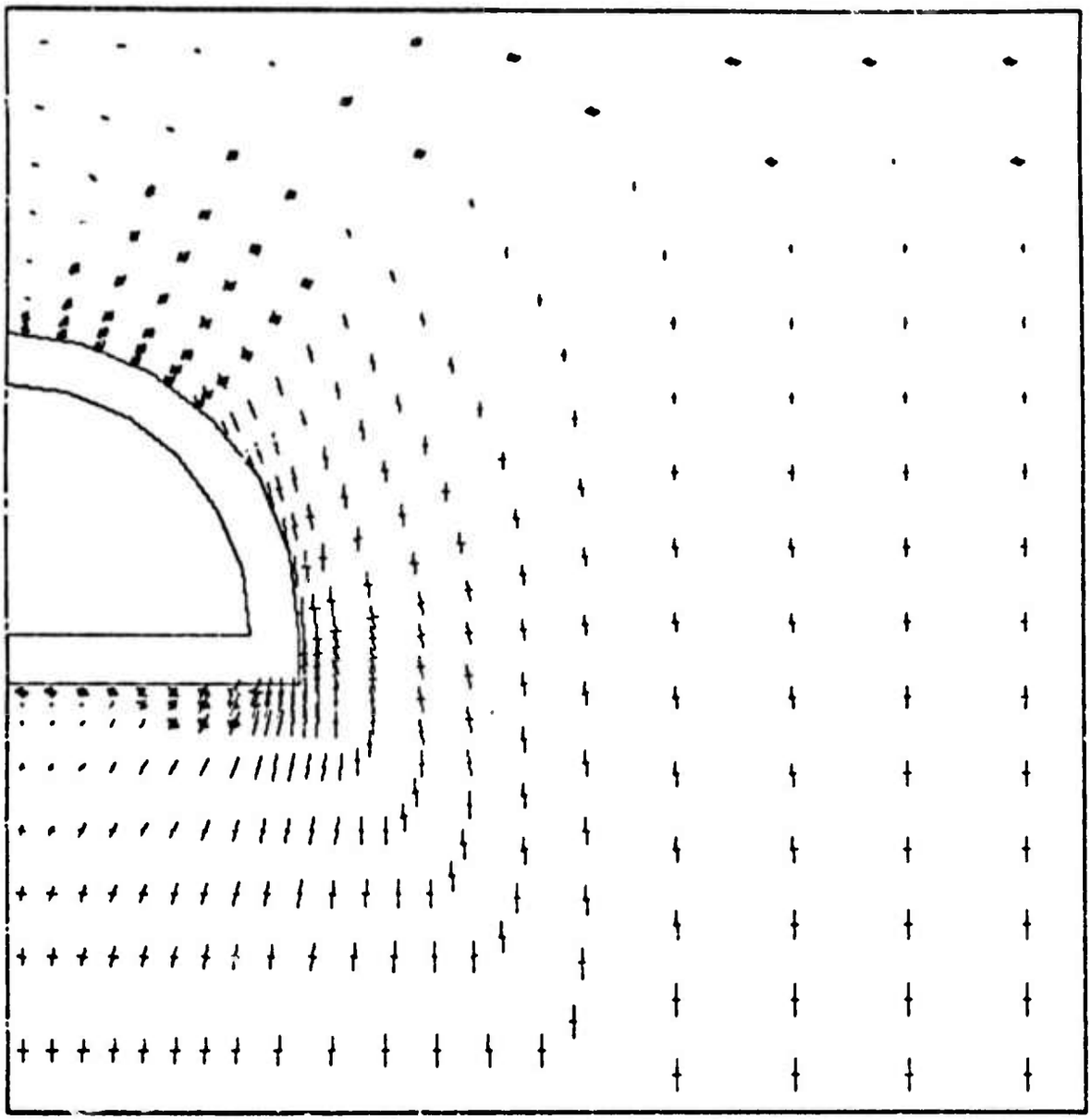

FIG. V-17 Initial Stress Distribution Around the Semi-circular Tunnel

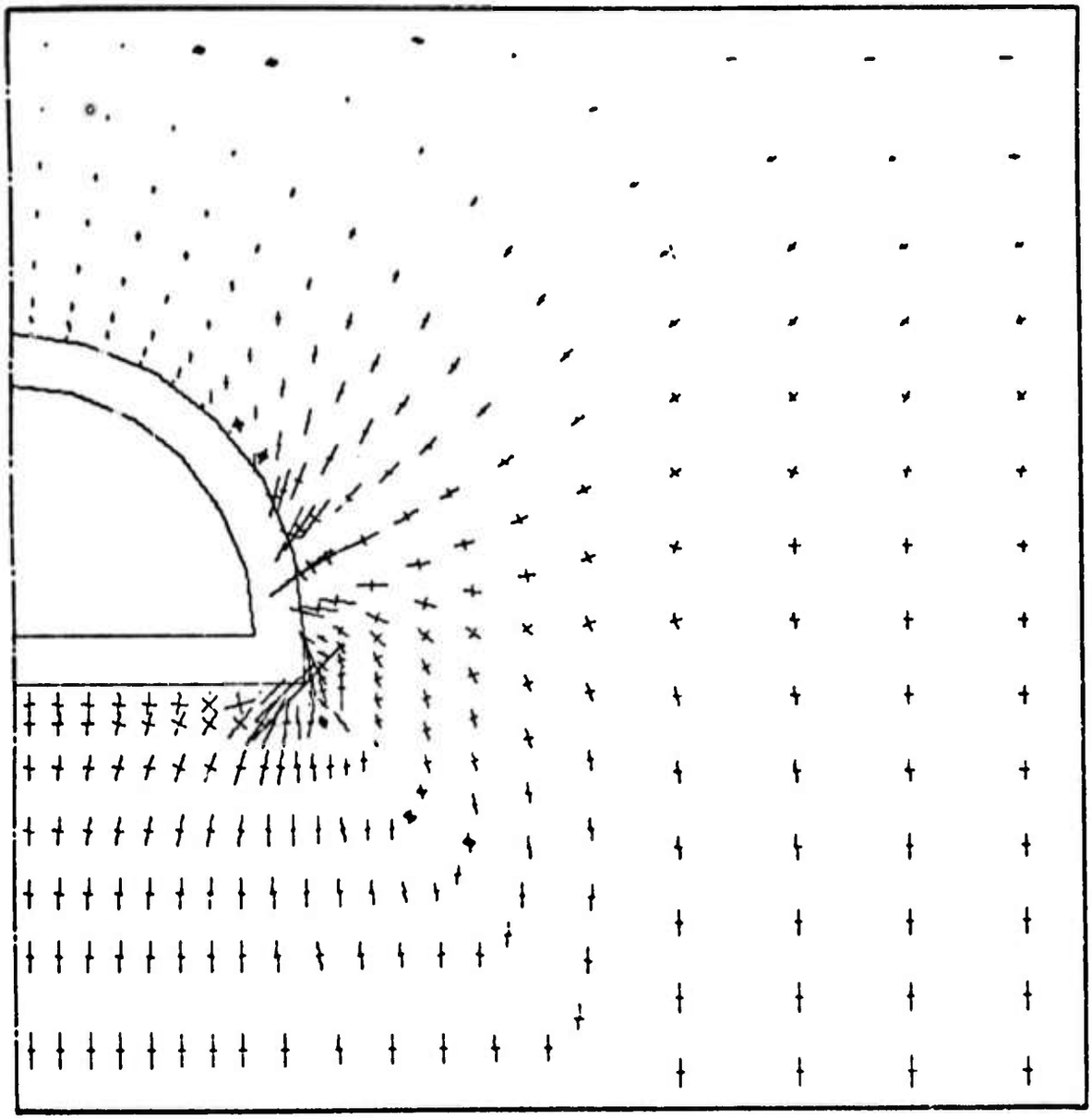

FIG. V-18 Final Stress Distribution Around the Semi-circular Tunnel

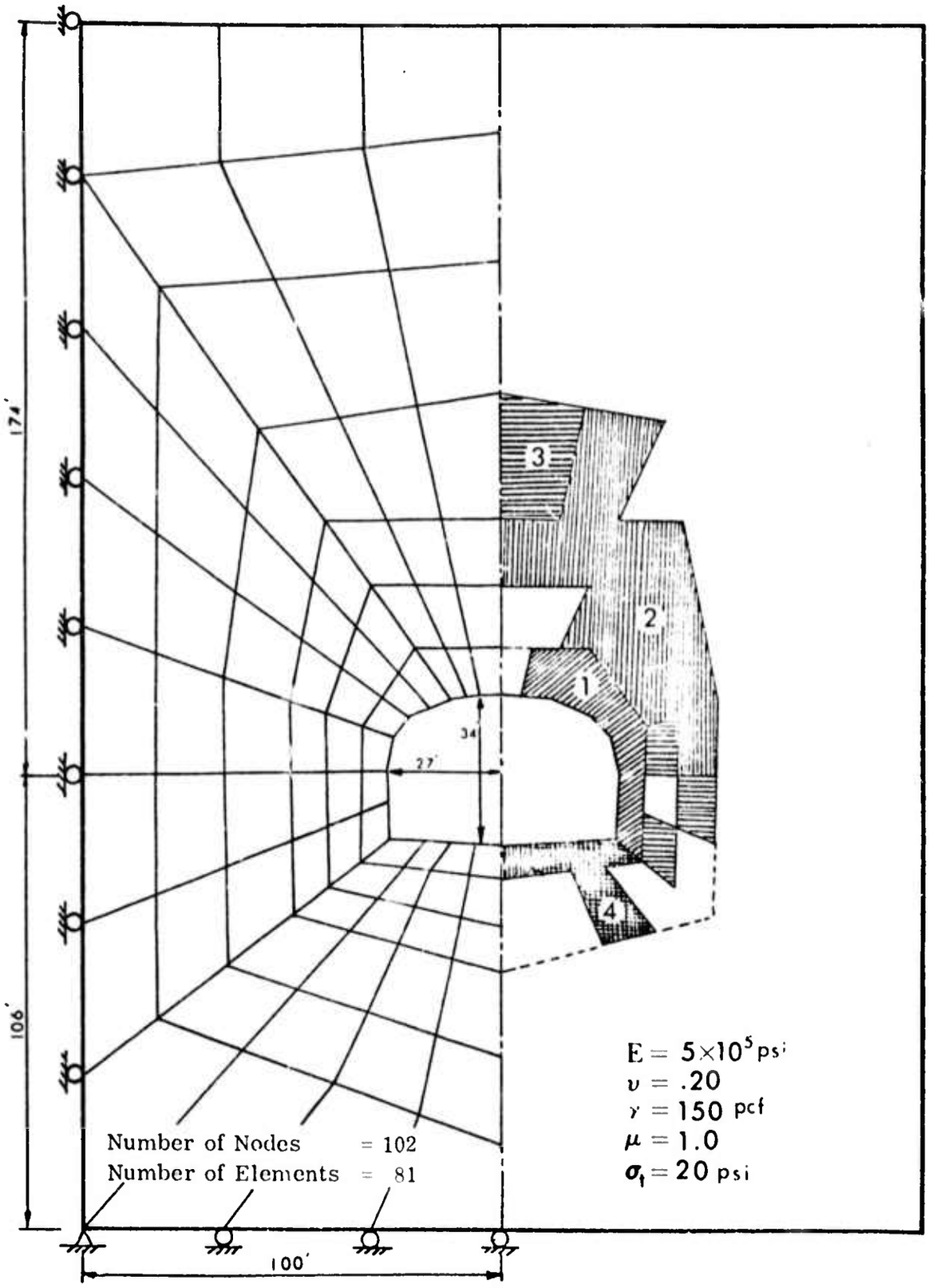

a. System Analyzed

b. Sequence of Cracking

FIG. V-19 Progressive Cracking Around an Eliptic Tunnel

It is noticed that the cracking sequence and the patterns of crack are not unique for a system. In fact, they are greatly influenced by the material properties. For example, if σ_t, the tensile strength, is the only varying parameter in the analysis, material having a higher value of σ_t would have less extensive cracking. Similarly, if μ, the internal coefficient of friction, is changed, the cracking sequence and the crack patterns will be different.

B. A Lined Tunnel

The system described in the preceding section was reanalyzed in three steps using $\mu = 0.8$ and $\sigma_t = 25$ psi (see Fig. (V-20)). Step one simulated excavation in a single step as in case A. Cracks appeared in the side wall of the tunnel as predicted by modified Griffith criterion and at the bottom by Griffith criterion. This was because of severe compressive stresses in the side wall while high tensile stresses occur at the tunnel invert and crown. Hatches in Fig. (V-20b) show the orientation of the cracks. In step two, concrete linirg was introduced. This provided the tunnel wall with some support due to the tendency of the concrete lining to deflect outwards under its own weight. The support effect is increased if increase in concrete temperature is allowed for or if the concrete/rock contact is pressure grouted. A region near the horizontal diameter developed double cracks in the first step. In the second step, one set of cracks in this region closed. No further cracking occurred at the end of this step (see Fig. (V-20c)). In the third step, a pressure of 2,000 psf was applied on the ground surface (Fig. (V-20d)). New cracks appeared at the base of the concrete lining, propagating downward at an angle of about 45 degrees to the right. Meanwhile the double crack appeared again near the horizontal diameter.

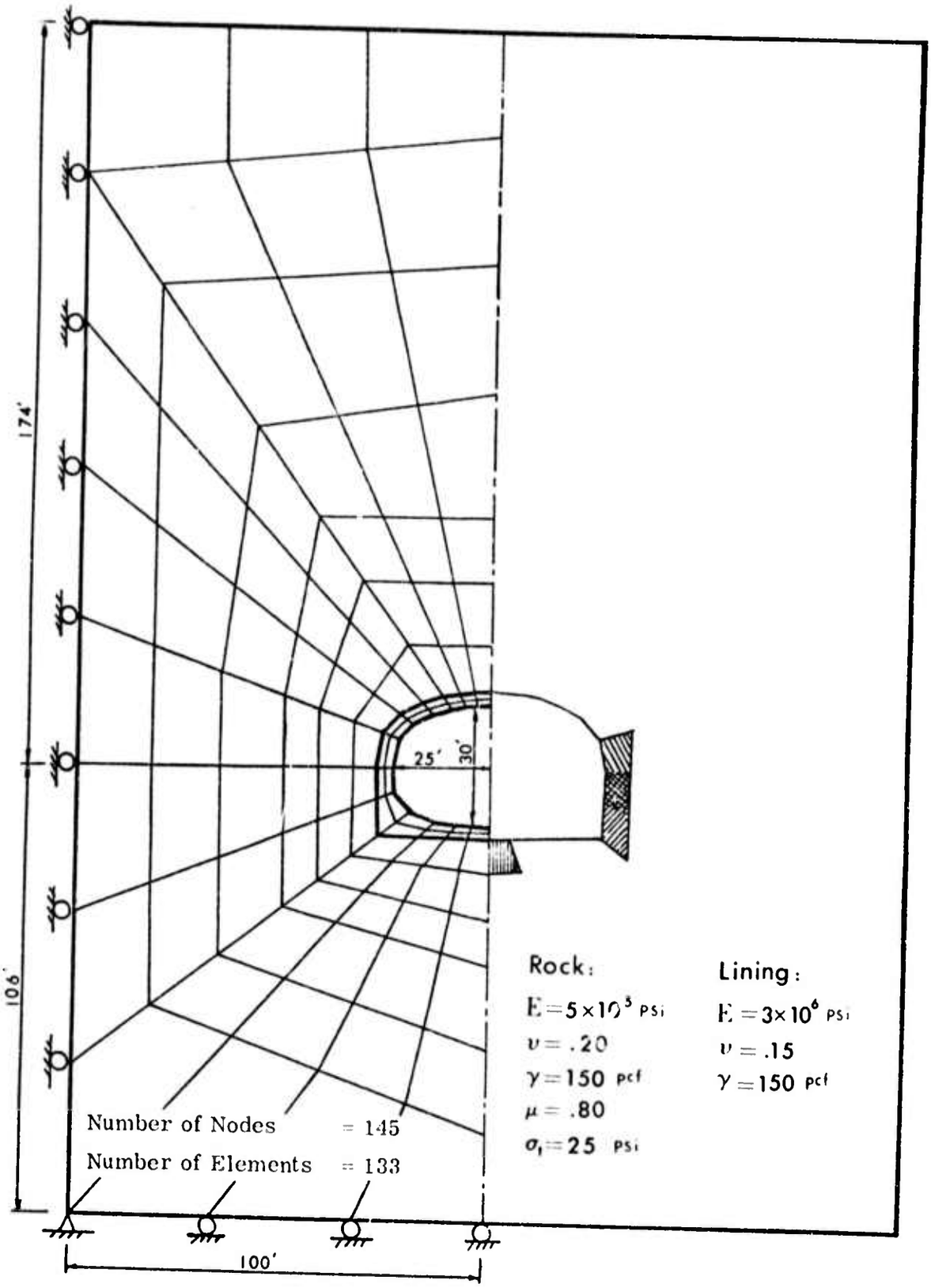

a. System Analyzed

b. Crack Orientations after Excavation

FIG. V-20 Incremental Analysis of An Elliptic Tunnel

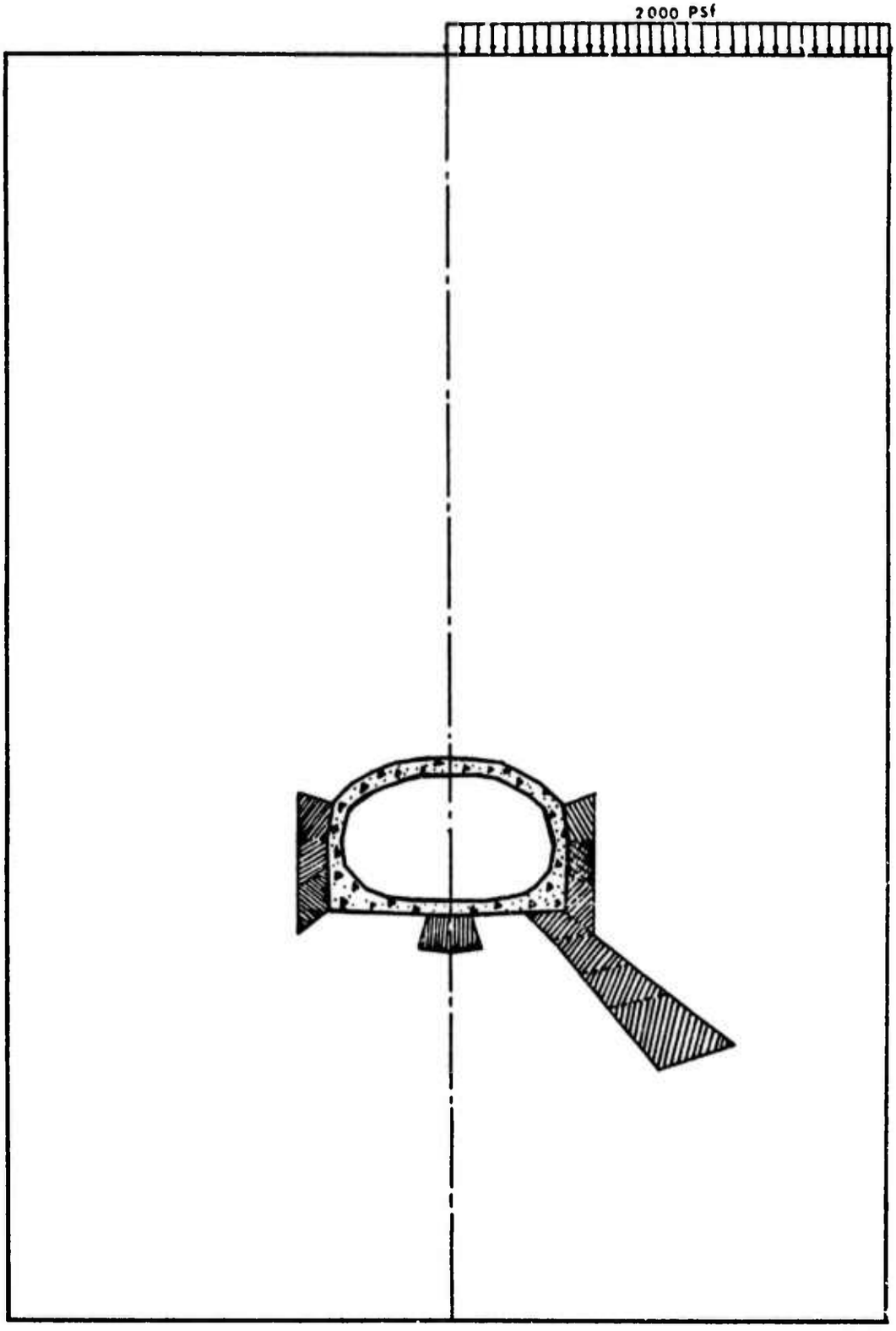

c. Crack Orientations After Placement of Lining

d. Crack Orientations After Application of Surface Loading

FIG. V-20 Incremental Analyses of an Elliptic Tunnel

5.7.4. Progressive Cracking in Blasting

The mechanism of breakage or fragmentation of a real rock caused by blasting is very complicated, yet the major mode of breakage is by brittle fracture. When a charge detonates in a borehole, blasting wave will propagate outward with very high velocity and pressure. The magnitude and direction of the velocity and pressure depend greatly on the properties of the charge and the rock. They also depend on the detonation process and the borehole geometry. Calculation of these quantities is by no means simple and various theories as well as empirical formulas have been proposed (e.g. Brown, 1956).

Due to the radial overflow of material accompanying the blasting wave, the pressure in both tangential and radial directions will decrease while radial cracks appear and propagate. Interaction between radial cracks and the tensile stress wave reflected by free surface may increase the tensile stress at the tip of those cracks which are parallel to the curved wave front. Tests on plexiglass mentioned by Persson et.al. (1970) concluded that cracks propagating in a direction at an angle 40 to 80 degrees to the normal of the free surface have a greater propagation velocity.

A system shown in Fig. (V-21) was analyzed as to simulate a bench type blasting . Inertial effects were not considered in this analysis, nor was decay of pressure due to gas entering the cracks allowed for. The ratio of the depth of rock to the diameter of the hole was 20. The effect of detonation of a charge was simulated as sudden application of a radial pressure on the perimeter of the hole. Three different values of the pressure intensity viz., 2000, 3000, 4000 psi, were considered. The

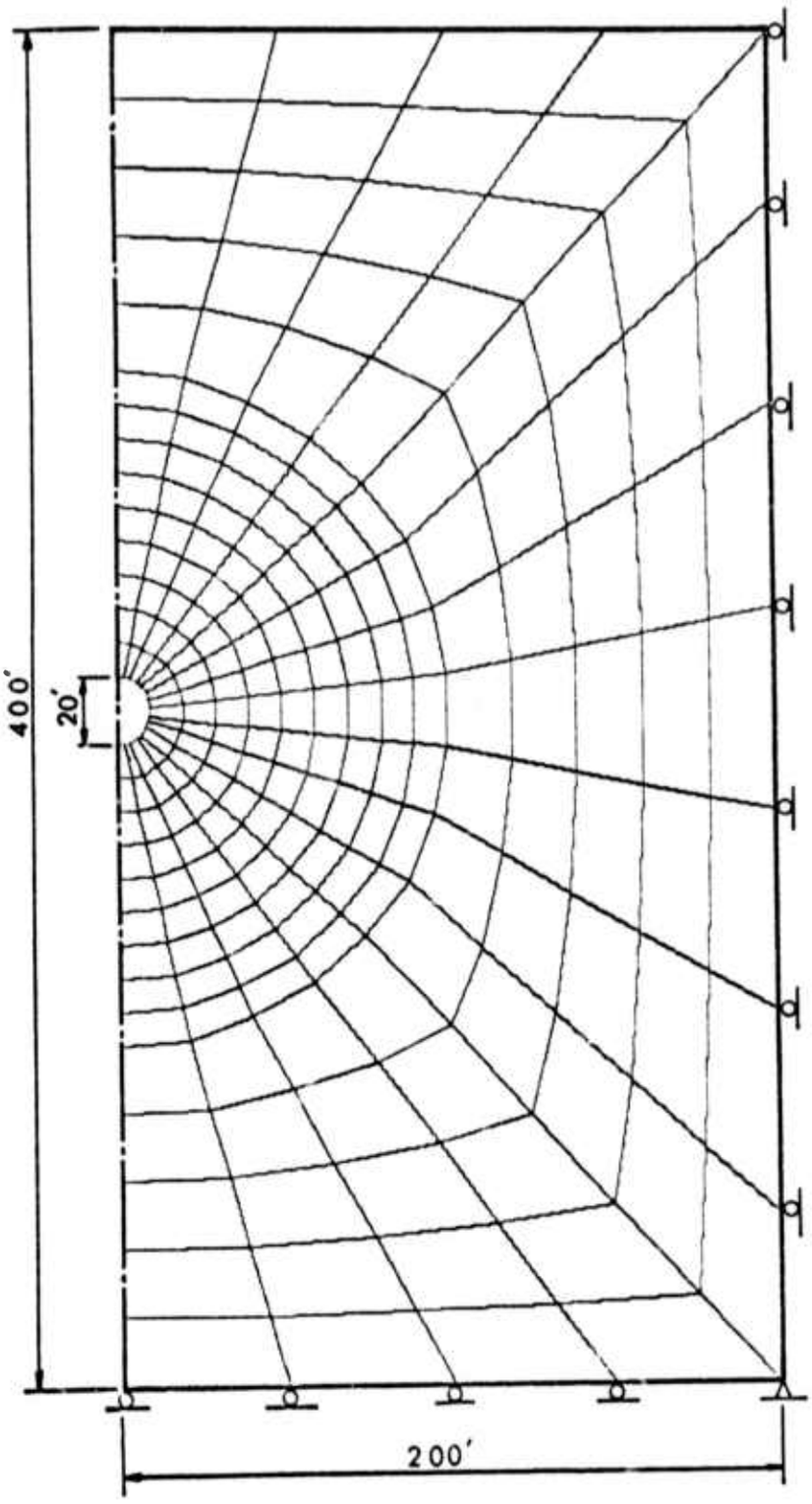

FIG. V-21. Finite Element Idealization of a Circular Tunnel

cracking sequences obtained are shown in Figs. (V-22), (V-23) and (V-24). At 2000 psi, only small radial cracks form near the top and the bottom of the hole. For pressure intensity equal to 3000 psi, cracking was severe around the hole, and three major cracks extended outward. Finally, for pressure equal to 4000 psi, the pressure front was pushed out further and radial fragmentation increased drastically with two major cracks propagating to the boundary. Inclination of these two major cracks to the normal of the free surface was 50 degrees and 70 degrees respectively.

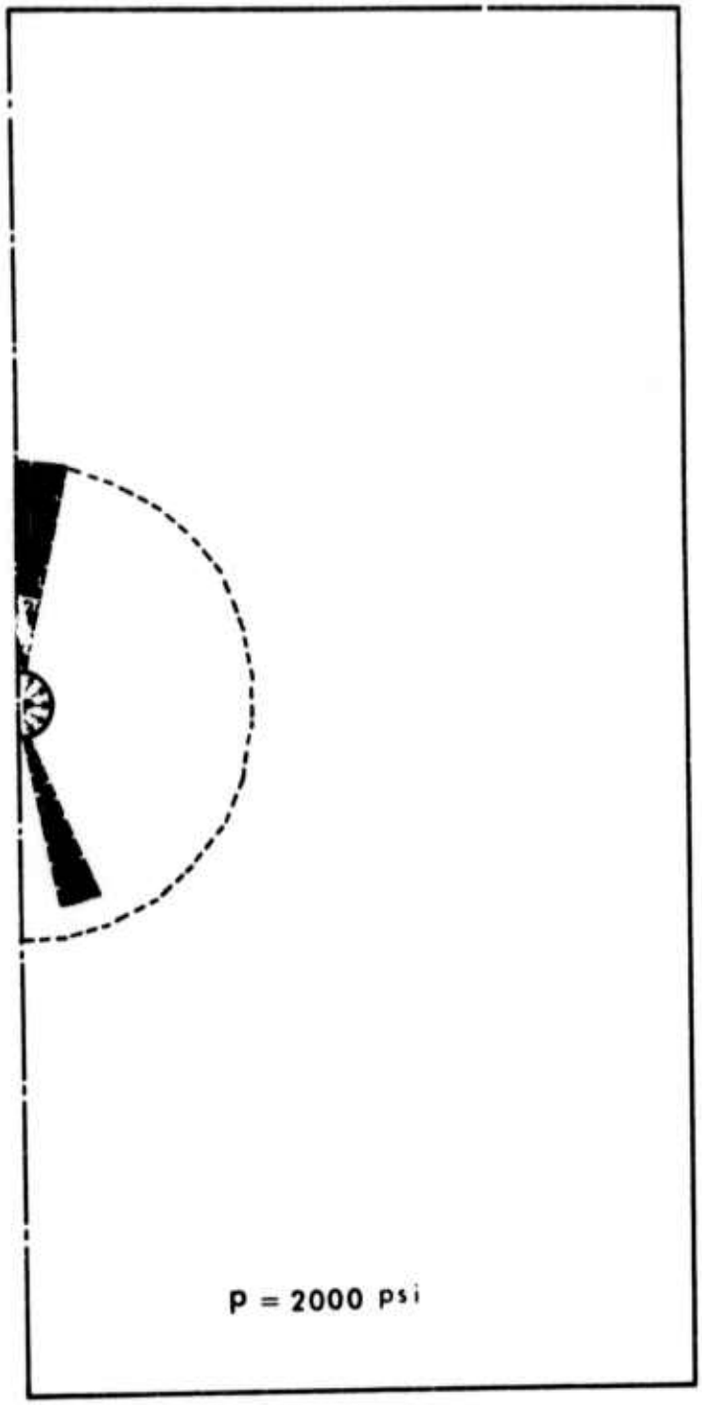

FIG. V-22. Sequential Cracking Due to Internal Pressure on Tunnel Surface - 2000 psi

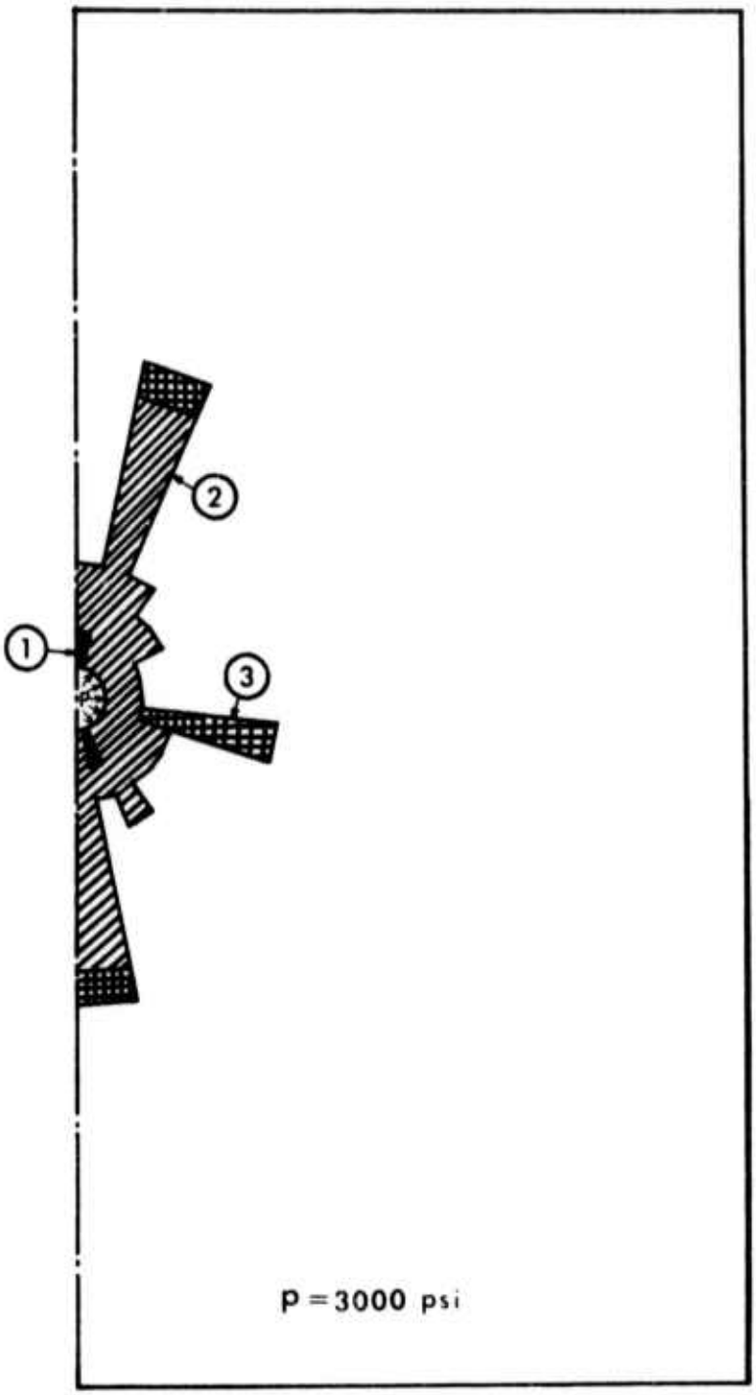

FIG. V-23 Sequential Cracking Due to Internal Pressure on Tunnel Surface - 3000 psi

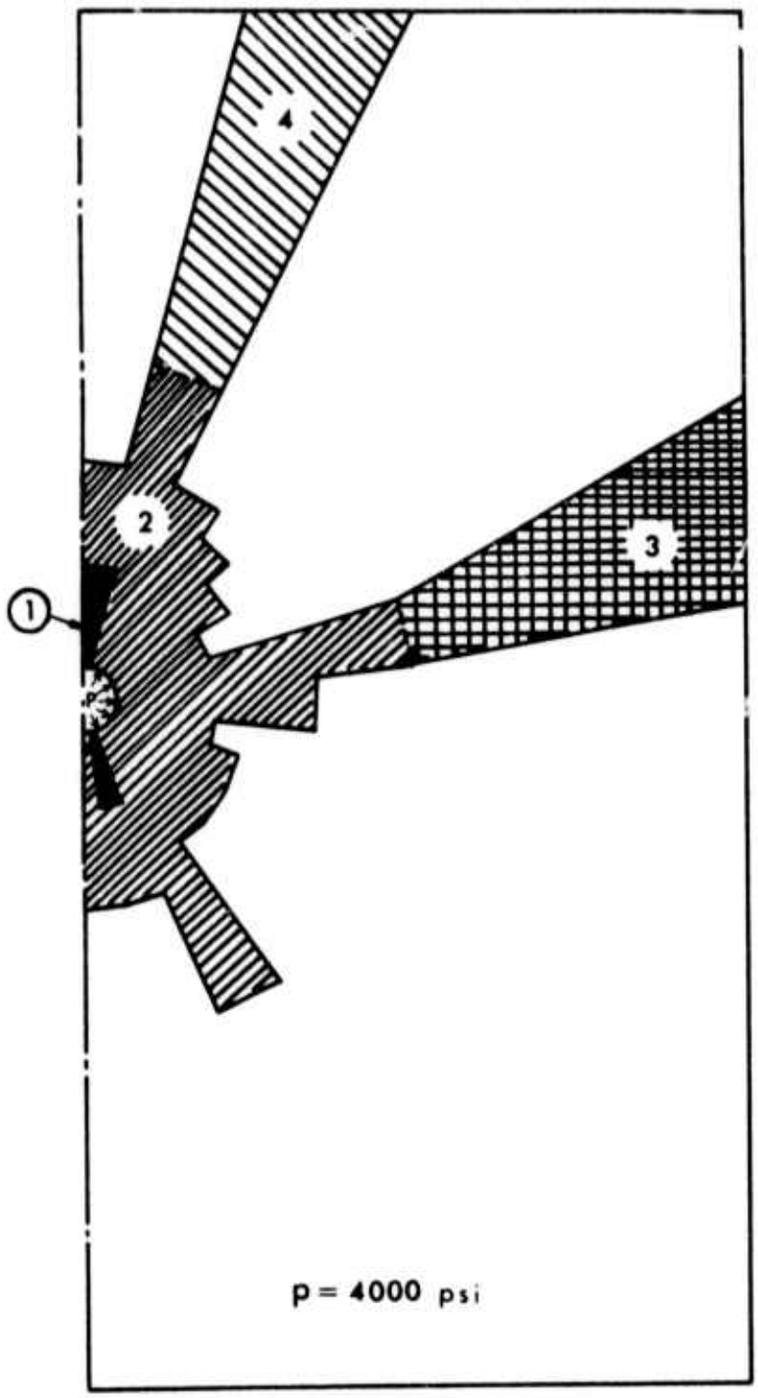

FIG. V-24 Sequential Cracking Due to Internal Pressure on Tunnel Surface - 4000 psi

CHAPTER VI. A PARAMETRIC STUDY OF STRESSES IN STEEL SUPPORTS FOR A TUNNEL

6.1. Statement of Work

The computer program for analysis of stresses and deformations in nonhomogeneous rock assuming elastic-plastic behavior was used in a parametric study of stresses in steel supports for a tunnel. Data for the problem were provided by the United States Bureau of Mines. Figures VI-1 to VI-4 show the configuration of the tunnel opening and the four different blocking systems studied. Figure VI-5 shows the steel support structure. The initial stress field was specified as hydrostatic pressure corresponding to an overburden depth of 1,000 feet and a material density of 165 pounds per cubic foot. The objective of the parametric study was to determine the influence of Young's modulus, Poisson's ratio, cohesion and angle of internal friction, upon the moments and stresses in the steel supports. The range of parameter values specified by the sponsor is shown in Table VI-1.

6.2. Method of Solution

6.2.1. Mechanism of Load Development

When a tunnel is excavated, the load carried by the material removed must be carried by the rock in the tunnel walls and by the unexcavated rock ahead of the face. Continued excavation at the face results in 'loss of support' further increasing the stress in the walls. For linear homogeneous isotropic elastic rock, it has been shown (Abel, 1967) that this effect is felt only in a region one diameter away from the face. If supports are installed immediately after excavation, they will share in this transfer of load as the face is advanced. Theoretically, after the excavation has progressed one

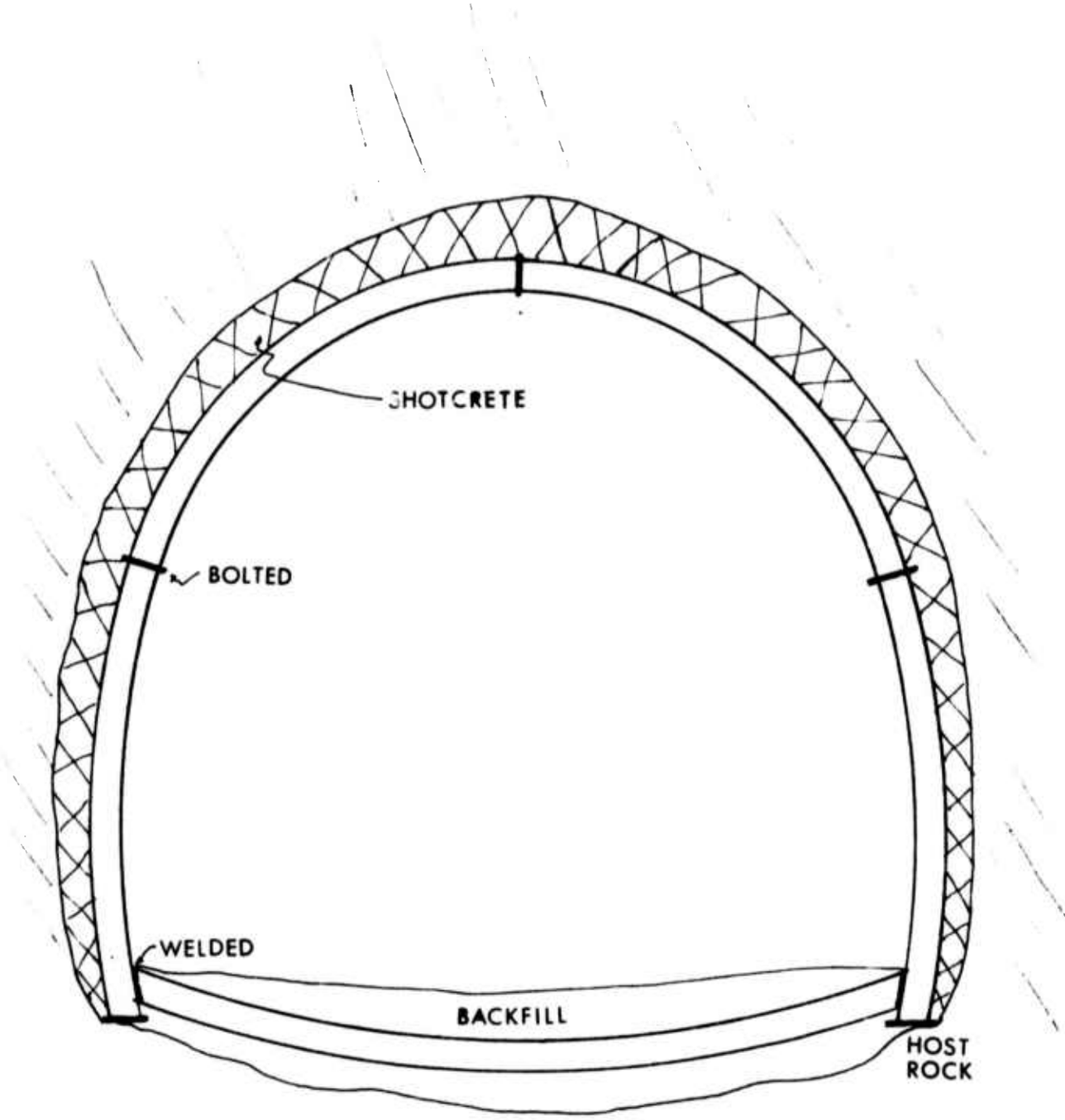

FIG. VI-1. Tunnel Excavation and Supports Case a (shotcrete)

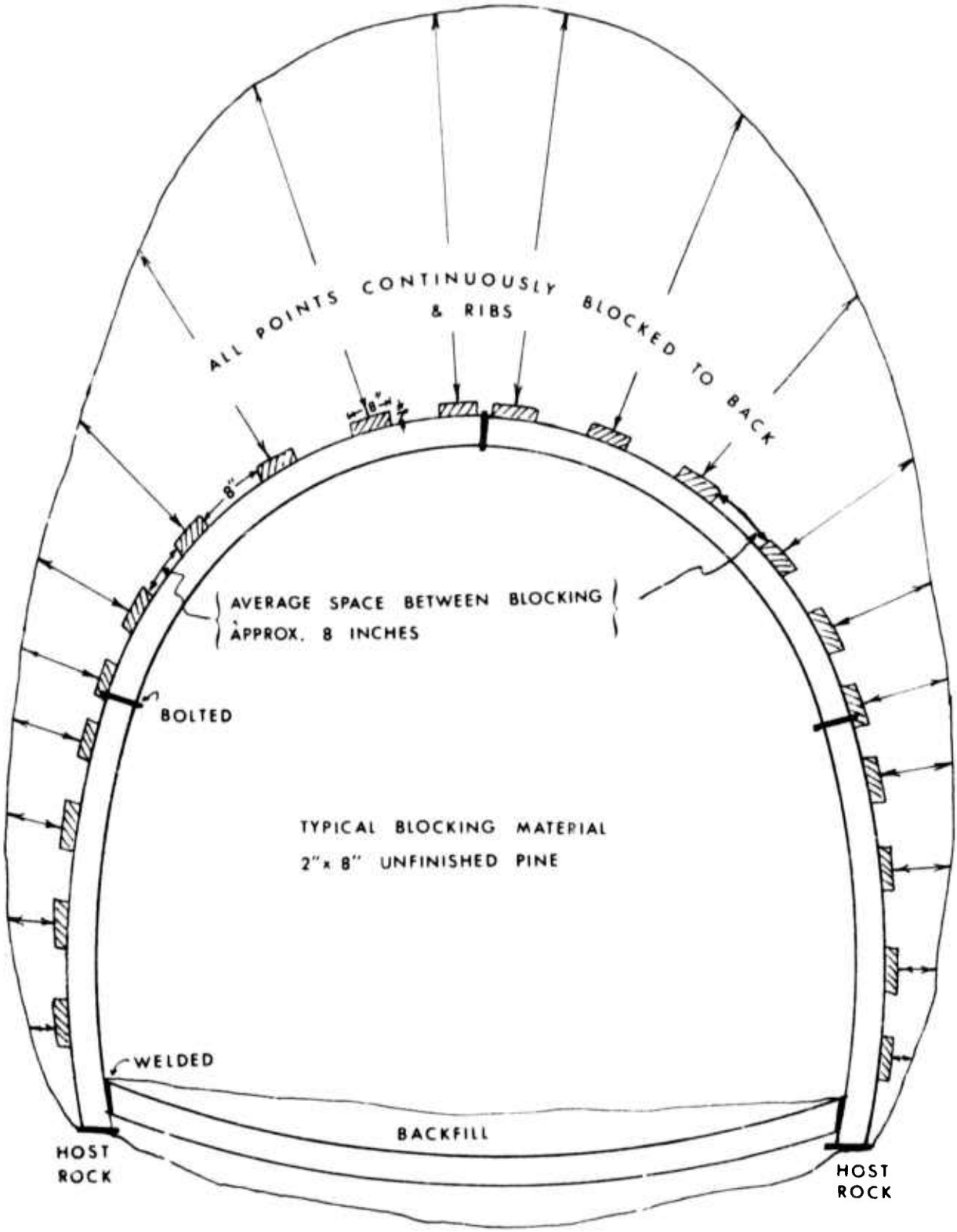

FIG. VI-2. Tunnel Excavation and Supports Case b

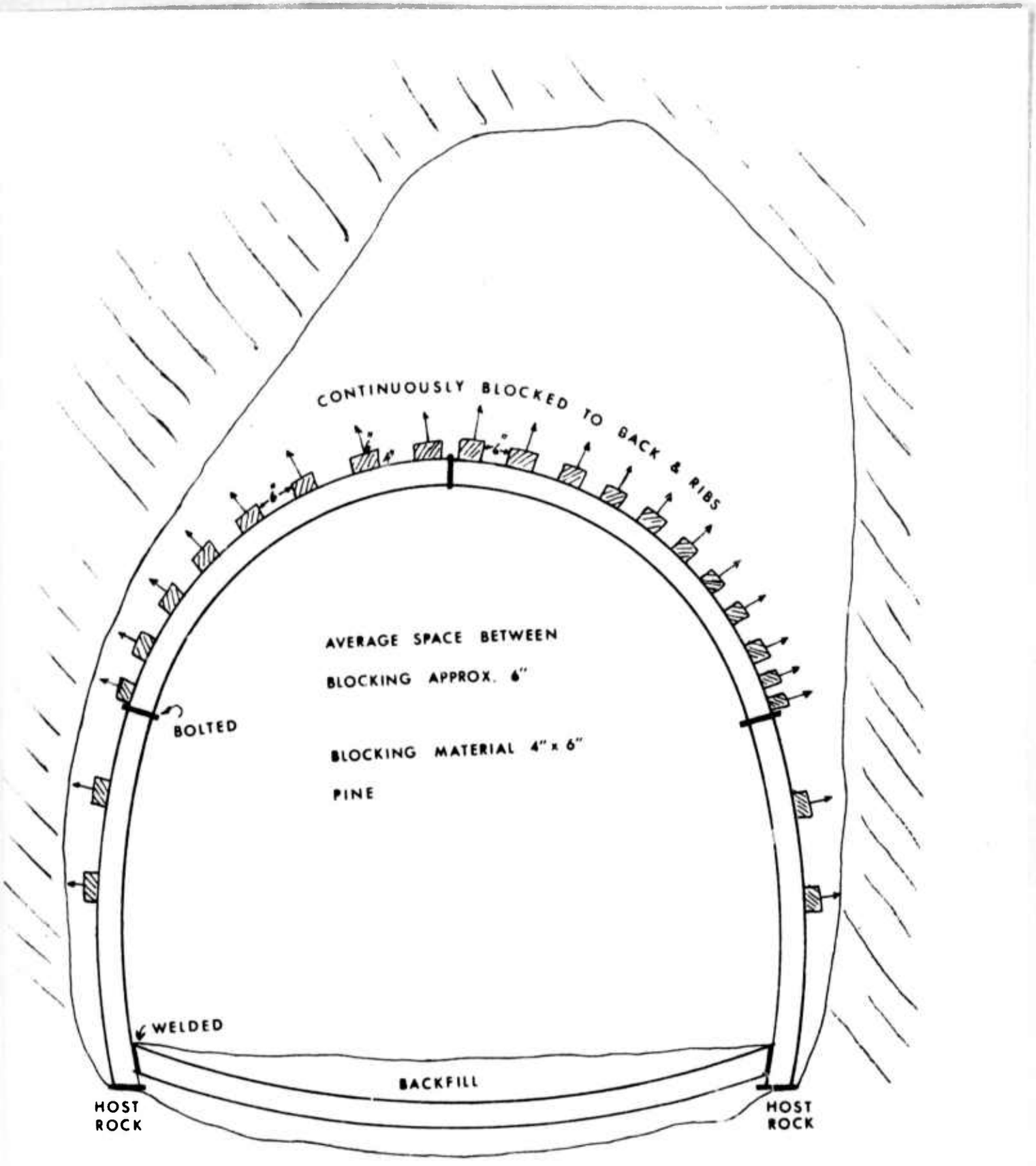

FIG. VI-3. Tunnel Excavation and Supports Case c (non-symmetrical)

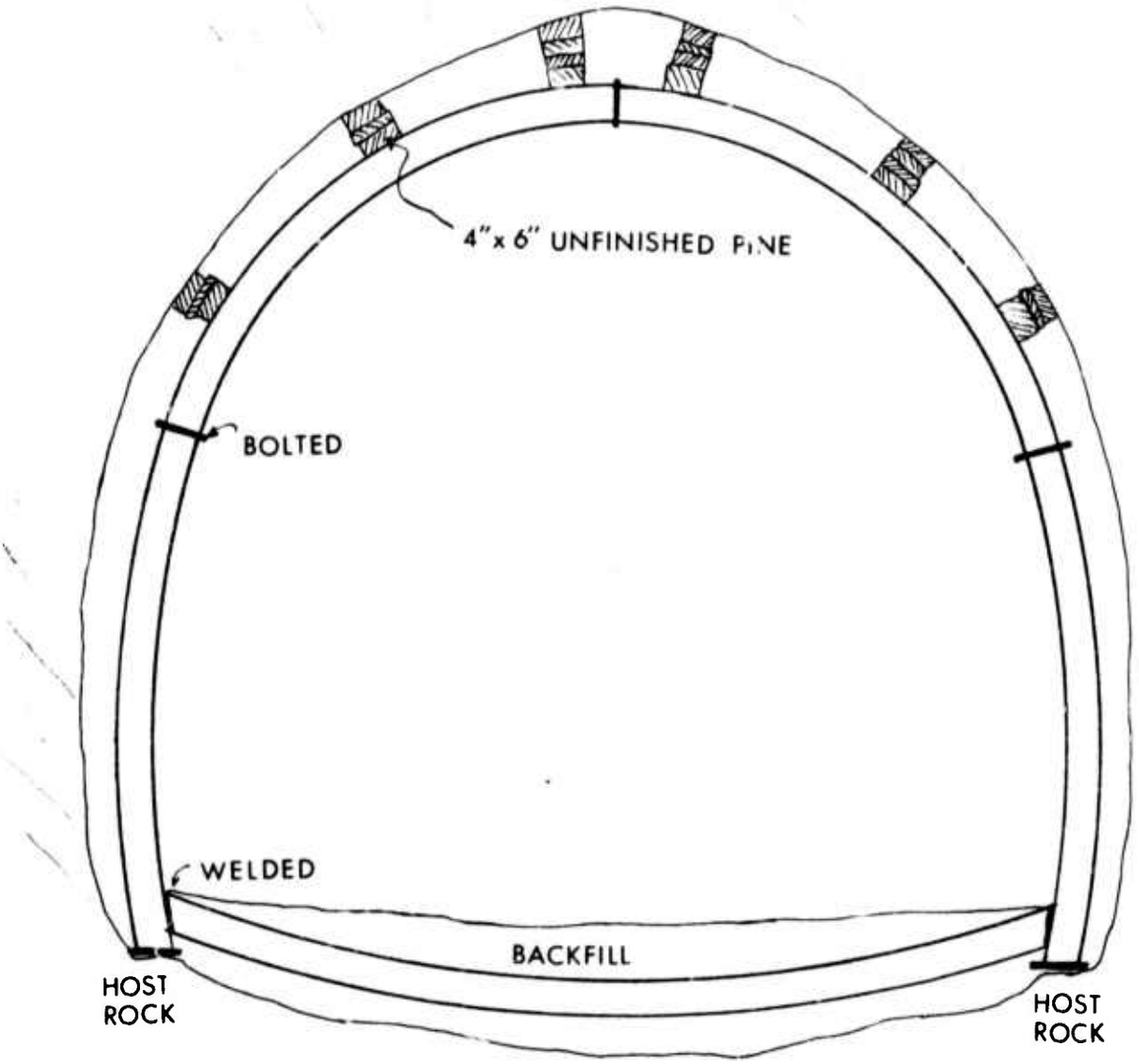

FIG. VI-4. Tunnel Excavation and Supports Case d

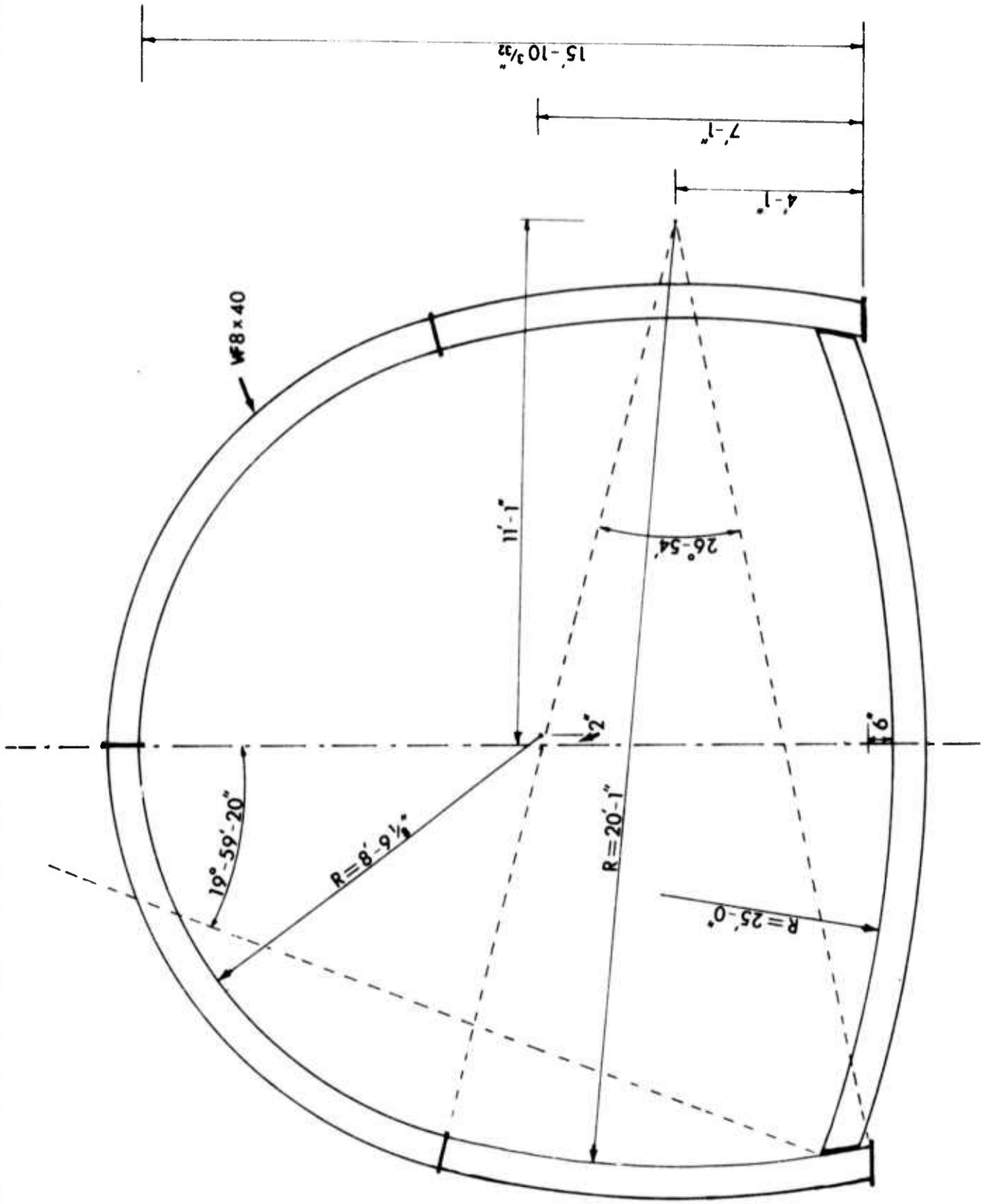

FIG. VI-5. Steel Support System for Cases a, b, c and d

PARAMETERS	MATERIAL			
	(a) Rock	(b) Shotcrete	(c) Steel	(d) Timber
Young's Modulus, E (psi)	$1 \times 10^6 - 10 \times 10^6$	2.71×10^6	30×10^6	1.5×10^6
Poisson's Ratio, ν	0.1 - 0.5	0.1	0.231	0.03
Cohesion, c (psi)	1000 - 5000	3300	---	---
Tan ϕ (ϕ = Angle of Internal Friction)	1.0 - 2.1	1.0	---	---
Material Density (pcf)	165.0	150.0	490.0	27.0

(a) Data furnished by sponsor.

(b) "Manual of Concrete Practice," Part 2, 1968, American Concrete Institute

$$E = w^{1.5} \ 33\sqrt{f'_c}$$

where w = 150 lb./c.ft.

f'_c = compressive strength, assumed as 2000 psi

(c) "Manual of Steel Construction," AISC

(d) "Wood Handbook," Forest Products Laboratory, Forest Research. The properties are for western white pine.

Table VI-1. Material Properties

diameter ahead of the support, there would be no further development of load on supports. Actually, it is observed (Abel, 1967) that rock movement continues for a long time before reaching stabilization. This results in continued growth in the load transferred to the supports. Also, exposure to atmosphere, loss of gouge material, and blasting damage may alter the mechanical properties of the rock mass resulting in increasing deformation and increasing support stresses. In summary, the load development may be associated with one or more of the following mechanisms:

a. Upon continued excavation at the face, the removal of rock results in increased rock load being transferred to the walls of the portion already excavated and the supports in that portion.

b. Time-dependent deformation of rock is resisted by the supports resulting in their taking on increasing load.

c. Change in material properties after installation of supports will result in additional deformation which in turn will lead to increased stresses in the supports resisting such deformation.

d. By blocking, a prestress may be introduced to support rock. Wedging of the blocks will give equal and opposite forces acting on the tunnel surface and the support structure.

In the work reported herein, the influence of various material properties upon support stresses was studied assuming load development primarily through mechanism (a) described above. The system in Figure VI-1 (case a) was analyzed to study the effect of variation of parameters and to rank them in order of importance. Calculations

were made varying each of the parameters between the limits given one at a time. The 'constant' values of other parameters were taken to be the midpoint of the specified range. The combination of parameter values corresponding to the worst stress in the supports was then used to analyze cases b, c, d shown in Figures VI-2 to Figure VI-4.

6.2.2. Assumptions Made in the Analysis

a. Extent of the Finite Model

When an underground opening is excavated, changes in the stress field and associated deformations occur in the entire rock mass. The principle of local action implies that these changes diminish with increasing distance from the opening. In the finite element model, a finite region is generally considered. On the boundary of this finite model, force or displacement boundary conditions have to be prescribed. These can be based on the assumption either of no change in the stress field or of no deformation. Neither of the two is true for finite distances from the opening and the two assumptions in fact give bounds to the correct solution. Nair (1968) and Kulhawy (1972), among others, have studied the effect of lateral dimension of the finite model and of the choice of boundary conditions on stresses and deformations in the vicinity of underground openings. For the present study, allowing for the specified hydrostatic initial stress field, a preliminary analysis showed that it would be adequate to model a region extending approximately seven diameters above the roof of the opening, five diameters horizontally on each side of the center-line and five diameters below the invert of the opening. This region is outlined as ABCD in Figure VI-6. The boundary conditions

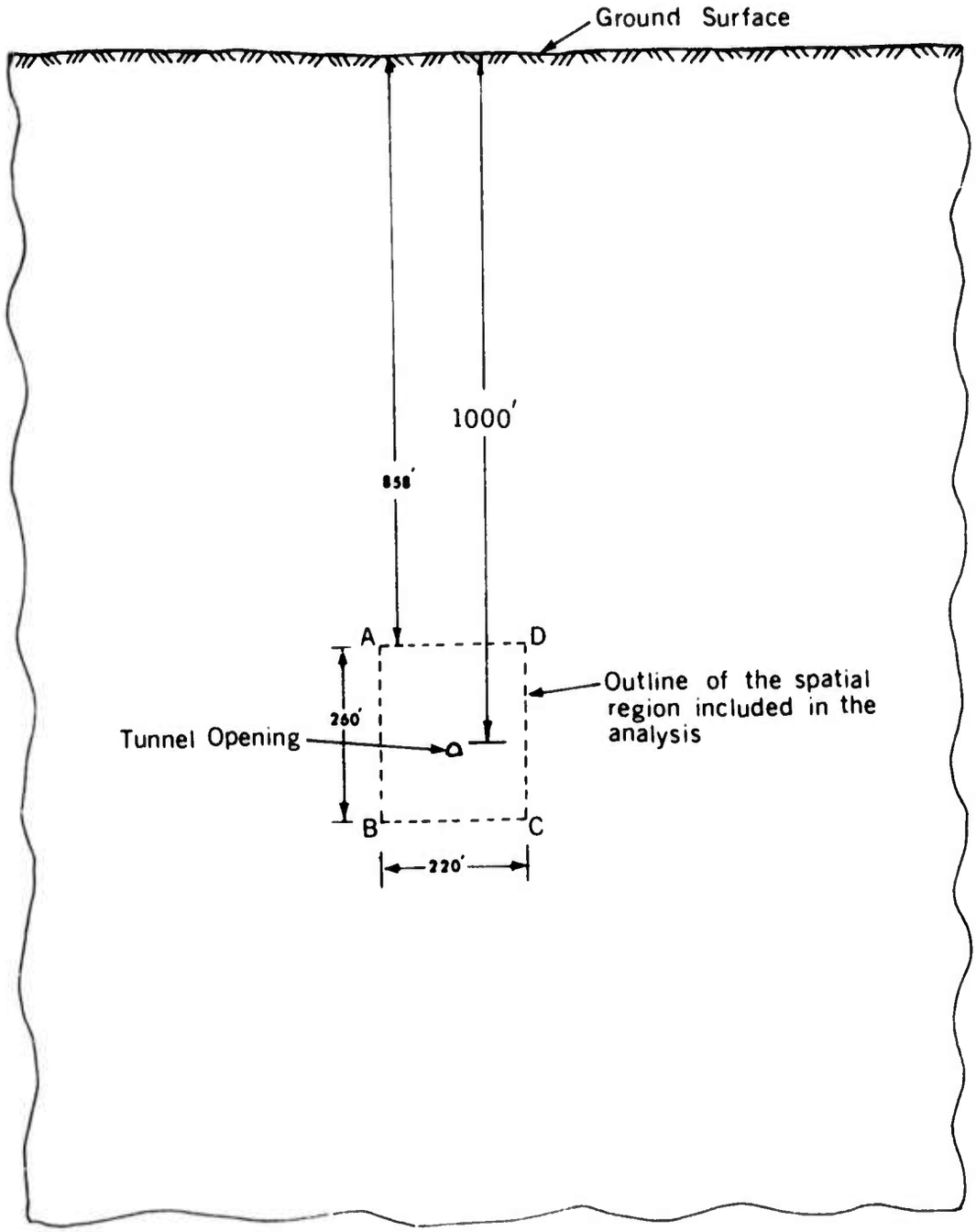

FIG. VI-6. Tunnel Opening, Overburden and Region Included in the Analysis

for the finite element model are illustrated in Figure VI-7. The overburden of the top 858 feet was replaced by an equivalent vertical load. The stress field on the vertical faces AB, CD was assumed to be unaffected by the sequence of operations in the opening and the vertical displacement of the horizontal section BC was set equal to zero.

b. Modelling of Support Structure and the Sequence of Operations

Starting with the initial stress state, the sequence of excavation, installation of supports and load development was simulated. The steel supports were assumed to be in plane stress whereas the rock and shotcrete were in plane strain. The spacing of steel supports was specified as three feet. Thus a three foot length of the tunnel was supported by each support ring. Figures VI-8 and VI-9 show a typical cross-section used in the finite element model. The cross-section of the steel rib was represented by five finite elements to obtain reasonably good distribution of stresses over the cross-section. The shotcrete and the rib were assumed to be bonded. If there is no bond between shotcrete and the rib, there is no load transferred through shear and the load transfer is entirely radial. This situation would be similar to case (d) except that the blocking would be continuous. For cases b, c, d, the wooden blocks were assumed to be axial members not transmitting any bending moments.

The shotcrete , the steel rib and the timber blocks were assigned the properties given in Table VI-1. It was assumed that C, Φ specified for the rock were obtained in triaxial tests on cylindrical specimens. It was assumed that the rock properties

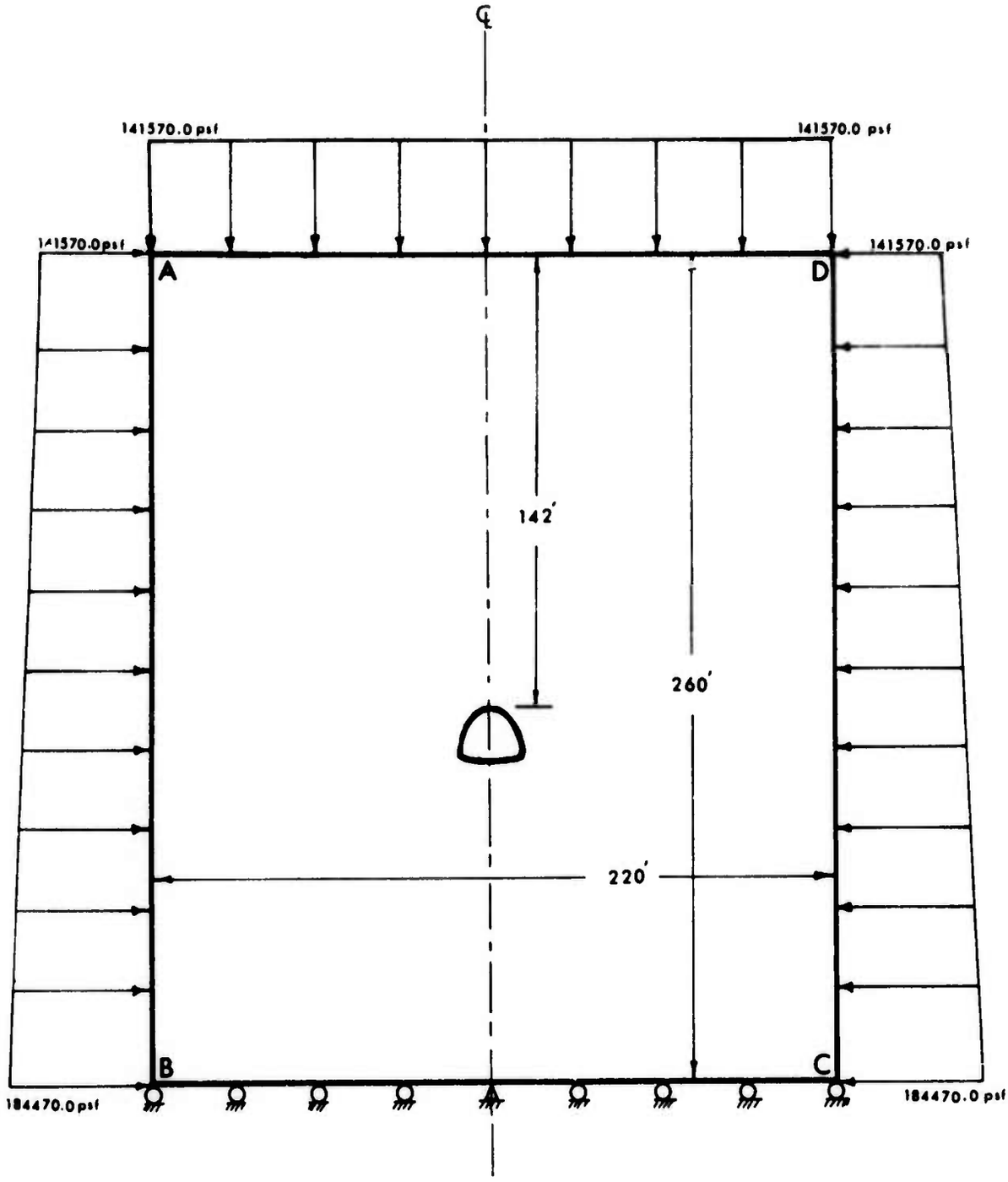

FIG. VI-7. Boundary Conditions on the Finite Element Model

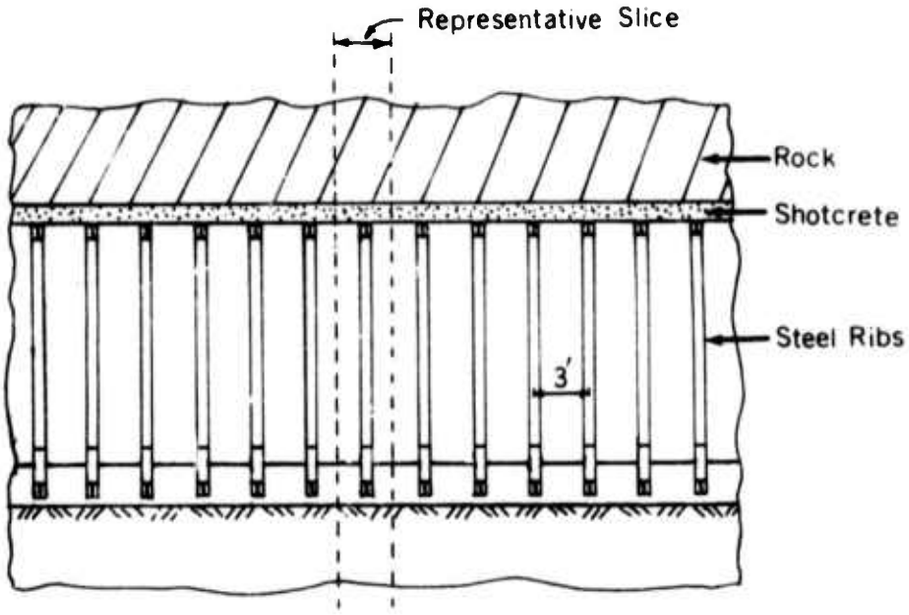

a. Longitudinal Cross-Section of Tunnel

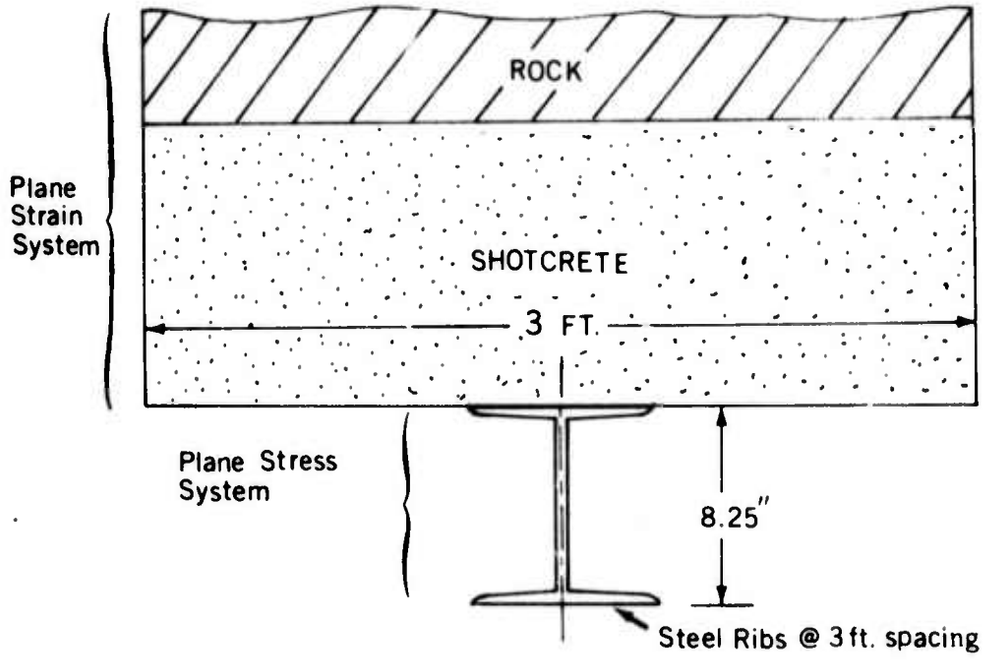

b. Representative Slice

FIG. VI-8. Longitudinal Cross-Section of Tunnel and Representative Slice

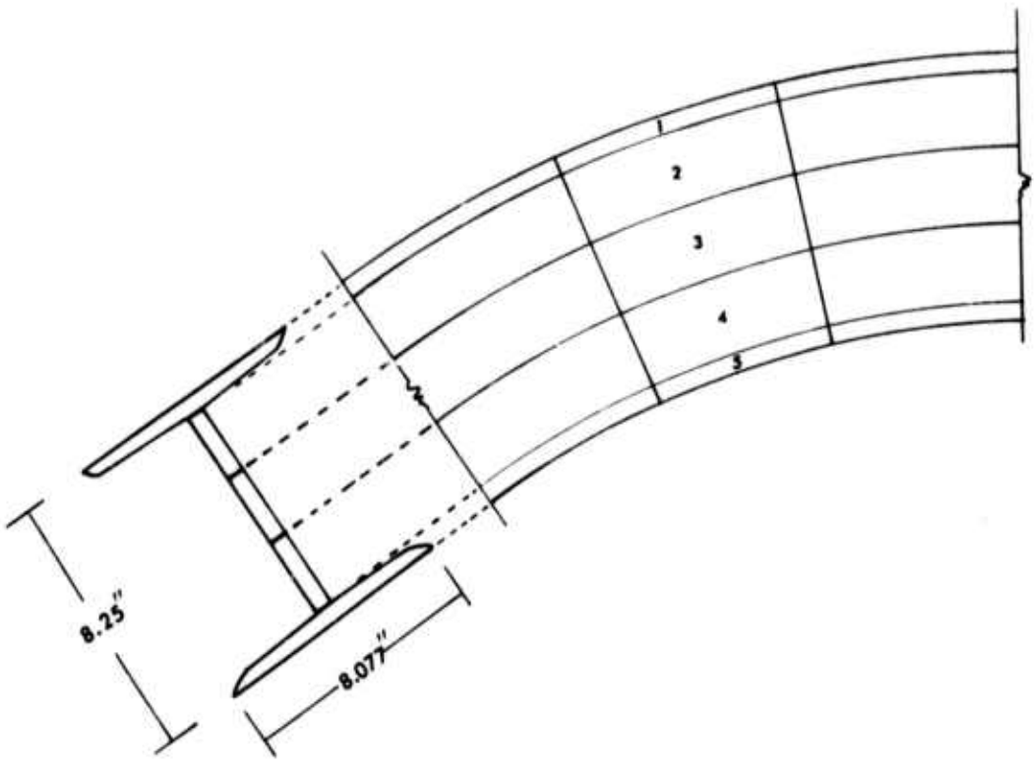

FIG. VI-9. Finite Element Representation of the Cross-Section of Steel Rib (5 Elements at Each Section)

do not change as a result of excavation of the opening. Additional studies considering the effect of such changes are reported in section 6.2.3.

In calculating load acting on the supports, it was assumed that, upon excavation, the gravity load due to the area shown shaded in Figure VI-10 was mobilized only fifty percent. The rest being supported by the unexcavated rock ahead of the working face. The balance fifty percent was assumed to become active upon loss of support due to continued excavation. This corresponds to mechanism (a) described in section 6.2.1. The geometry of the shaded area corresponded to the overbreak line in Figure VI-2, case b. It was assumed that the difference in excavation profiles in Figure VI-2 and VI-1 represented the rock load which could develop for cases a and d. For case b, the rock exerting the gravity load is shown shaded in Figure VI-11, the extent was arbitrarily taken as an average of 3.5 feet thickness beyond the excavation line. Similarly for case c, the extent (Figure VI-12) was arbitrarily taken as an average of 3.5 feet thickness beyond the excavation line.

6.2.3. Results

a. Preliminary

In studying the importance of material parameters, the quantities of interest were the maximum stresses in the steel member. It is customary to study the axial and shearing forces and bending moments in such structural components. Hence, these quantities were worked out. It should be noted that the basic output from the finite element analysis is the components of stress evaluated at the center of each of the five elements into which the steel member is divided. The moments and forces were obtained by numerical integration of the stress values.

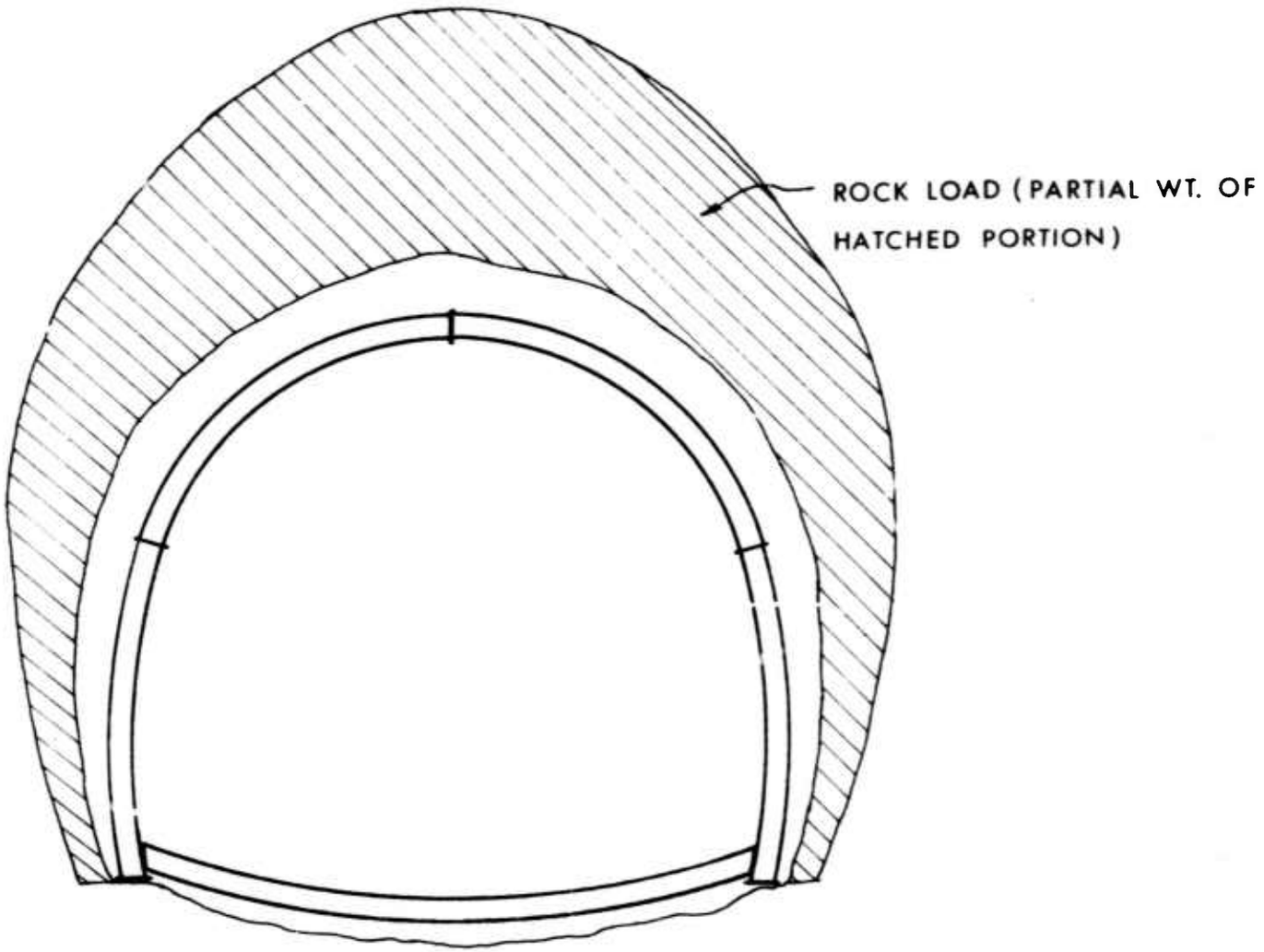

FIG. VI-10. Tunnel Cross-Section Showing Rock Load for Cases a and b

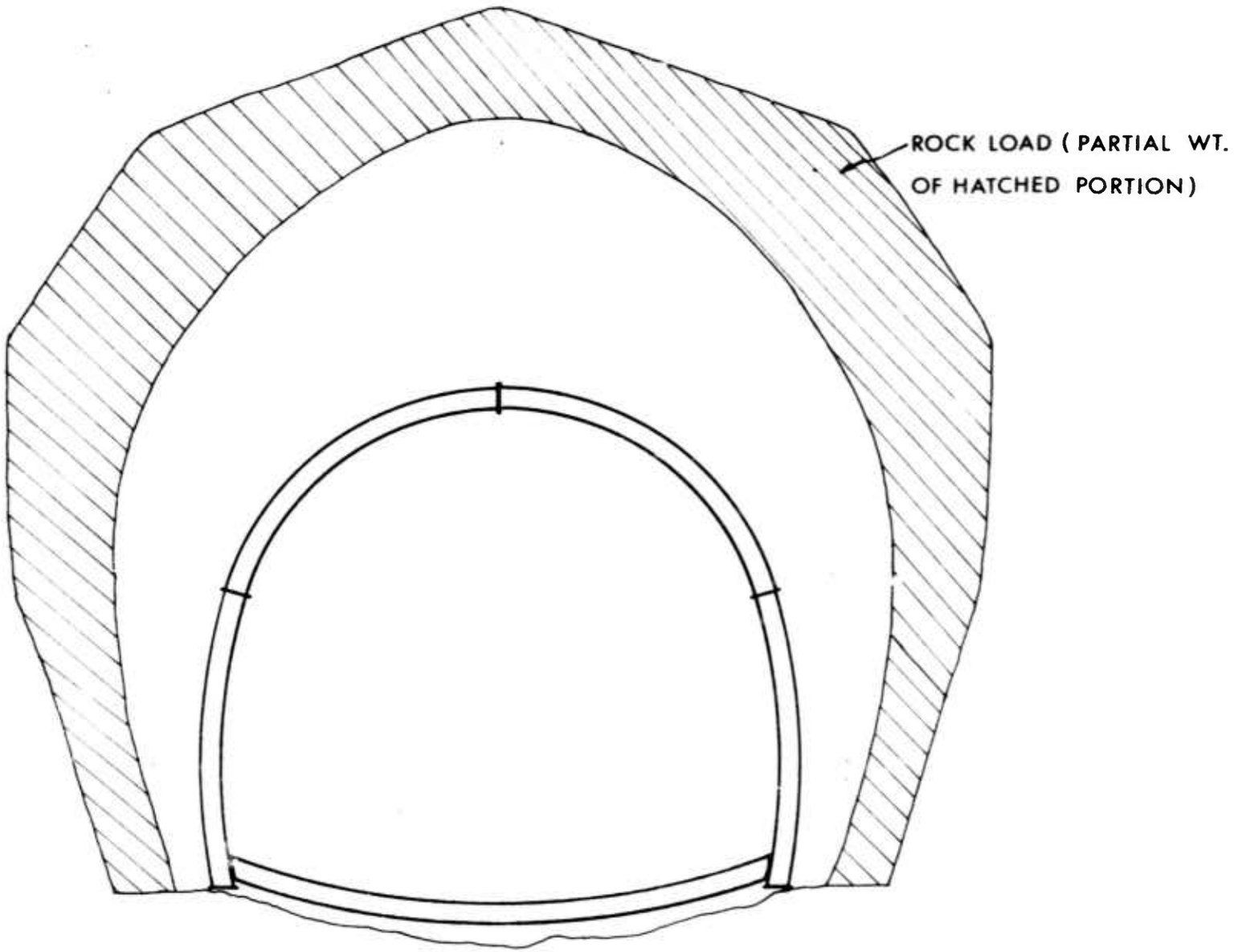

FIG. VI-11. Tunnel Cross-Section Showing Rock Load for Case b

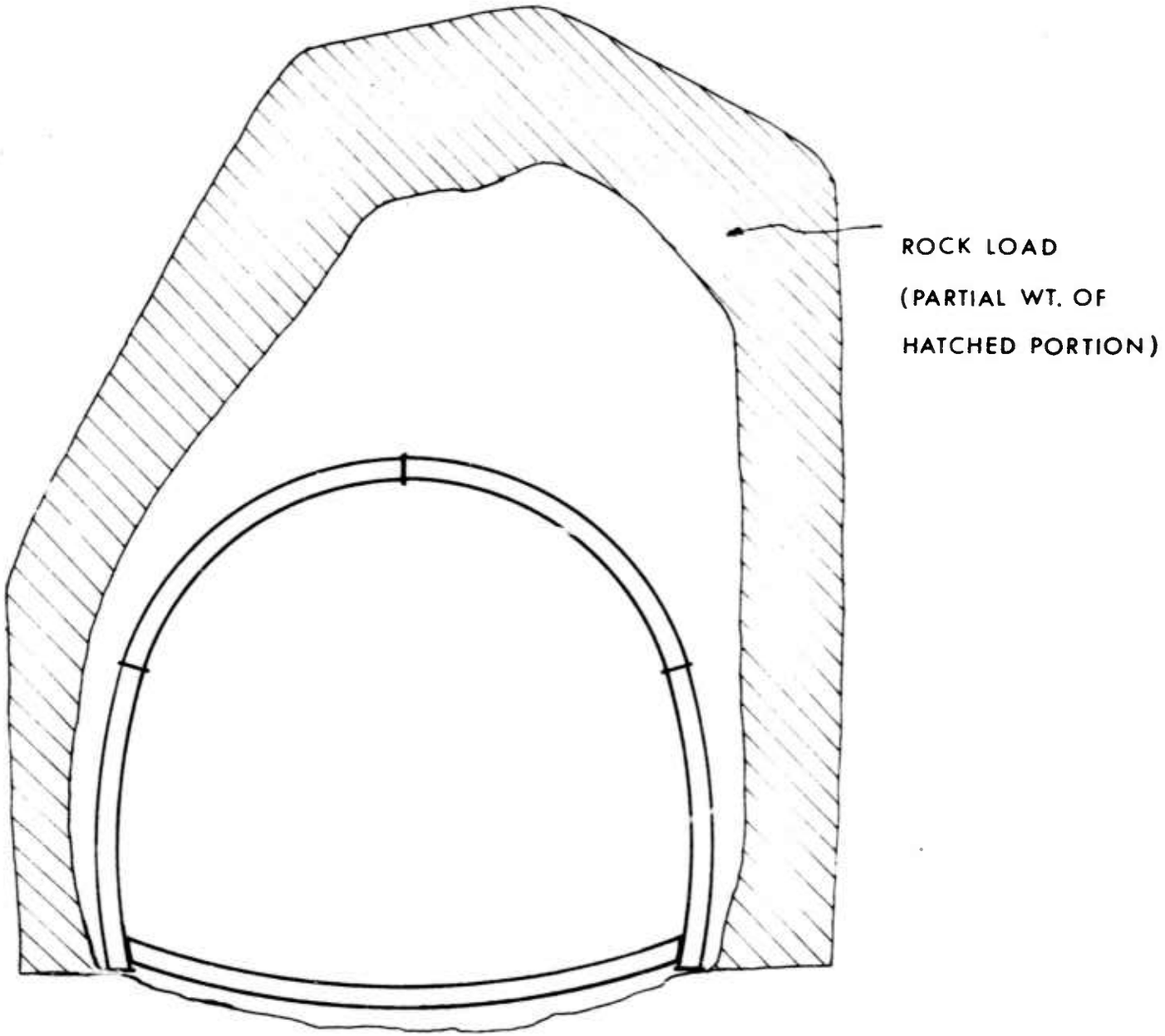

FIG. VI-12. Tunnel Cross-Section Showing Rock Load for Case c

Figures VI-13 and VI-14 show the cross-sections at which the stresses as well as the forces and moments in the steel rib were computed.

Rock load development was assumed to follow mechanism (a) of section 6.2.1. Additional studies using mechanism (c) and (d) are covered in section 6.2.4.

b. Influence of Material Properties

Four material parameters, viz., Young's modulus, Poisson's ratio, cohesion and angle of internal friction were to be considered to establish their order of importance in terms of their influence on the support forces.

For the specified range of the rock properties, the cohesion and the angle of internal friction did not influence the stresses in the structural supports. Figure VI-15 shows a plot of $J_1 = \sigma_1 + \sigma_2 + \sigma_3$, the first invariant of the stress tensor as the abcissa and $J_2^{\frac{1}{2}} = \left\{ \frac{(\sigma_1 - \sigma_2)^2 + (\sigma_2 - \sigma_3)^2 + (\sigma_3 - \sigma_1)^2}{6} \right\}^{\frac{1}{2}}$, the second invariant of the stress deviation tensor as the ordinate. The generalized Mohr-Coulomb yield criterion corresponding to the prescribed range of values of cohesion and angle of internal friction are shown and also the stress paths traced by points of critical locations around the tunnel opening.

The generalized Mohr-Coulomb yield law is,

$$\alpha \; J_1 + J_2^{\frac{1}{2}} = k$$

where: $\alpha = \dfrac{2 \sin\phi}{\sqrt{3}\,(3 - \sin\phi)}$

$k = \dfrac{6\,C \cos\phi}{\sqrt{3}\,(3 - \sin\phi)}$

ϕ = angle of internal friction

C = cohesion.

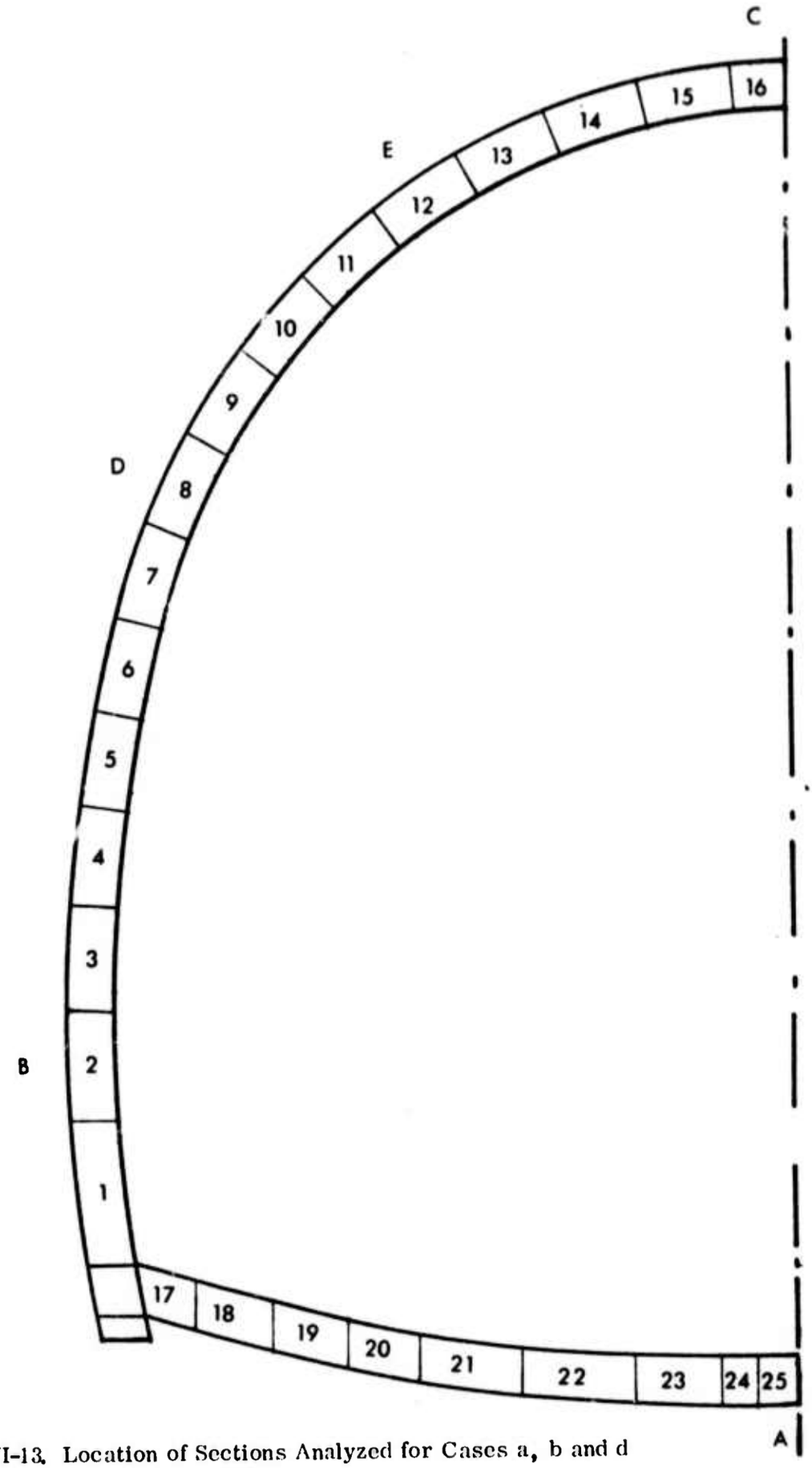

FIG. VI-13. Location of Sections Analyzed for Cases a, b and d

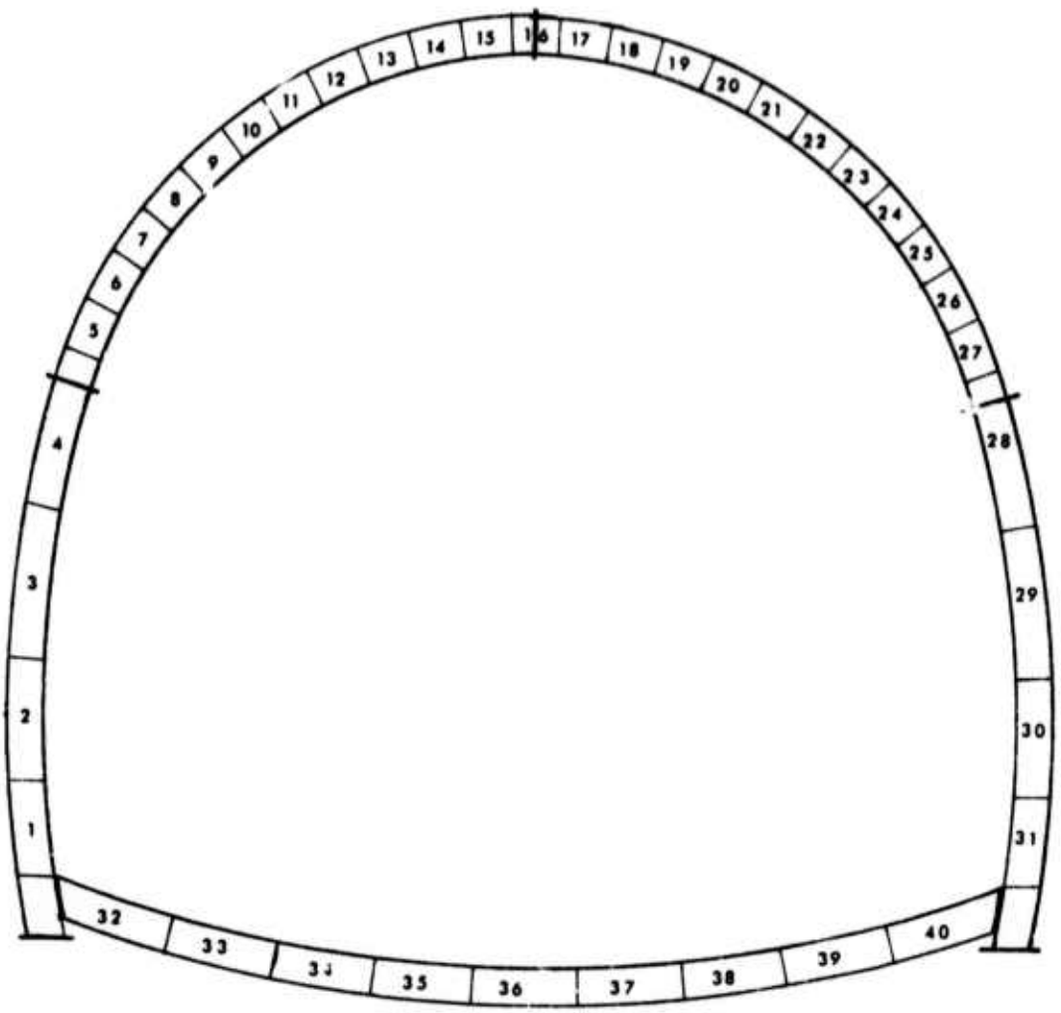

FIG. VI-14. Location of Sections Analyzed for Case c

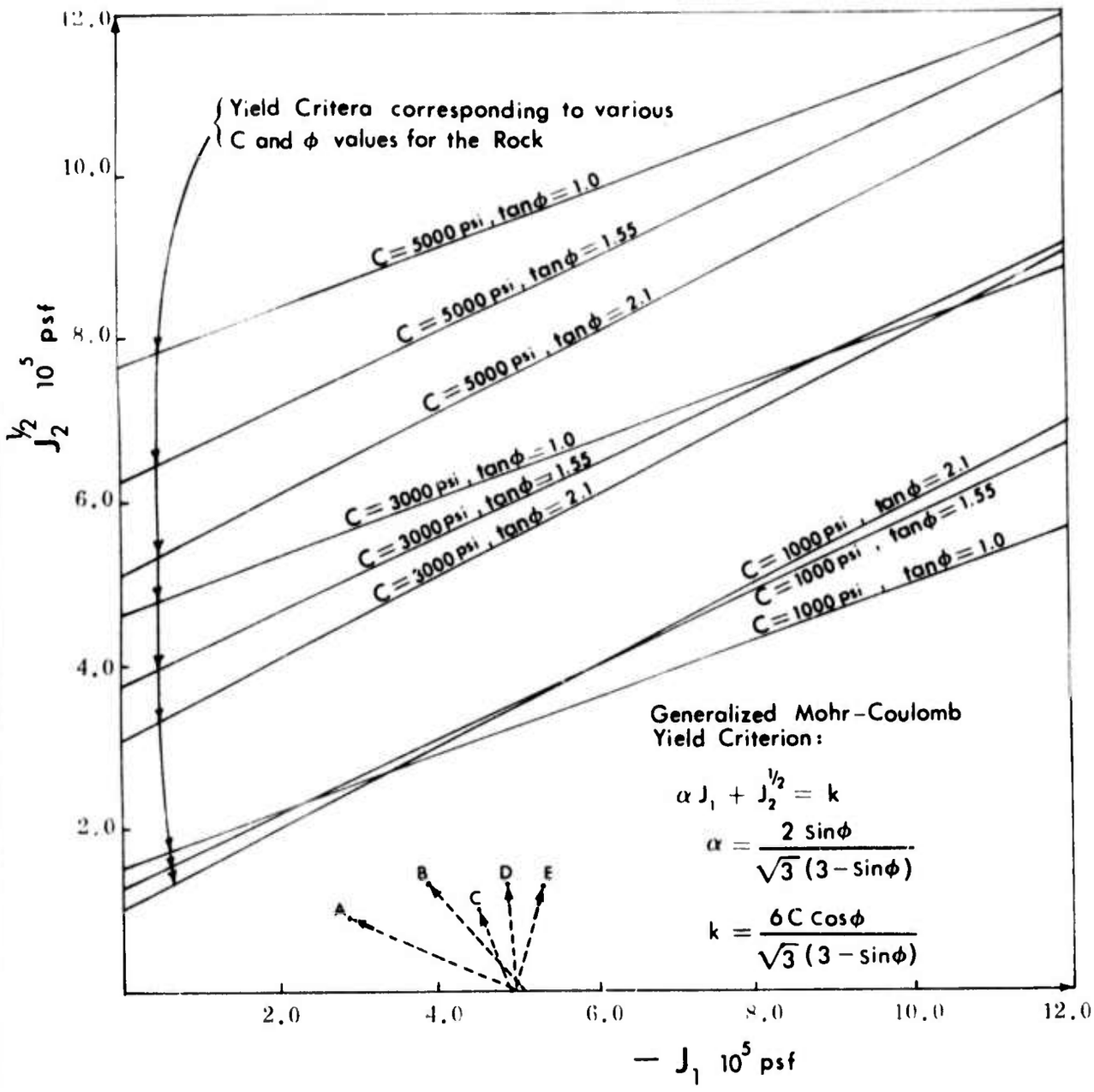

FIG. VI-15. Stress Paths for Points Around the Underground Opening
(for location of points see FIG. VI-13)

C and ϕ are determined from a triaxial test on a cylindrical specimen under axisymmetric radial stress. Derivation of the above equations is given by Singh (1972).

In Figure VI-15, paths A, B, C, D, E are traced by elements located around the face of the underground opening. Points A, C refer to elements at the invert and the crown, respectively, and points B, D, E correspond to elements on the side of the opening. The locations are indicated in Figure VI-13. The initial state in all cases is of hydrostatic stress. The terminal points represent the state after excavation. The development of rock load has little influence on the stress state in rock for the specified values of Young's modulus and Poisson's ratio. For all locations, the entire stress history was found to be well below the yield criterion.

Figures VI-16 through VI-18 show the influence of variation of Young's modulus upon bending moments and upon axial and shearing forces. Only sections with the worst forces have been plotted. The maximum bending moments were at section 16 (crown), the maximum axial force at section 5 (side) and the maximum shearing force at section 10. In all cases, decrease in elastic modulus of rock was seen to result in increased moments and forces. This is indeed to be expected. The load transfer to the structural support is dependent upon the tendency of the rock face to deform. Higher modulus implies less deformation for the same rock load and consequently less load transferred to the steel member. The decrease in support forces, with increasing Young's modulus, is rapid at first and then is less pronounced. This is due to the fact that rock deformation is proportional to reciprocal of the modulus. Also, for very large moduli, the strains are extremely small and difficulties arise with computational precision.

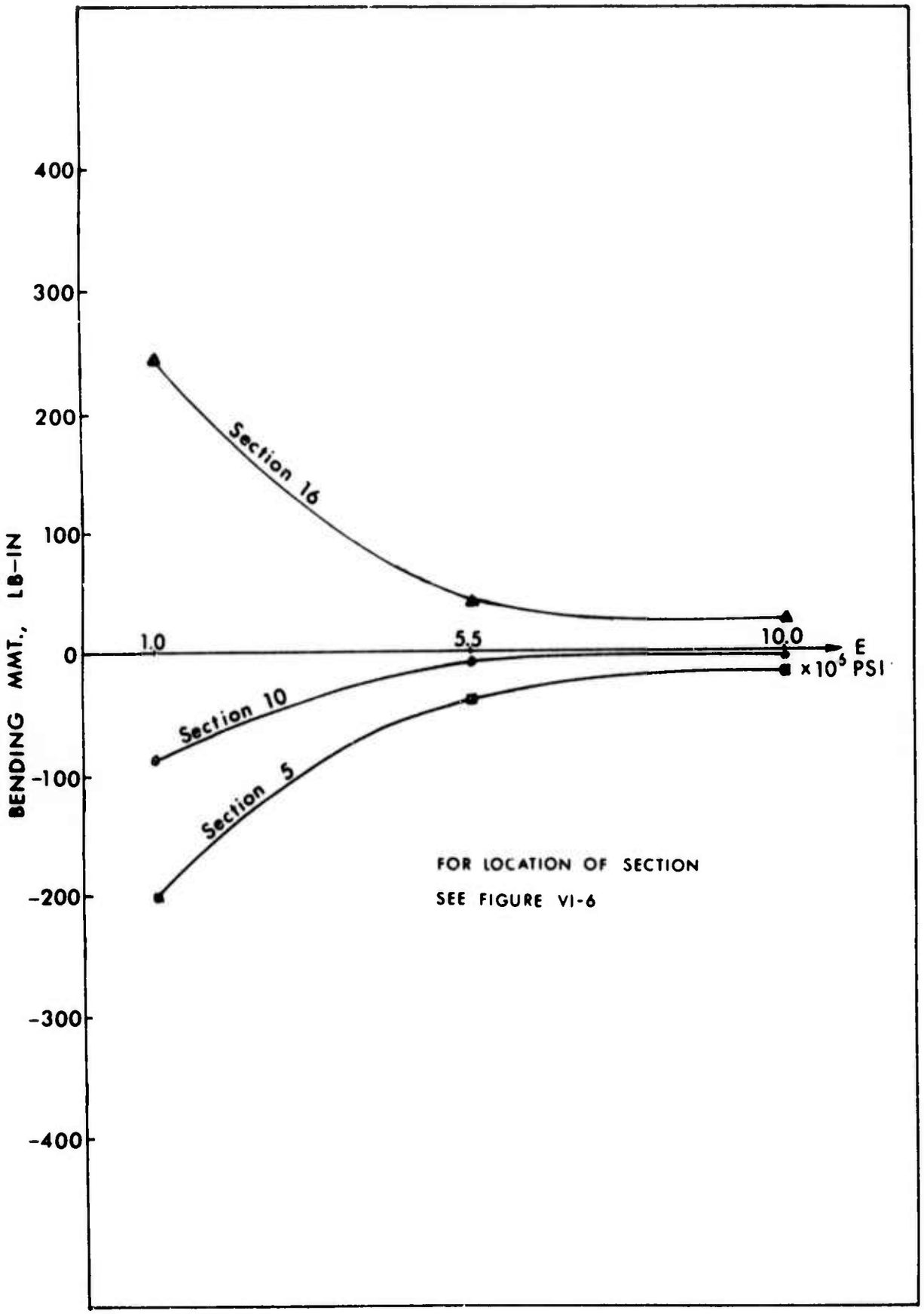

FIG. VI-16. Influence of Elastic Modulus on Bending Moments

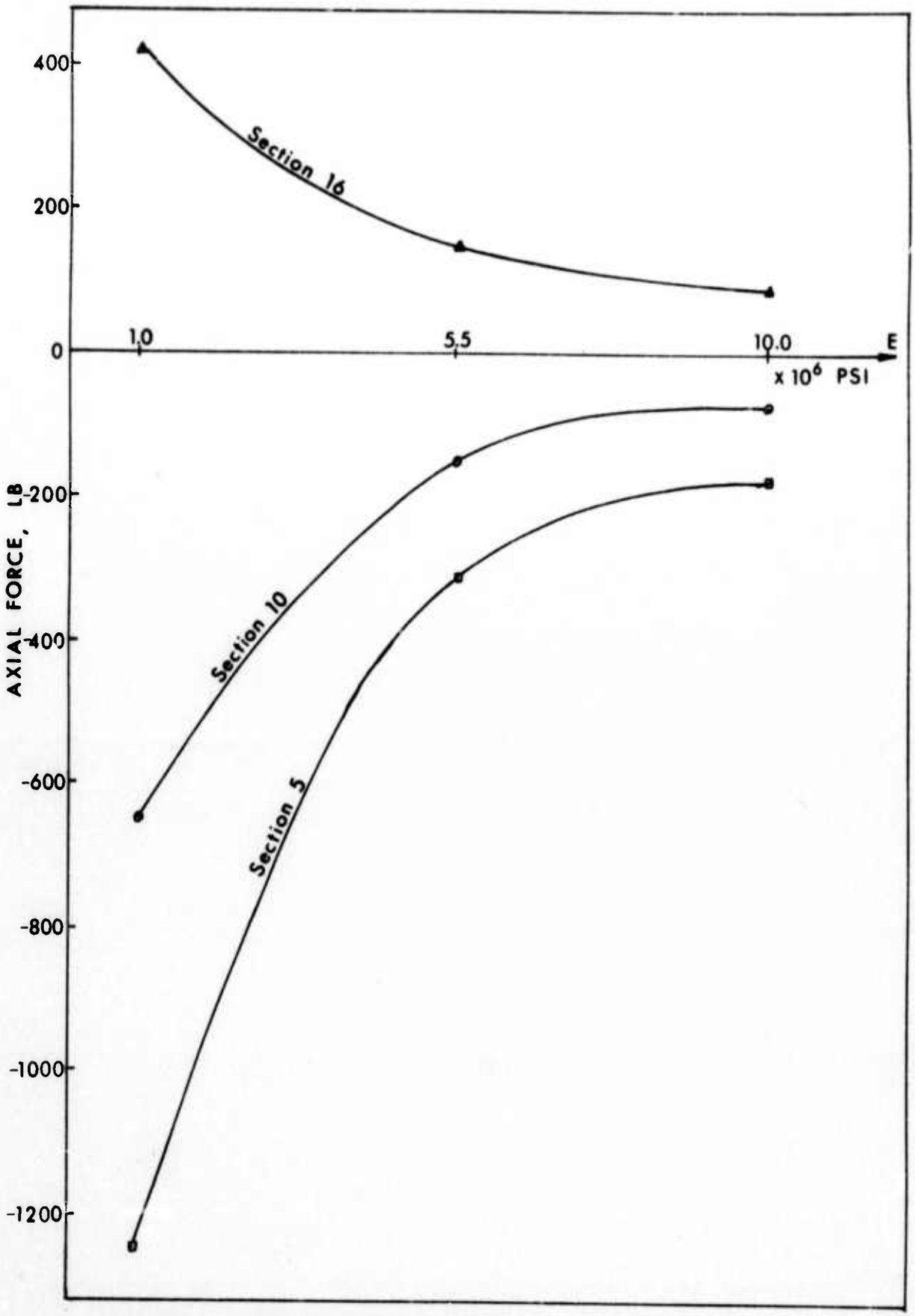

FIG. VI-17. Influence of Elastic Modulus on Axial Force

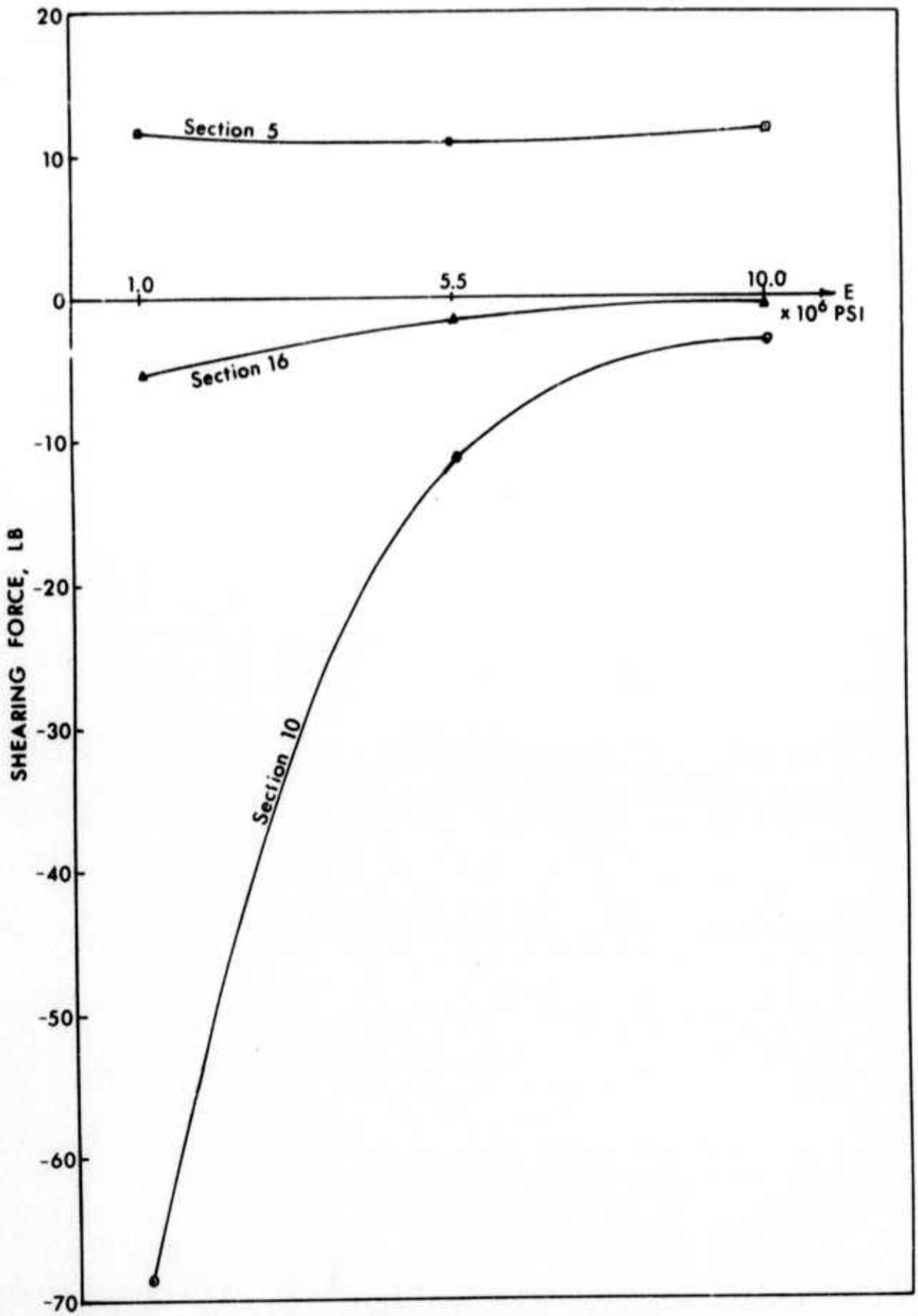

FIG. VI-18. Influence of Elastic Modulus on Shearing Force

Figures VI-19 through VI-21 show the influenee of the variation in the Poisson's ratio on the moments and axial and shear forees in the supports. Again, only results for the worst seetions have been plotted. In the erown and the side (section 16 and 5), an inerease in Poisson's ratio results in deereased bending moments whereas at seetion 10 the bending moment inereases somewhat. The higher Poisson ratio is assoeiated with a redistribution of stress in roek. This redistribution is refleeted in a more uniform stress distribution in the steel support.

For the speeified range of values for the material parameters, the bending moments and the shearing forees were insignifieant. The major effect was the axial foree in the member. Figure VI-22 shows the distribution of longitudinal stress for the mean values of rock parameters. An explanation for the bending effeet being very small may be found in the asssumption that the steel member is restrained by the shot-erete. Signifieant bending of the steel member must involve signifieant ehanges in eurvature. This is not possible for a member restrained from radial movement by relatively unyielding roek. Also, the roek properties are assumed to be unaffeeted by the exeavation proeess. This may not be true. There ean be eonsiderable ehange in deformability of a roek mass due to exeavation of the underground opening.

It is not possible to assign ranks to the parameters. It is elear however, that supports in lower elastie modulus roek will develop greater stresses. High value of Poisson's ratio has the effeet of redistributing stresses; deereasing the peaks and inereasing the lowest values.

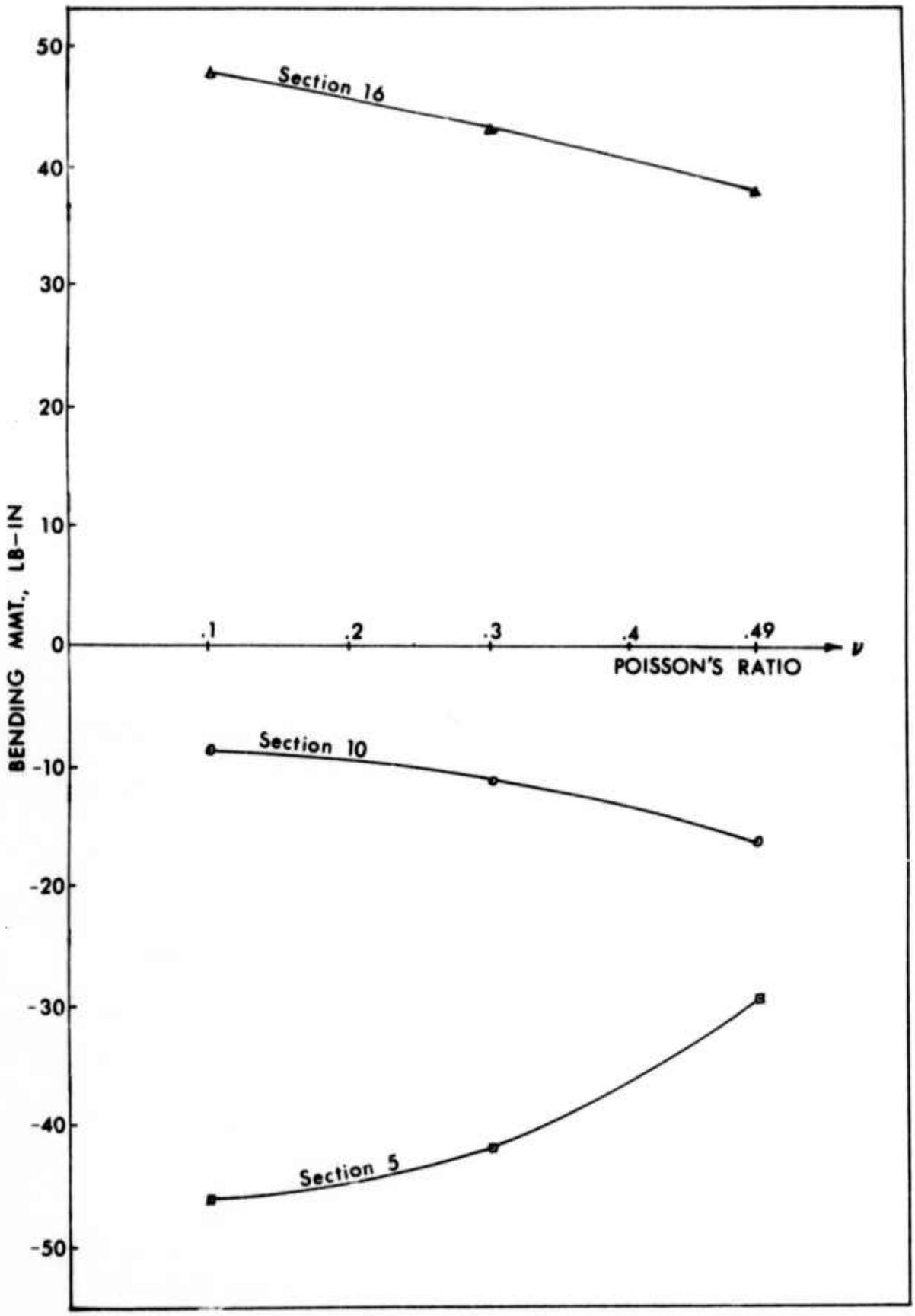

FIG. VI-19. Influence of Poisson's Ratio on Bending Moments

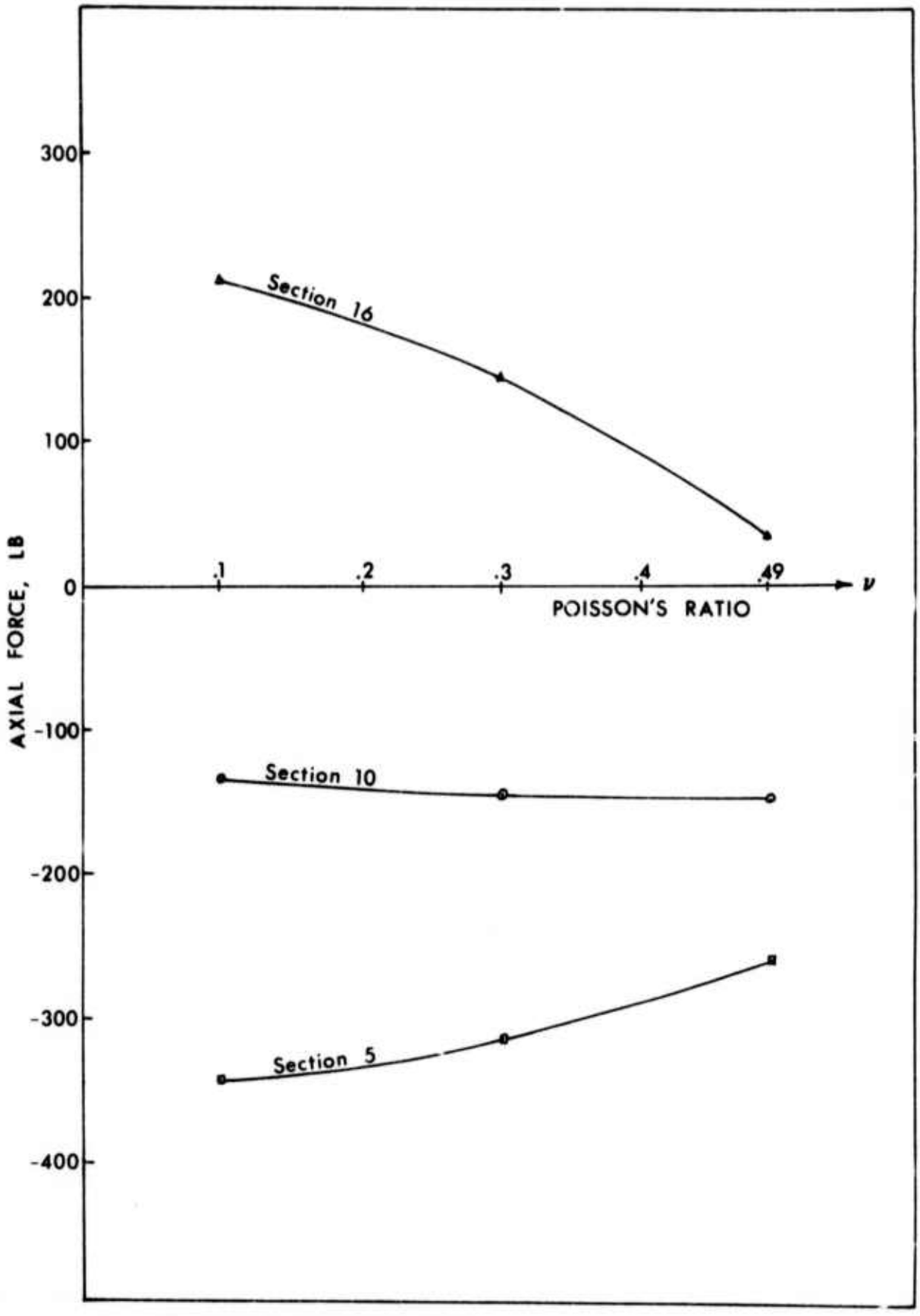

FIG. VI-20. Influence of Poisson's Ratio on Axial Force

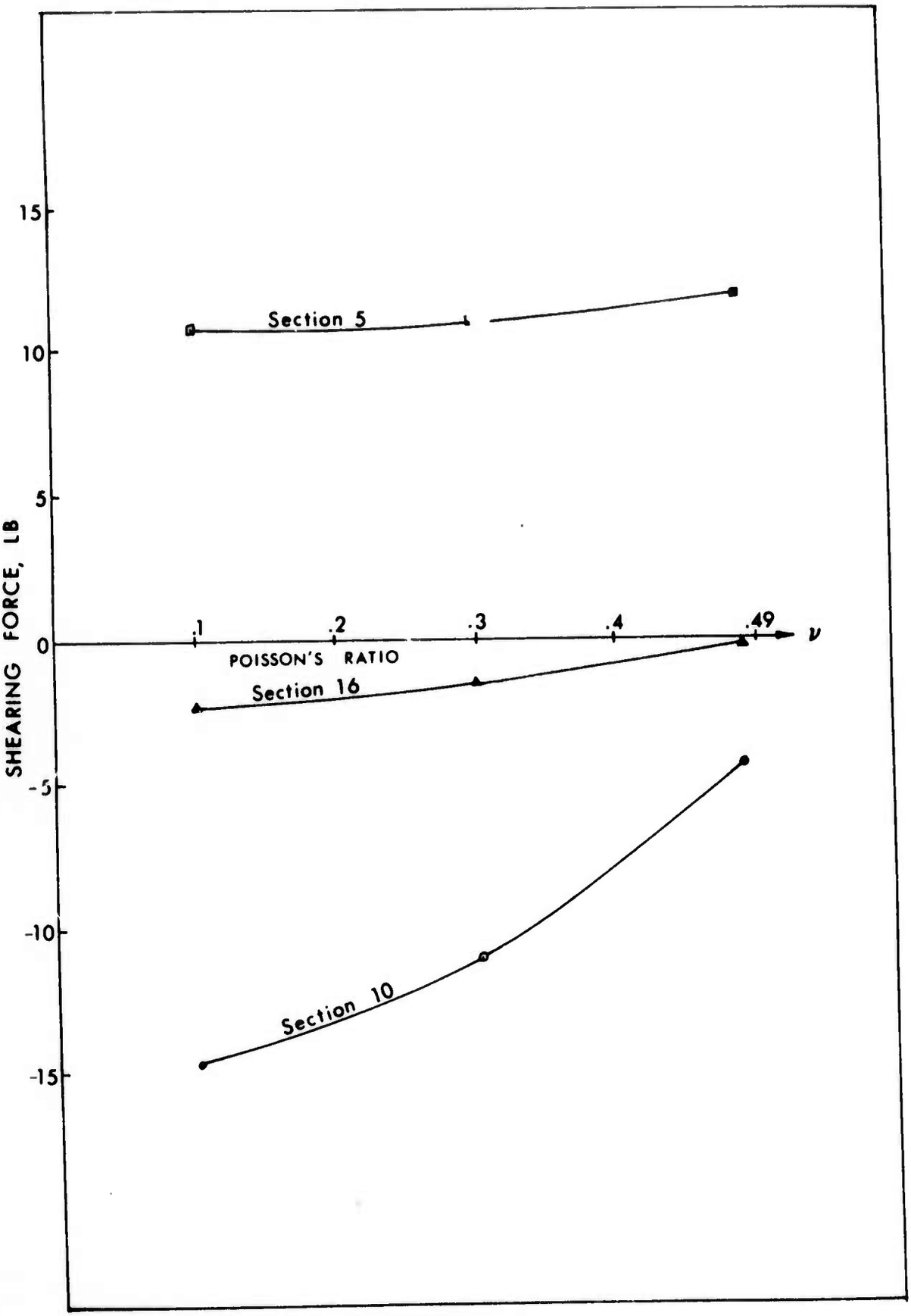

FIG. VI-21. Influence of Poisson's Ratio on Shearing Force

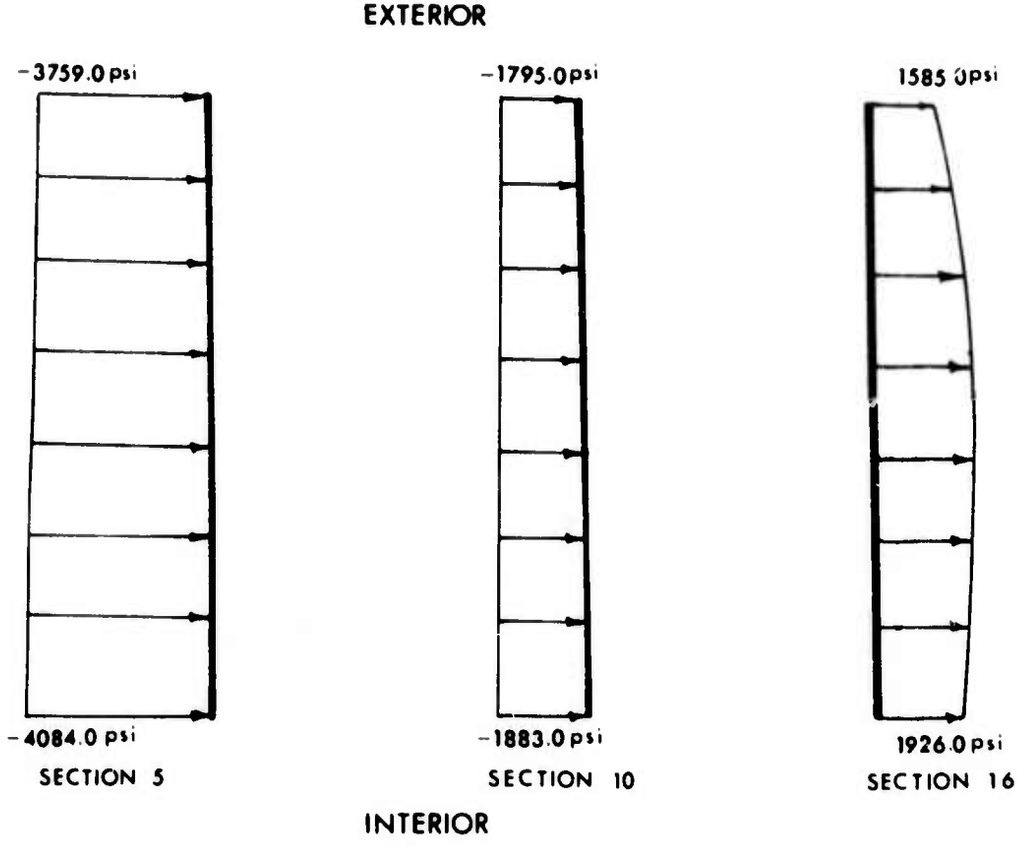

FIG. VI-22. Longitudinal Stress Distribution for Case (a) - Mean Values of E and ν

Using the lowest value, in the prescribed range, of Young's modulus and the minimum as well as the maximum values of Poisson's ratio, stresses for cases a, b, c, d (Figures VI-1 through VI-4) of different excavation profiles and blocking arrangements were determined. Figures VI-23 through VI-26 show the distribution of longitudinal stresses on critical section. A study was also carried out for case (a) in which no load transfer through shear between shotcrete and the rib was allowed (ribs unbonded to the shotcrete). Table VI-2 shows a comparison of forces for the cases (a) and (d). It was seen that the bending moments in case (d) were greater than those in case (a) in all portions of the rib except the invert section. Also the axial forces in these two cases are almost the same at the invert section but were different at other sections. These differences are due to the restraint offered by the shotcrete to radial deformation of the rib and due to the transfer of stresses between the rib and the shotcrete through shear. Results for the case of no load transfer through shear between the shotcrete and rib showed that the effect of bonding of rib to shotcrete on forces in the invert section is insignificant. The axial forces in the other parts of the steel rib were greater for the case where load transfer through bond was permitted. As would be expected, in case (c), where the tunnel cross-section and the rock load were unsymmetrical, the forces in the steel rib were also unsymmetrical. The axial force had a minimum value at section 22 and increased towards the invert on both sides of section 22 to 1137 lbs. at section 1 and 913 lbs. at section 31. (Figure VI-14 gives location of these sections of the steel ribs).

6.2.4. Additional Studies

Additional studies using values of Young's modulus less than the minimum of the

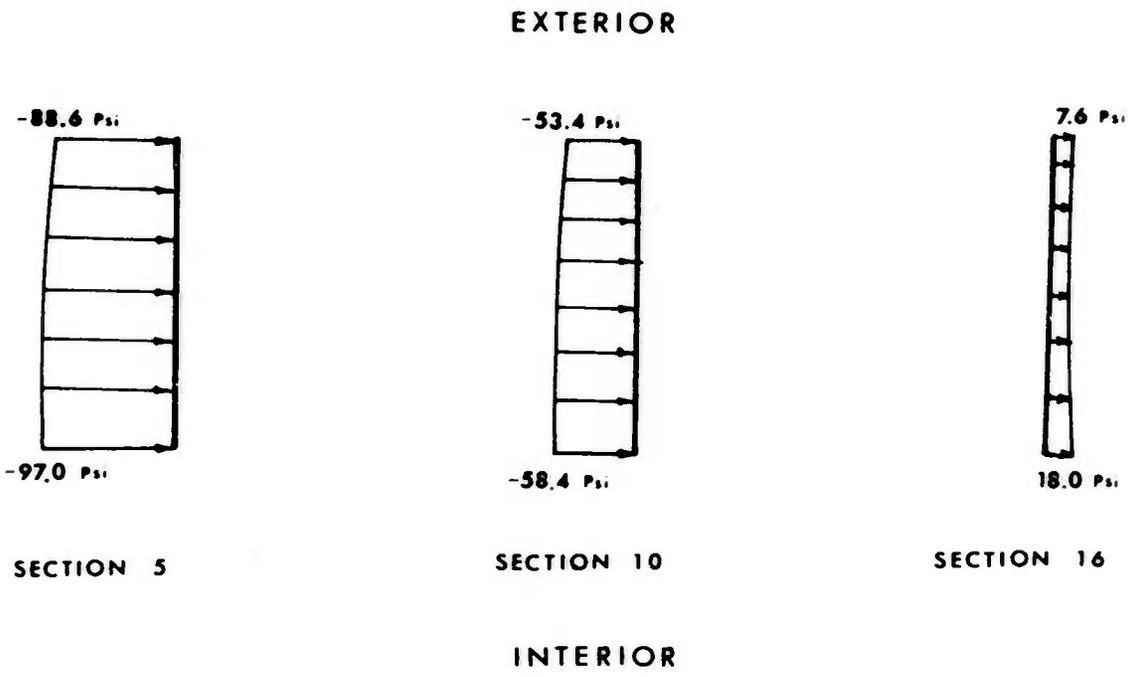

FIG. VI-23. Stress Distribution for Critical Combination of Rock Properties Case a

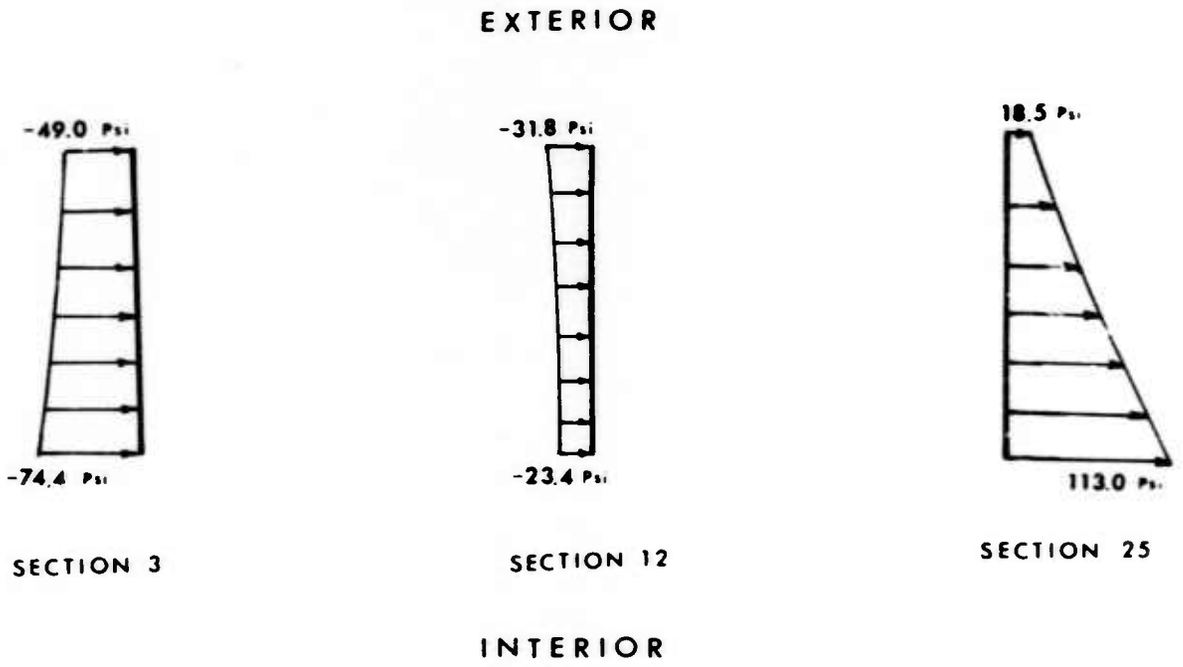

FIG. VI-24. Stress Distribution for Critical Combination of Rock Properties Case b

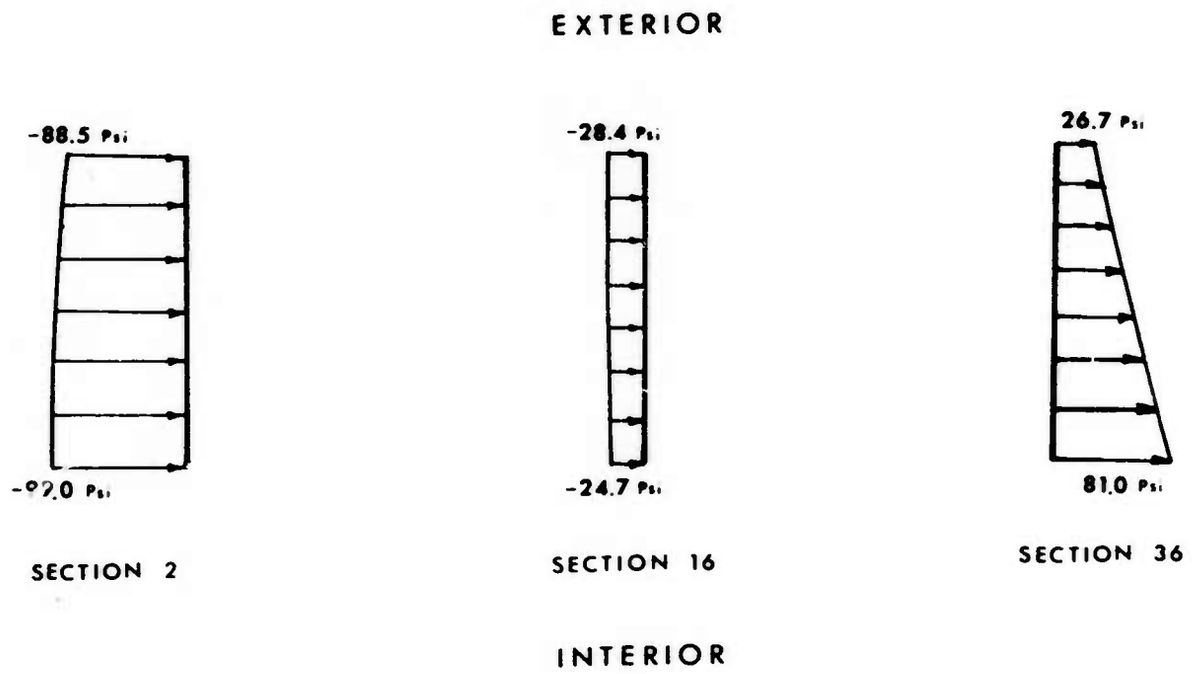

FIG. VI-25. Stress Distribution for Critical Combination of Rock Properties Case c

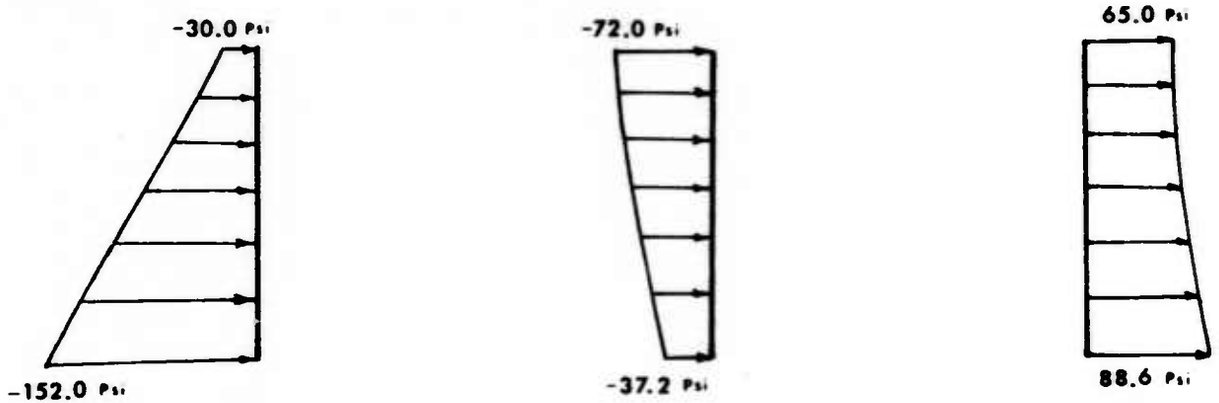

FIG. VI-26. Stress Distribution for Critical Combination of Rock Properties Case d

Section	case (a) Steel Rib Bonded to Shotcrete		case (a) Steel Rib Not Bonded to Shotcrete		case (d)	
	M (lbs.in.)	N (lbs.)	M (lbs.in.)	N (lbs.)	M (lbs.in.)	N (lbs.)
5	-212	-1325	-313	-791	-2341	-1003
16	+252	+ 605	+263	+158	+ 659	- 634
25	-814	+ 843	-718	+848	- 474	+ 892

Table VI-2. Comparison of cases (a) and (d)

range given in Table VI-1 were carried out to consider situations where the elastic modulus of roek in the vieinity of an underground opening may be significantly reduced by damage during exeavation or deterioration with exposure over a long time. The simulation assumed that after installation of supports and placement of shoterete, Young's modulus may reduce from an initial value of 1×10^6 pounds per square ineh. Different terminal values of Young's modulus used were 0.75×10^6, 0.67×10^6, 0.4×10^6, 0.25×10^6 pounds per square inch. Poisson's ratio was assumed to be 0.49 throughout. For case (a), the results are plotted in Figures VI-27 through VI-29. As might be expected, greater reduction in the elastie modulus was associated with greater bending moments and axial and shear forces. For reduetion of Young's modulus to 0.25×10^6 psi, the maximum longitudinal stress would be over 20,000 psi (Figure VI-30). Considering that deterioration of roek is more likely to oeeur in eases b and d, analysis were performed corresponding to a reduetion in Young's modulus from 1×10^6 to 0.4×10^6 pounds per square inch. Figure VI-31 shows the distribution of longitudinal stresses at critical sections for the cases a, b and d.

Another study considered mechanism (d) (section 6.2.1). In this, using ease b of Figure VI-2, the long struts or blocking points were assumed to be one-dimensional elements under a eompressive stress of 200 pounds per square ineh. Young's modulus and Poisson's ratio of rock were taken to be 1×10^6 psi and 0.49 respeetively. The struetural steel member was determined to have maximum axial foree of 25,520 pounds at section 12, maximum shearing foree of 1,604 pounds at seetion 8 and maximum bending moment of 28,700 pounds ineh at section 4. The maximum longitudinal stress was 2,750 psi in an element loeated in the flange of section 4. Distribution of longitudinal and shearing stresses at eritical seetions is shown in Figure VI-32.

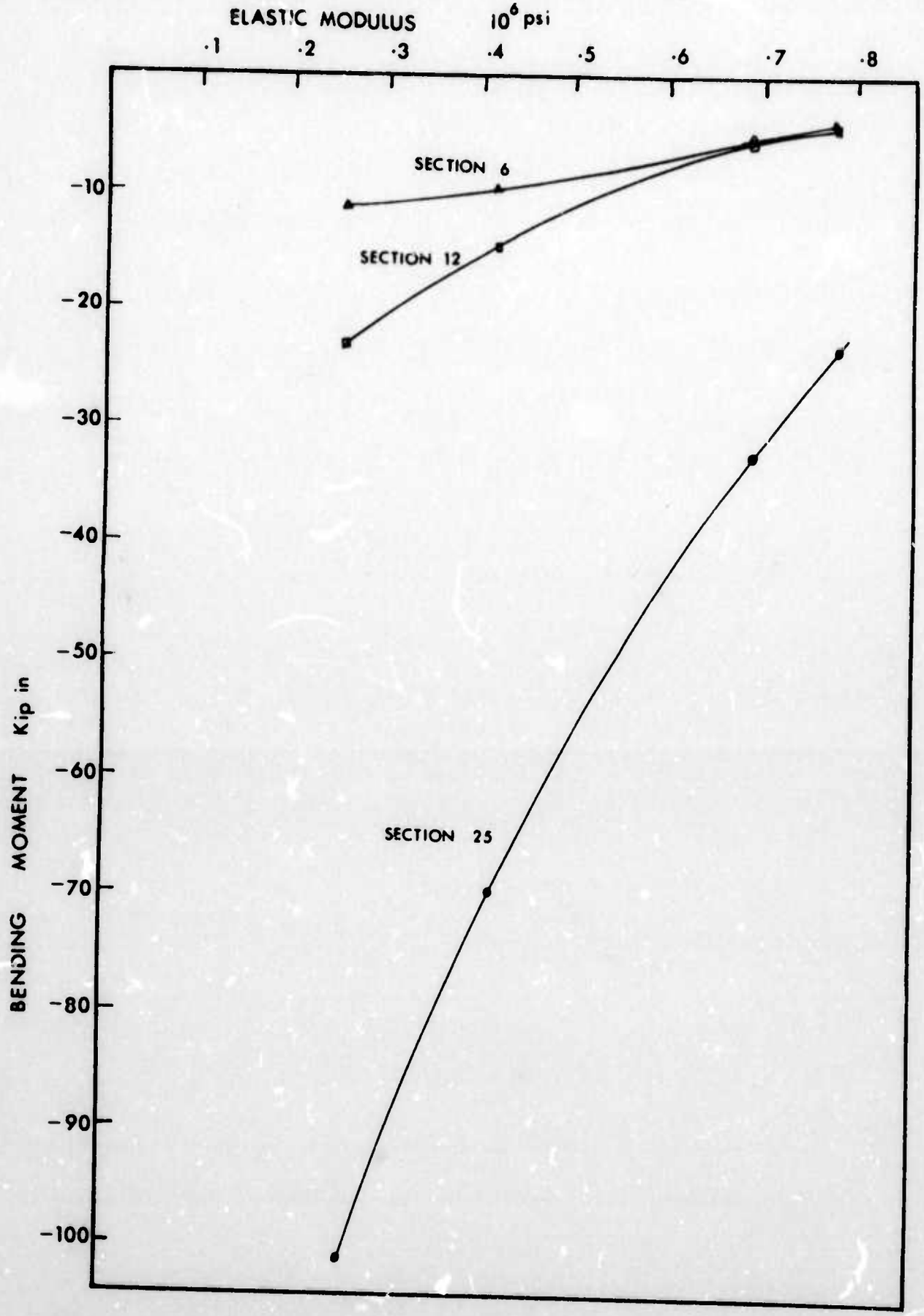

FIG. VI-27. Influence of Rock Deterioration on Bending Moment in Tunnel Supports

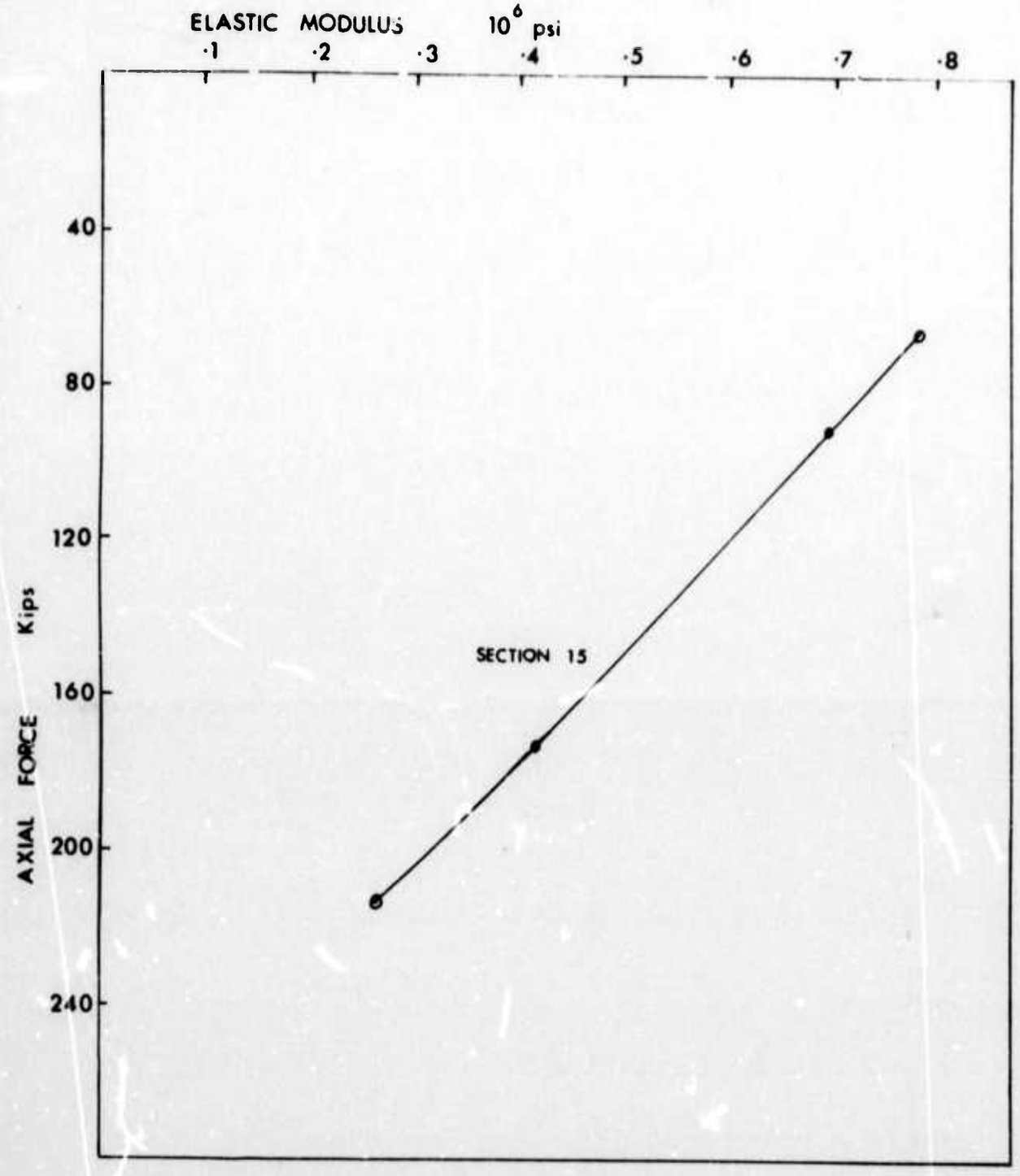

FIG. VI-28. Influence of Rock Deterioration on Axial Forces in Tunnel Supports

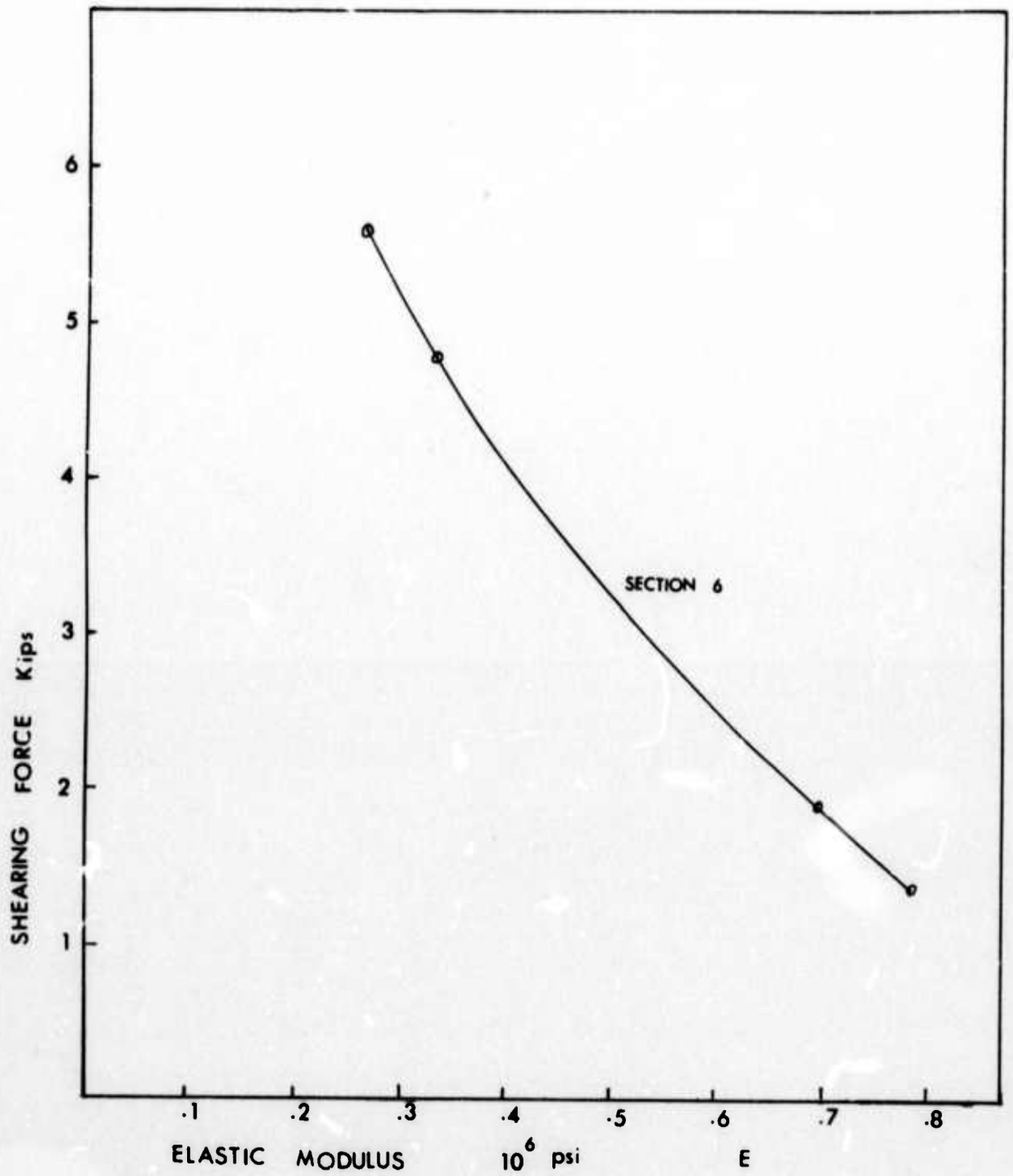

FIG. VI-29. Influence of Rock Deterioration on Shearing Force in Tunnel Supports

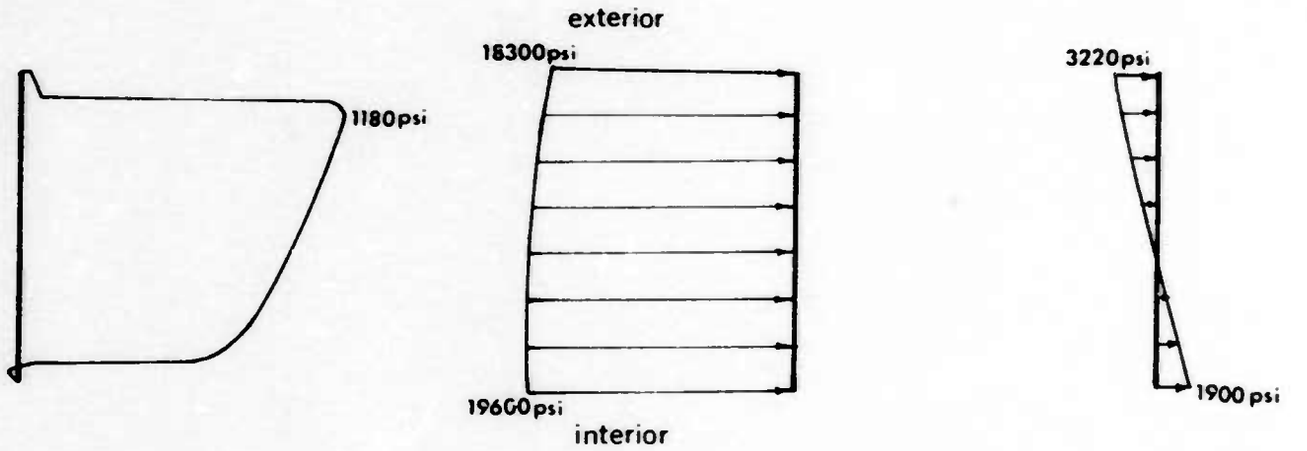

FIG. VI-30. Stress Distribution at Critical Sections Case a (Reduction of E from 1.0×10^6 to 0.25×10^6 psi)

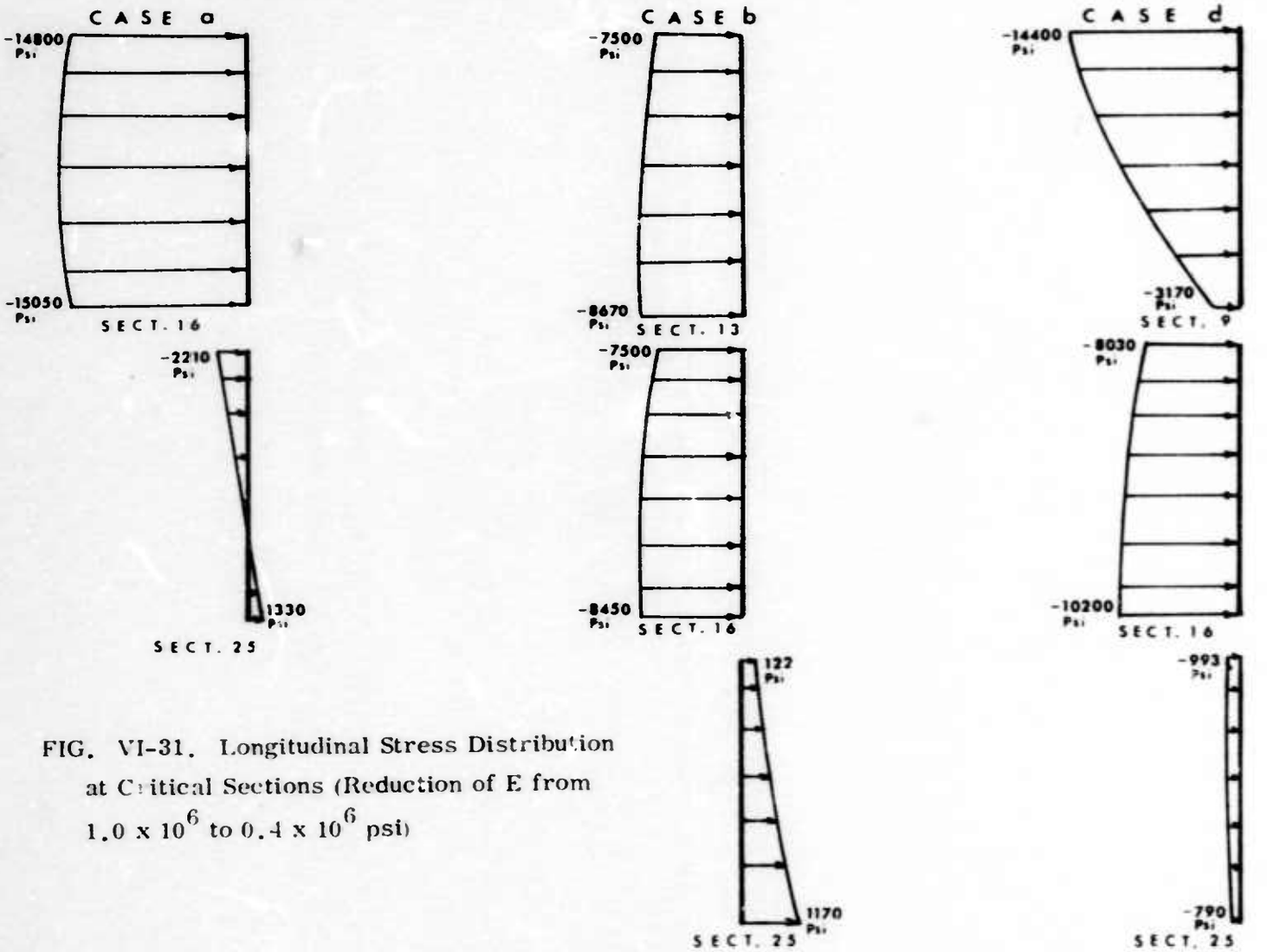

FIG. VI-31. Longitudinal Stress Distribution at Critical Sections (Reduction of E from 1.0×10^6 to 0.4×10^6 psi)

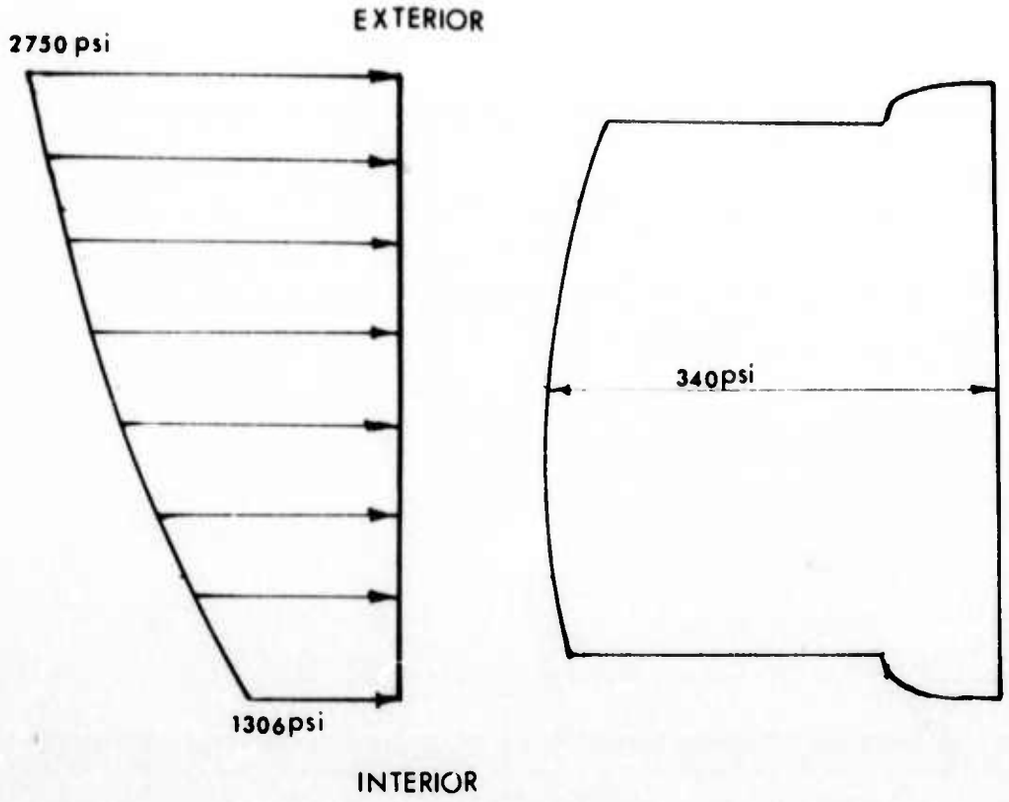

FIG. VI-32. Distribution of Longitudinal and Shearing Stresses on Critical Sections
Case (b) - 200 psi Stress in Struts

CHAPTER VII - DISCUSSION

Two different types of mechanical behavior of rock were considered. One treats rock as an isotropic elastic-plastic material following a generalized Mohr-Coulomb law and in the other, the rock is an isotropic linear elastic brittle material subject to fracture in accordance with Griffith's theory or the Modified Griffith theory. These two types of behavior are representative of a wide class of rock materials.

For analysis of stresses, deformation and progressive failure of nonhomogenous fissured rock, the finite element method is the most suitable. In the present research effort, previous attempts at finite element modeling of the two types of material behavior (elastic-plastic and elastic-brittle) were critically examined and their limitations noted. The present development eliminates several of the limitations. Analysis of elastic-plastic rock is based on Felippa's formulation of the incremental stress/incremental strain relationship. This is more general than and includes Prager-Naghdi's, Reyes' and Reyes-Deere's, and Yamada's formulations. In numerical procedures, the incremental approach was favored because of the poor convergence characteristics of the so called initial strain and initial stress methods. The procedures developed allow for incremental construction/excavation, arbitrary initial stresses, arbitrary geometry and considerable nonhomogeneity of of material. Nonmonotonic loading associated with sequential excavation was

properly allowed for.

For analysis of progressive failure of elastic-brittle rock, Griffith's theory and the Modified Griffith theory were used. Previous work used the no tension approach which is incorrect and unrealistic. In the present work, propagation of fracture was considered as a sequential phenomenon. The stress-redistribution associated with crack extension was allowed for as incremental cracking occured. Preexisting joints,whether open or closed,were considered. In all previous development, the location and orientation of fracture has to be known for a study of its propagation. In the present development, fractures can initiate at randomly oriented Griffith flaws assumed to be pre-existent everywhere in rock. Propagation follows initiation depending upon the Griffith criteria being satisfied.

The mathematical models of material behavior were fitted into appropriate variational formulations of the incremental elastostatic problem for the case of progressive fracture of elastic-brittle rock and the incremental plasticity problem for the case of progressive failure of elastic-plastic rock. Discretization of the governing functional by the finite element method gave the set of matrix equations leading to the problem solution. The procedural details of the finite element method are well known and therefore, were not reproduced in the present report.

The procedures developed were verified against existing theoretical solutions and experimental data. Excellent agreement was observed. Some typical

problems in rock mechanics and other areas were solved as illustrative applications.

The techniques developed are applicable to analysis of progressive failure through plastic yield or brittle fracture. In either case, arbitrary initial stress state, arbitrary geometrical configuration, arbitrary sequence of excavation/construction, can be considered and a history of sequential failure or fracture obtained. The methods can allow for pre-existing joints and fissures and are applicable to comparative stability studies based on stresses and deformations associated with excavation operations, evaluation of structural supports and loads on underground supports, safety analysis of openings, study of blasting effectiveness under certain conditions, evaluation of alternative mining sequences to obtain the safest construction sequence, etc.

The development was applied to a parametric study of the influence of rock properties on the stresses in steel supports using data supplied by the sponsor.

The experimental phase of the research program was concerned with development of modeling material so that materials with predetermined shape of the stress-strain curve could be produced in the laboratory. It should now be possible to carry out model tests on simulated rock to predict actual behavior at site as also to verify computational procedures. Certain assumptions made in the theory of plasticity are somewhat arbitrary. Model experiments would serve to verify them and permit evaluation of their influence on the significant parameters affecting stability of underground openings.

CHAPTER VIII - REFERENCES

Abel, J. F. Jr. (1967), "Tunnel Meehanies," Quarterly of the Colorado School of Mines, Vol. 62, No. 2.

Anderson, H. W. and Dodd, J.S. (1966), "Finite Element Method Applied to Rock Meehanies, Proe. 1st Cong. Int. Soc. for Rock Meeh., Lisbon, Vol. II, paper 7.17, pp. 317-321.

Argyris, J. H. (1960), Energy Theorems and Structural Analysis, Butterworth, London, 1960.

Aubin, J.P. (1972), Approximation of Elliptic Boundary-Value Problems, Wiley-Interscience.

Baker, L.E., Sandhu, R.S., and Shieh, W.Y. (1969), "Applieation of Elasto-Plastie Analysis in Rock Meehanies by Finite Element Method," Proeeedings, Eleventh Symposium on Rock Meehanies, Berkeley, California.

Batdorf, S.B., and Budiansky, B. (1949), "A Mathematieal Theory of Plastieity Based on the Coneept of Slip," NACA TN 1871, April 1949.

Bieniawski, Z. T. (1968), "Fracture Dynamies of Rock," Int. Jnl. Fraet. Mech., Vol. 4, No. 4, December 1968.

Bieniawski, Z.T. (1967), "Meehanism of Brittle Fraeture of Roek," Parts I, II, III, Int. Jnl. Rock Meeh. Min. Sci., V. 4, pp. 395-525.

Bock, Helmut (1971), "Computer Simulation of Second Order Faults," Roek Mechanies 3, pp. 225-238.

Bovee, R. B. and Ladd, C. C. (1970), M.I.T. Plane Strain Device, Researeh in Earth Physies, Phase Report No. 12, Massaehusetts Institute of Technology, Department of Civil Engineering, Cambridge, Massachusetts.

Braee, W.F. (1964), "Brittle Fraeture of Rocks," Part III, State of Stress in the Earth's Crust, ed. W.R. Judd, Am. Elservier Publishing Co., Ine., New York.

Braee, W.F. (1966), "Dilataney in the Fraeture of Crystalline Roeks," Jnl. Geoph. Res., Vol. 71, No. 16, pp. 3939-3953.

Brady, B.T. (1969a), "The Nonlinear Meehanieal Behavior of Brittle Roek, Part I, Stress-Strain Behavior During Regions I and II," Int. J. Roek Mech., Min. Sci., Vol. 6, No. 2, pp. 211-225.

Brady, B.T. (1969b), "The Nonlinear Mechanical Behavior of Brittle Rock, Part II, Stress-Strain Behavior During Regions III and IV," Int. J. Rock Mech. Min. Sci., Vol. 6, No. 3, pp. 301-310.

Brady, B.T. (1970), "A Mechanical Equation of State for Brittle Rock, Part I, The Pre-Failure Behavior of Brittle Rock," Int. J. Rock Mech. Min. Sci., Vol. 7, pp. 385-421.

Bresler, Boris, and Scordelis, A.C. (1963), "Shear Strength of Reinforced Concrete Beams," Jnl. A.C.I., January 1963.

Brown, F.W. (1956), "Determination of Basic Performance Properties of Blasting Explosives," Quarterly Colorado School of Mines, Vol. 51.

Budiansky, B. (1959), "A Reassessment of Deformation Theories of Plasticity," Journal of Applied Mechanics, Trans., ASME series E, Vol. 26, June, 1959.

Byskov, E., "The Calculation of Stress Intensity Factors Using the Finite Element Method with Crack Elements," Int. Jnl. of Fracture Mech., Vol. 6, No. 2, June, 1970.

Chan, S.K.; Tuba, I.S., and Wilson, W.K., "On the Finite Element Method in Linear Fracture Mechanics," Engr. Fracture Mechanics, Vol. 2, pp. 1-17.

Clough, R.W. (1960), "The Finite Element Method in Plane Stress Analysis," Proceedings, ASCE, 2nd Conference on Electronic Computation, Pittsburgh, Pa., September, 1960.

Clough, R.W. (1965), "The Finite Element Method in Structural Mechanics," Chapter 7, Stress Analysis, ed. O.C. Zienkiewicz and G.S. Holister, London, Wiley.

Clough, R.W., and Woodward, R.J. (1967), "Analysis of Embankment Stresses and Deformations," Journal of Soil Mech. and Foundations Div., Vol. 93, No. SM4, pp. 527-549, July 1967.

Desai, C.S. (1971), "Nonlinear Analyses Using Spline Functions," Journal of Soil Mechanics and Foundation Div., Vol. 97, No. SM10, pp. 1461, Oct. 1971.

Desai, C.S., and Holloway, D.M. (1971), Discussion to the paper "Nonlinear Analysis of Stress and Strain in Soils," Journal of the Soil Mech. and Found. Div., ASCE, Vol. 97, No. SM5, May 1971.

Desai, C.S., and Abel, J.F. (1972), An Introduction to the Finite Element Method, Von Nostrand.

Drucker, D.C. (1951), "A More Fundamental Approach to Plastic Stress-Strain Relation," Proc. First U.S. National Congress of Applied Mechanics, ASME, pp. 487-491.

Drucker, D.C., and Prager, W. (1952), "Soil Mechanics and Plastic Analysis or Limit Design," Q. App. Math., Vol. 10, pp. 157-165.

Drucker, D.C., Gibson, R.E., and Henkel, D.J. (1955), "Soil Mechanics and Work Hardening Theories of Plasticity," Paper No. 2864 Transactions, ASCE. 1955.

Duncan, J.M., and Goodman, R.E. (1968), "Finite Element Analysis of Slopes in Jointed Rock," Report No. S-68-3 to the USAE Waterways Experiment Station, Vicksburg, Office of Research Services, University of California, Berkley, California.

Duncan, J.M., and Chang, C.Y. (1970), "Nonlinear Analysis of Stress and Strain in Soils," Journal of Soil Mechanics and Foundations Div. Vol. 96, No. SM5, pp. 1629-1653, September, 1970.

Dunlop, P., and Duncan, J.M. (1969), "Slopes in Stiff-Fissured Clays and Shales," Journal of Soil Mechanics and Foundation Division, Vol. 95, No. SM2, pp. 467-492, March 1969.

Einstein, H.H.; Bruhn, R.W., and Hirschfeld, R.C. (1970), "Mechanics of Jointed Rock, Experimental and Theoretical Studies," Soil Mech. Publication No. 268, M.I.T..

E'Oliveira, Eduardo R. de Arantes (1968), "Completeness and Convergence in the Finite Element Method," Second Conf. on Matrix Methods in Structural Mechanics, WPAFB, Ohio.

E'Oliveira, Eduardo R. de Arantes (1968), "Theoretical Foundations of the Finite Element Method," Int. Jnl. of Solids and Structures, Vol. 4, pp. 929-952.

Evans, R.J., and Pister, K.S. (1966), "Constitutive Equations for a Class of Non-linear Elastic Solids," International Journal of Solids and Structures, Vol. 2, pp. 427-445.

Felippa, C. A. (1966), "Refined Finite Element Analysis of Linear and Nonlinear Two Dimensional Structures", Ph.D. thesis, University of California, Berkeley.

Felippa, C. A., and Clough, R. W., (1968), "The Finite Element Method in Solid Mechanics", Vol. 2 SIAM-AMS Proc. Numerical Solutions of Field Problems in Continuum Physics, Am. Math. Soc. Providence, R. I.

Gallagher, R. H., Padlog, J., and Bjilaard (1962). "Stress Analysis of Heated Complex Shapes", J. Am. Rocket Soc., Vol. 32, pp. 700-707.

Gallagher, R. H., and Oden, J. T. (1969), Recent Advances in Matrix Methods of Structural Analysis and Design , University of Alabama Press.

Green, A. E., and Naghdi, P. M. (1965), "A General Theory of an Elastic-Plastic Continuum", Arch. Rational Mech. Anal., Vol. 18, pp. 251-281.

Goodman, R. E., Taylor, R. L., and Brekke, T. L. (1968), "A Model for the Mechanics of Jointed Rock", Jnl. of Soil Mechanics & Foundation Division, Vol. 94, No. SM3, pp. 637-658.

Griffith, A. A., (1921), "The Phenomena of Rupture and Flow in Solids", Phil. Trans. Roy. Soc., London, Series A, Vol. 221.

Griffith, A. A., (1924), "The Theory of Rupture", Proc. 1st Cong. Appl. Mechanics, Delft.

Gross, B., Roberts, Jr., E., and Srawley, J. E. (1968), "Elastic Displacements for Various Edge-Cracked Plate Specimens," Int. J. Fract. Mech., Vol. 4. No. 3, September 1968.

Gross, B., and Srawley, J. E. (1964), "Stress-Intensity Factors for Single-Edge-Notch Specimans in Bending or Combined Bending and Tension By Boundary Collocation of a Stress Function", NASA TN D-2603,

Hahn, G. T., Hoagland R. G., Rosenfield, A. R., Simon R., and Nicholson G. D. "Influence of Microstructure on Fracture Propagation in Rock", Final Report to Bureau of Mines Contract No. HO 210006, Battelle, Columbus Laboratories, Columbus, Ohio.

Havner, K. S. (1969), "A Path Criterion for Deformation Plasticity Theory," Journal of the Engineering Mechanics Division ASCE, Vol. 95, No. EM3, June 1969.

Heuze, F. E., Goodman, R. E., and Bornstein, A. (1971), "Numerical Analyses of Deformability Tests in Jointed Rock - 'Joint Perturbation' and 'No-Tension' Finite Element Solutions," Rock Mechanics 3, pp. 13-24.

Hill, R. (1950), The Mathematical Theory of Plasticity, Oxford University Press.

Hoek, E.,and Bieniawski, Z. T. (1965), "Brittle Fracture Propagation in Rock Under Compression," Int. Jnl. Fract. Mech. 1, Vol. 3, pp. 137-155.

Holand, I., and Bell, K. (1970), "Finite Element Method in Stress Analysis," TAPIR, The Technical University of Norway, Trondheim, Norway, (2nd Print).

Ilyushin, A. (1945), "Relation Between Theory of St. Venant - Levy Mises and the Theory of Small Elastic Plastic Deformations," Prikladnia Matematika i Mekhanike, Vol. 9, pp. 207-218.

Irwin, G. R. (1958), "Fracture Mechanics," Proc. 1st Sym. Naval Struct. Mech., Ed. Goodier, Hoff.

Irwin, G. R. (1958), "Fracture" in Handbuck der Physik, Vol. 79, pp. 551-590, Springer-Verlag, Berlin.

Isakson, G., Armen, H., Pifko, A. B., and Levine, H. S. (1970), "Plastic Analysis of Structures," Grumman Research Department Report RE-380 J.

Jaeger, J. C., and Cook, N. G. (1969), Fundamentals of Rock Mechanics, Methwen and Co., Ltd..

Key, S. W. (1966), "A Convergence Study of the Direct Stiffness Method," Ph. D Dissertation, University of Washington.

King, I. P. (1965), "Finite Element Analysis of Two-Dimensional Time Dependent Stress Problems," Ph. D Thesis University of California, Berkeley.

Koiter, W. T. (1953), "Stress-Strain Relations, Uniqueness and Variational Theorems for Elastic-Plastic Materials with a Singular Yield Surface," Quart. App. Math., Vol. 11, pp. 350-354.

Koiter, W. T. (1960), "General Theorems for Elastic-Plastic Solids," Chapter IV, Progress in Solid Mechanics Ed. by Snedden and Hill, North Holland Publishing Co., Amsterdam.

Kondner, R. L. (1963), "Hyperbolic Stress Strain Response: Cohesive Soils," Journal of the Soil Mechanics and Foundations Division, ASCE, Vol. 89, No. SM1, pp. 115-143.

Kulhawy, F. H. (1972), "Analysis of Underground Openings in Rock by Finite Element Method," Semi-Annual Report to U.S. Bureau of Mines Contract, HO 210029, March 1972.

Kulhawy, F. H., and Duncan, J. M. (1969), "Finite Element Analyses of Stresses and Movements in Embankments During Construction," Contract Report S-69-8, USAE Waterways Experiment Station, Vicksburg, Mississippi, November, 1969.

Lajtai, E. Z. (1971), "Shear Strength of Weakness Plane in Rock," Int. Jnl. Rock Mech. Min. Sci., Vol. 6, pp. 499-515.

Lansing, W., Jensen, W. R., and Falby, W. (1965), "Matrix Analysis Methods for Inelastic Structures," Proceedings 1st Conference on Matrix Methods in Structural Mechanics, WPAFB, Dayton, Ohio.

Levy, N., Marcal, P. V., Ostergren, W. J., and Rice, J. R. (1971), "Small Scale Yielding Near A Crack in Plane Strain: A Finite Element Analysis," Int. Jnl. of Fracture Mechanics, Vol. 7, No. 2, June 1971.

Magri, F. (1972), "Variational Formulation for Every Linear Equation," International Symposium on Variational Methods in Engineering, Southampton, England.

Malina, H. (1970), "The Numerical Determination of Stresses and Deformations in Rock Taking into Account Discontinuities," Rock Mech., Vol. 2, pp. 1-16, 1970.

Marcal, P.V. (1968), "A Comparative Study of Numerical Methods of Elastic-Plastic Analysis," Jnl. AIAA, Vol. 6, No. 1, pp. 157-158.

Marcal, P. V.,and King, I. P. (1967), "Elastic-Plastis Analysis of Two-Dimensional Stress Analysis by the Finite Element Method," Int. Jnl. Mech. Sci., Vol. 9, pp. 143-155.

McClintock, F. A.,and Walsh, J. B. (1962), "Friction on Griffith Cracks in Rocks Under Pressure," 4th U.S. Natl. Cong. Appl. Mech., pp. 1015-1021.

Melay, R. W. (1969), "On the Finite Element Method in the Theory of Elasticity," No. D2-125154-1, Brochure Type Document, The Boeing Co., Washington.

Melkes, F. (1970), "The Finite Element Method for Nonlinear Problems," APLIKACE MATEMATIKY Svazek 15.

Melosh, R. J. (1963), "Basis for Derivation of Matrices for the Direct Stiffness Method," AIAA, Vol. 1, No. 7.

Mikhlin, S. G. (1965), The Problem of the Minimum of a Quadratic Functional, Holden-Day, San Francisco.

Naghdi, P. M. (1960), "Stress and Strain Relations in Plasticity and Thermoplasticity," Proceedings, 2nd Symposium on Naval Structural Mechanics, Pergman Press, pp. 121-169.

Nair, K., Sandhu, R. S.,and Wilson, E. L. (1968), "Time-Dependent Analysis of Underground Cavities Under Arbitrary Initial Stress Field," Proc. 10th Symposium on Rock Mechanics, Austin, Texas.

Neuber, H. (1969), "Anisotropic Nonlinear Stress-Strain Laws and Yield Conditions," Int. Jnl. Solids and Structures, Vol. 5, pp. 1299-1310.

Ngo, D.,and Scordelis, A. C. (1967), "Finite Element Analysis of Reinforced Concrete Beams," A.C.I. Jnl., March 1967.

Nilson, A. H. (1968), "Nonlinear Analysis of Reinforced Concrete by the Finite Element Method," A.C.I. Jnl., September 1968.

Oden, J. T. (1969), "A General Theory of Finite Elements:" I 'Topological Considerations', pp. 205-221; II 'Applications' pp. 247-260, International Journal of Numerical Methods in Engineering, Vol. 1.

Oden, J. T.,and Brauchli, H. J. (1971), "A Note on Accuracy and Convergence of Finite Element Approximations," Int. Jnl. for Numerical Methods in Engr., Vol. 3, pp. 291-294.

Oden, J. T. (1972), Finite Elements of Nonlinear Continua, McGraw Hill.

Paul, B., and Gangal, M. (1967), "Initial and Subsequent Fracture Curves for Biaxial Compression of Brittle Materials," Proc. 8th Sym. Rock Mech., Chapter 5, ed. C. Fairhurst.

Persson, P. A., Lundborg, N., Johansson, C. H. (1970), "The Basic Mechanisms in Rock Blasting," Proc. 2nd Cong. Int. Soc.Rock Mech.,Vol. 3, Belgrade.

Pian, T. H. H. (1968), "Variational Principles and Their Application to Finite Element Methods," Lecture Notes on "Finite Element Methods in Solid Mechanics," M.I.T., pp. 24-38.

Pian, T. H. H.,and Tong P. (1969), "Basis of Finite Element Methods for Solid Continua," International Journal of Numerical Methods in Engineering, Vol. 1, pp. 3-28.

Pian, T.H.H., Tong, P., and Luk, C.H. (1971), "Elastic Crack Analysis by a Finite Element Hybrid Method," M.I.T. Report, Proceedings, Third Conference Matrix Method in Structural Analysis, WPAFB, Ohio.

Prager, W. (1949), "Recent Developments in the Mathematical Theory of Plasticity," Jnl. App. Phys., Vol. 20, pp 235-241.

Prager, W. (1955), "The Theory of Plasticity: A Survey of Recent Achievements," (James Clayton Lecture), Proc. Instn. Mech. Engrs., Vol. 169, pp. 41-57.

Ramberg, W.,and Osgood,W. R. (1943), "Description of Stress-Strain Curves by Three Parameters," NACA-TN 902, July 1943.

Reyes, S. F. (1966), "Elastic-Plastic Analysis of Underground Openings by the Finite Element Method," Ph. D. Thesis,University of Illinois, Urbana.

Reyes, S. F.,and Deere, D. U. (1966), "Elasto-Plastic Analysis of Underground Openings by the Finite Element Method," Proceedings,First International Congress Rock Mechanics, Vol. 11, pp. 477-486, Lisbon.

Richard, R. M., and Goldberg, J. E. (1965), "Analysis of Nonlinear Structures: Force Methods," Journal of the Structural Division, ASCE, Vol. 91, St. 6.

Rivlin, R. S. (1960), "Some Topics in Finite Elasticity," Proceedings of the First Symposium on Naval Structural Mechanics," Pergamon Press, Inc., New York, pp. 169-198.

Salmon, M., Berke, L., and Sandhu, R. (1970), "An Application of the Finite Element Method to Elastic-Plastic Problems of Plane Stress," Technical Report AFFDL-TR-68-39, WPAFB, Ohio.

Sandhu, R. S., Wilson, E. L., and Raphael, J. M. (1967), "Two Dimensional Stress Analysis with Incremental Construction and Creep," Report No. SESM 67-34, Structural Engineering Laboratory, Univ. of California, Berkeley, Dec. 1967.

Sandhu. R. S., and Wilson, E. L. (1969), "Finite Element Analysis of Stresses in Mass Concrete Structures," Symposium on Impact of Computers on the Practice of Structural Engineering in Concrete, ACI, St. Louis, Missouri.

Sandhu, R. S. (1971), "Stresses, Deformations and Progressive Failure of Nonhomogenous Fissured Rock," Semi-annual Technical Report to U.S. Bureau of Mines, Contract No. HO 210017, August 1971.

Sandhu, R. S., and Pister, K. S. (1970), "A Variational Principle for Linear Coupled Field Problems," Int. J. Engrg. Sci., Vol. 8, pp. 989-999.

Sandhu, R. S., and Pister, K. S. (1971), "Variational Principles for Boundary Value and Initial-Boundary Value Problems in Continuum Mechanics," Int. Jnl. Solids and Structures, Vol. 7, pp. 639-654.

Sandhu, R. S., and Pister, K. S. (1972), "Variational Principles in Continuum Mechanics," Int. Symposium on Variational Methods in Engineering, Southampton, England.

Singh, R. D. (1972), Personal Communication

Sutherland, W. H. (1970), "AXICRP-Finite Element Computer Code for Creep Analysis of Plane Stress, Plane Strain and Axisymmetric Bodies," Nuclear Engineering and Design, Vol. II, pp. 269-285.

Swanson, S. R. (1970), "Development of Constitutive Equations for Rocks," Ph. D. Thesis, University of Utah.

Swedlow, J. L., Williams, M. L., and Yang, W. M. (1965), "Elasto-Plastic Stresses in Cracked Plates," California Institute of Technology, Report SM 65-19.

Tong, P., and Pian, T. H. H. (1967), "The convergence of the Finite Element Method in Solving Linear Elastic Problems," Int. Journal Solids Structures, Vol. 3.

Tottenham, H. (1970), "A Direct Numerical Method for the Solution of Field Problems," International Journal for Numerical Methods in Engineering, Vol. 2, pp. 117-131.

Toupin, R. A., and Bernstein, B. (1961), "Sound Waves in Deformed Perfectly Elastic Materials," The Journal of Acoustical Society of America, Vol. 33, No. 2, p. 217, February 1961.

Turner, M. J., Clough, R. W., Martin, H. C., and Topp, L. J. (1956), "Stiffness and Deflection Analysis of Complex Structures," J. Aero. Sci., Vol. 23, pp. 805-823.

Vainberg, M. M. (1964), Variational Methods for the Study of Nonlinear Operators," Holden-Day.

Vanderbilt University (1969), Applications of the Finite Element Method in Civil Engineering.

Walsh, J. B. (1965 a), "The Effect of Cracks on the Compressibility of Rocks," J. Geophys. Res., Vol. 70, No. 2, pp. 381-389.

Walsh, J. B. (1965 b), "The Effect of Cracks on the Uniaxial Elastic Compression of Rocks," J. Geophys. Res., Vol. 70, No. 2, pp. 399-411.

Walsh, J. B. (1965 c), "The Effect of Cracks in Rocks on Poisson's Ratio," J. Geophysical Res., Vol. 70, No. 20, pp. 5249-5257.

Walz, J. E., Fulton, R. E., and Cyrus, N. J. (1968), "Accuracy and Convergence of Finite Element Approximations," 2nd Conference on Matrix Methods in Structural Mechanics, WPAFB, Ohio.

Washizu, K. (1968), Variational Methods in Elasticity and Plasticity, Pergamon Press.

Wilson, E. L. (1963), "Finite Element Method in Two-Dimensional Problems," D. Engg. Thesis, University of California, Berkeley.

Wilson, E. L. (1965), "Structural Analysis of Axisymmetric Solids," Jnl. AIAA, Vol. 3.

Wilson, W. K. (1971), "Finite Element Methods for Elastic Bodies Containing Cracks," Westinghouse Research Laboratories, Scientific Paper 71-1E7-PDPSC-P1, October 29, 1971.

Wright Patterson Air Force Base Conferences on Matrix Methods in Structural Analysis 1965, Second Conference 1968, Third Conference 1971.

Yamada, Y., Yoshimura, N., and Sakurai, T. (1968), "Plastic Stress-Strain Matrix and its Application for Solution of Elastic Plastic Problems by the Finite Element Method," Int. Jnl. Mech. Sci., Pergamon Press, Vol. 10, pp. 343-354.

Yamamoto, Y. and Tokuda, N. (1971), "A Note on Convergence of Finite Element Solutions," International Jnl. of Numerical Methods in Engr, Vol. 3, pp. 485-493.

Ziegler, H. (1959), "A Modification of Prager's Hardening Rule," Quart. Applied Math., Vol 17, pp. 55-65.

Zienkiewicz, O. C. (1967), The Finite Element Method in Structural and Continuum Mechanics, McGraw Hill, New York.

Zienkiewicz, O. C., Valliappan, S. and King, I. P. (1968), "Stress Analysis of Rock as a 'No Tension' Material," Geotechnique, Vol. 18, No. 1, pp. 56-66.

Zienkiewicz, O. C., Valliappan, S. and King, I. P. (1969), "Elasto-Plastic Solutions of Engineering Problems, Initial Stress, Finite Element Approach," Int. Jnl. of Numerical Methods in Engr., Vol. 1, pp. 75-100.

Zlamal, M. (1968), "On the Finite Element Method," Numer. Math. 12, pp. 394-409.

APPENDIX A. GRIFFITH THEORY OF BRITTLE FRACTURE

A.1. The Original Griffith Theory of Brittle Fracture

Two different failure criteria were proposed by Griffith. They are the energy criterion and the stress criterion.

A.1.1. The Energy Criterion

An extended minimum potential energy theorem can be stated as:

> If an elastic solid body is deformed by certain specified boundary forces, the sum of the potential energy of the applied forces and the strain energy stored in the body will be either decreased or unaltered by the creation of cracks with traction-free surfaces.

Based upon this theorem and assuming the creation of new surfaces required only certain amount of surface energy, the failure criterion can be written as:

> The surface energy increased must be equal to the strain energy released such that the foregoing theorem is satisifed.

Mathematically the statement can be expressed by the following equation:

$$\frac{\partial}{\partial c}(W - S) = 0 \qquad (A.1)$$

where c = half length of the new crack
W = strain energy released
S = surface energy required to form the new crack.

Eq. (A.1) is considered as a necessary condition for stable fracture propagation.

It is understandable that stress is highly concentrated at crack tip when the radius of curvature of the crack tip is very small. The stress concentration may be counted for the failure of material at certain stress level lower than the strength of

the material. One major drawback of this failure criterion is that the critical orientation of the initial flaw which happens to be one of the important roles in the fracturing process, can not be generally defined. Following the energy criterion, the crack would propagate in the direction of the initial flaw. Apparently, this is just a special case of the general fracturing mode.

A.1.2. Stress Criterion

The stress criterion can be derived from the solution for stress distribution around the crack. Following Inglis (1913), the tangential stress on the boundary of an elliptic crack is given by (Fig. A.1)

$$\sigma_\eta = \left\{ (\sigma_1 + \sigma_2) \sinh 2\xi_o + (\sigma_1 - \sigma_2) \left[e^{2\xi_o} \cos 2(\beta - \eta) - \cos 2\beta \right] \right\} / (\cosh 2\xi_o - \cos 2\eta) \qquad (A.2)$$

where ξ , η = orthogonal curvilinear coordinates

ξ_o = ξ on the crack boundary

σ_1, σ_2 = major and minor principal stresses, positive in tension

β = angle between the major axis of the ellipse and σ_2 axis

Eq. (A.2) has been obtained on the assumption that the crack is very flat such that $\xi_o \ll 1$ exists.

From Eq. (A.2), it can be shown (Jaeger and Cook, 1969) that the maximum tensile stress at the crack tip is approximated by

$$\sigma_{max} = \frac{1}{\xi_o} \left[\sigma_1 \cos^2\beta + \sigma_3 \sin^2\beta - (\sigma_1^2 \cos^2\beta + \sigma_3^2 \sin^2\beta)^{\frac{1}{2}} \right] \qquad (A.3)$$

The condition $\partial\sigma_{max} / \partial\beta = 0$ yields

$$\cos 2\beta = - (\sigma_1 - \sigma_2) / (\sigma_1 + \sigma_2) \tag{A.4}$$

which defines β associated with σ_{max}, provided $\sigma_1 \neq \sigma_2$.

Eq. (A.4) also implies

$$\sigma_1 + 3\sigma_2 \geq 0 \text{ if } \sigma_1 > \sigma_2 \tag{A.5}$$

Substituting (A.4) in (A.3) we obtain

$$\sigma_{max} = - (\sigma_1 - \sigma_2)^2 / 4 \xi_o (\sigma_1 + \sigma_2) \tag{A.6}$$

Let σ_t denote the uniaxial tensile strength of the material, and consider two extremal cases:

(i) $\sigma_{max} = 2\sigma_1 / \xi_o$ when β is set equal to zero in Eq. (A.3) and the negative value of the square root is used to obtain the largest value of σ_{max}. σ_1 is tensile since $\sigma_1 + 3\sigma_2 \geq 0$ and $\sigma_1 > \sigma_2$. Then $\sigma_{max}\, \xi_o = 2\sigma_1 = 2\sigma_t$ or $\sigma_t - \sigma_1 = 0$. (A.7)

(ii) $\sigma_{max} = \dfrac{2\sigma_2}{\xi_o}$ when $\beta = \dfrac{\pi}{2}$

Mathematically σ_2 may not be tensile since Eq. (A.5) is satisfied alright, but physically, failure could not happen under this single condition. Therefore this becomes a limiting condition for Eq. (A.6). It then follows from Eq. (A.6) that

$$2\sigma_t = (\sigma_1 - \sigma_2)^2 / 4 (\sigma_1 + \sigma_2)$$

or

$$(\sigma_1 - \sigma_3)^2 - 8\sigma_t (\sigma_1 + \sigma_3) = 0 \tag{A.8}$$

Eqs. (A.4), (A.5), (A.7) and (A.8) constitute the failure criterion. They are summarized as follows:

$$\sigma_1 - \sigma_2 > 0$$

(i) $$3\sigma_1 + \sigma_2 \geqq 0$$

$$\sigma_t - \sigma_1 \leqq 0$$

$$\beta = 0 \qquad \text{(A.9)}$$

(ii) $$3\sigma_1 + \sigma_2 < 0$$

$$\sigma_t - \sigma_n \leqq 0$$

where $$\sigma_n = -\frac{1}{8}(\sigma_1 - \sigma_2)^2 / (\sigma_1 + \sigma_2) > 0$$

$$\cos 2\beta = -\tfrac{1}{2}(\sigma_1 - \sigma_2) / (\sigma_1 + \sigma_2)$$

A.2. Modification of Griffith Theory

The original Griffith theory did not allow for closing of crack subject to compressive stresses. When a crack closes, sliding may occur along the crack surfaces. A modification permitting crack closure was proposed by Brace (1960) and McClintock and Walsh (1962) and was further developed by Murrell (1964) and Hoek and Bieniawski (1965).

The modified theory is based on the assumption that the crack would close when the stress normal to the plane of crack is in compression and exceeds some critical compressive stress. After crack-closure, stresses are carried over the crack plane through interface friction. The material strength is increased and stress concentration at crack tip is reduced.

The conditions are stated as

$$\sigma_n = 0 \quad \text{if} \quad |\sigma_y| \leq |\sigma_c|$$

and

$$\sigma_n = -|\sigma_y - \sigma_c| \quad \text{if} \quad \sigma_y > \sigma_e \tag{A.10}$$

The interfaee friction and the effective interfaee friction are given by

$$\tau_f = -\mu \sigma_n = \mu |\sigma_y - \sigma_e| \text{ , if } \sigma_n > \sigma_e \tag{A.11a}$$

and

$$\tau = \tau_{xy} - \tau_f = \tau_{xy} - \mu |\sigma_y - \sigma_c| \tag{A.11b}$$

where σ_y = stress normal to the crack

σ_n = effective normal stress

σ_e = critical normal stress

μ = coefficient of friction

τ_{xy} = shearing stress along the crack

Following the similar procedure for deriving the stress criterion and making use of the condition $\frac{\partial \sigma_\eta}{\partial \eta} = 0$, we find

$$\sigma = 2(\sigma_c \xi_o - \eta \tau) / (\xi_o^2 + \eta^2) \tag{A.12}$$

$$\sigma_{max} = \frac{1}{\xi_o} (\sigma_e + \sqrt{\sigma_e^2 + \tau^2}) = \frac{2 \sigma_t}{\xi_o} \tag{A.13a}$$

and

$$\tau = 2\sigma + (\sigma_e / \sigma_t + 1)^{\frac{1}{2}} \tag{A.13b}$$

Eq. (A.11b) can be rewritten as

$$\tau = \tfrac{1}{2} (\sigma_1 - \sigma_2) \sin 2\beta + \mu (\sigma_1 \cos^2 \beta + \sigma_2 \sin^2 \beta - \sigma_e) \tag{A.14}$$

The condition $\partial \tau / \partial \beta = 0$ gives

$$\tan 2\beta = -\frac{1}{\mu} \text{ , provided } \sigma_1 \neq \sigma_2 \tag{A.15}$$

Substituting Eq. (A.15) in Eq. (A.14)

$$\tau = \tfrac{1}{2} (\sigma_1 - \sigma_2) (1 + \mu^2)^{\frac{1}{2}} + \mu (\sigma_1 + \sigma_2) - 2\sigma_c \qquad (A.16)$$

Eliminating τ between Eq. (A.13b) and Eq. (A.16)

$$(\sigma_1 - \sigma_2) (1 + \mu^2)^{\frac{1}{2}} + \mu (\sigma_1 + \sigma_2) = 4 \sigma_t (\frac{\sigma_c}{\sigma_t} + 1)^{\frac{1}{2}} + 2\mu \sigma_c \qquad (A.17)$$

If σ_c is negligible, Eq. (A.17) reduces to

$$(\sigma_1 - \sigma_2) (1 + \mu^2)^{\frac{1}{2}} + \mu (\sigma_1 + \sigma_2) = 4 \sigma_t \qquad (A.18)$$

Eq. (A.18) coincides with Mohr-Coulomb criterion if $2 \sigma_t = T$, where T is the cohesion of the material. Eq. (A.17) indicates that the modified criterion is of three-parameter type and Eq. (A. 18) gives a linear relationship between the principal stresses.

Another form of modified criterion was suggested by Hoek and Bieniawski (1966) and Bieniawski (1967):

$$\sigma_2 = \sigma_1 [(\sqrt{1 + \mu^2} + \mu) / (\sqrt{1 + \mu^2} - \mu)] - \sigma'_c \qquad (A.19)$$

where σ'_c = uniaxial compressive strength of the material. Eq. (A.19) has the advantage of using σ'_c which is much easier to measure than σ_t .

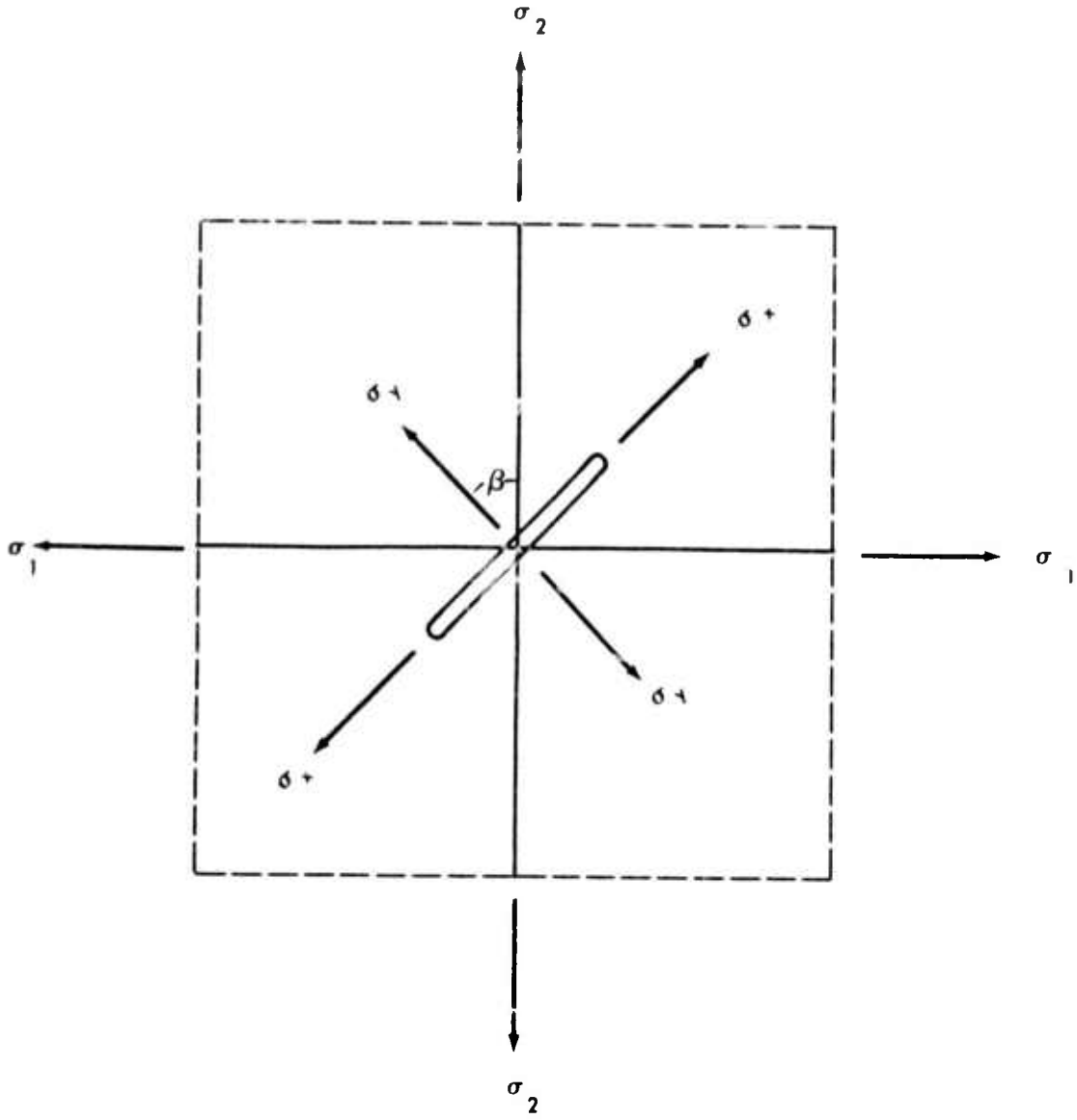

Fig. A-1. Griffith Crack

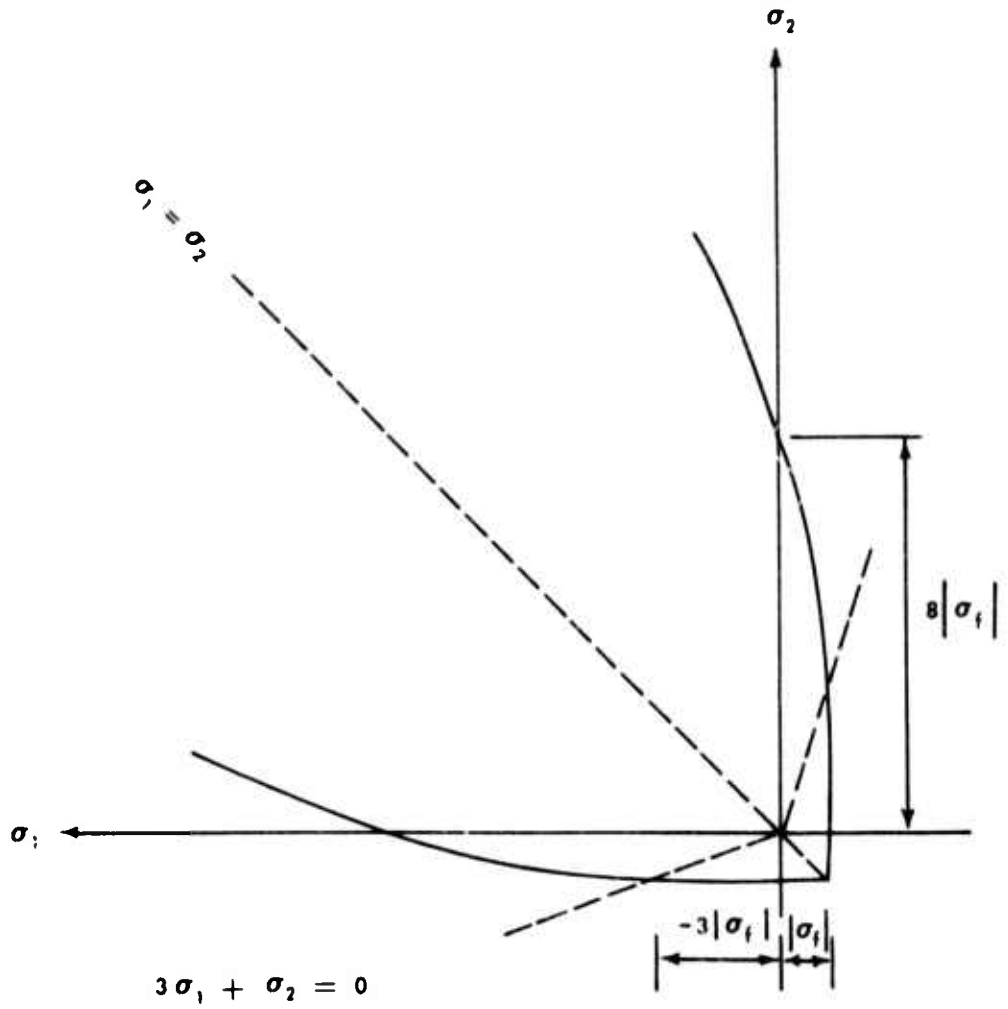

FIG. A-2. Griffith Criterion in $\sigma_1 - \sigma_2$ Space

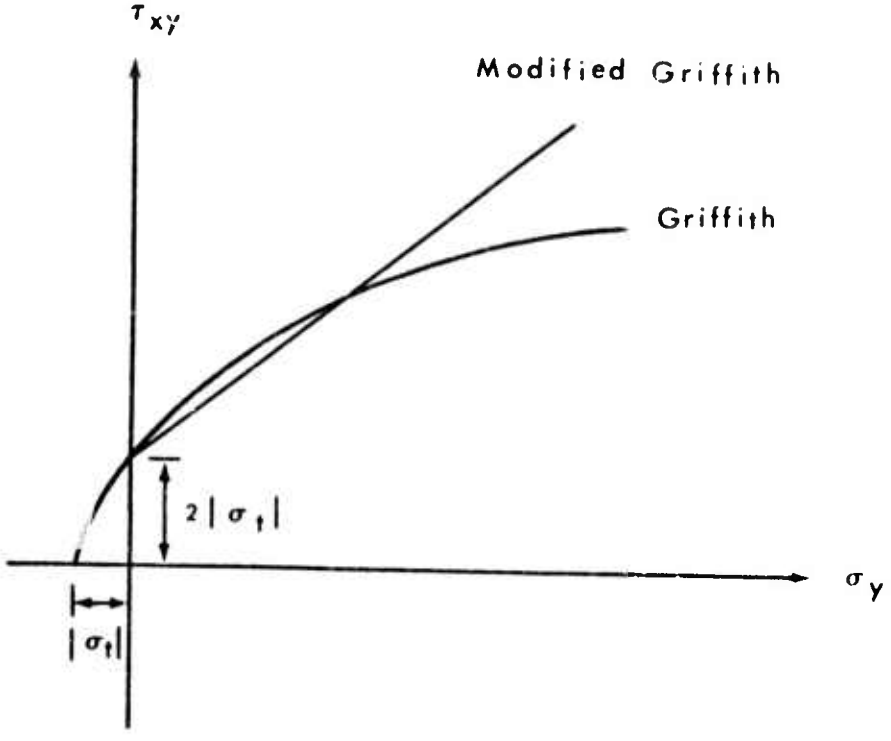

Fig. A-3 Mohr's Diagram for Griffith and Modified Griffith Criteria

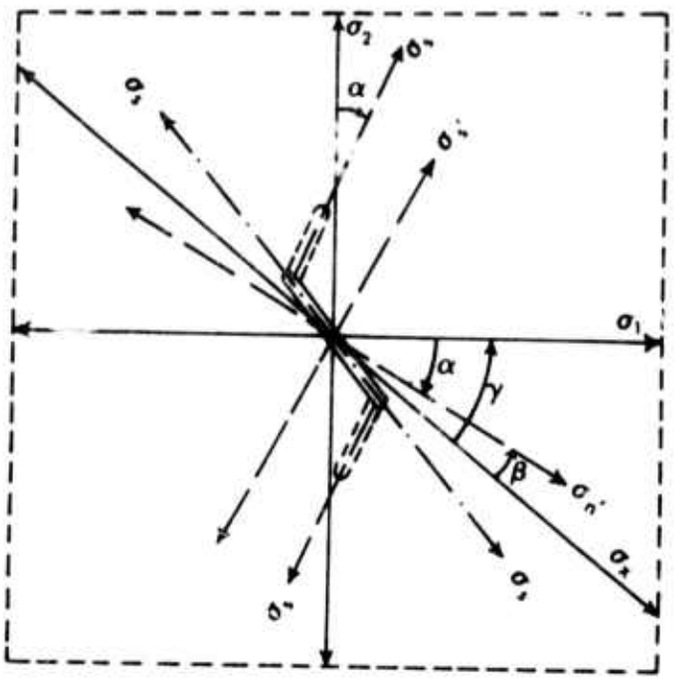

FIG. A-4. ANGLES RELATED TO CRACK PROPAGATION

σ_1, σ_2 stresses in reference configuration

σ_s, σ_n stresses referred to orientation of Griffith flaw

σ'_s, σ'_n stresses referred to orientation of crack extension

APPENDIX B. DEVELOPMENT OF TEST MATERIAL

B.1. The Experimental Program

The experimental program was intended to design laboratory materials whieh would simulate the stress-strain behavior of a wide variety of rock types. Consideration would be given to brittle, plastic and strain hardening response in both undrained and drained pore water conditions. Sinee the theoretieal solutions would be expeeted to operate with any eonsistent level of engineering parameters for both models and prototypes, it was not necessary to develop a true rock-like material. Instead, soils stabilized with additives such as hydrated lime could be used. Materials of this type may be eonstructed so as to show failure response ranging from elastie brittle to elastie-work hardening plastic. The variation may come about as a function of the eonsolidation pressure or of additive eoncentration. A speeial reason for using soil to model rock behavior was that the testing and modelling could be done using standard soil mechanics laboratory equipment with considerable saving in equipment costs and development time.

B.2. The Study Material

The study material was a brown silt from the lacustrine deposits south of Cleveland, Ohio. The oven-dried soil was combined with either hydrated lime or portland cement. After adding water, the soil was mixed and plaeed in a vaeuum extruder. The auger expelled the soil in a saturated condition through a final die, ready shaped for testing. Samples were sealed in four layers of plastie and wax and then cured in a humid room for period of 4 to 6 weeks.

A series of consolidated-drained triaxial tests indicated that a 4% lime-silt mixture might have the desired properties. As shown in Figure B-I, the full range of stress-strain response from elastic-brittle to strain hardening is available as a function of consolidation pressure. The stress levels are within the usable range of the plane strain device or of modelling applications. The testing program was terminated before plane strain tests could be conducted. The different boundary conditions in that test might have required modifications in the mix.

B.3. The Plane Strain Device

A plane strain device was purchased from the Massachusetts Institute of Technology soils laboratory. It has been shown to be satisfactory for the purpose of the tests intended. A rectangular sample 3.5 inch x 3.5 inch x 1.4 inch is restrained so as to allow the application of vertical stress by means of a piston, control of stress or strain in an orthogonal direction and the measurement of stress in the third orthogonal direction against a fixed plate. The system is designed to operate under a hydraulic back-pressure and measure pore-pressures during the test. Schematic drawings in Figures B-II to B-IV give details of the device and show elements of the sample loading and arrangement. A complete description of the device and its use are given by Bovee and Ladd (1970). Due to a curtailment of the scope of work, no tests were carried out under the current research program.

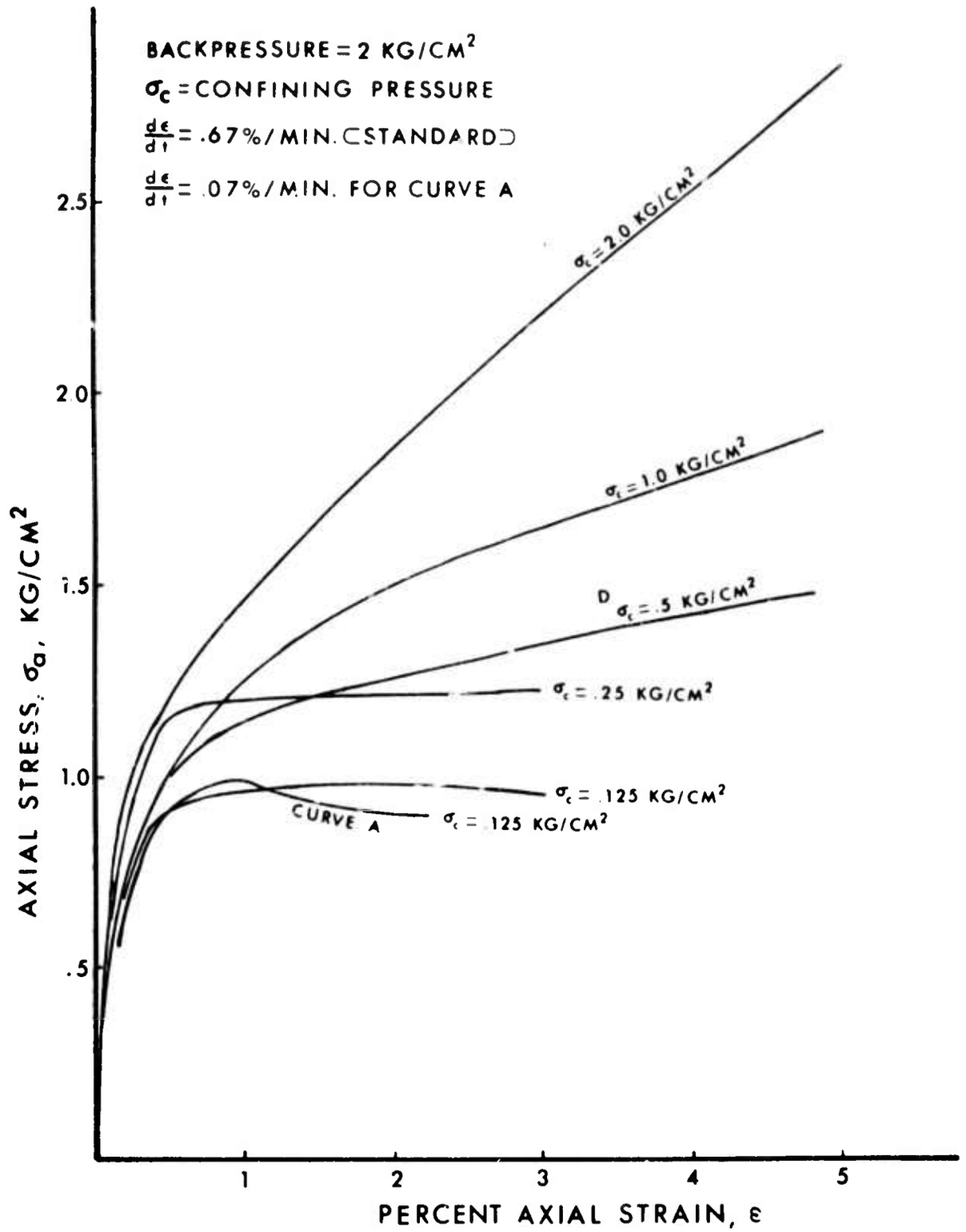

FIG. B-1. Stress-Strain Behavior of 4% Lime Silt (Triaxial Consolidated Drained Test)

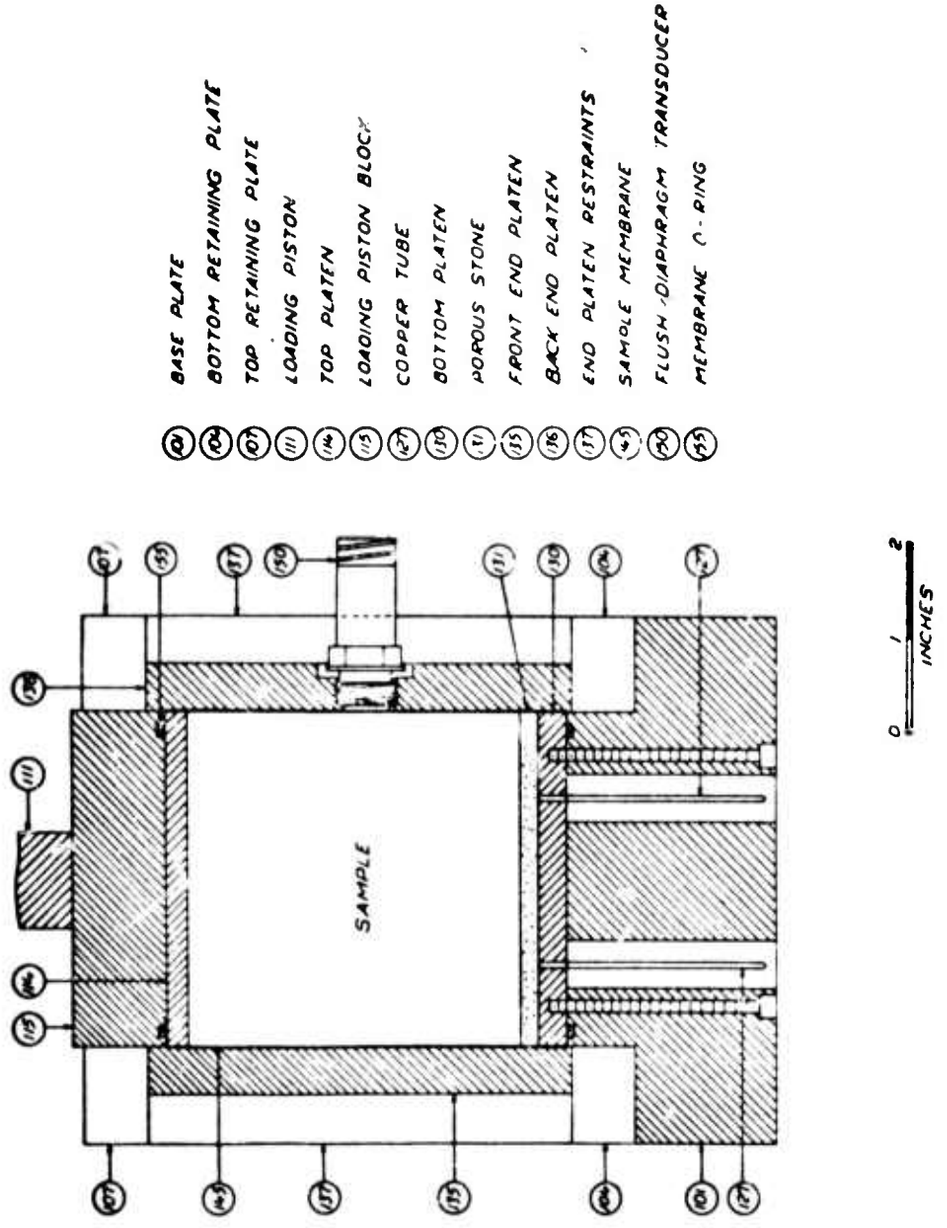

FIXED END PLATENS

(SIDE VIEW OF DEVICE)

FIG. B-II

(From Bovee-1970)

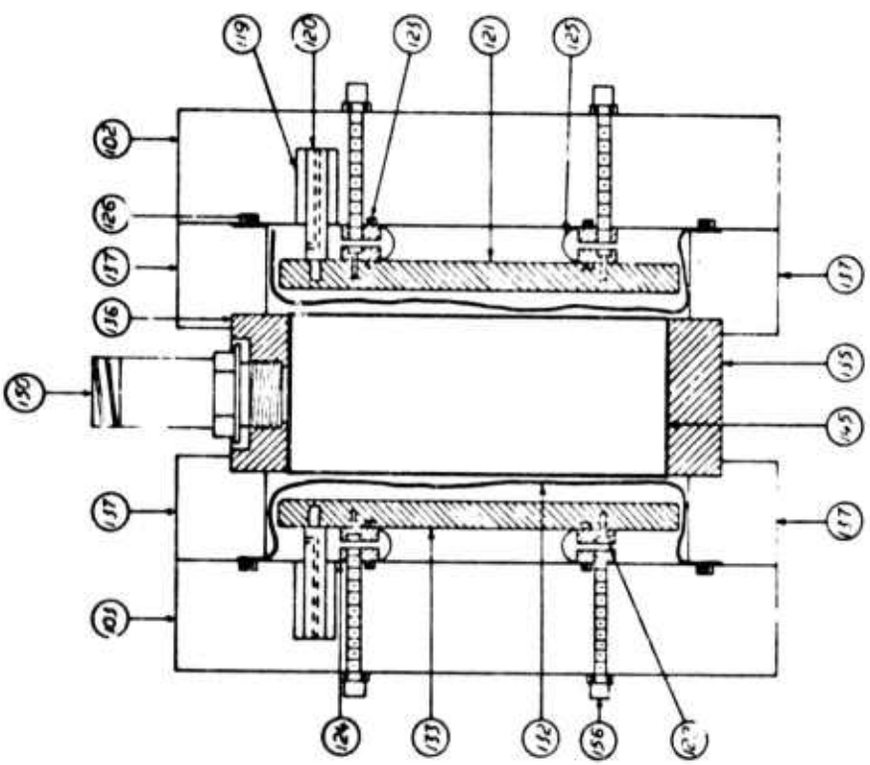

TOP VIEW OF PLANE STRAIN DEVICE

FIG. B-III

(From Bovee-1970)

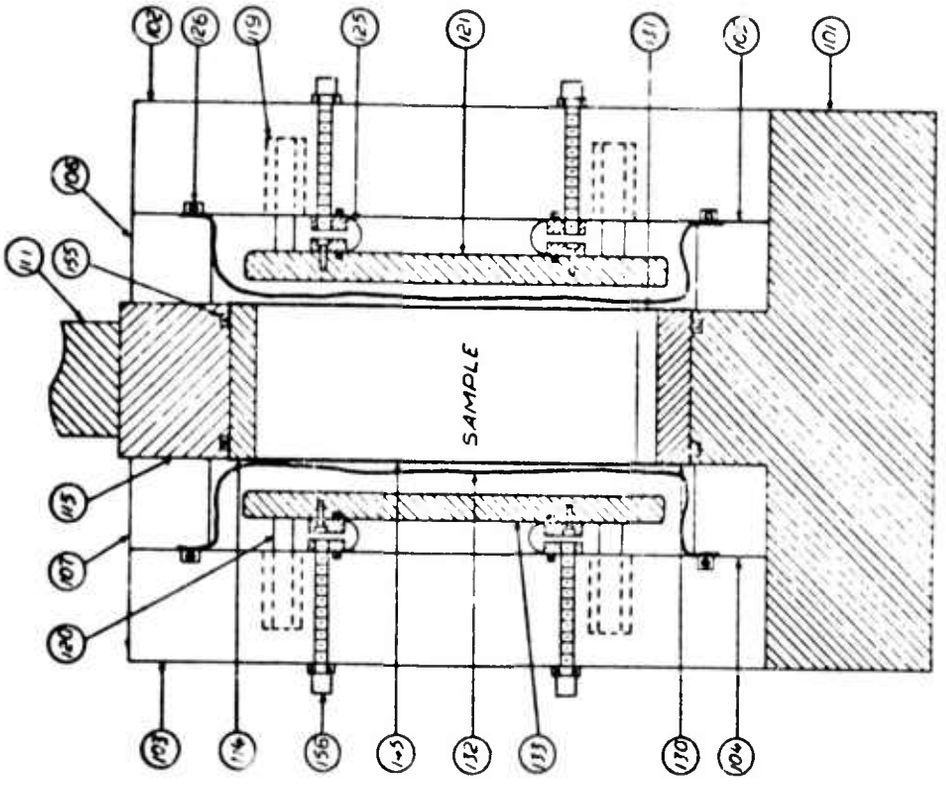

101 – BASE PLATE
102 – SIDE ASSEMBLY PLATES
103 – BOTTOM RETAINING PLATES
104 – TOP RETAINING PLATES
106 – LOADING PISTON
111 – TOP PLATEN
114 – LOADING PISTON BLOCK
115 – SIDE PLATEN GUIDE BUSHING
119 – GUIDE SHAFT
120 – RIGHT SIDE PLATEN
121 – SIDE PLATEN DIAPHRAGM
125 – CELL DIAPHRAGM O-RING
126 – BOTTOM PLATEN
130 – POROUS STONE
131 – CELL DIAPHRAGM
132 – LEFT SIDE PLATEN
133 – SAMPLE MEMBRANE
135 – MEMBRANE O-RING
136 – SIDE PLATEN DIAPHRAGM CAP SCREW

HORIZONTAL LOADING SYSTEM
(END VIEW OF DEVICE)

FIG. B-IV (From Bovee-1970)